

TRANSPORT OF IMMUNOGLOBULIN G  
ACROSS THE HUMAN PLACENTA

LINDA DEARDEN

Ph.D.

1983

ProQuest Number: U345206

All rights reserved

INFORMATION TO ALL USERS

The quality of this reproduction is dependent upon the quality of the copy submitted.

In the unlikely event that the author did not send a complete manuscript and there are missing pages, these will be noted. Also, if material had to be removed, a note will indicate the deletion.



ProQuest U345206

Published by ProQuest LLC(2015). Copyright of the Dissertation is held by the Author.

All rights reserved.

This work is protected against unauthorized copying under Title 17, United States Code.  
Microform Edition © ProQuest LLC.

ProQuest LLC  
789 East Eisenhower Parkway  
P.O. Box 1346  
Ann Arbor, MI 48106-1346



Thesis

1.6.1984

### ACKNOWLEDGEMENT

I wish to thank Dr. T. Harrison for his help and advice concerning culture of the BeWo cells; Mr. G. McTurk for use of Scanning Electron Microscope facilities; all members of the Anatomy Department for their help and encouragement; and Mrs. J. Butterworth for typing the manuscript efficiently and accurately at such short notice.

## CONTENTS

PAGE No.

### INTRODUCTION

<u>CHAPTER 1. Transmission of IgG across the human placenta.....</u>	1
--	---

### MATERIALS AND METHODS

<u>CHAPTER 2. Investigation of transport using human placental tissue...</u>	10
2-1 Examination of placenta .....	10
2-1.1. Term placenta .....	10
2-1.1.1. Light microscopic examination .....	10
2-1.1.2. Scanning electron microscopy (SEM) .....	10
2-1.1.3. Transmission electron microscopy (TEM) .....	11
2-1.2. First trimester placenta .....	11
2-1.2.1. Light microscopy .....	11
2-1.2.2. Transmission electron microscopy (TEM) .....	11
2-2. Perfusion of term placenta .....	12
2-2.1. Perfusion with tritiated IgG probe .....	14
2-2.1.1. Assessment of transport of tritiated IgG .....	17
2-2.1.2. Light microscopic autoradiography (LMARG) .....	17
2-2.1.3. Transmission electron microscopic autoradiography (TEM ARG) .....	18
2-2.2. Perfusion with colloidal gold-IgG (Au(18)-IgG) probe..	19
2-2.2.1 Assessment of transport of colloidal gold-IgG probe ..	19
2-2.2.2. Transmission electron microscopy (TEM) .....	19
2-2.2.3. Scanning transmission electron microscopy (STEM) .....	19
2-3. Preparation of the probes .....	19
2-3.1. Radiolabelling of human IgG .....	19
2-3.2. Ionic attachment of human IgG to colloidal gold particles .....	21
2-4. Validity of the probes .....	23
2-4.1. Tritiated IgG ( <sup>3</sup> H-IgG) .....	23

	<u>PAGE No.</u>
2-4.1.1. Immunoprecipitation (Ouchterlony) .....	23
2-4.1.2. Autoradiography of the Ouchterlony plate .....	23
2-4.1.3. Determination of the concentration of the <sup>3</sup> H-IgG probe .....	24
2-4.2. Colloidal gold-IgG (Au(18)-IgG) .....	24
2-4.2.1. Immunoprecipitation (Ouchterlony) .....	24
2-4.2.2. Tube immunoprecipitation .....	24
2-4.2.3. Negative staining of the gold-IgG complexes.....	25
2-4.2.4. Transmission electron microscopic immunoprecipitation .....	25
2-4.2.5. Sepharose-4B-protein A precipitation .....	26
2-4.2.6. Determination of the concentration of the colloidal gold probe .....	26
2-5. Tissue incubations .....	26
2-5.1. Term placenta incubated with <sup>3</sup> H-IgG .....	26
2-5.1.1. Light microscopic autoradiography (LM ARG) .....	27
2-5.2. Term placenta incubated with Au(18)-IgG .....	27
2-5.2.1. Transmission electron microscopy (TEM) .....	27
2-5.2.2. Scanning electron microscopy (SEM) .....	28
2-5.2.3. Replication of the surface of the tissue .....	28
2-5.3. First trimester placenta incubated with <sup>3</sup> H-IgG .....	28
2-5.3.1. Light microscopic autoradiography (LM ARG) .....	28
2-5.4. First trimester placenta incubated with Au(18)-IgG..	28
2-5.4.1. Transmission electron microscopy (TEM) .....	28
 <u>CHAPTER 3. Investigation of transport using placental tissue</u>	
<u>culture cells</u> .....	29
3-1. Examination of placental cells grown in tissue culture .....	29
3-1.1. Light microscopy .....	30
3-1.2. Transmission electron microscopy (TEM) .....	30
3-2. Incubation of cultured placental cells .....	30
3-2.1. Incubation with Au(18)-IgG .....	30

3-2.1.1.	Transmission electron microscopy (TEM) .....	31
3-3.	Examination of choriocarcinoma cells (BeWo) .....	31
3-3.1.	Light microscopy .....	33
3-3.2.	Transmission electron microscopy (TEM) .....	33
3-4.	BeWo cell incubations .....	33
3-4.1.	Short incubations with Au(18)-IgG .....	34
3-4.1.1.	Transmission electron microscopy (TEM) .....	34
3-4.2.	Long incubations with Au(18)-IgG .....	34
3-4.2.1.	Transmission electron microscopy (TEM) .....	35
3-4.3.	Incubation at 2 <sup>o</sup> C with Au(18)-IgG .....	35
3-4.3.1.	Transmission electron microscopy (TEM) .....	36

## RESULTS

<u>CHAPTER 4.</u>	<u>Investigation of transport using placental tissue .....</u>	<u>37</u>
4-1.	Normal placenta .....	37
4-1.1.	Term placenta .....	37
4-1.1.1.	Light microscopy .....	38
4-1.1.2.	Scanning electron microscopy (SEM) .....	38
4-1.1.3.	Transmission electron microscopy (TEM) .....	39
4-1.2.	First trimester placenta .....	40
4-1.2.1.	Light microscopy .....	40
4-1.2.2.	Transmission electron microscopy (TEM) .....	41
4-2.	Perfusion of normal term placenta .....	41
4-2.1.	Perfusion with <sup>3</sup> H-IgG .....	41
4-2.1.1.	Assessment of transport of <sup>3</sup> H-IgG .....	42
4-2.1.2.	Light microscopic autoradiography (LM ARG) .....	42
4-2.1.3.	Transmission electron microscopic autoradiography (TEM ARG) .....	45
4-2.2.	Perfusion with Au(18)-IgG .....	45
4-2.2.1.	Assessment of transport of Au(18)-IgG. ....	46
4-2.2.2.	Transmission electron microscopy (TEM) .....	46
4-2.2.3.	Scanning transmission electron microscopy (STEM) ....	46

4-3.	The Probes .....	47
4-3.1.	Tritiated IgG ( $^3\text{H}$ -IgG) .....	47
4-3.2.	Colloidal gold coupled to IgG (Au(18)-IgG) .....	47
4-4.	Validity of the probes .....	47
4-4.1.	$^3\text{H}$ -IgG .....	48
4-4.1.1.	Immunoprecipitation (Ouchterlony) .....	48
4-4.1.2.	Autoradiography of the Ouchterlony plate .....	48
4-4.1.3.	Determination of the concentration of the $^3\text{H}$ -IgG probe .....	48
4-4.2.	Au(18)-IgG .....	48
4-4.2.1.	Immunoprecipitation (Ouchterlony) .....	48
4-4.2.2.	Tube immunoprecipitation .....	49
4-4.2.3.	Negative staining of the colloidal gold-IgG complexes.	49
4-4.2.4.	Transmission electron microscopic immunoprecipitation.	49
4-4.2.5.	Sepharose-4B-protein A precipitation .....	49
4-4.2.6.	Determination of the concentration of the colloidal gold probe .....	50
4-5.	Tissue incubations. ....	50
4-5.1.	Term placenta incubated with $^3\text{H}$ -IgG .....	50
4-5.1.1.	Light microscopic autoradiography (LM ARG) .....	50
4-5.2.	Term placenta incubated with Au(18)-IgG .....	51
4-5.2.1.	Transmission electron microscopy (TEM) .....	51
4-5.2.2.	Surface examination of the tissue .....	52
4-5.3.	First trimester placenta incubated with $^3\text{H}$ -IgG .....	52
4-5.3.1.	Light microscopic autoradiography (LM ARG) .....	52
4-5.4.	First trimester placenta incubated with Au(18)-IgG....	53
4-5.4.1.	Transmission electron microscopy (TEM) .....	53

#### CHAPTER 5 Investigation of transport using placental tissue

<u>culture cells</u> .....	54
5-1. Placental tissue culture cells .....	54
5-1.1. Light microscopy .....	54
5-1.2. Transmission electron microscopy (TEM) .....	55
5-2. Incubation of placental tissue culture cells .....	56
5-2.1. Incubation with Au(18)-IgG .....	56

	<u>PAGE No.</u>
5-2.1.1. Transmission electron microscopy (TEM) .....	56
5-3. Choriocarcinoma cells (BeWo) .....	57
5-3.1. Light microscopy .....	57
5-3.2. Transmission electron microscopy (TEM) .....	57
5-4. BeWo cell incubations .....	60
5-4.1. Short incubations with Au(18)-IgG .....	60
5-4.1.1. Transmission electron microscopy (TEM) .....	60
5-4.2. Long incubations with Au(18)-IgG .....	61
5-4.2.1. Transmission electron microscopy (TEM) .....	61
5-4.3. Incubation at 2°C with Au(18)-IgG .....	63
5-4.3.1. Transmission electron microscopy (TEM) .....	63

## DISCUSSION

<u>CHAPTER 6. Discussion of methods and probes</u> .....	66
6-1 The methods .....	66
6-1.1. The perfusion system .....	66
6-1.2. The tissue incubations .....	68
6-1.3. Cell culture .....	68
6-1.3.1. Placental cells .....	68
6-1.3.2. Choriocarcinoma cells (BeWo) .....	69
6-2. The probes .....	70
6-2.1. Tritiated IgG ( <sup>3</sup> H-IgG) .....	70
6-2.2. Colloidal gold coupled to IgG(Au(18)-IgG) .....	71
<u>CHAPTER 7. Discussion of the results</u> .....	76
7-1. Light and electron microscopy of first trimester and term placenta .....	76
7-1.1. Light microscopy .....	76
7-1.2. Scanning electron microscopy (SEM) .....	77
7-1.3. Transmission electron microscopy (TEM) .....	77
7-2. The perfusion experiments .....	83
7-2.1. Perfusion with <sup>3</sup> H-IgG .....	83
7-2.2. Perfusion with Au(18)-IgG .....	84

	<u>PAGE No.</u>
7-3. The tissue incubations .....	85
7-3.1. Term placenta incubations .....	85
7-3.1.1. Term placenta incubated with <sup>3</sup> H-IgG .....	85
7-3.1.2. Term placenta incubated with Au(18)-IgG .....	85
7-3.2. First trimester placenta incubations .....	85
7-3.2.1. First trimester placenta incubated with <sup>3</sup> H-IgG .....	86
7-3.2.2. First trimester placenta incubated with Au(18)-IgG...	86
7-4. Tissue culture .....	87
7-4.1. Placental cells .....	87
7-4.1.1. Placental cells incubated with Au(18)-IgG .....	88
7-4.2. BeWo cells .....	89
7-4.2.1. BeWo cells incubated with Au(18)-IgG at 37°C .....	92
7-4.2.2. BeWo cells incubated with Au(18)-IgG at 2°C .....	94
<u>CHAPTER 8. General discussion of results</u> .....	97
 <u>CONCLUSION</u>	
<u>CHAPTER 9. Conclusion</u> .....	105
<u>APPENDICES</u> .....	108
<u>BIBLIOGRAPHY</u> .....	157
<u>FIGURES</u> .....	175

## INTRODUCTION

## CHAPTER 1 : The transmission of IgG across the human placenta

The human placenta is a versatile organ carrying out a diversity of functions during its relatively short life span of about 280 days.

It is involved in the transport of water and nutrients to the fetus, removal of waste products and exchange of gases. It also actively secretes both steroid-(Ryan, 1959; Zander, 1964) and peptide-containing hormones (Jones, et al., 1943; Midgely and Pierce, 1962). Another important role of the placenta is the selective transmission of antibodies or immunoglobulins to the fetus. These substances are essential, since they confer immunity or resistance to disease on the fetus thereby giving it protection during the first few months after birth until it begins synthesizing its own immunoglobulins.

Transmission of immunoglobulins to the fetus is an active process (Brambell, 1970). Antibodies to influenza virus (Mantyljarvi et al., 1970), small pox (Kempe and Benenson, 1953), diphtheria antitoxin (Neill et al., 1932; Barr et al., 1949; Osborn et al., 1952), and tetanus antitoxin (Ten Broeck and Bauer, 1923; Chandra, 1976) have all been detected in fetal serum. Evidence that these antibodies are maternal in origin comes from the finding that the baby of an agammaglobulinaemic mother was also agammaglobulinaemic at birth and during the neonatal period. However by the second month the baby was synthesizing its own gammaglobulins since it had not inherited its mother's genetic defect (Good and Zak, 1956). Active transport of immunoglobulins is indicated by the fact that in countries which have a high endemic rate of infectious diseases, infants have an elevated immunoglobulin level at birth (Good and Zak, 1956). Active transport of immunoglobulins has also been demonstrated in rhesus monkeys. Bangham et al. (1958) showed that transfer of immunoglobulins exceeded that of albumin by 15-20 times, yet the immunoglobulin molecule is twice the molecular weight of albumin.

Immunoglobulins can be divided into five major structural types- Immunoglobulin G (IgG), IgA, IgM, IgD and IgE. IgA, IgD, IgM and IgE are found only in trace amounts in fetal cord serum and these small amounts can be attributed to fetal synthesis (Loke, 1978). However, IgG levels in cord serum are often higher than the concentration found in the maternal serum (Kohler and Farr, 1966; Virella et al., 1972) which indicates that IgG is actively transported across the placenta (Gitlin et al., 1964; Kohler and Farr, 1966; Allansmith, 1968).

Immunoglobulin G has been shown to be composed of four peptide chains, two light and two heavy, linked by interchain disulphide bridges. Subsequent investigation has shown that IgG can be divided into four subclasses, IgG 1, IgG 2, IgG 3 and IgG 4 (Grey and Kungel, 1964; Terry and Fahey, 1964). These can be distinguished by structural differences located on the heavy peptide chains.

All four subclasses are transported to the fetus during gestation although some studies indicate that IgG 2 and IgG 4 are transported less efficiently (Wang et al., 1970; Hay et al., 1971; Virella et al., 1972).

Animal studies have shown that immunoglobulin G transmission occurs in a variety of ways (Fig 1). In the rabbit, it is accomplished via the yolk sac (Brambell, 1966; 1970). In rats, mice, cats and dogs the main transfer appears to take place after birth via the milk. In the primates it is accomplished via the placenta. The initial uptake of IgG appears to be by concentrative receptor mediated endocytosis, mediated by micropinocytic vesicles, but very little is known about the ultrastructural route taken by immunoglobulin G during transmission. A number of models for the transport process have been proposed. Brambell (1966) put forward a simple model based upon results from animal studies. He postulated that proteins were selectively absorbed to specific receptors on the walls of pinocytic vesicles. These vesicles then closed off and were transported across the cell. He suggested that attachment of the protein to the receptor within the vesicle

protected it from degradation by the lysosomal system. This model proposed the macropinocytic vesicles as the vehicles for protein transport. If this were the case then one would expect to find enzymes associated with these vesicles in the areas where the vesicles release their contents i.e. the basement membrane. Results from a study of the distribution of Cathepsin D, a common proteolytic enzyme associated with macropinocytic vesicles showed it was not present either in or below the basement membrane (Wild, 1976). On the basis of this evidence a different model for the transport process was proposed by Wild (1976). He suggested that selection of specific proteins occurred at the cell surface and involved binding of proteins to receptors over certain parts of the cell surface. These areas then invaginated forming coated micro-pinocytic vesicles, which transported the protein to the basal area of the cell. Wild proposed that it was the clathrin coating on the outer surface of these vesicles which protected them from fusion with, and subsequent degradation by, the lysosomal system. Any protein not bound by the receptors would be pinocytosed into macropinocytic vesicles which could then fuse with lysosomes, resulting in degradation of their contents.

An alternative model for transport was put forward by Hemmings and Williams (1976) based upon experimental results obtained using ferritin markers and  $^{125}\text{I}$  labelled IgG. They did not find any pinocytosed protein-probe-conjugate, attached to the periphery of vesicles, instead they found the markers lying free in the cytoplasm. They suggested a transport mechanism in which proteins diffused freely across the cell cytoplasm and selection occurred upon exit of the protein rather than on uptake.

It is difficult to extrapolate results from animal studies to the situation in man. Some studies have been made on human subjects (Dancis et al., 1961) but the risk to both mother and child prevents extensive experimentation. It is therefore more

acceptable to limit investigations to post delivery placentae.

Transmission of immunoglobulins in man is accomplished mainly via the placenta, although a small amount is thought to be transported in the colostrum (Ogra et al., 1977).

The discovery of the presence of immunoglobulins in amniotic fluid (Steigman and Lipton 1958; Wild, 1960; Usategui-Gomez and Stearns, 1969) led to the suggestion that transmission was accomplished by amniotic fluid swallowing and absorption via the intestine (Fig 2) as in many animal species (Brambell et al., 1954). Clinical observations by Wasz-Höckert et al., (1956) in infants with oesophageal atresia, a condition which prevents the fetus from swallowing the amniotic fluid showed that levels of diphtheria toxin in the infants was equivalent to that in their mothers' serum. This evidence suggests that transmission of immunoglobulins via the amniotic cavity is unlikely.

Investigation of transplacental transport has been undertaken using both whole IgG molecules and fragments produced by enzyme digestion. Digestion of IgG using papain (Porter, 1960) produces three fragments. Two of these are identical and are the univalent antibody fragments or Fab molecules (Fragment antigen binding). The third fragment does not combine with antigen and is the Fc portion (Fragment crystallizable).

Receptors for the Fc part of the IgG molecule have been demonstrated on the surface of the human placenta (Matre et al., 1975; Jenkinson et al., 1976; Matre, 1977) and a single population of membrane receptors which bind all four classes of IgG have been reported (Balfour and Jones, 1976). McNabb et al., (1976) showed that the different classes of IgG have different affinities. IgG 1 and IgG 3 bound with equal affinity, IgG 4 showed less affinity than IgG 1 and 3, and IgG 2 had the least affinity. These findings are in accord with the transport studies in which IgG 2 and 4 were found to be transported less efficiently than the other classes of IgG. (Wang et al., 1970; Hay et al., 1971; Virella et al., 1972).

Binding of IgG to receptors appears to be dependent on pH. Jones and Waldmann (1972) found that rat intestinal cells bound IgG selectively at low pH but lost this ability when the pH was raised to 7.4 or more. Rodewald (1976) also reported enhanced IgG binding at low pH. He proposed that pH changes could be an important factor in the transport mechanism; binding and uptake occurring at low pH and release of the ligand occurring where high pH was found, such as in the fluid permeating the basement membrane.

A similar observation has been made using human placental membranes (Balfour and Jones, 1976). A greater amount of labelled IgG was found to bind at pH 6.6 than at 7.8, however it is not known if high pH conditions exist on the fetal side of the basement membrane in the human placenta.

The receptor for the IgG molecule has been partially characterised by Niezgodka et al., (1980). They have isolated a water soluble glycoprotein fraction from human placental membrane using lithium diiodosalicylate. This fraction retains the ability to bind labelled IgG.

Some evidence suggests that binding of IgG by human placental membranes may be mediated by the Fc region of the immunoglobulin molecule. Balfour and Jones (1976) found that radio-iodinated Fc portions of IgG bound to human placental membranes to a much greater extent than Fab fragments. Similar results were obtained by Gitlin et al. (1964a) who injected <sup>125</sup>I labelled fragments of IgG into pregnant women and found that the concentration of Fc fragments in the foetal blood after delivery was 4 - 10 times that of the Fab fragments. However in further experiments (Gitlin et al., 1964b) in which relative rates of catabolism were taken into consideration, they found that both Fc and Fab fragments were both transported equally readily. Further evidence also suggests that there may be receptor sites for more than one area of the immunoglobulin molecule.

Gitlin and Gitlin (1976) have shown binding of Bence-Jones proteins to human placental membranes. These proteins are immunoglobulin light chains and so have no Fc region. Nevertheless the presence of Fc receptors on human placental membranes suggests that the Fc portion of the molecule has some function in binding or uptake of IgG. Fc receptors have also been demonstrated on Hofbauer cells (Moskalewski et al., 1975), and on endothelial cells (Matre, 1977). It has been suggested that the receptors in these areas may function to prevent immune complexes (formed by the reaction of maternal antibodies against incompatible fetal antigens) from entering the fetal circulation. Thus the placenta is given additional protection from maternal immunological attack.

The models put forward for transplacental protein transport suggest that coated vesicles play an important role particularly in receptor mediated uptake. Coated vesicles are known to occur in almost all cells and it has been shown by one dimensional peptide mapping (Pearse 1976;1978) that the major coated vesicles protein-clathrin-is highly conserved between several species. Often proteins which exhibit a high degree of conservation have an essential role in cell functioning eg. insulin and its role in blood sugar control.

It seems quite probable that coated vesicles have a vital role in protein uptake. Coated vesicles were first described as mediators of protein transport by Roth and Porter (1964) in the transmission of yolk protein in the mosquito oocyte. There are now a great many systems in which evidence indicates that coated vesicles are involved in protein uptake. For example  $\alpha_2$  macroglobulin (Maxfield, et al., 1978), ferritin (King and Enders, 1970), transferrin (Bliel and Bretscher, 1982), asialoglycoprotein (Wall et al., 1980) low density lipoprotein (Anderson et al., 1978, 1977), insulin (Pilch et al., 1983), Semliki Forest Virus (Marsh and Helenius, 1981) are all internalised into cells after first becoming associated with coated pits.

In some systems coated vesicles mediate the whole of transepithelial protein transport. For example in neonatal sucking rat jejunum (Rodewald, 1980) rat yolk sac (Huxham and Beck, 1981), rabbit yolk sac, (Moxon et al, 1976) and guinea pig placenta (King, 1977) coated vesicles have been found in apical, midcytoplasmic and basolateral regions. They have also been found associated with the Golgi where they are thought to play a part in the transport of secretory proteins.

In other studies the contents of the coated pits or vesicles appears to be transferred to large membrane bounded structures about 600 nm in diameter. These have been termed the receptosome by Willingham and Pastan (1980), and are very similar in morphology to the multivesicular bodies described by Martin and Spicer (1973). However they do not appear to contain lysosomal enzymes (Willingham and Pastan, 1981). The structure of coated pits and vesicles is quite well documented (see review: Uckleford, 1982). Placental coated vesicles are similar in structure to those isolated from other sources. They have a thickened glycocalyx on their luminal surface and a polygonal lattice of the protein, clathrin, on their cytoplasmic surface. The size of coated vesicles ranges from approximately 60nm to 200nm. Their size is dependent upon the ratio of the number of polygons in the lattice. These are either five or six-sided (Uckleford et al., 1977) but temporarily heptagons may occur during curvature induction (Heuser, 1980). Clathrin is the major protein of coated vesicles and has a molecular weight of 180,000. Smaller amounts of other proteins with molecular weights of 100,000, 45,000 and 32,000 have also been isolated (Uckleford and Whyte, 1977; Pearse, 1978). In other systems these molecules have been shown to be associated with trimers of clathrin to form an 8.4S lattice subunit. The trimeric subunit is known as the triskelion (Ungewickell and Branton, 1981). Each triskelion is apparently associated with two different types of light chain structures.

Since coated vesicles are responsible for the transport of so many different molecules (eg transferrin, ferritin,  $\alpha_2$  macroglobulin) it is perhaps not surprising that they sometimes contain more than one type of molecule. Huxham (1982) carried out a double labelling study in rat yolk sac, using IgG and ferritin conjugated to different sized particles of colloidal gold. He found both sizes of colloidal gold-probe located in the same coated vesicle.

In the human placenta there is evidence that IgG is taken up into coated vesicles. An immunoperoxidase ultrastructural study on human placenta by Lin (1980) showed localisation of IgG in small micropinocytic vesicles, similar in size to coated vesicles. Ockelford and Clint (1980) reported the presence of radioactivity in a coated vesicle preparation isolated from homogenised placental tissue incubated with labelled IgG. Pearse (1982) using an immunoblotting method demonstrated the presence of IgG in very pure preparations of coated vesicles isolated from human placenta. Booth and Wilson (1981) were unable to identify IgG in their isolates but these were mainly coated vesicles lattices.

The above data indicates uptake of IgG into coated pits at the placental maternal facing surface membrane but there is very little known about the ultrastructural route which the IgG takes to reach the basement membrane. This thesis aims to elucidate this route. Several types of experimental system were employed and two types of probe used in these systems. The probes were tritiated human IgG and human IgG covalently linked to 18 nm particles of colloidal gold.

The experimental systems were:-

1. Perfusion of the post-delivery human placenta with the IgG probes using an isolated cotyledon method.
2. Small groups of isolated chorionic villi incubated in defined media with IgG probes.

3. Tissue cultured placental cells incubated with the probes.
4. Tissue cultured placental choriocarcinoma cells incubated with the probes. In each case the tissue was subsequently examined using light and electron microscopy.

MATERIALS AND METHODS

## CHAPTER 2: Investigation of immunoglobulin G transport using human placental tissue

### 2-1 EXAMINATION OF THE HUMAN PLACENTA

#### 2-1.1. Term placenta

Term placentae from uncomplicated pregnancies were obtained from Leicester Royal Infirmary, by either elective Caesarian section or routine delivery. Small pieces were either fixed at the hospital or the whole placenta was transported back to the laboratory on ice for subsequent examination.

Human term placentae were examined using:- light microscopy, transmission electron microscopy and scanning electron microscopy.

##### 2-1.1.1. Light microscopic examination

A small piece of placenta was excised from a freshly delivered term placenta. It was teased out with fine forceps, mounted on a slide, covered with a coverslip and examined using Nomarski interference microscopy (Allen, et al., 1969), using a Zeiss photomicroscope.

Other small pieces of tissue were fixed with 3% glutaraldehyde in 0.1M phosphate buffer overnight and processed and embedded using the processing schedule shown in Appendix I. Thick (0.5 $\mu$ m) sections were cut using a Reichert ultramicrotome and mounted in a drop of water on a glass slide. The sections were dried down onto the slide using a hot plate at 65<sup>o</sup>C and stained with 1% toluidine blue. The sections were then mounted in DPX mountant, covered with a coverslip and examined with a Zeiss photomicroscope using bright field illumination.

##### 2-1.1.2. Scanning electron microscopy (SEM)

Small pieces of tissue were fixed overnight in 3% glutaraldehyde in 0.1M phosphate buffer and processed according to the processing schedule shown in Appendix II. They were then critical point dried (Anderson, 1950) and coated with approximately 25nm of gold in a Polaron Sputter coating unit.

The coated tissue was then examined using an ISI-60 scanning electron microscope.

#### 2-1.1.3 Transmission electron microscopic examination (TEM)

Thin sections (silver to gold in interference colour) were cut using resin embedded tissue prepared as described in Appendix I. The sections were collected on 200 mesh copper electron microscope grids (Agar aids) and stained with 10% methanolic uranyl acetate for 10 minutes and lead citrate (Reynolds, 1963) for 2 minutes in an atmosphere of sodium hydroxide. They were then examined using a Jeol 100CX transmission electron microscope operating at 80KV.

#### 2-1.2. First trimester placenta.

First trimester placenta from therapeutic terminations were obtained from Leicester Royal Infirmary. They were either fixed immediately or transported back to the laboratory on ice for subsequent examination. First trimester tissue was examined using light microscopy and transmission electron microscopy.

##### 2-1.2.1. Light microscopic examination.

First trimester tissue was prepared in the same way as the term placenta in Section 2-1.1.1. and examined using a Zeiss photomicroscope.

##### 2-1.2.2. Transmission electron microscopic examination (TEM)

First trimester tissue was prepared in the same way as the term placenta in 2-1.1.3 according to the processing schedule given in Appendix I.

## 2-2. PERFUSION OF TERM HUMAN PLACENTA

Perfusion of the human placenta was considered to be a useful method for examining the active transport of IgG across the placenta. By establishing an artificial circulation, which mimicked the in vivo situation it is possible to examine the transport route taken by an IgG probe across the placenta.

Since perfusion of the whole placenta is rarely possible because of damage to the tissue at parturition a single cotyledon was used for the experiments. The nature of the blood supply of the placenta is such that each cotyledon has its own circulatory system. It is therefore possible to examine transport across the human placenta using a single isolated cotyledon. The method used was similar to the isolated perfused cotyledon system used by Schneider et al., (1972), and Penfold et al., (1981).

### (i) The perfusion apparatus

The perfusion apparatus (Fig 3 ) consisted of a glass dish in which the placenta was contained and two "circuits". The fetal "circuit" was a closed "circuit", designed to mimick the arterial and venous blood systems of the placenta derived from the umbilical cord of the fetus. The maternal "circuit" was an open "circuit" designed to mimick the maternal blood supply to the placenta via the uterine spiral arterioles.

### (ii) The fetal "circuit" (Fig 4 A-I)

This consisted of a conical flask (the fetal reservoir), containing the perfusate buffer. This perfusate was composed of Hartman's sodium lactate buffer (Travenol), which had the following additives:- 10mM glucose (BDH); 4% dextran 70,000m.wt. (Sigma) and 60 µg/ml heparin (BDH). This reservoir was gassed with a mixture of 40% oxygen, 5% carbon dioxide, and 55% nitrogen. The perfusate was warmed by placing the reservoir in a water bath at 37°C. From the fetal reservoir, nylon tubing (OD=1.5mm, ID=1.0mm) connected a heat exchanger (Travenol miniprime), to maintain the temperature; a flow meter, to measure the flow rate of the buffer solution;

a mercury manometer (replaced by a more accurate strain gauge transducer for later experiments - see Appendix III for calibration method), to measure the pressure in the system; and an Ivac 531 infusion pump (later replaced by an LKB Varioperpex II peristaltic pump), to pump the buffer through the tubing systems. From the pump further tubing led to the glass dish in which the placenta was contained. The end of this tubing was modified to enable a nylon microcannula (Portex ID = 0.6mm, OD = 1.34mm) to be fitted.

A similar microcannula was connected to a second flow meter by nylon tubing and was directed back to the fetal reservoir via more tubing. Three-way sampling taps were introduced into the system just after the microcannulae (Fig 4) to allow samples of buffer to be taken during an experiment without disrupting the apparatus.

#### (iii) The maternal "circuit" (Fig 4 J-P)

This again consisted of a conical flask containing the perfusate (the maternal reservoir), sited in a water bath at 37°C. The perfusate consisted of Hartman's sodium lactate buffer and the same additives as the fetal reservoir. This solution was gassed with a mixture of 95% oxygen and 5% carbon dioxide. From the reservoir nylon tubing connected a heat exchanger; a peristaltic pump (Infusomat); a flow meter; and a mercury manometer, (later replaced by a strain gauge transducer). The tubing was connected to a nylon intravenous cannula (Portex, ID=1.7mm, OD=3.0mm) to which a glass microcannula was attached terminally (see section below).

#### (iv) Preparation of the microcannulae

The nylon microcannulae (Fig 5) used in the fetal part of the system were prepared before the experiment by placing a small drop of Araldite close to the tip of the microcannula and allowing this to dry to form a lip. This enabled the microcannula

to be sutured securely into place behind the Araldite, and thus prevent it from pulling out of the blood vessel during an experiment.

The microcannula for the maternal side of the apparatus (Fig 5) was made from a 100  $\mu$ l glass microcapillary tube (Bilbate), which had been drawn out to a fine point over a flame. The drawn end was melted slightly and glass-blown to produce a lip around the tip. This lip prevented the microcannula from pulling out of the tissue during the experiment. This glass microcannula was Araldited into the end of a nylon intravenous cannula taking care not to obscure the lumen and allowed to dry. This was then connected to the "maternal circuit".

#### (v) The placenta (Fig 4 Q-T)

The placenta was contained in a glass dish in a water bath maintained at 37°C. Above the dish was a reservoir containing Hartman's sodium lactate buffer at 37°C, which was used to keep the placenta moist and warm throughout the experiment by allowing the buffer to drip down on to it.

#### (vi) Selection of placentae suitable for perfusion

Both the maternal and fetal sides of the placenta were examined and only suitable placentae were selected. It was decided at the outset of the experiments that any placentae which were badly damaged, calcified, lardaceous, haematous, meconium stained, or had a battledore or velamentous insertion of the umbilical cord would be discarded. The ideal area for perfusion was a small cotyledon on the edge of the placental disc supplied by a distinct artery and vein.

#### 2-2.1 Perfusion of term placenta with tritiated IgG.

In order to mimick the maternal supply of IgG, tritiated human IgG was added to the buffer (with its additives) in the maternal reservoir. The method used to prepare the tritiated IgG is given in section 2-3.1.

A tritiated probe was used so that it would be possible to monitor transport of the probe by taking samples from the fetal circuit via the sampling taps in the perfusion system and assessing the presence of radioactivity by scintillation counting. This particular radioactive probe was also used so that the IgG within the tissue could be localised by autoradiography after the perfusion experiment.

Human placentae, were obtained after routine deliveries or elective Caesarian section from Leicester Royal Infirmary. A small sample of tissue was taken from an area not required for perfusion, and fixed in 3% glutaraldehyde in 0.1M phosphate buffer (pH 7.4). Care was taken to ensure this tissue was taken from an area similar to that which would be perfused so that the tissue could be used as a control for ultrastructural assessment of integrity of the experimental tissue. The placenta was then transported back to the laboratory on ice.

The placenta was placed in the glass container in the water bath at 37°C, and washed with warm buffer from the reservoir above, to remove any excess blood. The maternal surface of the placenta was then inspected to find a cotyledon suitable for perfusion. Usually this was a small intact cotyledon on the edge of the placental disc supplied by a single distinct fetal artery and vein.

The placenta was then placed with the fetal side uppermost. The chorionic membrane was peeled back, exposing the blood vessels clearly. The artery and vein supplying the chosen cotyledon were cut, and a nylon microcannula (as described in the section above) introduced into the artery and sutured into place. This microcannula was connected to the perfusion apparatus on the fetal side. Hartman's buffer, (containing the additives described in the section above) was pumped from the

fetal reservoir into the artery at a rate of 0.7ml/min, to wash the blood from the selected cotyledon. After a few minutes, all of the blood was removed, and the clear buffer solution could be seen flowing from the cut vein. The vein was then cannulated and connected to the perfusion system, returning the buffer to the fetal reservoir. Once cannulation was completed the closed fetal circuit of the perfusion system was established.

The placenta was then carefully turned over so that the maternal side was uppermost, taking care not to disturb the cannulae. The cotyledon being perfused could clearly be identified as it had a pale bloodless appearance (Fig 6). The glass microcannula, from the maternal side of the perfusion system, was gently introduced into the cotyledon through the basal plate (Fig 7). Hartman's buffer containing the additives listed above and the  $^3\text{H}$ -IgG probe was pumped from the maternal reservoir into the tissue at a rate of 0.7ml/min.

As soon as the maternal circuit was established a stop-clock was started and samples were taken from the venous return (via the three-way tap) of the fetal circulation every minute for 10 minutes then every 5 minutes until the end of the experiment. (Approximately 0.5ml was collected for each sample). A sample of fluid from the glass dish was taken at the end of the experiment to determine if there had been any leakage of the probe.

The perfusions were usually established 30-40 minutes after delivery of the placenta and the duration of the experiment was between 30-60 minutes. Throughout the course of the experiment the pressure in the system was monitored via the mercury manometers (or the pressure transducers) and was kept at approximately the same level in both "circuits", but was not permitted to rise above 60mm Hg. (higher pressure would cause rupture of the small capillaries in the tissue).

The flow rate of buffer through the arterial and venous vessels was also monitored. Wide fluctuations of the venous return flow indicated ruptured vessels (Elphick, 1981; personal communication). Details of the flow rates, pressure and general comments concerning the perfusion were noted for each placenta (Appendix IV).

At the end of the experiment the tissue located close to the tip of the maternal microcannula was excised and fixed in 3% glutaraldehyde, in 0.1M phosphate buffer (pH 7.4). The samples taken from the fetal venous during the experiment were assessed (see section 2-2.1.1 below) and if transport of the probe was demonstrated the control and experimental tissue were processed for transmission electron microscopy as given in Appendix I.

#### 2-2.1.1. Assessment of transport of the $^3\text{H}$ -IgG probe.

Aliquots (50  $\mu\text{l}$ ) of each of the samples taken from the fetal venous return were added to 5 ml of scintillation cocktail, and counted in a Packard Tricarb scintillation counter. The amount of radioactivity in each sample was expressed as disintegrations per minute and plotted on a graph against time.

#### 2-2.1.2. Autoradiography of the perfused tissue.

Thick sections (0.5-1.0  $\mu\text{m}$ ) were cut of control and experimental tissue, using a Reichert ultracut microtome and mounted on clean glass slides in a drop of distilled water and dried on a hot plate at 60°C. When cool to room temperature the slides were dipped in Ilford L4 Emulsion (Ilford), left to gel on a cold surface for 3-4 minutes, and then dried by placing approximately 20 cm away from a cool air source (an electric fan with no heater).

When dry they were packed into light-proof boxes with silica gel, sealed with tape, wrapped in a black plastic bag, sealed and stored at 4°C for 14 days. After this period of exposure the slides were developed in D19 developer (Kodak) for 5 minutes, washed briefly in distilled water, then fixed for 5

minutes in Kodaiix (Kodak), washed for 15 minutes in distilled water and dried on a hot plate. They were stained with a 1% solution of toluidine blue in 1% borax solution and examined light microscopically with a Zeiss Photomicroscope.

### 2-2.1.3. Transmission electron microscopic autoradiography (TEM ARG)

Thick sections (0.5  $\mu\text{m}$ ) were cut of both control and experimental tissue, and picked up on formvar/carbon coated gilded 200 mesh grids (Agar aids). Half of each group were stained with Reynolds lead citrate (Reynolds, 1963) for half an hour; the rest were left unstained. The time of staining was longer than normal since thick sections were being examined (Favard and Carasso, 1973).

The sections were processed for autoradiography using the method of Williams (1977) as follows: first they were coated with a 10nm layer of carbon in a Polaron Sputter Coater. The grids were then either attached to glass slides with a small piece of double sided Scotch tape or were placed on stubs (made from sections of glass rod) and held in place with a small drop of nail varnish. Those grids attached to the slides were dipped in Ilford L4 Emulsion, while those mounted on the stubs had the emulsion applied to them by means of a wire loop as described by Caro and van Tubergen (1962). The slides were dried in the same way as the autoradiographs for light microscopy (section 2-2.1.2). The grids on the stubs were allowed to air dry. All the specimens were then packed into light-tight boxes with silica gel and sealed with tape. They were then wrapped in black plastic and left to expose for 14 days at 4°C. After exposure they were developed in D19 developer (Kodak) for 3 minutes, washed briefly in distilled water and fixed for 3 minutes in Kodaiix (Kodak). They were then washed extensively in distilled water, and left to air dry. They were examined in a Jeol 100CX Transmission Electron Microscope (TEM).

### 2-2.2 Perfusion of term placenta with colloidal gold coupled to IgG.

The notation Au(18)-IgG will be used to refer to colloidal gold particles of size 18nm diameter coupled to IgG. The same perfusion procedure was followed as for the  $^3\text{H}$ -IgG probe except that the colloidal gold probe replaced the tritiated probe in the maternal reservoir. At the end of the perfusion it was often possible to identify the piece of tissue to be fixed as it was coloured pink by the gold probe.

#### 2-2.2.1. Assessment of transport of the Au(18)-IgG probe.

A 10 $\mu$ l aliquot of each of the samples taken from the fetal venous return of the perfusion apparatus was dried down on to a formvar/carbon coated 200 mesh electron microscope grid and examined in a Jeol 100CX TEM, for the presence of colloidal gold particles.

#### 2-2.2.2. Electron microscopic examination of the perfused tissue.

The tissue was processed for transmission electron microscopy as given in Appendix I. Thin sections (gold to silver interference colour) were cut using a Reichert ultracut microtome and picked up on 200 mesh copper grids. They were stained with 10% methanolic uranyl acetate for 10 minutes and Reynolds lead citrate for 4 minutes and examined in a Jeol 100CX TEM.

#### 2-2.2.3. Scanning transmission electron microscopy (STEM).

Thick sections (0.5-1.0 $\mu$ m) were cut and picked up as before on 200 mesh copper grids, stained with uranyl acetate for 60 minutes and lead citrate for 30 minutes and examined using STEM equipment on a Jeol 100CX TEM.

### 2-3. PREPARATION OF THE PROBES.

#### 2-3.1. Radiolabelling human IgG with N-succinimidyl propionate.

##### (i) Preparation of the protein

Human IgG (1mg) obtained from Miles was dissolved in 20 $\mu$ l of 0.1M borate buffer at pH 8.5 and kept on ice (0°C) until required. The borate buffer consisted of: boric acid (BDH), 6.18g/l; sodium tetraborate (Sigma), 9.54g/l; sodium chloride (BDH), 4.38g/l. The pH was adjusted with 1M HCl (BDH).

(ii) Radiolabelling of the protein

250 $\mu$ l of N-succinimidyl-2-(<sup>3</sup>H)-propionate (The Radiochemical Centre, Amersham) was dried down into the point of the conical base section of a glass bench centrifuge tube, under a gentle stream of nitrogen until all trace of the toluene solvent was removed. Then 20 $\mu$ l of IgG in borate buffer was added to the dry radiochemical in the tube and the two substances allowed to react in an ice bucket at 0°C for 15 minutes. The tube was shaken at intervals. The reaction was stopped by adding 0.5ml of 0.2M glycine (Sigma) in 0.1M borate buffer at pH 8.5 and left for 5 minutes at 0°C. (The glycine removes any radiochemical not bound to the IgG).

(iii) Separation of the <sup>3</sup>H-IgG and the <sup>3</sup>H-glycine.

A K9 chromatography column (LKB) was used to separate the mixture of tritiated IgG and glycine. Sephadex G50 fine (Sigma) weighing 1g was left to swell overnight in 20ml of 0.05M phosphate buffer at pH 7.5 with 0.25% gelatin added. After swelling, the column was packed with the Sephadex, and the radioactive sample was loaded carefully onto the top of the column. The sample was pumped gently through the column, using a Varioperpex 2120 peristaltic pump (LKB). The output from an ultra-violet absorption monitor (LKB 2138 Uvicord S) operated at wavelength 280nm was connected to an LKB 2210, 2-channel pen recorder. Fractions were collected using an LKB fraction collector (0.9ml/tube). Two peaks were observed on the chart recorder, the first peak corresponding to <sup>3</sup>H-IgG, the second to the glycine-radiochemical complex.

#### (iv) Radioactivity of the fractions.

To assess which tubes the radiolabelled IgG was localised in, 20ul samples of each of the fractions were added to 5ml of scintillation cocktail (Fisons) and counted in a Packard Tricarb scintillation counter. Increased radioactivity was found in two regions, corresponding to the two peaks on the chart recorder (IgG and glycine). Since the radioactivity for the IgG peak was spread over three or four tubes, these fractions were pooled and stored at 4°C until required.

#### 2-3.2. Ionic attachment of IgG to 18nm colloidal gold particles.

Colloidal gold is a useful marker for both scanning (Horisberger et al., 1975) and transmission electron microscopy (Faulk and Taylor, 1971). It is highly electron dense and uniform in shape (Fig 8) and because of these two characteristics it is very easy to identify in tissue sections. It is also non-toxic, easily prepared, stable and it is possible to make a wide range of sizes, from approximately 2nm in diameter up to 150nm. The 18nm diameter colloidal gold particles were prepared by reducing chloroauric acid ( $\text{HAuCl}_4$ ) with sodium citrate, using the method of Horisberger and Rosset (1977).

#### (i) Preparation of the protein.

Visking tubing was prepared by soaking overnight in distilled water. 2mg of human IgG (Miles) was dissolved in 1ml of 0.005M sodium chloride (BDH) and placed in the Visking tubing. The end was knotted and the protein dialysed extensively for 2 to 3 days against 0.005M sodium chloride. The IgG solution was then recovered and centrifuged at 3,000 rpm in a Gallenkamp laboratory centrifuge for 10 minutes ready for use.

(ii) Preparation of the colloid.

All glassware was soaked in either Decon 90 (Decon Laboratories Ltd) or chromic acid and rinsed thoroughly several times in running water, distilled water and finally in filtered distilled water. All solutions used to prepare the colloid were either filtered or centrifuged before use, since any slight contamination would cause flocculation of the colloid.

200ml of filtered distilled water and 5ml of 1% sodium citrate (BDH) was heated until boiling. 0.5ml of 4%  $\text{HAuCl}_4$  (chloroauric acid, BDH) was added to the boiling liquid and refluxed until no further colour change was observed. Initially the solution becomes purple in colour, and gradually changes to a red wine colour. The solution was left to cool.

(iii) Attachment of the protein to the colloid.

The pH of the colloid was tested by removing a small sample of the solution (about 1ml) into a vessel containing a few drops of 1% polyethylene glycol (PEG, m.wt.20,000). This prevents the pH electrode becoming coated with gold. The pH of the colloid was adjusted to between pH5.9 and pH7.0 with 0.2M KCl. (BDH). (The pH of the colloid is usually between pH4.0-5.0. In order for optimum attachment of the protein to the colloid to occur the pH must be close to the pI of the protein. The method for determining the optimum pH is given in Appendix V).

An aliquot (150 $\mu$ l) of the dialysed, centrifuged IgG solution was added to the colloid and swirled for 2 minutes. (The amount of protein required for attachment was determined as described in Appendix VI.) The solution was then stabilised by the addition of 6ml of 1% PEG, and then neutralised to pH 7.0 with 0.2M KCl.

#### (iv) Removal of unlabelled colloid.

The labelled colloid was concentrated by centrifugation in a Sorvall OTD-65 ultracentrifuge, at 28,000g (17,000 rpm) for 30 minutes at 4°C. (Any unlabelled colloid appears in supernatant.) The supernatant was discarded and the pellet resuspended in either Hartman's sodium lactate buffer or Hank's buffer (Flow), containing 0.6mg/ml PEG. The centrifugation process was then repeated, the supernatant removed and the pellet again resuspended in the buffer. It was then stored at 4°C until required.

### 2-4. VALIDITY OF THE PROBES

#### 2-4.1. Tritiated IgG (<sup>3</sup>H-IgG).

##### 2-4.1.1. Immunoprecipitation (Ouchterlony).

A solution of 1% agarose (Sigma) in phosphate buffered saline was boiled until the agarose had dissolved and then quickly poured onto a level clean glass plate and left to cool. When the agarose had set, wells were aspirated from the gel using a cutter and template kit (Miles). The well diameter was 4.0mm and centre to centre well distance was 7.0mm.

The centre well was loaded with 10µl of the radioactive probe and the surrounding six wells with 10µl of serially diluted anti-human IgG anti-serum (Sigma). The glass plate was kept for 24 hours at 4°C in a damp chamber sealed with parafilm. Presence or absence of a precipitation line between the centre well and the surrounding wells was then recorded.

##### 2-4.1.2. Autoradiography of Ouchterlony plate.

After results had been recorded for the Ouchterlony diffusion, the gels were washed in phosphate buffer for 48 hours to remove any unprecipitated <sup>3</sup>H-IgG, then dried on a hot plate at 50°C. In order to determine the position of the radioactivity on the gel, the cooled Ouchterlony plate was dipped in autoradiography emulsion K2 (Ilford). It was placed on a cold tray (4°C) to

gel and then dried about 20cm away from an electric fan, with no heat. The Ouchterlony plate was sealed in a light-tight box with some silica gel and left to expose at 4°C for four days. After this period the Ouchterlony plate was developed in the same way as an autoradiograph (three minute development in D19, short wash in distilled water, 3 minute wash in fixative). The formation of silver grains in the emulsion indicates exposure to a radioactive source.

#### 2-4.1.3. Determination of the concentration of the tritiated probe.

The concentration of the tritiated IgG was determined by scintillation counting of a 20µl sample in 5ml of scintillation cocktail and comparing the amount of radioactivity present with that present in the same quantity of a known standard.

#### 2-4.2 Au(18)-IgG.

##### 2-4.2.1. Immunoprecipitation (Ouchterlony).

The nature of the colloid probe was tested by Ouchterlony diffusion in the same way as the radioactive probe (given above in section 2-4.1.1.) In the centre well, 10µl of the gold-protein complex (Au(18)-IgG) was placed. This was allowed to diffuse for 24 hours, since the colloid-protein complex is large and diffuses more slowly than the anti-serum. After 24 hours the serially diluted anti-IgG anti-sera was added to the surrounding wells. Results were recorded after a further 24 hours.

##### 2-4.2.2. Tube immunoprecipitation.

Glass tubes (similar to those used for tube-gel electrophoresis) were half filled with a 1% agarose in phosphate buffered saline and left for a few minutes to gel. The Au(18)-IgG probe was mixed in equal volume with some of the 1% agarose solution and poured onto a glass plate. (A control tube was prepared in the same way, using Au(18) only). When this had solidified a circle of the gel was cut out and placed on top of the solid gel in the glass tube. The tube was then filled to within 1cm of the top

and again allowed to solidify. Rhodamine conjugated anti-IgG (100 $\mu$ l) was loaded onto the top of the gel and the tubes were kept in a damp chamber for 3 weeks. After diffusion the tubes were washed extensively for 24 hours in phosphate buffered saline solution and then examined under ultraviolet light for fluorescence.

#### 2-4.2.3. Negative staining of the gold-protein complex.

The gold-protein complex was examined using the negative staining method of Horrisberg and Rosset (1977). The surface of the colloid particles are coated with IgG, and by negative staining this protein "coat" can be seen as a pale halo around each gold particle.

A drop of the gold-protein probe was dried onto a formvar/carbon coated 200 mesh copper grid (Agar aids), and negatively stained with 1% potassium phosphotungstate solution (pH 12). The grid was examined with a Jeol 100CX TEM.

#### 2-4.2.4. Transmission electron microscopic immunoprecipitation.

Samples of the Au(18)-IgG probe (10 $\mu$ l) were mixed with 10 $\mu$ l samples of serially diluted anti-IgG (Sigma), and incubated for 1 hour at 37 $^{\circ}$ C. (Control tubes were prepared with colloidal gold only-Au(18)-instead of the gold-protein complex). The samples were then centrifuged for 5 minutes at 3,000rpm. After centrifugation the tubes were inverted twice to attempt to resuspend the pellet. (In the case of the control the pellet is easily resuspended, in the experimental the gold-IgG is bound by the anti-IgG and remains as a pellet). 10 $\mu$ l samples were then taken of each pellet (in the control a sample of the supernatant was examined), placed on formvar/carbon coated 200 mesh copper grids and examined in a Jeol 100CX TEM.

#### 2-4.2.5. Sepharose-4B-protein A incubations.

Protein A has the ability to bind and precipitate IgG. 50ul samples of the probe were taken and incubated with either 100ul of Sepharose-4B- protein A (Pharmacia) in PBS, or 100ul of Sepharose-4B (Pharmacia) overnight at 4°C. A similar incubation was carried out using 50ul of Au(18) only and 100ul of Sepharose-4B-protein A or Sepharose 4B only, again incubated overnight at 4°C. The tubes were scored for pink colouration the following day.

#### 2-4.2.6. Determination of the concentration of the Au(18)-IgG probe.

The concentration of the gold particles used in the experiments was assessed by comparing a sample of the probe with a known concentration of latex particles (0.9um diameter - Agar aids).

A 2ul sample of the gold colloid was dried down onto an electron microscope grid. Next a 2ul sample of a 0.1% solution of polylatex spheres was dried down onto the same grid. The grid was examined by transmission electron microscopy using a Jeol 100CX TEM and random areas of the grid photographed (Fig 9). The ratio of gold particles to latex was counted and thus the concentration of the gold solution determined and expressed as particles/ml. (See Appendix VII).

### 2-5. TISSUE INCUBATIONS

#### 2-5.1. Term placenta incubated with <sup>3</sup>H-IgG

Human placentae from Caesarian sections or normal deliveries, were obtained from Leicester Royal Infirmary and transported back to the laboratory on ice. Tissue preparations were made using the method of Ockleford and Clint (1980).

Groups of chorionic villi were washed and ligatured with a piece of nylon thread (Abulon) or a fine human hair, using a dissecting microscope. The thread was knotted tightly to prevent access of the culture medium to the lumen of the chorionic villi. A 6cm length of thread was left to transfer the tissue during the washes.

Some of the tissue preparations were incubated in microfuge tubes with 100 $\mu$ l of Medium 199 (Flow Laboratories), and 50 $\mu$ l of the  $^3\text{H}$ -IgG probe (pH7.4) and the rest were used as controls and incubated in microfuge tubes containing 150 $\mu$ l of Medium 199 only. All the tissue samples were placed in a water bath at 37°C, and shaken at a rate of 60 times/minute.

After 30 minutes incubation the tissue was washed 6 times in 1ml aliquots of Medium 199 (Ockleford and Clint, 1980). The nylon tail of the tissue preparation was twisted between the thumb and finger to aid washing. The tissue was then fixed in 3% glutaraldehyde in 0.1M phosphate buffer and processed for transmission electron microscopy as described in Appendix I.

#### 2-5.1.1. Light Microscopy Autoradiography (LM ARG).

Autoradiography was performed on the tissue as described in section 2-2.1.2.

#### 2-5.2. Term placenta incubated with Au(19)-IgG.

A second series of experiments were carried out using the same tissue incubation technique but this time using 150 $\mu$ l of the colloidal gold/protein complex in Hank's buffer (pH 7.2 and another series at pH 4.2). Portions of tissue were fixed after 30 and 60 minutes and processed and embedded in Spurr's low viscosity resin for examination by transmission electron microscopy as described in Appendix I.

#### 2-5.2.1. Transmission electron microscopic examination. (TEM)

Thin sections were cut (gold to silver interference colour) and picked up on 200 mesh copper grids. They were again stained with uranyl acetate and Reynolds lead citrate and examined using a Jeol 100CX TEM.

#### 2-5.2.2. Scanning electron microscopy (SEM)

Tissue was prepared, incubated and then fixed in 3% glutaraldehyde in 0.1M phosphate buffer. The tissue was processed for SEM as shown in Appendix II. The tissue was then examined in a ISI-60 scanning electron microscope.

#### 2-5.2.3. Replication of the surface of the tissue.

Tissue was prepared, incubated and fixed as for the SEM incubation experiment above (section 2-5.2.2) but processed according to the method given in Appendix VIII. In this experiment the tissue was incubated with 50nm particles of colloidal gold coupled to IgG (Au(50) ).

#### 2-5.3. First trimester placenta incubated with <sup>3</sup>H-IgG

The tissue incubation experiments were repeated using first trimester placentae from therapeutic terminations of pregnancy performed at Leicester Royal Infirmary.

#### 2-5.3.1 Light microscopic autoradiography (LM ARG).

Tissue was fixed and processed for light microscopy autoradiography (LM ARG), as described in section 2-5.1.1.

#### 2-5.4. First trimester placenta incubated with Au(18)-IgG probe.

The experiment was carried out using the method described in section 2-5.2.

#### 2-5.4.1. Transmission electron microscopy examination.

Sections were cut and stained for TEM examination as described in section 2-5.2.1.

## CHAPTER 3: Investigation of Immunoglobulin G transport using placental tissue culture cells.

### 3-1. Examination of normal placental cells grown in tissue culture

Attempts were made to culture trophoblast cells from human term placenta, by a standard method given in Appendix IX. However, as has been reported by other workers (Taylor and Hancock, 1973), it was not possible to culture such cells for periods of longer than 7-10 days, owing to fibroblastic overgrowth.

Aladjem et al. (1975;1980) reported a method for inhibiting stromal growth in normal cultures of trophoblast, using high density plating of cells and culturing in low O<sub>2</sub> and high CO<sub>2</sub> atmosphere with a low nutrient supply. This method (Lueck and Aladjem, 1980) was used to grow long term cultures of human trophoblast.

#### (i) The culture method

Human placentae were obtained from Caesarian sections at Leicester Royal Infirmary. About 20g of tissue was taken from areas with a normal appearance. These pieces were washed in Hanks balanced salt solution and finely minced into 1mm<sup>2</sup> pieces with sterile scissors and forceps. The finely minced tissue was then transferred to a 150ml sterile conical flask to which 0.25% trypsin/EDTA solution (Gibco) was added. The tissue was digested until the solution began to look cloudy and the number of cells present assessed using a haemocytometer. (Concentration of cells required was approximately  $1 \times 10^6$ ). The cell suspension was centrifuged at 3,000rpm in a Gallenkamp laboratory centrifuge for 5 minutes to concentrate the cells. The supernatant was discarded and the digestion reaction stopped by resuspension of the cells in Ham's F12 culture medium (Flow) containing 30% fetal calf serum (Sera Lab.) and 100units penicillin/100ug streptomycin per ml. The cells were again centrifuged to remove the residual trypsin and resuspended in

10ml of Ham's F12 medium with 30% fetal calf serum (FCS) with the antibiotics as described above and dispensed into 50ml culture flasks (Nunc). The flasks were sealed tightly and kept at 37°C for 14 days then the cells were fed by replacing half of the medium with fresh medium. The flasks were again tightly sealed and incubated at 37°C for a further 21 days when the flasks were assessed for growth.

### 3-1.1. Light microscopic examination of the cells.

After 5 weeks of growth the cells were examined using a Zeiss inverted microscope.

### 3-1.2. Transmission electron microscopic examination.

Cells were also fixed and processed for electron microscopy examination.

## 3-2 Incubation of cultured placental cells.

### 3-2.1. Incubation of cells with Au(18)-IgG.

#### (i) Preparation of the cells.

The cells were fed with fresh culture medium 24 hours prior to the incubation experiments to ensure they were in an active state.

#### (ii) The incubation

Cells were incubated with Au(18)-IgG using a method similar to that used by Dickson et al. (1981) who examined the uptake of  $\alpha_2$  macroglobulin into Swiss 3T3 cells. The cells were placed on ice at 2°C for 30 minutes. Then the culture medium was removed and replaced by 5ml of the Au(18)-IgG probe in Hank's buffer. The cells were incubated with the Au(18)-IgG probe on ice at 2°C for 4 hours. They were then washed six times with cold culture medium (2°C). Then one flask was fixed

immediately and the rest were transferred to an incubator (37°C) and warmed for 60 minutes before fixation with cold 3% glutaraldehyde in 0.1 M phosphate buffer. The increase in temperature of the culture medium during the 60 minutes warming is shown in Fig 10.

#### 3-2.1.1. Transmission electron microscopy (TEM).

The cells were processed and embedded for examination by electron microscopy using the processing schedule given in Appendix X. Thin sections were examined using a Jeol 100CX transmission electron microscope.

#### 3-3. Choriocarcinoma cells (BeWo).

The BeWo cell line initially used was a gift from Professor W. Page-Faulk of the Queen Victoria Hospital, Department of Transplantation Biology, and later supplies were purchased from The American Type Culture Collection. The culture method given below was that recommended for the cells obtained from The American Type Culture Collection. The method used to grow the cells obtained from Professor Page-Faulk can be found in Appendix XI.

##### (i) The culture method

The medium used to culture the cells was Ham's F-12 medium with 15% heat inactivated FCS added and no antibiotics. Several types of FCS were tested (see Appendix XII) to find one which promoted optimum growth. (The serum was heat inactivated by incubating at 56°C for 30 minutes).

The cells were delivered in a frozen state, so were thawed rapidly by warming in the hand, and dispensed in to Ham's medium, with 15% FCS. The solution was centrifuged at 3,000 rpm in a Gallenkamp laboratory centrifuge for 5 minutes to remove the storage medium. The supernatant was discarded and the cells resuspended in fresh culture medium.

The cells were examined after 24 hours and it was found that only a few of them settled and spread onto the base of the culture flask. The cells were then fed by removing the old culture medium and adding 6 ml of filter sterilised conditioned medium (medium which had previously contained actively growing cells), and 2ml of Ham's F12 medium with 15% FCS. The conditioned medium was added to provide the cells with trace nutrients and thus aid their growth.

The cells did not show signs of growing after 4 days of feeding with conditioned medium, so it was decided to add "feeder" cells in the form of human myeloma cells, (this was again to try to provide the cells with nutrients which they may have been lacking). These cells grow in suspension when cultured this way. The mixed culture of cells were fed every other day by removing 3ml of the culture medium and replacing it with 3ml of fresh medium. When several flasks of cells had been obtained by subculture (see section below), some of the cells were put aside for long term storage by freezing (see Appendix XIII).

(ii) Procedure for subculturing cells.

When the culture flask contained a large number of cells, they were subcultured as follows. The old culture medium was removed and 1-2ml of trypsin-EDTA (Gibco) was added to the flask. Detachment of the cells from the base of the flask was observed using an inverted microscope (Nikon) and took 5-8 minutes at 37°C. The digestion reaction was stopped by the addition of culture medium in excess. The solution of cells and medium was transferred to a sterile centrifuge tube and spun at 3,000 rpm for 5 minutes in a Gallenkamp laboratory centrifuge. The supernatant was discarded and the cells resuspended in fresh culture medium and dispensed into 2-3 new flasks.

### 3-3.1 Light microscopy of the BeWo cells.

Cells were grown on sterile glass coverslips in the culture flasks by the method described above (section 3-3 (i)). They were either fixed in 3% formalin for 15 minutes and then transferred to phosphate buffered saline (PBS), or fixed with 3% glutaraldehyde in 0.1M phosphate buffer overnight. They were then examined using phase contrast microscopy or Nomarski differential interference contrast microscopy using a Zeiss photomicroscope.

### 3-3.2. TEM examination of the BeWo cells.

Cells were grown in either Linbro wells (Flow Laboratories), plastic Petri dishes (Sterilin or Nunc), or plastic culture flasks (Sterilin). The culture medium was removed and the cells fixed with 3% glutaraldehyde overnight. They were then processed for electron microscopic examination as shown in Appendix X. Groups of cells were localised using a dissecting microscope. Over each group a gelatin capsule, filled with prepolymerised resin, was inverted and the cells polymerised in an oven at 60°C for 36 hours. The gelatin capsules were then snapped from the plastic vessel while still hot thus peeling the cells from the base of the plastic vessel.

Some of the cells were reorientated by sawing the block with a small fret-saw and re-embedding. Thin sections, silver to gold in interference colour, were cut using a Reichert ultracut microtome, collected on 200 mesh copper grids and air dried. They were stained with 10<sup>-4</sup> methanolic uranyl acetate and Reynold's lead citrate and examined in a Jeol 100CX transmission microscope.

### 3-4 The BeWo cell incubations.

### 3-4.1. Short incubations with Au(18)-IgG.

#### (i) Preparation of the probe.

The colloidal gold-protein (Au(18)-IgG) was suspended in Hank's buffer for these experiments. Hank's buffer was used instead of culture medium because the gold colloid flocculated in the culture medium used to grow the cells.

Control experiments were carried out using unlabelled 18nm particles of colloidal gold (designated by the notation Au(18) ) in Hank's buffer. The pH of both the colloidal gold-IgG and the colloidal gold alone was 7.2.

#### (ii) Preparation of the BeWo cells.

Cells were grown in culture flasks and fed with fresh medium 24 hours before the experiment to ensure they were actively growing.

#### (iii) The incubation procedure.

The culture medium was removed from the culture flasks and in one case replaced with medium containing the probe, and in the other replaced with the control solution of Au(18) only. The two flasks were incubated at 37°C for 30 minutes and the probe/medium mixture removed and the cells fixed with 3% glutaraldehyde.

#### 3-4.1.1. Transmission electron microscopy (TEM)

The cells were processed for electron microscopic examination as given in Appendix X.

### 3-4.2. Long incubations with Au(18)-IgG.

#### (i) Preparation of the probe.

The probe was prepared as for the short incubations section 3-4.1.

(ii) Preparation of the BeWo cells.

The cells were prepared as for the short incubations sections 3-4.1.

(iii) The incubation method.

For this experiment the same method as in section 3-4.1. was used but the incubation time was increased. In this case the cells were incubated with the gold-protein probe for 18 hours. Again a control experiment was carried out using colloidal gold only. After incubation the cells were washed briefly with warm culture medium before fixation with 3% glutaraldehyde in phosphate buffer.

3-4.2.1. Transmission electron microscopy (TEM).

The cells were processed and embedded using the schedule given in Appendix X. Thin sections were examined using a Jeol 100CX transmission electron microscope.

3-4.3. Incubation at 2°C with Au(18)-IgG.

The incubation schedule used was based on that used by Dickson et al. (1981).

(i) Preparation of the cells

The cells were again grown in plastic culture flasks. Ten flasks of cells were used, and divided into two groups. The experimental group were fed the day before with serum-free medium (to prevent cross reaction between any fetal calf IgG in the fetal calf serum). The control group were fed with serum-free medium plus 2mg/ml free IgG (in order to saturate the IgG receptors on the cell surface).

#### (ii) The incubation

On the day of the experiment the cells were cooled to almost freezing by placing on ice at 2°C for 1 hour, then the culture medium was removed and replaced in the case of the experimental group with the gold-protein probe (at 2°C), and the control group with colloidal gold only. The cells were incubated at 2°C for 4 hours. They were then washed 6 times with cold serum-free culture medium and one flask from each group was fixed in 3% glutaraldehyde in phosphate buffer. The remaining flasks were transferred to a hot room at 37°C and flasks from each group fixed at 1, 5, 10 and 30 minutes. The increase in the temperature of the medium was recorded at five minute intervals (Fig 11).

#### 3-4.3.1. Transmission electron microscopy

The fixed tissue was processed for electron microscopic examination using the method given in Appendix X. Thin sections were cut and examined using a Jeol 100CX transmission electron microscope.

## RESULTS

## CHAPTER 4: Results from studies of human placental tissue

### 4-1 THE HUMAN PLACENTA

#### 4-1.1. Term placenta

The placenta, together with the umbilical cord and the fetal membranes constitutes the "afterbirth" which is discharged during the third stage of labour. The human placenta is a flat discoid organ (Figs 12 & 14) which has a diameter of approximately 20cm and a weight of about 500g. The two sides of the placental disc are very different in appearance. The umbilical cord is attached to the chorionic plate on the fetal side of the placenta (Fig 12). The position of attachment of the cord is usually central, although placement of the cord to one side is quite common. A network of blood vessels (Fig 12) radiate out from the point of attachment of the cord, across the placental surface. A thin membrane - the chorion - covers the blood vessels (Fig 13). The blood vessels are derived from the three main vessels in the umbilical cord (two arteries and one vein). Nomenclature of the vessels changes according to their position on the placenta. There is a series of transitions from umbilical vessels through chorionic vessels to cotyledonary vessels which serve the cotyledons of the placenta.

The other side of the placenta (the maternal side) is known as the basal plate (Fig 14), and it is this side which is attached to the endometrium. It consists of a number of lobes and gives the placenta a cobblestone appearance. The lobes, which consist of one or more cotyledons, are separated by grooves which are known as the placental septa (Fig 15). Each cotyledon has its own blood supply derived from the blood vessels of the umbilical cord. If the placenta is cut longitudinally through a cotyledon it can be seen that the trophoblastic tissue is organised into a branching tree-like structure (Fig 16).

#### 4-1.1.1. Light microscopy

Examination of this tree-like structure by Nomarski interference microscopy shows that a main branch or stem villus divides up into intermediate and terminal structures (Fig 17). Occasionally the position of the fetal capillaries can be seen (Fig 18).

The histology of the trophoblastic tissue can be seen in Figs 19 & 20, which are low power light micrographs of thick 0.5µm sections of resin embedded tissue stained with 1% toluidine blue. There is an outer darker layer of syncytiotrophoblast which has a surface microvillus border. Many nuclei can be seen although there are no cell boundaries since this tissue layer is a syncytium. This layer tends to be more densely staining than the other layers due to the large number of dark nuclei and other dense granules and inclusions. Examination of the tissue at higher power shows many large vacuoles and smaller vesicular structures are present (Fig 20). Deep to the syncytiotrophoblast is the cytotrophoblast. This layer consists of cells resting on a basement membrane. In first trimester placenta these cells form a complete layer beneath the syncytiotrophoblast (Fig 37) but by term cells are much fewer in number, and in many areas the syncytiotrophoblast is in direct contact with the basement membrane (Fig 20). Below the cytotrophoblast cells and the basement membrane is the stroma (Fig 19 & 20). This is composed of connective tissue, fibroblasts, Hofbauer cells and collagen fibres. Within the stroma are the fetal blood capillaries (Fig 20).

#### 4-1.1.2. Scanning electron microscopy (SEM)

The branching nature of the trophoblast is shown particularly well when the tissue is examined using scanning electron microscopy (Fig 21). The surface microvilli are also clearly visible (Fig 22).

#### 4-1.1.3 Transmission electron microscopy (TEM)

Ultrastructural examination of human placental tissue reveals a considerable difference in appearance between the syncytiotrophoblast and the cytotrophoblast (Fig 23). The syncytiotrophoblast has a much more electron dense appearance than the underlying cytotrophoblast cells. This is owing to the many nuclei which are present in the syncytiotrophoblast (Fig 24) and the high concentration of organelles in the syncytial cytoplasm. The syncytial nuclei are more electron dense than those of the cytotrophoblast cells, owing to the presence of more heterochromatin, around the margin of the nuclear envelope (Fig 23). Large numbers of nuclear pores are present in the syncytial nuclear envelope.

A characteristic feature of the syncytiotrophoblast is its surface microvillous border (Fig 23&24). In vivo this layer is in contact with the maternal blood. At the base of the microvilli membrane invaginations are found. These may be smooth membrane pits, or there may be a protein coating on the membrane - coated pits (Fig 26 & 28). These membrane invaginations contribute to the general vesiculated appearance which is a prominent feature of the syncytiotrophoblast (Fig 25). This extensive vesiculation is mainly owing to a high concentration of a wide size range of vesicles and vacuoles within the syncytial cytoplasm and the vesicular profiles of the endoplasmic reticulum. Large vacuoles are often found close to the syncytial nuclei - juxtannuclear vacuoles (Fig 29). Sometimes the lumen of coated vesicles just below the syncytial surface appear to be joined to the intervillous space by a tube-like structure (Fig 27 & 28). Some of the larger vesicular profiles appear to have electron dense material within them (Fig 30). Mitochondria are present in the syncytiotrophoblast (Fig 30) and also contribute to the vesiculated appearance. Very darkly staining droplets are found in the syncytial cytoplasm, and these do not appear to be bounded by a limiting membrane (Fig 29). Fine

filaments are also present in the syncytiotrophoblast (Fig 27) and desmosomes could be seen between the syncytiotrophoblast and cytotrophoblast (Fig 31). Below the syncytiotrophoblast is the cytotrophoblast layer. This is composed of individual cells resting on a basement membrane (Fig 29). In the early placenta (first trimester) these cells form a continuous layer beneath the syncytiotrophoblast (Fig 37), but by term this layer is incomplete and the syncytiotrophoblast is often in direct contact with the basement membrane (Fig 24 & 25). The cytotrophoblast layer is more electron-lucent than the syncytiotrophoblast and contains fewer organelles (Fig 32 & 33). The cytotrophoblast cells have microvilli on their surface which interdigitate with the syncytiotrophoblast (Fig 32). Sometimes desmosomes are found near these interdigitations (Fig 32). The cytotrophoblast nuclei are pale staining and the chromatin is finely dispersed. There is some heterochromatin scattered in the nucleoplasm and the remainder is located in a thin layer around the nuclear envelope (Fig 36). Nucleoli (Fig 36), mitochondria (Fig 32), and endoplasmic reticulum are present in the cytotrophoblast cells (Fig 32 & 33), although there is much less endoplasmic reticulum than in the syncytiotrophoblast. Fine filaments (Fig 33), coated vesicles (Fig 35), vesicles containing electron dense material (Fig 32), and Golgi, often located close to the nucleus (Fig 34), are also common features of the cytotrophoblast.

#### 4-1.2. First trimester placenta

First trimester placentae were obtained by a suction-evacuation method and so were delivered as fragments of tissue.

##### 4-1.2.1. Light microscopy

Examination of thick (0.5 $\mu$ m) sections of resin embedded first trimester tissue (Fig 37) showed a similar morphology to that of term placenta. The tissue could again be divided into an upper syncytiotrophoblast layer and a layer of cytotrophoblast

cells beneath. In first trimester placentae the cytotrophoblast cells form a complete continuous layer under the syncytiotrophoblast. The syncytiotrophoblast has its characteristic microvillus border, and the cytoplasm again has a highly vesiculated appearance. Juxtannuclear vacuoles are seen as well as smaller vesicles and vacuoles (Fig 37). The syncytial nuclei have a characteristic electron dense appearance owing to the presence of darkly staining heterochromatin (Fig 37). Occasionally some of the cytotrophoblast cells are more darkly staining than those normally found (Fig 37), they have a more syncytiotrophoblast - like appearance but still retain the limiting membrane characteristic of cytotrophoblast cells. Such morphology suggests that these cells may be in the process of forming syncytiotrophoblast. Below the cytotrophoblast is the connective tissue stroma (Fig 37) containing the fetal blood capillaries.

#### 4- 1.2.2. Transmission electron microscopy (TEM)

Examination of first trimester placental tissue by transmission electron microscopy showed the presence of many of the organelles and features found in term placentae (Fig 38). In the syncytiotrophoblast many vesicles and vacuoles were present. Mitochondria, endoplasmic reticulum and electron dense droplets not bounded by a limiting membrane-probably lipid-were also found (Fig 38). In the cytotrophoblast cells, mitochondria, endoplasmic reticulum and other vesicular inclusions were present (Fig 39). Densely staining bodies were also found in the basement membrane (Figs 38 & 39).

### 4-2. PERFUSION OF THE HUMAN PLACENTA

#### 4-2.1. Perfusion with $^3\text{H}$ -IgG

A total of seven of the perfusion experiments were successful, i.e. the flow rates of both the maternal and fetal circuits were stable throughout the experiment and the pressure in the system did not rise above 60mmHg. Of these successfully perfused placentaethree showed transport of the tritiated probe as measured by scintillation counting of samples taken from the venous return

circuit of the perfusion apparatus, during the experiment.

#### 4-2.1.1. Assessment of transport of the probe.

The amount of radioactivity in the samples was calculated and expressed as disintegrations per minute. These data were then plotted on a graph against time (Fig 40). An increase in the amount of radioactivity in the samples indicated that transport of the probe had taken place.

The results given below are for the placentae which showed an increase in the amount of radioactivity in the sample with increase in length of time of perfusion i.e. transport of the tritiated probe.

#### 4-2.1.2. Light microscopy autoradiography (LM ARG)

Placentae which showed transport of the tritiated probe were examined by autoradiography. A small piece of the perfused cotyledon was embedded in resin and 0.5 $\mu$ m sections were cut and autoradiographed. Control tissue was excised prior to the perfusion experiment. It was taken from a cotyledon of the same placenta not required for the perfusion experiment. Care was taken to ensure the tissue was taken from a similar sized cotyledon in a similar position to the one which was to be perfused. The tissue was processed and embedded in the same way as the experimental tissue and sections were cut from it and autoradiographs made. Sections of resin alone without contained tissue were cut and were autoradiographed as a second control.

The presence of radioactivity in developed autoradiographed sections is manifested by the presence of silver grains. The location of the grains indicates the position of the radioactive source within a certain radius around the silver grain (the radius of the circle depends on several factors such as the thickness of the emulsion, type of radiation). It is therefore possible to identify the position of the radioactive source in the tissue within certain confidence limits.

Autoradiography of the tissue perfused with tritiated IgG showed silver grains in the epithelial region of the trophoblast, with a few grains over the stroma and some over the capillary endothelial cells (Fig 41). In the control tissue a few silver grains were found scattered over the tissue (Fig 42), and in the control resin sections a few grains were also found. The number of silver grains found over the control tissue sections was not significantly different from the number of grains found over the control resin sections and so it was concluded that the silver grains in both these cases were a result of random background radiation.

(i) Epithelial association.

The distribution of radioactivity in the tissue was investigated using the counting method described in Appendix XIV. The results of the counts are presented as histograms in Fig 43 and in Table 1. Statistical comparisons were made between each of these areas using the Students t-test. For the experimental tissue a significant difference was found between the epithelium and the stroma ( $p < 0.01$ ), and between the epithelium and the background area ( $p < 0.01$ ). A significant difference was also found between the experimental epithelium and the control epithelium ( $p < 0.01$ ).

	Number silver grains $\times 10^{-3}$ in each $1\mu\text{m}^2$ of tissue		
	EPITHELIUM	STROMA	BACKGROUND
Experimental	5.06	0.4	0.2
Control	2.1	0.32	0.26
	Significant $P < 0.01$	Not signif- icantly different.	Not signif- icantly different.

Table 1 showing average number of silver grains  $\times 10^{-3}$  in  $1\mu\text{m}^2$  of tissue.

(ii) Vesicle association.

Many of the silver grains in the experimental tissue sections appeared to be localised over large vesicles (Fig 44 & 45). To show that this localisation was not a random distribution but a true association, a schema was devised to test this distribution statistically. This is described in Appendix XV. Briefly the method involved the generation of a population of random numbers from random tables (Appendix XVI) and plotting these on ordinate and abscissa axes on transparent acetate sheets. The acetate sheet was placed over the photomicrographs of the autoradiographs and the number of random dots falling over syncytial vesicles expressed as a percentage of the total number of random dots. This was compared statistically by the Students t-test to the percentage of silver grains falling over syncytial vesicles. Fig 46 shows a histogram of the results. A significant difference ( $p < 0.01$ ) was found between the dots and silver grain data for the experimental tissue but not for the control data.

	REAL SILVER GRAINS	RANDOM DOTS	
Experimental	66.93%	35.16%	$p < 0.01$
Control	46.0%	39.0%	

Table 2 showing average % of real and random silver grains in  $1\mu\text{m}^2$  tissue.

(iii) Endothelial association

In addition to the vesicular association, a population of silver grains appeared to be localised close to the fetal capillary endothelial cells (Fig 47). To investigate this apparent association, photomicrographs for both the experimental and control tissue were assessed for the number of silver grains found around the perimeter of the endothelial capillaries using a MOP-AM02 (Kontron Messgerate). The data were expressed as numbers of

grains per 1 $\mu$ m perimeter of tissue and plotted on a histogram (Fig 48). Since the data did not follow a normal distribution the control experimental data were compared using the Mann-Whitney U-Test. This test is the most powerful test which can be used on non-parametric data (i.e. data which does not follow the normal distribution). A significant difference ( $p < 0.01$ ) was found between the experimental and control data.

	GRAINS/ $\mu$ m x $10^{-3}$
Experimental	5.0.
Control	0.7.
	significant $p < 0.01$ .

Table 3 to show average number of silver grains x  $10^{-3}$  in a 1 $\mu$ m length of tissue.

#### 4-2.1.3. Transmission electron microscopy autoradiography (TEM ARG)

Silver grains were visible in the experimental grids. Some grains were found in the syncytial layer apparently over vesicular structures (Fig 49 & 50) while others were found in the stroma (Fig 49 & 51). However, it was not possible to conduct a detailed statistical analysis on the data since there were not sufficient silver grains present for such a study.

#### 4-2.2. Perfusion of the placenta with Au(18)-IgG

A total of nine of the perfusions were successful i.e. the flow rates were stable throughout the experiment and the pressure in the system did not rise above 60mmHg. Of these one showed a pink colouration of the cotyledon being perfused, near to the point of insertion of the microcannula.

#### 4-2.2.1. Assessment of transport of the probe.

Samples taken from the fetal venous return during the perfusion experiment were examined by transmission electron microscopy for the presence of gold-IgG complexes. No gold particles were found by this method.

#### 4-2.2.2. Transmission electron microscopy (TEM) of perfused tissue.

Ultrastructural examination of the perfused tissue showed it to be intact and undamaged, when compared with the ultrastructure of control tissue excised and fixed prior to the perfusion experiments.

Gold-IgG complexes, characterised by highly electron dense particles of uniform size and shape were seen distributed over the tissue in a variety of locations. They were found:

- (i) Close to the microvilli on the surface of the syncytiotrophoblast (Fig 52 & 53)
- (ii) In close proximity to the non-microvillar surface of the syncytiotrophoblast (Fig 54).
- (iii) Lying very close to coated regions on the surface of the syncytiotrophoblast, i.e. coated pits (Fig 55-57).
- (iv) Enclosed within coated vesicles (Fig 60)
- (v) Enclosed within smooth membrane vesicles (Fig 58 & 59).
- (vi) Lying apparently free in the cytoplasm (Fig 61)
- (vii) Located in the basal lamina (Fig 61)
- (viii) Lying free in the stromal core (Fig 61)
- (ix) In the endothelial cells of the fetal blood vessels (Fig 61)

#### 4-2.2.3. Scanning transmission electron microscopy examination (STEM)

Since the total number of gold particles seen per section by TEM was generally low, thicker sections were cut and examined by STEM. This method permits the examination of much thicker sections than normally possible with conventional transmission electron microscopy with little loss in resolution. It was

predicted that more gold particles could be observed per section using this method and that it would be possible to determine if the particles were actually within vesicles. Stereo-pair photomicrographs were prepared from STEM examination and this added depth to the photographs if viewed with stereo viewing glasses (Fig 62-67). However it was not possible to find any more gold particles by this method than could be found by conventional TEM.

#### 4-3. THE PROBES

##### 4-3.1. $^3\text{H}$ - IgG

A total of 9ml of tritiated IgG was collected from the condensation reaction between the N-succinimidyl-propionate and the human IgG.

##### 4-3.2. Au(18)-IgG

The preparation of a solution of colloidal gold involves reduction of aurochloric acid ( $\text{HAuCl}_4$ ) solution by sodium citrate. As the reaction proceeds a colour change takes place. Initially the solution of gold chloride is a yellow colour. When added to the boiling sodium citrate and distilled water solution it turns a dark purple colour. As the reaction continues the solution becomes lighter in colour. At the end of the reduction process the final solution is a clear deep red wine colour. Addition of the protein to this solution produces a slight darkening of this red wine colour. Addition of too much protein results in a flocculation of the solution which is accompanied by a change in colour of the solution to cloudy blue. Gold which had been coated with protein was concentrated by centrifugation and the resultant pellet of Au-IgG complexes resuspended in Hanks buffer (containing PEG) to give a total volume of 20ml of probe.

#### 4-4 VALIDITY OF THE PROBES

#### 4-4.1. <sup>3</sup>H-IgG

A small sample (10 $\mu$ l) of <sup>3</sup>H-IgG was used to test the validity of the probe using Ouchterlony double immunodiffusion.

##### 4-4.1.1. Ouchterlony double immuno-diffusion

The tritiated IgG was diffused against anti-human IgG and after 24 hours a precipitation line was formed between the centre well containing the radioactive probe and the surrounding wells containing the serially diluted anti-IgG anti-sera. The intensity of the precipitation line decreased with decrease in concentration of the anti-sera and indicated that the probe was human IgG (Fig 68).

##### 4-4.1.2. ARG of the Ouchterlony plate

After four days of exposure the sensitive emulsion on the Ouchterlony plate was blackened due to exposure to the radioactive source (Fig 69).

##### 4-4.1.3. Determination of the concentration of the <sup>3</sup>H-IgG probe.

The concentration of the probe was 60 $\mu$ g protein / ml.

#### 4-4.2. Validity of the Au(18)-IgG probe.

The validity of the colloidal gold probe was tested by Ouchterlony double immunodiffusion, negative staining of the gold-protein complexes and immunoprecipitation.

##### 4-4.2.1. Ouchterlony double immuno-diffusion

Since gold-protein complexes are large and therefore have a slow diffusion rate, 10 $\mu$ l was placed in the centre well of the Ouchterlony plate and was allowed to diffuse for 24 hours before adding the serially diluted antibody to the outer wells. However no precipitation line was obtained in this experiment.

#### 4-4.2.2. Tube immunoprecipitation

No precipitation line was obtained.

#### 4-4.2.3. Negative staining of Au(18)-IgG complexes.

Negatively stained preparations of the Au(18)-IgG probe examined by TEM showed a distinct pale halo, representing the protein around a central dark electron dense gold particle (Fig 70). Control samples of negatively stained Au(18) only lack this pale halo (Fig 71). The pale halo phenomenon is not a focusing artefact since the "wobbler" focusing facility on the microscope was used in both cases.

#### 4.4.2.4. TEM immunoprecipitation.

Transmission electron microscopic examination of the pellets produced by incubation of the gold-protein probe with anti-IgG showed clumps of electron dense particles characteristic of colloidal gold (Fig 72). In the case of the control where Au(18) only was incubated with anti-IgG no clumping of the gold was seen (Fig 73).

#### 4-4.2.5. Sepharose-4B-protein A incubations.

It is well known that protein A has an affinity for IgG and so a test for the validity of the Au(18)-IgG probe was devised using a commercially prepared reagent Sepharose-4B-protein A. The probe was incubated with either Sepharose-4B-protein A or Sepharose-4B only. Control experiments were carried out using Au(18) incubated with Sepharose-4B-protein A or Sepharose-4B. The results of the incubations are shown in Fig 74 & 75. Only the incubation between Sepharose-4B-protein A and Au(18)-IgG showed a pink coloured pellet indicating the presence of the colloidal gold-protein probe retained by the Sepharose even after washing of the pellet several times with PBS (Fig 74).

4-4.2.6. Determination of concentration of the probe.

The concentration of the Au(18)-IgG probe was  $2,000 \times 10^9$  particles of gold colloid per ml.

4-5 TISSUE INCUBATIONS

4-5.1. Term placenta incubated with  $^3\text{H}$ -IgG

4-5.1.1. Light microscopy autoradiography (LM ARG)

Silver grains were found over the tissue incubated with  $^3\text{H}$ -IgG, with fewer grains present over the tissue not exposed to  $^3\text{H}$ -IgG, and a background number of grains over sections of resin which contained no tissue. Statistical analysis showed no significant difference between the number of grains found over the tissue incubated without the presence of the  $^3\text{H}$ -IgG probe and the number of grains found over the resin sections with no included tissue. The silver grains in both cases were attributed to random background radiation.

The silver grains over the experimental tissue were quantitated for the epithelial and stromal areas using the method described in Appendix XIV, and compared statistically with data obtained from the control tissue, using the Students t-test. The results obtained are given in Table 4 below:

Number of silver grains $\times 10^{-3}$ in each $1\mu\text{m}^2$ of tissue		
EXPERIMENTAL	CONTROL	SIGNIFICANCE
epithelium 1.7	epithelium 0.3	$p < 0.01$
stroma 0.1	stroma 0.2	not significant

Table 4 Showing the results of the statistical comparison between experimental and control tissue.

A significant difference was found between the distribution of silver grains over the experimental tissue and the control tissue. Fig 76 shows the distribution of silver grains over the experimental tissue. Fig 77 shows silver grains located over control tissue.

#### 4-5.2. Incubation with Au(18)-IgG

##### 4-5.2.1. Transmission electron microscopy (TEM)

###### (a) pH.4.2

TEM examination of the tissue incubated with the Au(18)-IgG probe for 30 minutes at pH.4.2 showed electron dense spherical bodies characteristic of the Au(18)-IgG probe distributed over the tissue. They were found:

- (i) lying very close to the surface of the syncytiotrophoblast (Figs 78 & 79).
- (ii) on the surface microvilli (Figs 78 & 80).
- (iii) lying near to coated pits (Fig 78).
- (iv) enclosed in larger non-coated membrane bounded vesicles (Fig 79).
- (v) scattered in the cytoplasm of the tissue not bounded by membrane (Fig 81)

###### (b) pH 7.0

Transmission electron microscopic examination of pieces of term chorionic villi incubated with Au(18)-IgG (pH 7.0) for 30 minutes at 37°C showed association of gold particles with the surface and some uptake of the probe into the tissue. Gold particles were found:-

- (i) associated with the microvillous surface of the tissue (Fig 82)
- (ii) localised in large vesicular structures (Fig 83 & 84).
- (iii) apparently lying free in the cytoplasm (Figs 85 & 86)

Tissue incubated with the probe for 60 minutes at 37°C showed very little surface association of the probe. Gold particles were found:-

- (i) Lying free in the syncytiotrophoblast layer (Fig 87); some particles were seen which may have been enclosed by a membrane but the plane of the section made it difficult to distinguish this (Fig 88).
- (ii) lying adjacent to the cytotrophoblast cells (Figs 87 - 89).
- (iii) lying adjacent to the basal lamina (Figs 88, 90, 91, 92).
- (iv) within vesicular structures in the cytotrophoblast cells (Figs 93 & 94).

#### 4-5.2.2. Surface examination of the tissue

Attempts to distinguish gold particles on the placental microvillous surface, by scanning electron microscopy and replication methods were unsuccessful for technical reasons.

#### 4-5.3. First trimester placenta incubated with $^3\text{H}$ -IgG.

Pieces of first trimester placental tissue were incubated in buffer containing the tritiated IgG probe. Control experiments were carried out by incubating pieces of first trimester tissue in buffer alone for the same period of time as the experimental tissue. The tissue was then fixed and embedded and 0.5 $\mu\text{m}$  sections were cut and prepared for autoradiographic examination.

##### 4-5.3.1. Light microscopy autoradiography (LM ARG)

Silver grains were found over the tissue incubated with the  $^3\text{H}$ -IgG probe. A few grains were found on the control tissue incubated in culture medium only, and these were attributed to background radiation.

The distribution of silver grains over the syncytiotrophoblast, cytotrophoblast and stroma in both the control and experimental situation was quantitated as given in Appendix XIV. The resultant data were compared using the Students t-test and the results obtained are given in Table 5.

Number of silver grains $\times 10^{-3}$ in each $1\mu\text{m}^2$ of tissue			
EXPERIMENTAL		CONTROL	SIGNIFICANCE
syncytiotrophoblast	0.3	syncytiotrophoblast	0.4 not significant
cytotrophoblast	0.8	cytotrophoblast	0.2 significant $p < 0.01$ .
stroma	0.9	stroma	0.3 significant $p < 0.01$

Table 5 showing the results of statistical comparison between experimental and control tissue.

A significant difference was found between the experimental cytotrophoblast tissue and the control cytotrophoblast tissue, ( $p < 0.01$ ), and between the experimental stromal tissue and the control stromal tissue ( $p < 0.01$ ). Fig 95 shows the distribution of silver grains over the experimental tissue and Fig 96 shows the control tissue.

#### 4-5.4. First trimester placenta incubated with Au(18)-IgG.

##### 4-5.4.1. Transmission electron microscopy (TEM)

TEM examination showed the presence of gold-IgG complexes:-

- (i) associated with microvilli on the surface (Fig 97)
- (ii) associated with non-microvillous areas on the surface (Fig 97)
- (iii) within vesicular structures in the cytotrophoblast (Fig 98).
- (iv) near the basement membrane (Fig 99).

## CHAPTER 5: Results from studies using human placental cells in tissue culture.

### 5-1 Tissue culture of normal human placenta

Immediately after dispensing the cells into culture flasks the cultures were examined with an inverted microscope. Initially the cultures were found to contain a large amount of red blood cells and it was difficult to see the placental cells. However after two weeks of culture most of the blood cells had disappeared and clumps of tissue could be seen adhering to the base of the culture flasks.

#### 5-1.1. Light microscopy

Examination of the cultures after five weeks, showed a layer of cells to be present around the clumps of tissue (Fig 100). Sometimes these clumps of tissue could be detached by repeated vigorous washing of the cultures and the detached clump transferred to a slide for examination at high power using Nomarski interference microscopy. By focusing at different levels the tissue clumps were found to consist of several layers of cells. Around the periphery of these tissue clumps were villus-like structures (Figs 103-105) and other long filopodial filaments (Figs 103 & 106) which often had a bulbous structure attached to the end (Fig 106). In one case a villus-like structure was found floating in the medium and was fixed and processed for examination by electron microscopy (Figs 129 & 181).

Light microscopy of thick (1 $\mu$ m) sections stained with toluidine blue cut vertically through these long term placental cultures showed a central mass of tissue composed of both light and dark staining cells (Fig 101), and some individual cells on either side of this clump (Fig 102). Some very densely staining bodies were seen in many of the cells (Figs 102 & 103). The tissue clump appeared to show some differentiation into syncytial and cytotrophoblast tissue (Fig 102). The upper darker syncytial

portion possessed a layer of surface microvilli (Fig 107) and the underlying tissue was pale and cytotrophoblast-like; stromal-type regions could also be identified in the tissue (Fig 107). In some cases the individual cells on either side also appeared to be distinguishable into light and dark regions. Also in this area there were fine fibres visible deep to the individual cells (Fig 107).

#### 5-12 Transmission electron microscopy

Electron microscopy of thin sections of long term placental cell cultures confirmed ultrastructurally the apparent division into syncytial and cytotrophoblast tissue seen in the light microscope (Fig 107). On the outer edge of the main tissue clump some dark cells were found while within the centre of the mass were the lighter cytotrophoblast elements (Fig 108), the basement membrane (Fig 109), and the stromal areas. The darkly staining bodies seen within many of the cells in the light microscopic examination were more prominent and appeared to contain some membrane elements (Fig 107).

Many organelles commonly found in normal placental tissue were found by transmission electron microscopic examination of these cell cultures. Surface microvilli (Fig 110) were present on the surface of the syncytial-like cells. Both coated and uncoated membrane invaginations were present between the microvilli (Fig 110). Mitochondria, endoplasmic reticulum and other vesicular structures were found in the syncytial-like cell cytoplasm (Fig 110). Fine filaments and numerous ribosomes were seen (Fig 110) and in some cells large numbers of desmosomes were present (Fig 111). Densely staining droplets were sometimes seen which were not bounded by a limiting membrane (Fig 112).

In the paler staining cytotrophoblast-type cells the complement of organelles included mitochondria, endoplasmic reticulum,

ribosomes and large vesicular structures (Fig 113). Other smaller vesicular profiles (Fig 113) were also seen and fine filaments were present in the cell cytoplasm (Fig 115). The stromal areas in the tissue were composed mainly of collagen-type fibres (Fig 114). The cells at the edges of the tissue mass contained a similar range of inclusions and organelles, that is mitochondria, endoplasmic reticulum, vesicles and electron dense droplets (Fig 116). Between these individual cells were fibres similar to collagen (Fig 116).

Transmission electron microscopy of the villus-like structure isolated from the culture medium showed it to be composed of cells (Fig 117). They were not organised into a villus morphology as is found in normal placenta, nor was there any obvious differentiation into syncytiotrophoblast-like tissue and cytotrophoblast-like tissue. No surface microvilli were seen. Many of the cells were highly vacuolated (Fig 117 & 118) and contained a variety of organelles such as mitochondria, endoplasmic reticulum, some small vesicular structures (Fig 117) and non-membrane-bounded electron dense droplets (Fig 117).

## 5-2. Incubations of normal placental tissue culture cells

### 5-2.1. Incubation with Au(18)-IgG.

#### 5-2.1.1. Transmission electron microscopy (TEM)

Transmission electron microscopy of cells incubated with Au(18)-IgG for 4 hours at 2°C, then washed six times in cold culture medium and fixed immediately, showed an association of the gold - IgG complexes with the cell surface microvilli (Fig 119). Particles of gold were also seen lying near coated pits on the cell surface (Fig 120).

Cell cultures examined after washing with cold culture medium and then warming for 60 minutes before fixation showed gold particles in large electron-lucent vesicles (Fig 121).

### 5-3 BeWo Cells

The normal morphology of BeWo cells was examined using both light and electron microscopy.

#### 5-3.1. Light microscopy

Nomarski interference microscopy of BeWo cells, showed both clusters of cells and some individual cells. In many of the cell groups the individual cell membranes were not distinct although in some cases it was possible to distinguish them (Fig 125). Some of the cells appeared to have more than one nucleus (Fig 122) and might have been in the process of dividing.

Nomarski interference microscopy revealed more than one layer of cells in the cultures (Fig 123 & 128). Around the edges of the cells, filopodial structures could be seen (Fig 124), and in some areas villus-like outgrowths could be seen (Figs 126 & 127). Other villus-like structures were also noted above the clump of tissue (Fig 129), attached to the sheet of cells by a fine filament (Fig 129 (i)). Light microscopy of thick (1 $\mu$ m) sections of resin embedded cells stained with toluidine blue (Fig 130) showed sheets of cells with many nuclei of irregular shape. No cell membrane could be seen. In the cytoplasm there were very densely staining droplets present (Fig 130).

#### 5-3.2. Transmission electron microscopy (TEM)

Transmission electron microscopy of BeWo cells showed them to possess many features and organelles similar to those found in normal placental tissue (Fig 145). Transverse sections through some of the cells showed that they were divided into two distinct layers, a darker upper layer and a lighter lower layer comparable to the dark syncytiotrophoblast and the lighter cytotrophoblast layer found in normal placental tissue (Fig 131). Also some cells were found which had part of an adjacent cell on their surface (Fig 133) and where this was found there were interdigitations between the cells (Fig 131) similar to those found between the syncytiotrophoblast and the cytotrophoblast of normal placental tissue. A similarity was noted between the

general appearance of the BeWo cells and first trimester placental tissues (Fig 132).

Many of the organelles and inclusions found in the BeWo cells were similar in appearance to those found in normal placental tissue. The nuclei of the BeWo cells were more irregular in shape than those found in normal placenta with many invaginations or lobes (Fig 134). A small amount of condensed chromatin was found near the edges of the nuclear envelope (Fig 139). Nucleoli were very prominent in the BeWo cells and often more than one was found (Fig 135). Sometimes the nucleolus was located near the margin of the nuclear envelope (Fig 136).

The nuclear envelope of the BeWo cells was a normal trilaminar structure, often highly invaginated (Fig 135). Nuclear pores were present in high density in the membrane (Figs 137 & 138). Tangential sections showed a central dense granule (Fig 137).

Microvilli and longer filopodial structures were present on the cell surface (Fig 140). Fig 141 shows microvilli cut in transverse section and shows the presence of filaments around the periphery. Occasionally some of these microvillous structures were found deeper in the cells (Fig 142). A definite layer of filaments is present just beneath the cell surface (Fig 141). Microtubules are distributed throughout the cytoplasm of the cells (Fig 143). Some were noted near the nucleus (Fig 146). A large number of microtubules were found around the centriole (Fig 144). Microfilaments were also numerous throughout the cytoplasm of the cells (Fig 143 & 146). Some of the bundles of filaments seen were of a similar dimension to cyto-keratin filaments (Fig 147).

Centrioles were sometimes found in the BeWo cells (Figs 148 - 150). Pericentriolar structures can also be seen grouped around the centriole (Fig 148 & 149). Several Golgi bodies usually grouped together, were situated in the cytoplasm often adjacent

to the nucleus (Fig 151). Mitochondria were present frequently clustered into groups (Fig 152). Desmosomes were found both intracytoplasmically (Figs 153 & 154), and between adjacent cells (Fig 154). Glycogen was abundant, (Fig 154) and non-membrane bounded densely staining droplets were present in the cytoplasm of the BeWo cells. These droplets sometimes had a darker staining band around the periphery (Fig 153). Intracytoplasmic membrane systems (annulate lamellae) were found in the BeWo cells (Fig 156 - 159). They were composed of parallel arrays of membranous cisternae with small annuli or fenestrations at regular intervals (Figs 156 - 159).

Myelin figures were sometimes seen in the BeWo cells (Fig 160). Occasionally cytoplasm containing organelles or other inclusions were found at the centre of these bodies (Fig 160).

Endoplasmic reticulum was abundant (Fig 162). Lysosome - like structures and multivesicular bodies were present in the BeWo cells (Fig 161 & 163). Coated vesicles were seen in a variety of locations:

- (i) at the base of the microvillar surface of the cells (Fig 141).
- (ii) between adjacent cells (Figs 164 & 165)
- (iii) adjoining desmosomes (Fig 166).
- (iv) joining larger smooth membrane vesicles (Fig 167 - 170).
- (v) in the cytoplasm surrounded by actin filaments (Fig 171).
- (vi) joined to the cell surface by tube-like structures (Fig 172-175).

Tube-like structures, similar to those seen associated with coated vesicles were also seen joining larger vesicles (Fig 178).

A structure similar to an iron-binding organelle, described by Ockleford and Menon (1977) in normal placental tissue, was noted on the BeWo cell surface (Fig 176). Dead cells (Fig 177) and other structures which could not be identified were also seen (Fig 179). The villus-like upgrowths noted in light microscopic examination of the BeWo cells (Fig 180), were examined by transmission electron microscopy (Fig 181). They were found to

be composed of a number of cells, some of which appeared to be degenerating. The basal part of the structure seen in Fig 181 was attached to the base of the flask during culture. This area was composed of two cells, which appeared healthy by morphological criteria.

One of these cells was almost completely surrounded by the other and the surrounded cell was lighter staining with fewer organelles, resembling the cytotrophoblast of normal placental tissue. The darker cell has microvilli on its surface and resembles the syncytiotrophoblast of normal tissue.

An outgrowth from one cell was noted which had a strange morphology (Fig 182). It appeared as a dark mass of tissue with a "cauliflower" shape, protruding from a BeWo cell. Higher power examination showed it had a variety of inclusions contained within the "florets" of the "cauliflower". Lipid, glycogen, mitochondria, membrane fragments and various vesicles were identified (Fig 182). Where this structure was in contact with the BeWo cell below there were larger interdigitations between the pieces of tissue and the cell. The BeWo cell itself appeared to have a normal morphology (compare with Fig 185). Further sections of the area showed that at the region of contact between the tissue "growth" and the BeWo cell there were many microvilli (Figs 183 & 184).

#### 5-4. BeWo Cell Incubations.

##### 5-4.1. Short incubations of BeWo cells with Au(18)-IgG.

###### 5-4.1.1. Transmission electron microscopy (TEM)

Transmission electron microscopy of cells incubated with Au(18)-IgG for 30 minutes showed uptake of a few particles of the probe. Particles of the probe were found:-

- (i) in coated vesicles (Fig 186)
- (ii) in large electron-lucent vesicles in the cytoplasm of the cells (Fig 187).

In the control incubations, where the cells were incubated with Au(18) only, for 30 minutes, particles of gold were again seen in large pale vesicles (Fig 188).

## 5-4.2. Long incubations of BeWo cells with Au(18)-IgG.

### 5-4.2.1. Transmission electron microscopy

Transmission electron microscopy of BeWo cells incubated with both the Au(18)-IgG probe and the Au(18) showed uptake of the probes. Gold particles were found localised in a family of structures which will be termed cytoplasmic bodies (CB's). These may be classified as follows:

- (i) small electron-lucent bodies (Fig 189, 190), sometimes containing small vesicles within them (Fig 189).
- (ii) large electron-lucent bodies containing smaller vesicles within them (Fig 173), sometimes the membrane of these large bodies appeared to have coated regions (Figs 191 - 194).
- (iii) large bodies of low electron density, again sometimes containing small vesicles (Figs 195 & 196) or sometimes containing glycogen (Fig 195).
- (iv) large bodies with very dense inclusions (Figs 197 & 198).

It was noted that there were fewer gold particles in the small electron-lucent bodies (only one or two particles), whereas the pale bodies seemed to contain many more particles. Within these bodies the particles appeared to be grouped together (Figs 195 & 199). Similarly there seemed to be less particles in the very dense bodies. Where small vesicles were found in the large bodies the gold particles were located close to these vesicles (Fig 191 & 194).

To show statistically that the appearance of the gold particles into CB's is a sequestration phenomenon the number of gold particles per CB was compared to the number of gold particles in the rest of the cytoplasm using the method given in Appendix XVII. Briefly the number of particles contained in each CB was computed so that a final figure of number of particles per unit area of CB was obtained. CB's which did not contain any gold were also included. The number of gold particles in the cytoplasm

was computed and expressed in the same way. Data was prepared for both the Au(18)-IgG incubations and the Au(18) only incubations (Table 6), and compared using the Mann-Whitney U-test.

	Incubation with Au(18)	Incubation with Au(18)-IgG
Number of particles in $1\mu\text{m}^2$ of cytoplasmic body	$66.2 \times 10^{-3}$	$124.2 \times 10^{-3}$
Number of particles in $1\mu\text{m}^2$ of cytoplasm	$0.824 \times 10^{-3}$	$2.298 \times 10^{-3}$

Table 6 Data from gold-probe and gold only incubations.

Using this data it was investigated:

- (a) if there was a sequestration of gold particles into CB in both the incubation with Au(18)-IgG and the incubation with Au(18) only, and
- (b) if there was a significant difference in the amount of gold particles sequestered into the CB's in the two incubations i.e. if there were more in the CB's in the Au(18)-IgG incubations than in the Au(18) only incubations, indicating that there were specific IgG receptors on the surface of the cells.

A significant difference ( $p < 0.01$ ) was found between the number of particles contained in the cytoplasmic bodies and the number of particles found in the cytoplasm in both the Au(18)-IgG incubations and the Au(18) only incubations, indicating that there is a sequestration of gold particles into the bodies. However no significant difference was found between the number of particles present in the Au(18)-IgG incubations and the Au(18) only incubations.

### 5-4.3. Incubation of BeWo with probe at 2°C followed by warming.

#### 5-4.3.1. Transmission electron microscopy

Transmission electron microscopic examination of cells incubated with the experimental Au(18)-IgG probe and the control Au(18) probe for four hours at 2°C followed by timed warming periods showed adherence of both types of probe to the surface and uptake into the cells. The increase in temperature of the culture medium during warm up of the cells is given in Fig 11.

Different quantities of the probe were found in different regions of the cell according to the duration of the warming period. The location of gold particles in the cells are presented in Table 7.

Both the experimental and control incubations fixed without warming showed gold particles attached to the cell surface, associated with both the microvilli (Figs 200 & 201) and the non-microvillous surface (Fig 200). Some gold particles were found associated with coated pits on the cell surface (Fig 201). In the experimental incubation some gold particles were found in small smooth membrane vesicles (Figs 202 & 203). Some uptake into the cells seemed to have occurred in both cases as some gold particles were seen within the tissue enclosed in membrane - bound structures (Figs 204 & 205). Also in the experimental incubations some gold was found in a tube-like structure just below the cell surface (Fig 206).

After 5 minutes warming fewer gold particles were present on the surface of the cells in both the control and experimental incubations (Figs 207 & 208). Again gold particles were found associated with the microvilli and the non-microvillar surface (Fig 207 & 208).

Fixation after 10 minutes warming showed only a few particles of gold associated with the cell surface in both the incubations (Figs 209 - 211). Gold particles were found in smooth vesicles (Figs 212 & 213) in both incubations. In the experimental incubation particles of gold were found in coated vesicles (Fig 214), in large dense vesicular structures (Fig 215), and lying free in the cytoplasm (Figs 216 & 217). After 30 minutes warming very little gold was present on the cell surface (Fig 218 & 219), in either incubation. In the experimental incubation, particles of gold were found between the basal interdigitations of adjacent cells (Fig 220), lying free within the cytoplasm of the basal interdigitations (Fig 221) and lying free on the basal surface of the cell where it was attached to the base of the culture flask (Fig 222 & 223).

TABLE 7 : CHANGE IN THE CELLULAR DISTRIBUTION OF GOLD PARTICLES ON WARMING FOR DIFFERENT TIME PERIODS.

REGION OF GOLD PARTICLE LOCALISATION.	TIME AFTER WARMING	EXPERIMENTAL CELLS INCUBATED WITH Au(18)-I <sub>2</sub> G AT 0°C			CONTROL CELLS INCUBATED WITH Au(18) AT 0°C			
		0 MIN.	5 MIN.	10 MIN.	30 MIN.	0 MIN.	5 MIN.	10 MIN.
ASSOCIATED WITH MICROVILLI ON THE CELL SURFACE		+++	++	+	+++	++	+	+
ASSOCIATED WITH THE NON MICROVILLIOUS CELL SURFACE		+++	+	+	+++	+	+	
ASSOCIATED WITH COATED PITS ON THE CELL SURFACE		+		+		+		
ASSOCIATED WITH SMOOTH NON-COATED PITS ON THE CELL SURFACE					+			
ENCLOSED WITHIN COATED VESICLES								
ENCLOSED WITHIN SMALL SMOOTH VESICLES		+		+			+	
ENCLOSED WITH LARGE VESICLES ( 100m dia)		+		+		+		
LYING FREE IN THE CYTOPLASM				+				
ASSOCIATED WITH THE BASAL CELL SURFACE				+				

KEY = + 5 particles ++ 5 particles +++ 20 particles.

## CHAPTER 6 : DISCUSSION OF THE METHODS AND PROBES USED.

A number of different techniques have been used to investigate the route taken by human immunoglobulin G, when it is transported across the human placenta. These include perfusion studies, tissue incubations and cell culture systems. Two immunoglobulin probes, tritiated IgG and IgG coupled to colloidal gold, have been used in these experimental systems to study the transport process at both the light and electron microscope level.

For clarity the experimental methods and the probes will be discussed in this chapter and the results obtained using these methods will be discussed in Chapter 7.

### 6-1. THE METHODS

The inaccessibility of the human placenta in pregnancy prevents direct examination of its transfer function, and although animal models have contributed greatly to a general understanding of placental function there are many interspecies differences and one cannot assume that findings from animal studies apply to the situation in man.

#### 6-1.1. The Perfusion System

The anatomy and circulation of the human placenta make it an ideal organ for perfusion techniques. In addition perfusion would appear to produce less disruption of placental integrity than the methods discussed below.

One of the first attempts to perfuse both fetal and maternal circulations was carried out by Krantz et al., (1962), using the entire placenta and piercing the basal plate with multiple tubes to simulate the original input through the spiral arterioles. This technique is usually unsuccessful since intervillous perfusion is usually inadequate owing to tissue damage caused by incomplete abscission or uneven abscission. It is extremely rare to find a whole placenta free from damage. Nesbitt et al., (1970) note that only 10% of placental tissue available is suitable for investigation because of tissue damage.

The isolated cotyledon perfusion method (Schneider et al., 1972) exploits the fact that each cotyledon has its own individual circulation, therefore a suitable, undamaged cotyledon can be selected and only this small volume is perfused, rather than the whole placenta. Although the mechanisms for in vitro maintenance are elaborate, the duration of perfusion is rarely greater than six hours (Stromberg, 1980).

One of the main criticisms of perfusion studies is that the tissue may be degenerating and therefore any results obtained from such studies may not be a true reflection of the situation in vivo. Several studies have investigated the physiological vitality of the placenta during perfusion experiments. Challier et al., (1976) measured oxygen consumption during perfusions and found them similar to that in vivo in a number of species. However Penfold et al., (1981), showed that all types of plastic tubing investigated lost a certain amount of gas across their walls and a moderate oxygen consumption could be measured even without a placental preparation in the circuit. Georke et al., (1961) measured glucose consumption and found it remained constant for about twelve hours at a rate of 1g / kg of placenta / hour. Penfold et al., (1981) carried out extensive studies and examined pH levels, potassium concentrations, lactate dehydrogenase, ATP and nucleotide levels. They concluded that normal physiological conditions were approximated and viability of the tissue was maintained after 1-2 hours perfusion. A study by Schneider et al., (1972), using three substances known to be transported by different transport mechanism in the placenta, demonstrated that these mechanism were all operating during perfusion experiments. Evidence for the ultrastructural integrity of the perfused tissue comes from electron microscopic examination of tissue from perfusion experiments described in this thesis, and together these results indicate that for a limited period at least the perfused placenta is intact and functions in a similar way to that in vivo.

### 6-1.2. Tissue Incubations.

Incubation of placental tissue in culture medium with a probe provides an alternative method to the perfusion system to investigate the same problem.

Preparation of tissue for such incubations is considerably quicker than that for perfusion experiments and so offers the advantage that the placental tissue is fresher and degeneration is not as advanced. Comparison of results between the two types of experiments permits their validation. Comparison of tissue fixed at delivery with incubated tissue by electron microscopy has demonstrated the ultrastructural integrity of the incubated tissue (Tighe et al., 1967 ; Ockleford and Menon, 1977; Ockleford and Clint, 1980).

Evidence for tissue function under incubation conditions comes from a study by Ockleford and Clint (1980) who demonstrated active uptake of a radiolabelled macromolecule over a period of 1 hour at 37°C using this tissue incubation method.

### 6- 1.3. Cell Culture

#### 6-1.3.1. Placental cells

There has been varying degrees of success in establishing trophoblast cells in monolayer culture from human placenta (Gey et al., 1938; Loke and Borland, 1970; Taylor and Hancock 1973; Stromberg et al., 1978). It was soon discovered that monolayers of trophoblast cells could only be maintained successfully for a short period of time in primary culture (7-10 days) owing to fibroblastic overgrowth. It was not possible to subculture and maintain cell lines derived from these cultures using standard tissue culture techniques. Although most methods for culture of trophoblast cells recommend the use of first trimester placentae (Stromberg, 1980), Lueck and Aladjem (1980) had very successful results using term placentae. They reported successful inhibition of stromal growth using a high density plating, low manipulation method. This produced hypoxic conditions during the first three

weeks of culture, fibroblast growth was inhibited and trophoblast proliferated. Cultures were successfully maintained in their laboratory for four passages over an eight month period. Cell morphology and determination of hPL levels in the culture medium confirmed the structural integrity and metabolic viability of the cells. This method was used to culture trophoblast cells for the incubation experiments described in this thesis. Electron microscopic examination of cells grown in this way show them to retain all the ultrastructural characteristics of trophoblast cells. Electron dense syncytial elements and microvilli are present on the surface of the cells, and below this are the more electron-lucent cytotrophoblast and stromal elements.

#### 6-1.3.2. Choriocarcinoma cells

The BeWo cell line are trophoblastic cells derived from a human choriocarcinoma. The cell line was originally established by Hertz (1961) by serial transplantation in the hamster cheek pouch. It was later established in tissue culture by Pattillo and Gey (1968). The BeWo cells retain the morphology, and biochemistry of trophoblastic tissue. Immunofluorescence studies have shown the presence of keratin fibres in these cells indicating their ectodermal origins (Ockleford, unpublished observations). Biochemical studies have shown they produce HCG and other placental hormones (Pattillo and Gey, 1968). Electron microscopic examination of these cells in this study (section 5-3.2.) show they possess many trophoblastic features, for example they have a microvillous border at their surface. Some cells were found to have some more electron dense tissue below the surface microvilli as if the cell was differentiating into syncytiotrophoblast and cytotrophoblast layers. The cells were found to possess most of the organelles found in trophoblast cells, as well as some additional structures which it was not possible to characterise. Although the cells are difficult to grow, requiring frequent medium changes owing to high glucose metabolism, they are an ideal cell to investigate trophoblast transport.

## 6-2. THE PROBES

The two probes used in the systems described above were 1) tritiated IgG and 2) IgG coupled to colloidal gold particles. Tritiated IgG permits visualisation, via autoradiography, of the localisation of IgG during transport, while the colloidal gold-IgG complexes permit visualisation of transport at the ultrastructural level and identification of the cellular components involved.

### 6-2.1. Tritiated IgG.

Human IgG was labelled using N-succinimidyl propionate (NSP). NSP reacts with proteins at pH 8.5 substituting a CH<sub>3</sub> and CH<sub>2</sub> group on to the amino terminal regions of the IgG molecule by a condensation reaction (see Fig 224) (Ockleford and Clint, 1980). The amino terminals are situated in the Fab portion of the IgG molecule (Edelman et al., 1969). Since it is the Fc part of the molecule which mediates binding to the syncytiotrophoblast receptors (Gitlin and Gitlin, 1974; Jenkinson et al., 1976), it is unlikely that this relatively minor change at the opposite end of the molecule would interfere with the binding.

Tritiated IgG is a useful probe in investigating uptake and transport across placental tissue. It is simple and quick to prepare and it is easily detected at the light microscope level by autoradiographic techniques. The main disadvantage is that it is not possible to localise the exact source of the radioactivity. However methods are available to calculate the most likely source within certain confidence limits.

The validity of the <sup>3</sup>H-IgG probe was demonstrated by Ouchterlony immunodiffusion. A single precipitation line demonstrated that IgG was present and subsequent autoradiography of the Ouchterlony plate showed radioactivity was present in this precipitation line.

### 6-2.2. Colloidal gold-IgG.

Colloidal gold was first proposed as a specific electron dense marker for transmission electron microscopy (TEM) by Faulk and Taylor (1971), and later for scanning electron microscopy (SEM) by Horisberger et al., (1975). It is now a well known, widely used probe and specific markers have been produced using a variety of macromolecules. For example antibodies (Gerber et al., 1973), lectins (Bauer et al., 1972), enzymes (Geoghegan and Ackerman, 1977), various proteins (Romano and Romano, 1977; Schwab and Thoenen, 1978), polysaccharides (Horisberger and Rosset, 1977; Horisberger et al., 1978 a) and glycoproteins (Geoghegan and Ackerman, 1977; Horisberger et al., 1978 b; Horisberger and Vonlanthen, 1978) have all been successfully linked to colloidal gold particles. The gold markers have been used to label a number of different systems, such as bacteria (Bauer et al., 1974; Faulk and Taylor, 1971; Garland et al., 1975), slime moulds (Horisberger et al., 1978 b), kidney cells, blood platelets, lymphocytes, viruses (Romano and Romano, 1977), yeasts (Bauer et al., 1972; Gerber et al, 1973; Horisberger and Rosset, 1976; 1977; Horisberger and Vonlanthen, 1977; Horisberger et al., 1978 a), plant protoplasts (Burgess and Linstead, 1977), blood platelets (Romano and Romano, 1977), neurones (Schwab and Thoenen, 1978), hepatocytes (Horisberger and Vonlanthen, 1977), pancreatic tissue (Roth et al., 1978), red blood cells (Horisberger and Rosset, 1977; Horisberger and Vonlanthen, 1979). A comprehensive bibliography of gold labelling studies is given by Goodman et al. (1980).

Gold markers can be produced in a range of sizes from 2 - 150nm (Horisberger and Rosset 1977; Horisberger and Volanthen, 1979; Horisberger et al., 1975) by varying the amount of reducing agent present during colloid preparation. Provided gold particles of sufficiently different sizes are used, multiple marking experiments can be conducted using different proteins.

Much of the basic methodology for the preparation of colloidal gold - macromolecule conjugates is now established (Geoghegan and Ackerman, 1977; Geoghegan et al., 1978; 1980; Horisberger and Rosset, 1977; Horisberger, 1979; Goodman et al., 1980). Scrupulously clean glassware is essential throughout the preparation as contamination interferes with monodispersion of the colloid (Geoghegan and Ackerman, 1977). Two methods are available for the preparation of the gold colloid. Small particles (2 - 5nm in diameter) are produced by reductions of a solution of aurochloric acid with phosphorus saturated ether (Faulk and Taylor, 1971). Larger colloidal gold particles (18-150nm in diameter) are prepared by reducing aurochloric acid with sodium citrate (Frens 1973; Horisberger and Rosset, 1977).

Particles of colloidal gold in water carry a net negative charge (Weiser, 1949). Addition of electrolytes alters the electrochemical environment and allows the particles to adhere and flocculate (Weiser, 1949). Flocculation can be prevented by addition of a protective protein coat to the particles (Jirgensons and Straumanis, 1964). This is achieved by mixing the colloidal gold solution with a suitable amount of soluble protein (Faulk and Taylor, 1981).

The optimal amount of protein or macromolecule required to stabilize a gold solution is determined by exposing constant amounts of gold to increasing amounts of macromolecule. Sodium chloride solution is then added to flocculate any unstabilized gold particles (Horisberger and Rosset 1977). Flocculation is seen as a change in colour of the gold solution from red to light blue which can be determined visually or spectrophotometrically (Horisberger and Rosset, 1977). Thus the minimum concentration of macromolecule at which the addition of a fixed amount of sodium chloride does not cause flocculation can be quantitated accurately (Horisberger and Rosset, 1977).

The phenomenon of protein binding to the gold particles is not well understood, however electrostatic forces are thought to be active (Horisberger and Rosset, 1977). Resistance to salt induced flocculation suggests very tight binding, and the protein appears to effectively screen the gold from ionic effects (Goodman et al., 1981). Some studies indicate that stabilization of the gold colloid is dependant on the size of the particles, and the molecular weight of the protein (Horisberger and Rosset 1977; Roth and Binder, 1978). Adsorption of proteins to colloidal gold is dependant upon pH, and is influenced by the interfacial tension, solubility and electric charge of the macromolecules (Geoghegan and Ackerman, 1977). Efficient adsorption of the protein to the gold occurs at, or just on the basic side of the pI of the protein (Geoghegan and Ackerman, 1977; Goodman et al., 1980). At its pI the protein is least soluble and is in a neutral state; maximum surface tension also occurs at the pI. It is suggested that at its pI the protein is in a weakly hydrated state and would be most readily absorbed onto the hydrophobic surface of the colloidal gold particles. (Goodman et al., 1980). There is some debate as to whether the protein is absorbed as a monolayer around the gold particle, (Horisberger and Rosset, 1977; Roth et al., 1978) or as several layers of protein described as a multilamellar arrangement (Goodman et al., 1980; 1981) . A multilamellar protein shell might affect the stability of the probe since some of the probe could desorb from the gold. This would result in the presence of free competing proteins in the solution and reduce the labelling efficiency of the probe. There is some evidence for desorption of protein. <sup>125</sup>I-tetanus toxin conjugated to colloidal gold was incubated with rat serum for 14 hours at room temperature. After this time 9% of the initial radioactivity was found in the supernatant (Schwab and Thoenen, 1978). The stability of the probe is enhanced by the addition of polyethylene glycol (PEG) to the solution. Tritiated ConA-colloidal gold was incubated with conditioned medium in the absence of PEG for 3 hours at 37°C, and 40% of the initial radioactivity was in the supernatant.

When PEG was present during the incubation, release of radioactivity was only 15% (Goodman et al., 1980; 1981). In most methods describing the preparation of gold-protein probes PEG is routinely added to the final buffer in which the probe is to be stored. (Horisberger and Rosset, 1977; Goodman et al., 1980; 1981; Geoghegan and Ackerman, 1977).

Different protein-gold probes appear to have different stabilities. 5nm gold particles labelled with antisera were stable for at least six months at 5°C (Faulk and Taylor, 1971). HRP - colloidal gold retained its activity for at least 14 months (Geoghegan and Ackerman, 1977). Most authors recommend storage at 4°C under sterile conditions or with a preservative added. Freezing destroys the complex (Faulk and Taylor, 1971).

In the experiments performed in this study, the IgG-gold probe was washed before use to remove any desorbed proteins which might have been present in the solution and remove any gold particles which were no longer coated with protein due to this desorption. The colloidal gold-protein preparation has several distinct advantages as an electron microscope marker. It is quick and straightforward to prepare as well as being relatively inexpensive. It is easily identifiable by TEM as very electron dense uniform particles which cannot be confused with other cell or tissue components. Only a small amount of protein is needed to label the colloid, and the macromolecules immobilized in the gold particles retain their specific binding properties (Horisberger, 1979; Goodman et al., 1980; 1981). The probe may be prepared in a range of sizes thus permitting multiple labelling studies (providing the sizes of colloidal gold particles are significantly different).

There are a few disadvantages which include the fact that as the particle size increases so does the heterogeneity of the solution so some caution is necessary when considering multilabelling studies (Goodman et al., 1980; 1981). It is not a suitable

probe for quantitation of receptors since only the smallest sizes will not interfere significantly with binding. A study by Horisberger and Vonlanthen (1979) used three different sized markers to label red blood cells and found that binding was less than that for the total calculated number of receptors. Therefore care must be taken when interpreting such studies as absence of the marker does not necessarily imply that there is an absence of receptors, merely that a steric hindrance phenomenon may be operating. However the colloidal gold system has a definite advantage over other marker systems such as ferritin, which since it is often an intrinsic molecule of some cell systems may confuse and complicate the final interpretation.

The colloidal gold-IgG probe was validated by 1) immunoprecipitation with anti-IgG and examination of the resultant pellet by electron microscopy and 2) immobilisation by a Sepharose - protein A preparation. Protein A is known to have affinity for IgG and the retention of the gold in the preparation, shown by the pink colour, indicates that IgG and the colloidal gold particles are closely associated.

## CHAPTER 7:DISCUSSION OF THE RESULTS

### 7-1. Light and electron microscopy of term and first trimester human placental tissue.

There are many comprehensive histological and ultrastructural studies of the human placenta at all stages of its development (Getzowa and Sadowsky, 1950; Boyd and Hughes, 1954; Wislocki and Dempsey, 1955; Alvarez, 1964; Strauss et al, 1965; Boyd and Hamilton, 1966; 1967; Salazar and Gonzalez-Angulo, 1967; Boyd et al., 1968 a and b; Boyd and Hamilton, 1970; Okudaira et al., 1971; Stein et al., 1974; Fox and Agrofojo-Blanco, 1974; Wynn, 1975; Fox, 1978 a and b; Dearden and Ockleford, 1983).

#### 7-1.1. Light microscopy

In this study the structure of both first trimester and term placenta was examined by light and electron microscopy and the organelles and other inclusions described by the above authors were identified.

Examination of pieces of placental tissue at the light microscope level show a tree-like structure with a central core region which contained the fetal capillaries and red blood cells.

Sections of resin embedded material stained with toluidine blue showed the tissue to be composed of an outer darker layer of syncytiotrophoblast, with a microvillous surface. Electron dense nuclei were scattered throughout the cytoplasm and large and small vesicular structures could be distinguished. Sometimes densely staining droplets were seen.

Beneath the syncytiotrophoblast were paler staining cytotrophoblast cells resting on a basement membrane. At term these cytotrophoblast cells were sparse in distribution and the syncytiotrophoblast was often in direct contact with the basement membrane. In first trimester placenta these cytotrophoblast cells form a

more or less continuous layer beneath the syncytiotrophoblast layer.

Occasionally cells of an intermediate morphology between cytotrophoblast and syncytiotrophoblast were seen. These may have been cells in the process of forming syncytiotrophoblast, and have previously been reported to be present by Boyd and Hamilton (1970). Beneath the basement membrane a central or core region is present which contains the fetal capillaries and connective tissue fibres and cells, also specialised macrophages called Hofbauer cells. Occasionally the fetal capillaries lie directly adjacent to the syncytiotrophoblast tissue which is extremely thin. These areas are termed vasculo-syncytial membrane (VSM'S). It has been suggested that they are specialised regions adapted to facilitate gas exchange (Baker et al., 1944; Getzowa and Sadowsky, 1950; Becker and Bleyl, 1961). Evidence in favour of this idea comes from the finding that a deficiency of VSM'S is associated with a high incidence of fetal hypoxia (Fox 1967). Although the capillary and trophoblastic walls are thinner overall in the vasculo-syncytial membranes, immunofluorescence staining of polymeric cytoskeletal proteins in these areas show no obvious local reduction in the thickness of this component of the epithelium (Ockleford et al., 1981). Other features discernable at the light microscope level in placental tissue are groups of syncytial nuclei which are termed syncytial knots. It has been suggested that this grouping of nuclei together is a sequestration phenomenon (Fox, 1965) collecting together aged nuclei as they are replaced by the proliferative activity of the cytotrophoblast. This idea is supported by the fact that only those nuclei in the knots show morphological changes associated with ageing (Fox, 1965; Boyd and Hamilton, 1970). Also villi with knots have a higher total number of nuclei than villi without knots. Sometimes syncytial knots from adjacent villi fuse together forming an intervillous bridge. (In vitro fusion of knots has been demonstrated by Jones and Fox,

1977). It has been suggested that these bridges form an internal strut system and absorb stress and strain within the placenta. Clint et al., (1979) observed by scanning electron microscopy, a population of villi which did not possess any blood vessels. They suggested that these were anchoring villi and had a similar function to these intervillous bridges of absorbing stress and strain. Rupture of such bloodless structures would not have such potentially dangerous consequences as would rupture of normal villi resulting in a possible fatal mixing of fetal and maternal blood.

#### 7-1.2. Scanning electron microscopy (SEM)

Scanning electron microscopic examination of both term and first trimester showed the tissue to be covered with numerous microvilli. These are just visible with the light microscope and were first described as a "brushborder" by Katschenko (1885). The distribution of the microvilli on the syncytiotrophoblast surface is variable with some areas of tissue completely lacking microvilli (Wislocki and Bennett, 1943; Boyd and Hamilton, 1967; Ludwig, 1974; Clint et al., 1979).

#### 7-1.3. Transmission electron microscopy (TEM)

Examination of tissue by transmission electron microscopy showed the typical morphology of placental tissue.

The syncytial nuclei have a distinctive appearance with coarse chromatin scattered throughout the nucleoplasm and aggregated around the edge of the nuclear envelope. Tangential sections through the nuclei show the presence of numerous nuclear pores, a characteristic of synthetic activity (Tighe et al., 1967).

Endoplasmic reticulum of both the rough and smooth type is found in abundance in the syncytiotrophoblast and contributes extensively to the vesiculated appearance of the cytoplasm.

Mitochondria are numerous in the syncytium throughout gestation although are sometimes difficult to see since they often have more indistinct cristae than those in the syncytiotrophoblast (Boyd and Hamilton, 1970).

Golgi complex is present in the mature placenta but is difficult to see owing to the intense vesiculation of the syncytial cytoplasm, because this organelle is smaller and less well defined than would be expected of a secretory tissue. It is more easily visible in the young placentae.

Ribosomes are abundant both in the syncytial cytoplasm and attached to endoplasmic reticulum.

Polymeric cytoskeletal proteins including microtubules, microfilaments and intermediate filaments have been found in the syncytiotrophoblast. Wislocki and Bennett (1943) described a birefringent layer immediately below the syncytial plasma membrane. A definite layer of filaments composed of microtubules (Ockleford and Whyte, 1977) and actin filaments (Ockleford et al., 1981) has been identified in this area using immunofluorescent techniques. Ockleford et al., (1981) proposed the name syncytioskeletal layer for this region. Cytokeratins are the only type of intermediate filaments which have been identified in the syncytioskeletal layer (Ockleford, Dearden and Badley 1983) and this finding supports the view that trophoblast is an ectodermal derivative.

Residual bodies containing myelin figures are sometimes seen in the syncytial cytoplasm (Tighe et al., 1967). Glycogen is abundant in the syncytium both in clusters and individual particles. Lipid droplets are most numerous in young placentae and are very sparse at term. Secretion granules are present in the syncytiotrophoblast and contribute to the vesiculated appearance of the syncytial cytoplasm.

There is an abundance of vesicles and vacuoles in the syncytiotrophoblast and these are the main contributors responsible for the highly vesiculated appearance of the syncytial cytoplasm. Large and small vacuoles such as juxtannuclear vacuoles, lagoons, receptosomes, lysosomes and multivesicular bodies are found as well as large and small vesicles such as macropinocytic vesicles and micropinocytic smooth and coated vesicles.

Desmosomes are occasionally found lying free in the syncytial cytoplasm. These are evidence for the formation of syncytiotrophoblast from the fusion of underlying cytotrophoblast cells. Intercellular junctions are also found between the syncytium and the underlying cytotrophoblast cells.

The cytotrophoblast is the germinative layer of the trophoblast and DNA synthesis and mitotic figures are confined to the cytotrophoblast nuclei (Richart, 1961; Galton 1962). Evidence for the production of syncytiotrophoblast from cytotrophoblast cells comes from the occurrence of cells with a morphology intermediate between that of a cytotrophoblast cell and the syncytiotrophoblast (Yoshida, 1964; Boyd and Hamilton, 1966). Other evidence comes from remnants of membrane and desmosomes occasionally found in the syncytial cytoplasm (Pierce and Midgely, 1963; Carter, 1964; Enders, 1965).

Microvillus-like projections are found on the surface of the cytotrophoblast cells interdigitating with those from adjacent cells and with the basement membrane. The cytotrophoblast nuclei are more uniform in shape than the syncytial nuclei and are more electron-lucent with more finely dispersed chromatin. There are usually one or two nucleoli present. It has been suggested that this reflects the less differentiated state of the cytotrophoblast (Stein et al., 1974). Nuclear pores are seen in tangential sections through the nuclear envelope. The cytotrophoblastic endoplasmic reticulum is poorly developed and has few attached ribosomes. Mitochondria in the cytotrophoblast are not as numerous as in the syncytiotrophoblast. They have well defined

cristae (Boyd and Hamilton, 1970) and a pale matrix (Dempsey and Luse, 1971). The Golgi complex is more conspicuous than in the syncytiotrophoblast since the cisternae are more dilated. Vesicles in the Golgi area have been seen fusing with the Golgi cisternae (Rhodin and Terzakis, 1962). A few ribosomes are found attached to the endoplasmic reticulum and there is an abundance of ribosomes lying free in the cytoplasm (Tighe et al., 1967). A network of fine filaments is reported to be present in the cytotrophoblast cells (Tighe et al., 1967; Boyd and Hamilton, 1970). A small amount of lipid is present in the form of droplets (Boyd and Hamilton, 1970). Myelin figures have not been reported to be present. Glycogen is present in large amounts in young placenta (Yoshida, 1964) and diminishes towards term. Secretion granules are less common in the cytotrophoblast than in the syncytiotrophoblast. Lysosomes, multivesicular bodies, macropinocytic and micropinocytic vesicles are found in the cytotrophoblast but are fewer in number than those found in the syncytiotrophoblast.

A few tight junctions are found between the cytotrophoblast cells but the majority of the connections between them are desmosomal.

The main difference between term placenta and first trimester tissue was that first trimester placenta had a complete layer of cytotrophoblast present beneath the syncytiotrophoblast.

## 7-2 THE PERFUSION EXPERIMENTS

### 7-2.1. Perfusion with tritiated IgG

Transport of IgG across the human placenta was demonstrated using a perfused isolated cotyledon system. Samples taken from the venous return supply of the apparatus during the experiments showed an increase in radioactivity with time indicating active transport of the  $^3\text{H}$ -IgG probe. Autoradiography of perfused tissue showed a statistically significant distribution of silver grains (representing the location of the probe). Silver grains were found associated with (i) the syncytial tissue - in large light microscopically visible vesicles and (ii) the endothelial cells of the fetal capillaries. The association of silver grains with the large syncytial vesicles may be comparable to the findings of Willingham and Pastan's (1981). These authors report that after initial uptake, proteins are transferred to a large smooth vesicular structure which they term the receptosome. On the other hand it may be that some of the silver grains originate from radioactive probe localised in coated vesicles in the syncytiotrophoblast. However it is not possible to resolve this question at the light microscope level.

There are several possible criticisms of such an experiment, some of which were discussed in Chapter 6. Another possible criticism would obviously be that the distribution of the probe in the tissue could be a result of diffusion of the probe into the tissue or diffusion of the probe through damaged areas of tissue. Alternatively the appearance of radioactivity in the tissue could be owing to tritium exchange rather than transport of the  $^3\text{H}$ -IgG. Random diffusion of the probe is unlikely since the results obtained indicate specific localisation of the probe in certain areas of the tissue. By the same reasoning tritium exchange is also unlikely. Diffusion of the probe through damaged areas of tissue is also unlikely since light microscope examination of the tissue showed it to be intact.

These perfusions using  $^3\text{H}$ -IgG as a probe give an indication of the regions of the tissue which are involved in the transport process at the light microscope level. However they give no indication of the actual sequence of events which occur and which organelles within the tissue are involved. Attempts to examine the distribution of the probe in the perfused tissue at the electron microscope level, by electron microscope autoradiography, were unsuccessful owing to the small amount of radioactivity in the thin sections.

#### 7-2.2. Perfusion with Au(18)-IgG

Perfusion studies using the gold-IgG probe permitted evaluation of the distribution of the probe at the electron microscope level and identification of the organelles involved in the transport of IgG. Electron microscopic examination of the perfused tissue showed it to be intact and undamaged. Particles of the gold probe were found associated with both the microvillar and non-microvillar surface of the syncytiotrophoblast, closely associated with coated pits on the syncytial surface, enclosed within coated pits, enclosed within smooth membrane vesicles, lying apparently free in the cytoplasm in the basal lamina, in the stroma and in the endothelial cells of the fetal blood capillaries. These results suggest that after initial binding with the surface the probe is enclosed within vesicular structures, then at some point it is released, crosses the basal lamina and enters the endothelial cells. However, it is not possible from these experiments to suggest that the probe is first associated with coated vesicles then uncoated structures or that the coated vesicles lose their coatings or if the probe becomes associated with both coated and non-coated vesicles. These experiments again do not give any indication of the sequence of transport of the probe.

### 7-3. TISSUE INCUBATIONS

#### 7-3.1 Term placenta

##### 7-3.1.1. Term placenta incubated with $^3\text{H}$ -IgG

Autoradiography of tissue incubated with  $^3\text{H}$ -IgG showed a similar distribution of radio-active probe to that found in the perfusion experiments. A statistically significant association of silver grains was found within the syncytial epithelium. In these experiments there were not sufficient data to investigate any possible association between vesicles in the syncytium and the probe nor between the endothelial cells of the fetal capillaries. This was probably owing to the fact that tissue was fixed after 30 minutes incubation and that this was not a sufficiently long period of time for a build-up of transported probe to be apparent. The tissue again appeared to be intact and undamaged when examined by light microscopy.

##### 7-3.1.2. Term placental tissue incubated with Au(18)-IgG

The incubations carried out at both pH 7.0 and 4.2 showed similar results. Particles of the gold-IgG probe were found (i) associated with the microvillar surface of the syncytiotrophoblast, (ii) within large membrane bounded vesicles and (iii) scattered in the cytoplasm. These results are comparable with the results of tissue incubations with  $^3\text{H}$ -IgG and are also similar to the perfusion results. Longer incubations with Au(18)-IgG at pH 7.0 showed particles of probe localised within vesicles of the cytotrophoblast cells and near the basal lamina.

These results will be discussed more fully in conjunction with the findings from the tissue culture incubations.

#### 7-3.2. First trimester placenta incubations.

The selective transport of IgG begins at about 3 months and increases progressively during gestation (Adinolfi, 1975). During the first

trimester of pregnancy the cytotrophoblast cells form a continuous layer beneath the syncytiotrophoblast. These become reduced in number as pregnancy progresses and at term very few are present (Boyd and Hamilton, 1970). It is possible that during the early stages of pregnancy when transfer of IgG is low, the complete layer of cytotrophoblast cells may be acting as a physical barrier to its passage. As pregnancy progresses the transport could then increase as the layer becomes incomplete. Tissue incubations using first trimester placenta were carried out to investigate this proposal.

#### 7-3.2.1. $^3\text{H}$ -IgG incubations

A statistically significant number of silver grains were found associated with the cytotrophoblast layer of the tissue incubated with tritiated IgG.

A significant association was also found between the probe and the stromal experimental tissue. These results suggest that there has been transfer of IgG through the cytotrophoblast tissue and into the stromal region of the tissue. No significant association with the endothelial cells of the fetal capillaries was found.

#### 7-3.2.2. Incubation with Au(18)-IgG

Electron microscopic examination of incubated tissue showed IgG complexes associated with both the microvillar and non-microvillar surfaces of the tissue, and also associated with vesicular structures within the cytotrophoblast cells, as well as near the basement membrane. These results confirm transport of the probe across the tissue through the cytotrophoblast layer, and suggest that it is not the cytotrophoblast layer which is inhibiting the transport of IgG early in pregnancy but that the rate limiting step in the transport process occurs at the level of the endothelial cells of the fetal capillaries. A plausible suggestion would be that the receptor, or some other molecule involved in the transport of IgG across the fetal capillaries, is only activated after about three months of gestation.

## 7-4 TISSUE CULTURE

### 7-4.1. Tissue culture of normal human placental cells

Placental cells were cultured from normal human placentae using the long term culture method of Lueck and Aladjem (1980) by inducing hypoxia conditions in the cultures and thus suppressing fibroblast overgrowth. This method results in the growth of clumps of cells some of which appear to have tubular/fingerlike outgrowths. In some cases these resemble the villous morphology found in normal placenta.

Sections of resin embedded cell clumps stained with toluidine blue and examined by light microscopy showed that the clumps of cells could be divided up into a dark outer layer and a paler inner area similar to the syncytiotrophoblast and cytotrophoblast layers respectively, found in normal placental tissue. Stromal-type areas could also be identified.

Ultrastructural examination showed this same organisational pattern and many of the organelles seen in normal human placental tissue were identified. For example in the syncytiotrophoblast - like regions, microvilli, coated and uncoated pits and vesicles, mitochondria, endoplasmic reticulum and other vesicular profiles were present. Desmosomes, ribosomes and fine filaments were noted. In some areas large numbers of desmosomes were found which suggests that cell fusion has occurred. It may be that some of these cultured cells are attempting to behave as they would in vivo where cytotrophoblast cells fuse to give rise to syncytiotrophoblast tissue (Pierce and Midgely, 1963; Carter, 1964; Enders, 1965).

In both light and electron microscopic examinations very densely staining bodies were observed in some areas of the tissue clumps, usually near the surface. It is possible that these may be endocytosed red blood cells. It was noted that the initial cultures contained a large number of red blood cells but these progressively disappeared and were absent after a few weeks. Ultrastructurally

these bodies have the appearance of lipid residues and most likely are derived from the cholesterol rich erythrocyte membrane. This is particularly likely as lipid membrane is not readily degradable by lysosomal hydrolases and persists within residual bodies as myelin figures (Mahadevan and Tappel, 1968 a & b). Placental tissue has been shown to be capable of endocytosing red blood cells in a scanning electron microscopy study by Clint et al., (1979).

The paler staining cytotrophoblast cells contained the organelles normally found in this tissue in vivo. For example filaments, mitochondria, endoplasmic reticulum, vesicles and ribosomes were all present. Stromal areas were identified by large quantities of collagen-type fibres.

The villus-like upgrowths of the cellular clumps also indicates an "attempt" by the cells to differentiate, although ultrastructural examination showed that they were not organised as a normal villus and there was no differentiation of the tissue into syncytiotrophoblast and cytotrophoblast regions. Various organelles were present within them. Some rounded floating pieces of tissue were noted in the cultures. These could have been pieces of the villous structures which had detached or could be analogous structures to the syncytial sprouts reported by Boyd and Hamilton (1970), which detach from the placenta and appear in the maternal circulation. Similar floating structures have been noted in donkey trophoblast cell cultures (Whyte, 1983, personal communication). Ultrastructural examination of the structures found in the cultures showed them to be composed of degenerating tissue.

#### 7-4.1.1. Incubation studies using Au(18)-IgG

Incubation of cells with Au(18)-IgG probe at 2°C for 4 hours enables binding and subsequent saturation of the receptors, while internalisation by pinocytosis is inhibited and receptor mediated endocytosis is greatly reduced. By removal of the probe by washing the cells in cold culture medium, and then subsequent warming, the route of the receptor associated probe has been followed.

Fixation of the cells immediately after washing at 2°C showed association of a few particles of gold with the cell surface. After 60 minutes incubation, particles of the probe were found within large vesicular structures, indicating some uptake and transport of the probe had taken place.

#### 7-4.2. BeWo cells

This choriocarcinoma cell line has some similarities with the normal cultured placental cells. Microvillous or filopodial structures were found around the edges of the BeWo cell clumps and some upgrowth structures were observed attached to the cells below by fine filaments.

In some electron micrographs the tissue appeared to be divided into two layers, a darker upper layer and a lighter layer beneath, similar to the division of normal human placenta into electron-dense syncytiotrophoblast and electron-lucent cytotrophoblast.

Ultrastructural examination of the cells showed all the organelles common to normal placental tissue to be present. The nuclei of the BeWo cells were often irregular in shape with many invaginations. Invagination of the nuclear envelope is often a sign of an abnormal or malignant cell (Lutzner & Jordan, 1968). This feature is sometimes found in normal cell types and in these cases is usually correlated with function. For example both smooth and striated muscle nuclei have been shown to be elongated in shape in the relaxed phase and highly invaginated after contraction (Lane, 1965; Franke & Schinko, 1969). Some nuclei are known to change shape as the cell ages eg. the nuclei of polymorphonuclear neutrophil leucocytes become segmented and lobed with increasing age (Ghadially, 1975). In the case of the BeWo cells it is likely that their highly invaginated nuclear shape is a sign of their high metabolic rate. They are a very active cell line producing a variety of placental hormones and have a high glucose requirement.

Other cells which have high metabolic rates have also been reported to have invaginated nuclei, for example the cells of silk-spinning glands of certain insects have highly irregular shaped nuclei (Lozinski, 1911).

The nucleoli of the BeWo cells were usually prominent and often more than one was present. Sometimes the nucleolus was located near the margin of the nuclear envelope. Ghadially (1975) reports that this is often the case in the rapid growth phase of tumours. Numerous nuclear pores were found in the BeWo cells. In some tangential sections the pores were visible as circular annuli. Each annulus often exhibited a dense granule in the centre similar to that described by Rhodin (1963). The number and size of nuclear pores present in a cell has been correlated with metabolic activity. It has been reported that active tissues have larger and a greater number of pores whereas cells with diminished metabolic activity have a reduced number (Merriam, 1962; Yasuzumi et al., 1967; Blackburn & Vinijchaikul, 1969; Sucker - Franklin, 1968).

Generally there was only a small amount of heterochromatin present in the BeWo cell nuclei, most of the chromatin being in the active euchromatin form. This again correlates with an active cell.

The BeWo cells possessed microvilli and longer filopodial structures on the surface of the cells. These are characteristic features of normal placental tissue and indicate the origin of this cell line.

A definite layer of filaments was often seen just below the surface microvilli and may correspond to the syncytioskeletal layer described by Ockleford et al., (1981). Similar filaments were seen within the microvilli when they were cut in transverse section. Other filaments were seen apparently randomly distributed throughout the cytoplasm, some were gathered into bundles. These were probably cytokeratin filaments since they were of a similar size to these filaments. Microtubules were also found throughout the cytoplasm, adjacent to the nucleus. Immunofluorescent staining of BeWo cells

using antitubulin has shown labelling over the cells with discrete areas labelled which are distant from the nucleus. These could correspond to microtubule organising centres (Ockleford, Dearden and Badley, 1983). Centrioles were occasionally found in the BeWo cells and often pericentriolar material was found near them. Centrioles are seldom observed in normal placental tissue but material similar to the pericentriolar material does occur.

Golgi bodies were found, often grouped together in the cytoplasm. In one case five were found close to each other and adjacent to the nuclear envelope. The presence of large numbers of Golgi is again indicative of a high metabolic rate.

Mitochondria were present in the BeWo cells. These were often found grouped together in clusters. Many desmosomes were observed both within the cells and between adjacent cells. Desmosomes are sometimes found in the syncytiotrophoblast of normal placental tissue and it is well known that the mechanism of syncytiotrophoblast formation is by fusion of the underlying cytotrophoblast cells (Pierce & Midgely, 1963; Carter, 1964; Enders, 1965). The desmosomes found in the syncytiotrophoblast are thought to be the membrane remnants of this fusion. It is possible that the BeWo retain part of this ability and the presence of desmosomes in the cells indicates that the cells are attempting to form syncytiotrophoblast.

Intracytoplasmic membrane systems or annulate lamellae occurred in the cytoplasm. These were composed of parallel arrays of cisternae with small annuli or fenestrations at regular intervals. The occurrence of annulate lamellae is documented in vertebrate and invertebrate germ cells, embryonic cells and some tumour cells. Very occasionally they have been found in somatic cells. The structure of annulate lamellae closely resembles the structure of nuclear envelope and when they occur close to the nucleus they are orientated parallel to it. Because of this similarity to nuclear envelope it has been suggested that it is derived from it.

The functional significance of annulate lamellae is unknown although there are a number of theories which have been put forward. These include that they are fragments of nuclear membrane left behind after mitosis; they carry genetic material from the nucleus to the cytoplasm; they provide a framework for the collection and assembly of certain substances during certain stages of development; and they provide membrane material for subsequent morphogenetic activities. There is very little evidence to support any of these ideas. Perhaps the most likely theory is that annulate lamellae have a role in cell growth and differentiation, since they are more developed and occur more frequently in embryonic and tumour cells (Kessel, 1968). Other organelles found in the BeWo cells included densely staining droplets which were probably lipid since there was no enclosing membrane around them; glycogen was abundant, ribosomes were found. There were also a variety of vesicular and vacuolar structures. These included coated vesicles, larger vesicles with coated areas on their membrane and also multivesicular bodies. In some cells coated vesicular structures appeared to be connected to the surface of the cell by a membrane tubular structure. Other structures were found within the BeWo cells which could not be identified, for example the "cauliflower-shaped" outgrowth. The 'florets' of this structure contained a variety of organelles and other inclusions but did not appear to have any organised arrangement. It is possible that cells which are degenerating are extruded into the surrounding medium in this form. Similar rounded raised structures have been seen on the surface of BeWo cells examined by scanning electron microscopy (Ockleford, unpublished observations). Small fragments of tissue were also noted floating in both the BeWo culture medium and the placental tissue culture medium. These may represent pieces of the extruded structures since when examined by electron microscopy they appeared to be composed of degenerated tissue.

#### 7-4.2.1. Incubation with Au(18)-IgG

Incubation of BeWo cells with Au(18)-IgG probe for 30 minutes at 37°C resulted in uptake of the gold into the cells. The probe was

found in coated vesicles and within large electron-lucent vesicular structures. However cells which were incubated with Au(18) on its own also showed uptake into large electron-lucent vesicles. Incubation of the cells with either Au(18)-IgG or Au(18) alone for a longer period (18 hours) showed accumulation of the probe in a range of vesicular structures from small vesicles to very large lysosomal type structures. Statistical analysis of the number of particles in the cytoplasm of the cell and these vesicular structures or cytoplasmic bodies (CB's) showed that there was a definite sequestration of the gold particles into the CB's but no significant difference between the number of particles in CB's in the experimental situation (incubation with Au(18)-IgG) or the control situation (incubation with Au(18) only).

It was noted that in the CB's which contained smaller vesicles within them, the gold particles were not enclosed within these small vesicles but were closely associated with the outside. A similar finding was reported by Haigler et al. (1979) using an epidermal growth factor-ferritin probe in a human carcinoma cell line. They suggested that the vesicle fusion process with larger multivesicular bodies inverts the vesicles as they enter. This membrane 'flipping' phenomenon can be caused by pH changes and will be discussed more fully later.

Some of the larger vesicles were found to possess coated areas suggesting fusion of coated vesicles with them. In this size of vesicle the gold particles were usually close to the edge of the vesicle whereas in the larger CB's they were more centrally located and often clumped together. This could be owing to the acidic nature of these lysosomal structures which would cause clumping of the protein coated gold particles.

It was noted that there were always many more gold particles in these larger vesicles than in the smaller ones. It is possible that either the probe is stored here or that this is its final destination and it is transported no further. Evidence in favour

of this latter suggestion comes from the fact that large CB's were found which had a much denser appearance similar to the residual lysosomal bodies found in other tissues, and these also contained large numbers of gold particles.

Overall the results appear to suggest that both Au(18) particles alone and IgG coated particles are taken up effectively by the tissue. At 37°C both fluid phase endocytosis and receptor mediated endocytosis would be occurring at the same time. The build-up of gold particles in the large cytoplasmic bodies would be a consequence of this phenomenon. The fluid phase pinocytic pathway may be masking the less obvious transport pathway occurring by receptor mediated endocytosis. Ockleford and Clint (1981) suggested that two uptake pathways exist. They proposed that uptake of protein in large endocytic vesicles is responsible for approximately 80% of uptake. They also reported that this mode of uptake is sensitive to pharmacological agents and low temperature. The other uptake pathway, mediated by micropinocytic vesicles, was shown to be less sensitive to low temperature. The following experiments were based on this information and were designed to investigate the receptor mediated route of uptake.

#### 7-4.2.2. Incubation of BeWo cells with Au(18)-IgG probe at 2°C

BeWo cells were incubated with either Au(18)-IgG or Au(18) only for 4 hours at 2°C. This was in order to saturate all the surface IgG receptors. The cells were then washed with cold medium to remove all traces of unbound probes and then cells were either fixed immediately (to show the distribution of probe bound to receptors or otherwise tightly adherent to the cell surface) or after warming to 37°C for a specific period of time (to show internalisation). Although fluid phase pinocytosis occurs at 37°C, it would not be visualised by these experiments since the washing procedure ensures that there are no gold particles remaining in the fluid when the cells are warmed.

Results of these incubations showed different quantities of gold particles localised on different areas of the cell depending on the length of incubation. A similar distribution was found for both the Au(18)-IgG and Au(18) only incubations.

Many particles were found associated with both microvillar and non-microvillar surfaces of the cells fixed immediately after washing. Some particles of gold were found associated with coated pits on the cell surface. In the Au(18)-IgG incubations some particles were found enclosed in both small smooth vesicles and within larger vesicles. In the control situation (ie Au(18) only incubations) particles of gold were found in the larger vesicles only. After five minutes warming fewer particles were present on the cell surface than those fixed immediately after washing. No particles were found within the cells but in the Au(18) only incubation some particles of gold were found associated with smooth pits on the cell surface. After 10 minutes warming a few particles of gold were found on the cell surface, and none were found associated with coated pits in the Au(18) only incubations, although some were seen in the Au(18)-IgG situation. It was at this 10 minute incubation that the results found in the two incubations differed. In the Au(18) only incubations some particles were found within small smooth vesicles while in the Au(18)-IgG incubations gold particles occurred in small smooth vesicles, large vesicles and lying free in the cytoplasm.

After 30 minutes warming only a very few particles of gold were seen on the cell surface. In the Au(18) only incubations no gold was found within the cell but in the Au(18)-IgG incubations gold was found near the basal lamina. These results again imply that both the Au(18)-IgG probe and the Au(18) only are taken up by the cells by a common mechanism. It is possible that there are two micropinocytotic routes operating. Non-specific binding sites on the surface may bind the Au(18) particles while specific IgG receptors may bind the Au(18)-IgG particles. These receptor - ligand complexes

may then be internalised either within the same vesicles or in separate vesicles. Huxham (1982) identified two different ligands in the same coated vesicle. If the two ligand-receptor complexes were internalised in the same vesicle, selection of IgG for specific transport must take place at a later stage. Selection of some sort does seem to occur since it was only in the Au(18)-IgG incubations that probe was found lying free in the cytoplasm and basal lamina. Since the pathway seems to be the same for both Au(18) and Au(18)-IgG probes upto the point of inclusion into large vesicular bodies in the cytoplasm a possible suggestion is that selection occurs at this point possible by a similar mechanism to that of virus infection. This will be discussed later.

GENERAL DISCUSSION

## CHAPTER 8 General Discussion of all experiments

The location of the probe in each of the experimental situations was very similar i.e. associated with the surface microvilli, associated with coated pits, within both smooth and coated vesicles and enclosed in larger vesicular structures with coated regions. Probe was also found free in the cytoplasm close to the basal lamina, and associated with the endothelial cells of the fetal capillaries. This correlation between location of the probes in each of the experiments is evidence that a similar transport mechanism is operating in each case and also validates the experimental methods used.

Other workers have described localisation of a variety of protein probes in similar organelles in a variety of cell systems. For example EGF - ferritin, in human carcinoma A-431 cells (Haigler et al., 1979), low density lipoprotein in human carcinoma cells (Anderson, et al., 1981; Goldstein, et al., 1979),  $\alpha_2$  macroglobulin in Swiss 3T3 cells (Dickson et al., 1981) and many others.

Schlessinger (1980) carried out uptake studies using several different polypeptide hormones and suggested that the internalisation process could be divided into several stages; the initial stage being binding of the ligand to the membrane receptors. Binding of the IgG-probe to the surface placental membrane was seen in all of the experiments. However binding does not necessarily ensure that the bound ligand will be transported. Insulin is known to bind to human placental membranes (Gitlin and Gitlin, 1976) but is not readily transported across the placenta, at least in the early stages of gestation. Binding may be the initial step in transport but this evidence suggests that an additional mechanism is required to complete the transfer.

The next stage in the internalisation process as described by Schlessinger (1980) is clustering or aggregation of the ligand in coated pits. A study by Anderson et al. (1976) showed that coated

pits are clustering regions for low density lipoprotein. Subsequently many ligands have been found to cluster in these pits including  $\alpha_2$  macroglobulin and epidermal growth factor (Willingham et al., 1979; Willingham et al., 1981 ).

Definite clustering of probe was not seen in either perfusion experiments, tissue incubations or placental or BeWo cell incubations, although there was some association of probe with coated pits. The absence of clustering is probably owing to the concentration of probe used in the experiments and the time of fixation of the tissue. Dickson et al., (1981) reported that in their studies the degree of clustering was dependent on the probe concentration. In the perfusion experiments transport of the probe was taking place over a large area and consequently the probe was diluted by a large factor. Under such circumstances it was unlikely that there would be enough probe present in one area to show the clustering phenomenon. In the tissue incubations the experiments were conducted at 37°C and at this temperature internalisation occurs very rapidly. Since the tissue was also washed at 37°C, one would expect most of the probe to have been internalised by the time the tissue was fixed so it would be unlikely to find any probe on the surface of the tissue. Results from cells incubated with gold probe at 2°C and fixed immediately after washing with cold medium showed a diffuse distribution of gold particles over the surface of the tissue. Little internalisation occurs at 2°C and no clustering of the probe was found.

In addition the concentrations of probe used in the incubation experiments was very high in order to saturate all the receptors on the surface. It is possible that any clustering was masked by the diffuse labelling of the surface particularly as coated pits occupy only a small proportion of the surface plasma membrane. (In cultured fibroblasts, Willingham & Pastan (1981) estimated that coated pits occupied less than 2% of the cell surface). It is possible that clustering may have been inhibited at 2°C if the membrane lipids freeze at that temperature thus preventing lateral movement and

aggregation which depend upon membrane fluidity. Schlessinger (1980) proposed that neither the binding or aggregation processes consumed energy and they occurred as a result of simple biophysics. The first changes which use metabolic energy are a result of rapid alterations in the dynamic properties of the plasma membrane. He suggests that changes occur in the rate of lateral or rotational motion of the receptor molecule as a consequence of interaction with neighbouring molecules and these changes are likely to play a key role in the first stages of membrane signalling. Such signals could be transmitted rapidly to the interior of the cell and may induce changes in ion permeability across the membrane. This messenger could in turn activate cytoplasmic enzymes which could then introduce specific covalent changes.

Recent reports indicate that insulin and EGF can induce covalent modifications of cellular components. The binding of EGF to isolated membranes results in a marked stimulation of phosphorylation of intrinsic proteins in the presence of  $^{32}\text{P}$  labelled ATP (Carpenter et al., 1979). Das (1980) has recently demonstrated that cytoplasmic extracts from EGF treated 3T3 cells contain substances that can stimulate DNA synthesis in isolated nuclei from spleen cells of adult frogs. This indicates that the interaction between EGF and its membrane receptor leads to the generation of cytoplasmic proteins which can stimulate DNA synthesis.

Various models have been proposed for the mechanism by which internalisation of protein within coated pits occurred. It is generally accepted that the coated pits pinch off from the plasma membrane and form coated vesicles. However the mechanism of invagination and detachment from the surface is not clear. Kanaseki and Kadota (1969) proposed a model of membrane motility for coated vesicle formation. They proposed that extensive hexagonal lattices of clathrin existed beneath the plasma membrane and that binding of the ligand to the surface receptor resulted in some of the hexagons in the lattice being converted into pentagons. This

alteration would thus result in curvature of the membrane. However, there is no evidence for the existence of such extensive sheets of clathrin lattice and an alternative model of coated pit formation was put forward by Ockleford (1976) and Ockleford & Whyte (1977). This model proposed that vesicle formation is similar to membrane patching. The stages in coated pit formation in this model include binding of the ligand to a receptor molecule which either spans the plasma membrane or is connected to a linking molecule. Binding of ligand acts as a trigger and permits the binding of clathrin. The addition of further units of receptor - linker clathrin permits polymerisation of the clathrin molecules resulting in curvature of the membrane, and formation of a coated vesicle. It is possible that the cytoskeletal components of the tissue may be involved in invagination of coated pits since it has been shown that during mitosis coated pits formed on the surface of the plasma membrane do not invaginate (Fawcett, 1965). During mitosis the cytoskeleton of the cell undergoes reorganisation and it is possible that the temporary suppression of invagination is a consequence of this reorganisation. Thus cytoskeletal components are implicated in coated pit and vesicle function. Calmodulin also appears to be implicated in coated pit formation. Salisbury *et al.* (1981) found that inhibition of uptake into coated pits occurred when a calmodulin inhibitor was used. He suggested that calmodulin is involved in conversion of submembraneous clathrin to form the coat, or in recruitment of cytoplasmic pools of clathrin into the membrane. Calmodulin is one of the proteins specifically found associated with coated vesicles.

Whether coated vesicles transport the internalised protein to its destination is unknown. This seems unlikely since Ockleford and Whyte (1977) examined the distribution of coated vesicles and found that the majority were always very close to the surface membrane and coated vesicle profiles were seldom seen deeper in the tissue. It is generally thought that soon after coated vesicle formation the clathrin dissociates and is recycled back to the surface to participate in further internalisation events (Anderson *et al.*, 1977; Goldstein *et al.*, 1979; Pearse, 1980; Heuser, 1980).

In the human placenta there is evidence that IgG is associated with vesicular structures. Johnson et al. (1982) demonstrated an association between IgG and the syncytiotrophoblast using immunofluorescent labelling techniques on cryostat sections of term placentae. They also found a punctate pattern of staining suggestive of discrete vesicular structures and suggested these might be involved in IgG transport. Lin (1980) also noted the presence of IgG in vesicular structures in the syncytiotrophoblast, using an immunoelectron microscope technique although it was not possible to definitely identify these as coated pits. King (1977) reported localisation of IgG-horseradish peroxidase (HRP) probe in syncytiotrophoblast coated vesicles. Pearse (1982) isolated a highly pure fraction of coated vesicles from human placenta and was able to show IgG was contained within these vesicles, although Booth & Wilson (1981) reported they could not find IgG in their vesicle preparations but were able to find transferrin. However the method used by Pearse produced a purer and less disrupted coated vesicle fraction. Ockleford and Clint (1980) also report localisation of  $^3\text{H}$ -IgG to coated vesicle enriched fractions in their wide aperture counting studies.

Recently the existence of coated vesicles as separate entities from the plasma membrane has been questioned (Wehland et al., 1981). Several sections through apparent coated vesicles profiles have shown them to be connected to the plasma membrane by a slender stalk. In addition they suggest that if clathrin molecules were recycling back to the plasma membrane one would expect to find 'pools' of free clathrin within the cytoplasm. Experiments have failed to demonstrate the existence of such 'pools' (Wehland et al., 1981). The model for internalisation proposed by Wehland et al. (1981) is that the clustered ligand is transferred to a large uncoated intracellular vesicle which is formed either as an invagination from the adjacent plasma membrane or through an opening in the lattice, and that coated vesicles are really pits which never leave the surface. They suggest that the vesicular structures seen by various other workers (Anderson et al. 1977; Roth and Porter, 1964; Friend and Farquhar, 1967) could possibly be joined to the surface beyond the plane of

sections. Coated vesicles have been isolated from various tissues by homogenisation (Kanaseki and Kadota, 1969; Pearse, 1976; Blitz et al., 1977; Woodward and Roth, 1978; Keen et al., 1979) He suggests these are artifacts of the preparation method. It is well known that artificial vesicular structures can be produced from lipid preparations (Simons et al., 1982). However very recently Fan et al. (1982) have presented direct evidence supporting the existence of coated vesicles. This work has shown (by serial sections through 3T3 L1 cells incubated with cationic ferritin) that 47% of apparent coated vesicles were true vesicles and were not connected to the surface since they contained no ferritin, whereas the other 53% were coated pits containing ferritin.

Another recent study using human fibroblasts also demonstrated the existence of coated vesicles as intermediates in absorptive endocytosis (Peterson & Van Deurs, 1983). This evidence suggests that coated vesicles do play an important role in endocytosis.

In both the BeWo cell incubations and the cultured placental cell incubations carried out in this study, ultrastructural examination showed smooth vesicular profiles with small coated areas. This suggests that large vesicular receptosome structures identified by Wehland et al. (1981) may also play a part in endocytosis. Structures of the same order of magnitude were also found in the perfused tissue incubation experiments. These receptosomes are similar to the multivesicular bodies described by Martin & Spicer (1973), however it has been shown that receptosomes do not contain lysosomal enzymes (Willingham & Pastan, 1981). Willingham & Pastan (1981) report that these receptosomes mediate ligand transport and move through the cytoplasm by saltatory movement. In their internalisation studies carried out using  $\alpha_2$  macroglobulin coupled to colloidal gold they report an initial association of probe with coated pits. After 10 minutes incubation at 37°C the cell surface was entirely clear and the gold-probe was localised exclusively in the receptosome structures.

After 30 minutes gold was found in primary lysosomes and after 2 hours the gold was localised in larger heterogenous lysosomes. In addition they also report gold localised in small vesicles in the vicinity of the Golgi apparatus after 2 hours incubation. Results from the perfusion experiments, tissue and cell incubations show a similarity to this model. In the overnight incubations of gold-IgG with the BeWo cells a large build-up of probe was found in lysosome-like structures indicating that fusion of the transporting vesicles with lysosomes may be part of the transmission system. There may also be a parallel with the virus infective pathway. This utilizes the low pH developed in the phagolysosome to aid transmission of the genetic components of virus particles across the phagolysosomal membrane into the compartment of the cytoplasm with access to nuclear pores. Entry into the cell nucleus of the viral nucleic acid thus results in infection. Simons et al. (1982) demonstrated that Semliki Forest virus particles (SFV) bound preferentially to the surface microvilli of hamster kidney cells and were internalised via coated pits. The coated vesicle loses its clathrin coat and then the SFV particle is transferred to the endosome or receptosome. The endosome or receptosome then fuses with the phagolysosome. It is here where most proteins would be degraded. However the acidity of the phagolysosomes appears to induce a change in the virus membrane which enables it to fuse with the phagolysosomal membrane. The process takes place so quickly that the virus is expelled into the cytoplasm of the cell without being destroyed by the degradative enzymes of the lysosome.

Simons et al. (1982) found that the infectious pathway of the virus particles could be interrupted using lysosomal inhibitors. These do not inhibit binding of the SFV to the cell membrane or movement of virus particles into the lysosome but they do prevent it from passing out into the cytoplasm. It seems that the inhibitors interfere with the fusion of viral and lysosomal membranes by decreasing the acidity of the lysosome.

Differences in pH have also been shown to play an important role in the binding and release of proteins. Jones and Waldman (1972) showed in rat intestinal cells that pH differences altered the binding ability of the cells for IgG. At pH 7.4 the rat cells lost the ability to bind IgG. It is possible that differences in pH between tissue compartments may play a far greater role in the transport of substances than has been previously realised and further investigations of the influence of pH on stages in human placental transport of IgG is needed.

CONCLUSION

## CHAPTER 9 CONCLUSION

A considerable amount of new information has been obtained from the results of the preceding experiments.

(1) Evidence is presented concerning the transport of IgG across the human placenta, which is consistent with the majority of other recent work. That is, there is an association between IgG and the syncytiotrophoblast. The IgG probes used have been located in coated pits, coated vesicles, smooth vesicles, and larger vesicular structures. These findings support the model that uptake of IgG occurs initially by receptors which localise in coated pits.

Transport of the ligand from coated vesicles to smooth vesicles is not fully understood and a number of mechanisms have been proposed. Firstly, a possible explanation may be that coated pits never actually leave the surface but transfer their contents to smooth vesicles to which they are joined. However there is evidence in some systems for the existence of complete coated vesicles (Fan et al., 1982) and these have been shown to contain a variety of ligands. Another possibility is that the coated pits form coated vesicles which deliver their contents to smooth vesicular structures and then recycle back to the surface (Rodewald, 1980) or that once the coated vesicle is formed it loses its clathrin coating and forms a smooth vesicle. Although there is evidence that there are no 'pools' of free clathrin (Wehland et al., 1981) this does not necessarily imply that clathrin recycling does not occur. Triskelions of clathrin may be associated with intermicrovillar membrane individually. However, whatever the mechanism involved, at least partial uncoating must occur to enable fusion of coated pits or vesicles with other organelles. Evidence for fusion of coated vesicles with smooth vesicles is given in the experiments presented here. Both coated vesicular structures were seen adjoining smooth vesicles and smooth vesicular profiles were seen which contained coated areas of membrane. At some stage during transport of IgG, across the placenta, the probes appeared to be liberated from the vesicular organelles as they were found lying free in the cytoplasm. This might be accomplished in a similar way to the infectious cycle

of virus particles, where they are liberated in the cytoplasm at the stage of fusion with the lysosome. Once free in the cytoplasm, subsequent transport to the basal lamina and endothelial capillaries might be accomplished by diffusion.

(2) It has been demonstrated that although IgG does not reach the fetal circulation early in gestation, uptake and transport of IgG into placental tissue definitely occurs, and the cytotrophoblast cells, although they form a continuous layer beneath the syncytiotrophoblast, do not form a barrier to IgG transport.

(3) Ultrastructural examination of the BeWo cells has provided observations of structures typical of the transformed state and the tissue of origin.

(4) Extensive documentation is presented showing the in vitro differentiation of cultured cells towards the villous state of the parent tissue. Cytoplasmic differences in the cells were noted which appeared to mimic the appearance and mutual positioning of cytotrophoblast and syncytiotrophoblast in vivo.

(5) Bulbous projections were also noted in the cultured cells both attached to the tissue and floating free in the culture medium and may relate to the budding off and deportation of trophoblast in vivo.

Obviously further investigation into the IgG transport system is required. Electron microscopic examination of tissue (either incubated or perfused with probe) permits only a small area of tissue to be examined. In all the experiments only a small amount of probe was seen in each section examined. Ockleford and Dearden (1983) have calculated that 20,000 micropinocytic events occur over the 20 minute period of a typical perfusion experiment. That is 100 events per minute in the volume of tissue enclosed in an ultrathin tissue section. Therefore the number of coated vesicles one would expect to see in a thin section is small.

It is possible to show by a calculation (see Appendix XVIII) that uptake of IgG is an active concentrative phenomenon. The internal volume of an average coated vesicle can be calculated since the size range of coated vesicles is known. Pearse (1982) showed that a coated vesicle contains an average of 4 IgG molecules. The weight of 4 IgG molecules can be calculated and since the weight of IgG and volume of coated vesicle lumens are known the concentration of IgG within a coated vesicle can be determined. The concentration of IgG within an average vesicle has been calculated as approximately 12.2mg/ml. This is in the range of concentration found in human serum. Since this is an average value then it can be assumed that 50% of vesicles have above average concentration and this implies uptake into coated vesicles may be a selective process. In addition, and much more important, this calculation assumes the vesicle lumen contains no other material. However, there is an unquantified but substantial amount of glycocalyx material acting as a solvent excluder. Therefore the concentration calculated is a minimum estimate.

Although electron microscopic examination is a vital method for the investigation of transport systems its main limitation is that a very large amount of tissue has to be examined to give a correct interpretation of the situation.

The most successful experiments reported here were those using tissue culture cells. These could provide the experimental model of choice for the uptake systems since serial sections of such cells are expected to allow the best description of the mechanism of the uptake situation in an intact physiological and viable system.

APPENDICES

## APPENDICES

- I Processing schedule for examination of tissue by Transmission Electron Microscopy (TEM).
- II Processing schedule for examination of tissue by Scanning Electron Microscopy.
- III Calibration of Transducerunits used in the perfusion equipment.
- IV Placental perfusion experiments - details of flow rates, pressure, and other parameters.
- V Calculation of optimum pH for coupling IgG to colloidal gold.
- VI Calculation of optimal amount of protein (IgG) required to coat colloidal gold particles.
- VII Calculation of concentration of colloidal gold probe.
- VIII Method used for replication of the surface of placental tissue.
- IX Method of culturing placental cells.
- X Processing schedule for examination of cultured cells by Transmission Electron microscopy.
- XI Method of culturing BeWo cells obtained from Professor Page-Faulk.
- XII Method used to test a number of different fetal calf sera.
- XIII Method of freezing BeWo cells for long term storage.

APPENDICES (cont)

- XIV Counting method used to assess amount of radioactivity in perfused tissue.
- XV Method used to assess distribution of silver grains located over syncytial vesicles.
- XVI Random table used in Appendix XV.
- XVII Method used to demonstrate sequestration of gold particles into BeWo CB's in overnight gold incubation.
- XVIII Calculation of concentration of IgG in a coated vesicle.

## APPENDIX I

### Processing schedule for examination of placental tissue by transmission electron microscopy.

<u>SOLUTION</u>	<u>TIME</u>
2% OsO <sub>4</sub> in 0.1M phosphate buffer (pH7.4)	60min.
30% Alcohol in distilled water	15min.
50% Alcohol in distilled water	15min.
70% Alcohol in distilled water	15min.
90% Alcohol in distilled water	15min.
100% Alcohol	15min.
100% Alcohol dried over Ammonium Sulphate	2 changes of 15min each.
Propylene Oxide	3 changes of 1min each.
Propylene Oxide/Spurr's low viscosity resin(Agar aids) 50:50	Overnight.
Fresh Spurr's resin	At least 3 hours.
Embed in gelatin capsules polymerise at 60°C for 36 hours.	

### Mixture of components used for Spurr's low viscosity resin (Spurr's, 1969)

NSA	26g
VCD	10g
ERL	4g
Stir for 5min.	
S1	0.4g
Stir for 5min.	

## APPENDIX II

### Processing schedule for examination of tissue by Scanning Electron microscopy

Tissue is fixed over-night in 3% glutaraldehyde in 0.1M phosphate buffer (pH7.4) then processed as given below:-

<u>SOLUTION</u>	<u>TIME</u>
30% Alcohol in distilled water	15min.
50% Alcohol in distilled water	15min.
70% Alcohol in distilled water	15min.
90% Alcohol in distilled water	15min.
100% Alcohol	15min.
100% Acetone	At least 1 hour

Critically point dry by replacement with carbon dioxide. The critical point occurs at a pressure of 1200 PSI and a temperature of 31.5°C. Coat with 25nm gold in a Polaron Sputter Coater Unit.

### APPENDIX III

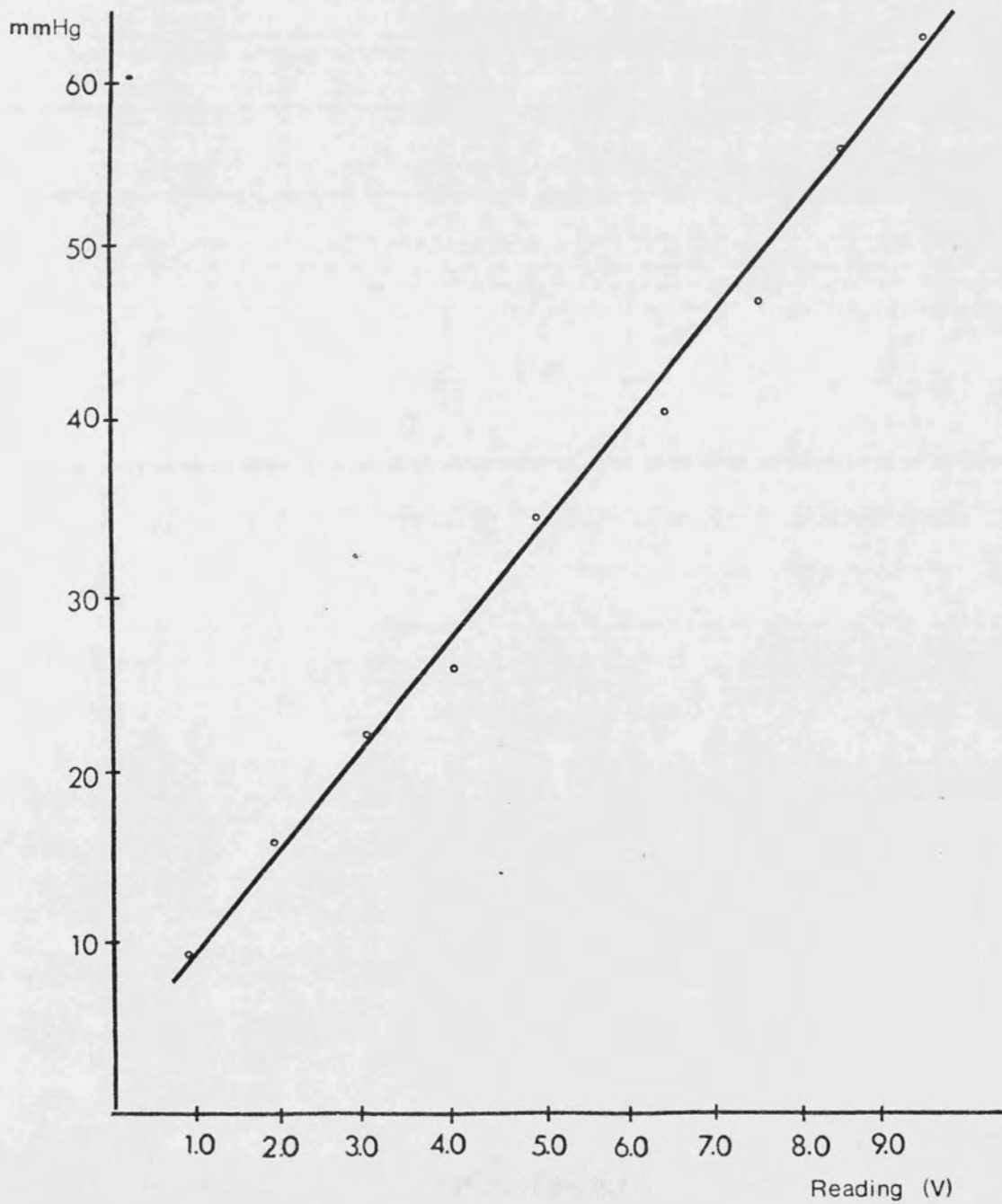
#### Calibration of Transducers

The transducers used in the perfusion apparatus were calibrated by comparing a series of pressures with a mercury manometer. Results were plotted as a calibration curve for each channel. (see graphs over)

The transducer reading could thus be converted to mm Hg for the purpose of the experiment.

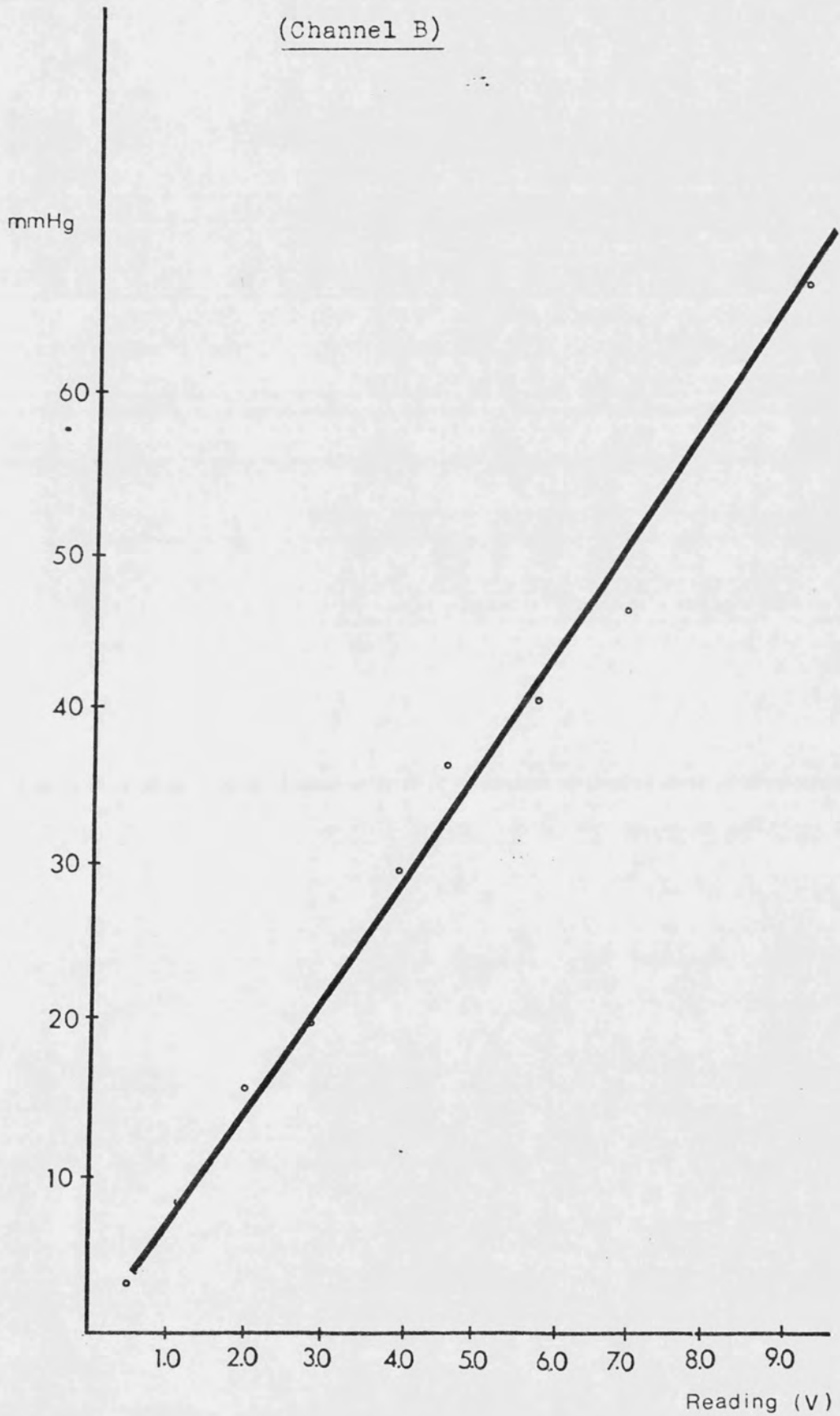
Calibration curve for transducer

(Channel A)



Calibration curve for transducer

(Channel B)



Appendix IV Placental perfusion experiments-details

PLACENTAL PERFUSION

Date: 11.2.81

Series No: 1.1

Maternal side conditions

Flow rate ..... 1.9mls/min .....  
Pressure mmHg ..... 5 .....  
Gas mixture ..... 95% O<sub>2</sub>; 5% CO<sub>2</sub> .....  
Additives ..... Au<sub>18</sub>-IgG (dilution: 1ml in 100mls buffer) .....  
Temperature ..... 37°C .....  
Buffer ..... Hartmans .....

---

Foetal side conditions

Flow rate (arterial) ..... 0.9mls/min .....  
Flow rate (venous) ..... - .....  
Pressure mmHg ..... - .....  
Gas mixture ..... 40% O<sub>2</sub>; 55% N<sub>2</sub>; 5% CO<sub>2</sub> .....  
Additives ..... - .....  
Temperature ..... 37°C .....  
Buffer ..... Hartmans .....  
Sample Times ..... 0, 30, 60 mins .....  
Fixation Times ..... 0, (at hospital) 100, (at end of experiment) mins .....  
Time after delivery perfusion established ..... 40 mins .....  
Comments on morphology ..... Normal .....

---

Additional Comments

PLACENTAL PERFUSION

Date: 22.2.81

Series No: 1.2

Maternal side conditions

Flow rate .0.78mls/min.....  
Pressure mmHg .15.....  
Gas mixture .95% O<sub>2</sub>; 5% CO<sub>2</sub>.....  
Additives .Dextran 75 (5mls); Au<sub>18</sub>-IgG (dilution: 1ml/100mls of buffer).....  
Temperature .37°C.....  
Buffer .Hartmans.....

---

Foetal side conditions

Flow rate (arterial) .0.78mls/min.....  
Flow rate (venous) .0.44 - 0.53mls/min.....  
Pressure mmHg .12.....  
Gas mixture .40% O<sub>2</sub>; 55% N<sub>2</sub>; 5% CO<sub>2</sub>.....  
Additives .Dextran 75 (5mls).....  
Temperature .37°C.....  
Buffer .Hartmans.....  
Sample Times .None.....  
Fixation Times .0, (at hospital) 120, (at end of experiment) mins.....  
Time after delivery perfusion established .90 mins.....  
Comments on morphology .Normal.....

---

Additional Comments

PLACENTAL PERFUSION

Date: 28. 4. 81

Series No: 1.3

Maternal side conditions

Flow rate 0.26mls/min  
Pressure mmHg 12  
Gas mixture 95% O<sub>2</sub>; 5% CO<sub>2</sub>  
Additives 4% Dextran; 10mM Glucose; Au<sub>198</sub>-IgG  
Temperature 37°C  
Buffer Hartmans

---

Foetal side conditions

Flow rate (arterial) 0.75mls/min  
Flow rate (venous) 0.75mls/min  
Pressure mmHg 7  
Gas mixture 40% O<sub>2</sub>; 55% N<sub>2</sub>; 5% CO<sub>2</sub>  
Additives 4% Dextran; 10mM Glucose; Heparin (6mgs/100mls)  
Temperature 37°C  
Buffer Hartmans  
Sample Times 0, 1, 2, 3, 4, 5, 6, 7, 8, 9, 10, 15, 20 mins  
Fixation Times 0, (at hospital) 60, (at end of experiment) mins  
Time after delivery perfusion established 35mins  
Comments on morphology extra lobe

---

Additional Comments

PLACENTAL PERFUSION

Date: 28.4.81

Series No: 1.4

Maternal side conditions

Flow rate ... 0.29mls/min.....  
Pressure mmHg ... 5.....  
Gas mixture ... 95% O<sub>2</sub>; 5% CO<sub>2</sub>.....  
Additives 4% Dextran; 10mM Glucose; Au<sub>18</sub>-IgG.....  
Temperature 37°C.....  
Buffer Hartmans.....

---

Foetal side conditions

Flow rate (arterial) 0.82mls/min.....  
Flow rate (venous) 0.87mls/min.....  
Pressure mmHg 1.5.....  
Gas mixture 40% O<sub>2</sub>; 55% N<sub>2</sub>; 5% CO<sub>2</sub>.....  
Additives 4% Dextran; 10mM Glucose; Heparin (6mgs/100mls).....  
Temperature 37°C.....  
Buffer Hartmans.....  
Sample Times 0, 1, 2, 3, 4, 5, 6, 7, 8, 9, 10, 15, 20 mins.....  
Fixation Times 0, (at hospital) 95, (at end of experiment) mins.....  
Time after delivery perfusion established 75 mins.....  
Comments on morphology Large, normal.....  
.....

---

Additional Comments

PLACENTAL PERFUSION

Date: 12.5.81

Series No: 1.5

Maternal side conditions

Flow rate .0.6mls/min.....  
Pressure mmHg .18.....  
Gas mixture .95% O<sub>2</sub>; 5% CO<sub>2</sub>.....  
Additives .4% Dextran; 10mM Glucose; Au<sub>18</sub>-IgG (dilution: 50mls + 10mls buffer).....  
Temperature .37°C.....  
Buffer .Hartmans.....

---

Foetal side conditions

Flow rate (arterial) .0.79mls/min.....  
Flow rate (venous) .0.26 - 0.7mls/min.....  
Pressure mmHg .15.....  
Gas mixture .40% O<sub>2</sub>; 55% N<sub>2</sub>; 5% CO<sub>2</sub>.....  
Additives .4% Dextran; 10mM Glucose; Heparin (6mgs/100mls ).....  
Temperature .37°C.....  
Buffer .Hartmans.....  
Sample Times .0, 1, 2, 3, 4, 5, 6, 7, 8, 9, 10, 15, 20 mins.....  
Fixation Times .0, (at hospital) 55, (at end of experiment).....  
Time after delivery perfusion established .25 mins.....  
Comments on morphology .Normal.....  
.....

---

Additional Comments

PLACENTAL PERFUSION

Date: 26.6.81

Series No: 1.6

Maternal side conditions

Flow rate 0.49mls/min  
Pressure mmHg 10  
Gas mixture 95% O<sub>2</sub>; 5% CO<sub>2</sub>  
Additives 4% Dextran; 10mM Glucose; Au<sub>18</sub>-IgG (dilution 50mls + 10mls of buffer)  
Temperature 37°C  
Buffer Hartmans

---

Foetal side conditions

Flow rate (arterial) 0.75mls/min  
Flow rate (venous) 0.78 - 0.35mls/min  
Pressure mmHg 9 - 15  
Gas mixture 40% O<sub>2</sub>; 55% N<sub>2</sub>; 5% CO<sub>2</sub>  
Additives 4% Dextran; 10mM Glucose; Heparin (6mgs/100mls)  
Temperature 37°C  
Buffer Hartmans  
Sample Times 0, 10, 20, 30, 40 mins  
Fixation Times 0, (at hospital) 75, (at end of experiment) mins  
Time after delivery perfusion established 35 mins  
Comments on morphology Small, 29 weeks

---

Additional Comments Good perfusion, area fixed was coloured purple with the Au<sub>18</sub>-IgG probe

PLACENTAL PERFUSION

Date: 13.7.81

Series No: 1.7

Maternal side conditions

Flow rate .0.29mls/min.....  
Pressure mmHg .12.....  
Gas mixture .95% O<sub>2</sub>; 5% CO<sub>2</sub>.....  
Additives .4% Dextran; 10mM Glucose; Au<sub>18</sub>-IgG (dilution: 50mls + 10mls buffer).....  
Temperature .37°C.....  
Buffer .Hartmans.....

---

Foetal side conditions

Flow rate (arterial) .0.53mls/min.....  
Flow rate (venous) .0.35mls/min.....  
Pressure mmHg .10.....  
Gas mixture .40% O<sub>2</sub>; 55% N<sub>2</sub>; 5% CO<sub>2</sub>.....  
Additives .4% Dextran; 10mM Glucose; Heparin (6mgs/100mls).....  
Temperature .37°C.....  
Buffer .Hartmans.....  
Sample Times .35 mins.....  
Fixation Times .0, (at hospital) 80, (at end of experiment) mins.....  
Time after delivery perfusion established .45 mins.....  
Comments on morphology .Eccentric cord.....

---

Additional Comments

PLACENTAL PERFUSION

Date: 22.7.81

Series No: 1.8

Maternal side conditions

Flow rate 0.7mls/min  
Pressure mmHg 12  
Gas mixture 95% O<sub>2</sub>; 5% CO<sub>2</sub>  
Additives 4% Dextran; 10mM Glucose; Au<sub>18</sub>-IgG (dilution: 50mls + 10mls buffer)  
Temperature 37°C  
Buffer Hartmans

---

Foetal side conditions

Flow rate (arterial) 0.78mls/min  
Flow rate (venous) 0.87mls/min  
Pressure mmHg 15  
Gas mixture 40% O<sub>2</sub>; 55% N<sub>2</sub>; 5% CO<sub>2</sub>  
Additives 4% Dextran; 10mM Glucose; Heparin (6mgs/100ml)  
Temperature 37°C  
Buffer Hartmans  
Sample Times 0, 50, mins  
Fixation Times 0, (at hospital) 95, (at end of experiment) mins  
Time after delivery perfusion established 45 mins  
Comments on morphology Large, normal

---

Additional Comments No flow on maternal side for first 30 mins of perfusion. Found this was due to blocked cannula. This was freed and re-inserted and perfusion continued for a further 20 mins.

PLACENTAL PERFUSION

Date: 1.12.81

Series No: 1.9

Maternal side conditions

Flow rate .0.78mls/min.....  
Pressure mmHg ..10.....  
Gas mixture ....95% O<sub>2</sub>; 5% CO<sub>2</sub>.....  
Additives .4% Dextran; 10mM Glucose; Au<sub>18</sub>-IgG (dilution: 50mls + 10mls buffer)  
Temperature 37°C.....  
Buffer ..Hartmans.....

---

Foetal side conditions

Flow rate (arterial) .0.77mls/min.....  
Flow rate (venous) ....0.....  
Pressure mmHg .....15.....  
Gas mixture ..40% O<sub>2</sub>; 55% N<sub>2</sub>; 5% CO<sub>2</sub>.....  
Additives .4% Dextran; 10mM Glucose; Heparin (6mgs/100mls).....  
Temperature ..37°C.....  
Buffer .....Hartmans.....  
Sample Times ..None.....  
Fixation Times ..0, (at hospital) 60, (at end of experiment) mins.....  
Time after delivery perfusion established ..30 mins.....  
Comments on morphology ..Eccentric cord.....  
.....

---

Additional Comments Cotyledon did not pale very much.

PLACENTAL PERFUSION

Date: 5.3.31

Series No: 2.1

Maternal side conditions

Flow rate .....1.5mls/min.....  
Pressure mmHg ...3.....  
Gas mixture .....95% O<sub>2</sub>; 5% CO<sub>2</sub>.....  
Additives .....4% Dextran; 10mM Glucose; Tritiated IgG.....  
Temperature .....37°C.....  
Buffer .....Hartmans.....

---

Foetal side conditions

Flow rate (arterial) ...3.5mls/min.....  
Flow rate (venous) .....11mls/min.....  
Pressure mmHg .....0.5.....  
Gas mixture ...40% O<sub>2</sub>; 55% N<sub>2</sub>; 5% CO<sub>2</sub>.....  
Additives 4% Dextran; 10mM Glucose; Heparin.....  
Temperature .....37°C.....  
Buffer ..Hartmans.....  
Sample Times ....0, 10, 20, 30, 40 min.....  
Fixation Times ...0(at hospital), at end of experiment.....  
Time after delivery perfusion established ..75min.....  
Comments on morphology ..Normal.....  
.....

---

Additional Comments

PLACENTAL PERFUSION

Date: 17.3.31

Series No: 2.2

Maternal side conditions

Flow rate ... 6mls/min .....  
Pressure mmHg 4.5 .....  
Gas mixture .95% O<sub>2</sub>; 5% CO<sub>2</sub> .....  
Additives .4% Dextran, 10mM Glucose, Tritiated IgG .....  
Temperature ..... 37°C .....  
Buffer .. Hartmans .....

---

Foetal side conditions

Flow rate (arterial) .. 2.5mls/min .....  
Flow rate (venous) ..... 2mls/min .....  
Pressure mmHg ..... 0.5 .....  
Gas mixture ... 40% O<sub>2</sub>; 55% N<sub>2</sub>; 5% CO<sub>2</sub> .....  
Additives .. 4% Dextran; 10mM Glucose; Heparin .....  
Temperature ..... 37°C .....  
Buffer ... Hartmans .....  
Sample Times ..... 0, 10, 20, 30min .....  
Fixation Times ..... 0 (at hospital); at end of experiment. ....  
Time after delivery perfusion established ... 60min .....  
Comments on morphology ..... Normal .....  
.....

---

Additional Comments

PLACENTAL PERFUSION

Date: 19.3.31

Series No: 2.3

Maternal side conditions

Flow rate ....4.7mls/min.....  
Pressure mmHg ..5.....  
Gas mixture .....95% O<sub>2</sub>; .5% CO<sub>2</sub>.....  
Additives .4% Dextran; .10mM Glucose; Tritiated IgG.....  
Temperature ...37°C.....  
Buffer ...Hartmans.....

---

Foetal side conditions

Flow rate (arterial) ...3.7mls/min.....  
Flow rate (venous) ....3.7mls/min.....  
Pressure mmHg ....1.....  
Gas mixture .....40% O<sub>2</sub>; .55% N<sub>2</sub>; .5% CO<sub>2</sub>.....  
Additives .4% Dextran; .10mM Glucose; Heparin.....  
Temperature ..37°C.....  
Buffer ...Hartmans.....  
Sample Times ....0, .10, .15, .20, .25 mins.....  
Fixation Times ...0. (at hospital); at end of experiment.....  
Time after delivery perfusion established .....50min.....  
Comments on morphology ..Normal.....  
.....

---

Additional Comments

PLACENTAL PERFUSION

Date: 23.3.81

Series No: 2.4

Maternal side conditions

Flow rate .. 5mls/min .....

Pressure mmHg ... 3.5 .....

Gas mixture ..... 95% O<sub>2</sub>; 5% CO<sub>2</sub> .....

Additives .. 4% Dextran; 10mM Glucose; Tritiated IgG .....

Temperature .. 37°C .....

Buffer ..... Hartmans .....

---

Foetal side conditions

Flow rate (arterial) .. 6.3mls/min .....

Flow rate (venous) ..... 0.5mls/min .....

Pressure mmHg ..... 1 .....

Gas mixture ..... 40% O<sub>2</sub>; 55% N<sub>2</sub>; 5% CO<sub>2</sub> .....

Additives ..... 4% Dextran; 10mM Glucose ; Heparin .....

Temperature ..... 37°C .....

Buffer ..... Hartmans .....

Sample Times ..... 0, 2, 4, 6, 8, 10, 15, 20 min .....

Fixation Times ..... 0 (at hospital); at end of experiment .....

Time after delivery perfusion established ..... 90min .....

Comments on morphology .. Eccentric cord .....

.....

---

Additional Comments

PLACENTAL PERFUSION

Date: 23.3.31

Series No: 2.5

Maternal side conditions

Flow rate ..... 3.5mls/min .....  
Pressure mmHg ..... 1.5 .....  
Gas mixture ... 95% O<sub>2</sub>; 5% CO<sub>2</sub> .....  
Additives . 4% Dextran; 10mM Glucose; Tritiated IgG .....  
Temperature .... 37°C .....  
Buffer .... Hartmans .....  
.....

Foetal side conditions

Flow rate (arterial) . 4.3mls/min .....  
Flow rate (venous) ..... 4.2mls/min .....  
Pressure mmHg ..... 1.5 .....  
Gas mixture ... 40% O<sub>2</sub>; 55% N<sub>2</sub>; 5% CO<sub>2</sub> .....  
Additives . 4% Dextran; 10mM Glucose; Heparin .....  
Temperature ..... 37°C .....  
Buffer .... Hartmans .....  
Sample Times . 0, 2, 3, 4, 5, 6, 7, 8, 9, 10, 15, 20, 25, 30 min .....  
Fixation Times .. 0 (at hospital) at end of experiment .....  
Time after delivery perfusion established . 45min .....  
Comments on morphology ..... Normal .....  
.....

Additional Comments

PLACENTAL PERFUSION

Date: 24.3.81

Series No: 2.6

Maternal side conditions

Flow rate ....3.5mls/min.....  
Pressure mmHg ...1.5.....  
Gas mixture .....95% O<sub>2</sub>: 5% CO<sub>2</sub>.....  
Additives ...4% Dextran; 10mM Glucose; Tritiated IgG.....  
Temperature ....37° C.....  
Buffer .....Hartmans.....

---

Foetal side conditions

Flow rate (arterial) ...4.5mls/min.....  
Flow rate (venous) .....4mls/min.....  
Pressure mmHg .....0.5.....  
Gas mixture .....40% O<sub>2</sub>: 55% N<sub>2</sub>: 5% CO<sub>2</sub>.....  
Additives ...4% Dextran; 10mM Glucose; Heparin.....  
Temperature .....37° C.....  
Buffer ....Hartmans.....  
Sample Times 0, 1, 2, 3, 4, 5, 6, 7, 8, 9, 10, 15, 20, 25, 30min  
Fixation Times .....0 (at hospital), at end of experiment.....  
Time after delivery perfusion established .....60min.....  
Comments on morphology .....Eccentric cord.....  
.....

---

Additional Comments

PLACENTAL PERFUSION

Date: 24.3.31

Series No: 2.7

Maternal side conditions

Flow rate .... 5.4mls/min.....  
Pressure mmHg .... 5.....  
Gas mixture ..... 95% O<sub>2</sub>; 5% CO<sub>2</sub>.....  
Additives ..... 4% Dextran; 10mM Glucose; Tritiated IgG.....  
Temperature ..... 37°C.....  
Buffer ... Hartmans.....

---

Foetal side conditions

Flow rate (arterial) . 4.5mls/min.....  
Flow rate (venous) ..... 3mls/min.....  
Pressure mmHg ..... 1.....  
Gas mixture ..... 40% O<sub>2</sub>; 55% N<sub>2</sub>; 5% CO<sub>2</sub>.....  
Additives ... 4% Dextran; 10mM Glucose; Heparin.....  
Temperature ..... 37°C.....  
Buffer ..... Hartmans.....  
Sample Times 0, 1, 2, 3, 4, 5, 6, 7, 8, 9, 10, 15, 20, 25, 30min  
Fixation Times .. 0 (at hospital) at end of experiment.....  
Time after delivery perfusion established ..... 45min.....  
Comments on morphology ..... Normal.....  
.....

---

Additional Comments

## APPENDIX V

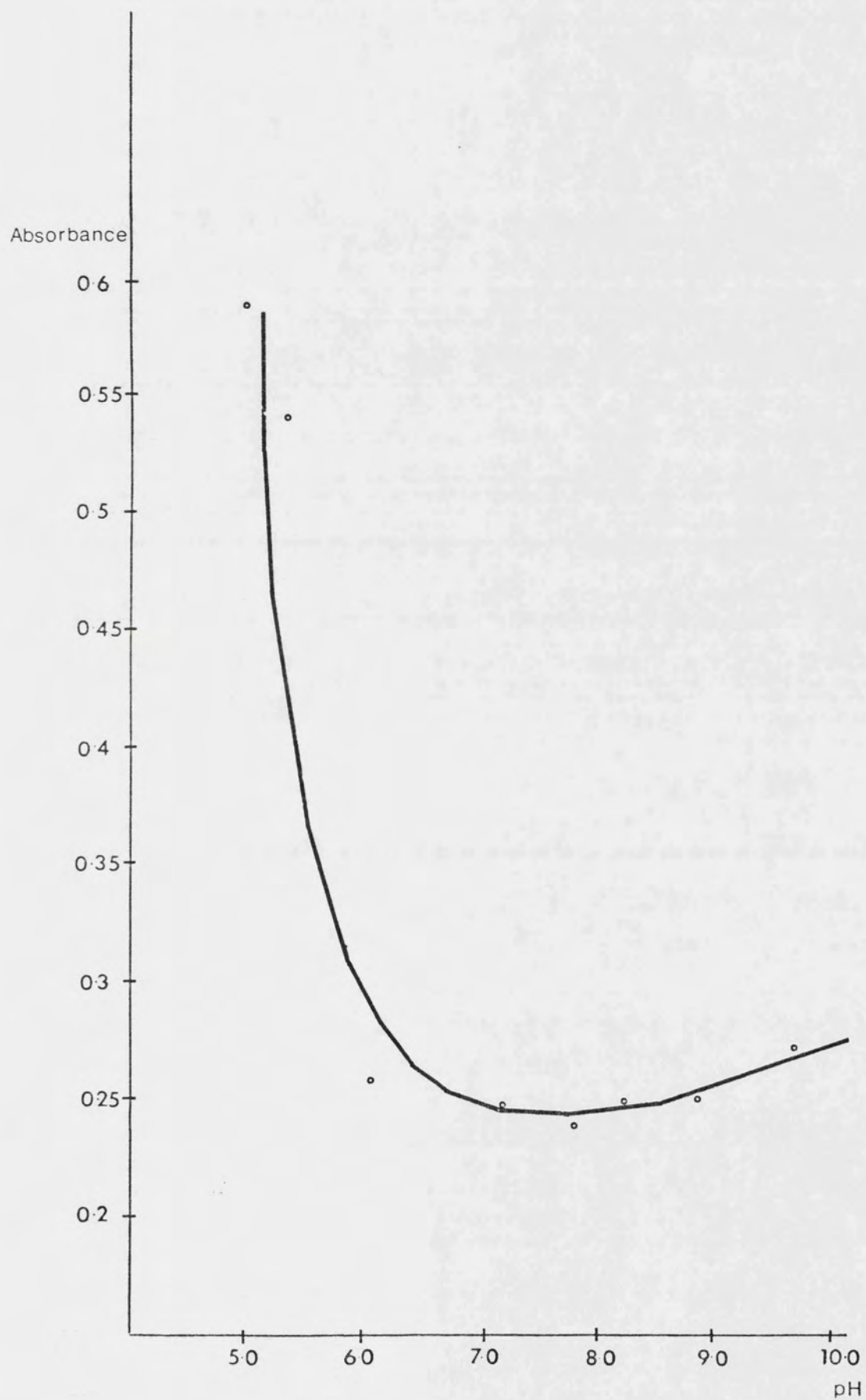
### Calculation of optimum pH for coupling IgG to colloidal gold

Adsorption of protein onto colloidal gold particles occurs at a pH close to the pI of the protein. The optimal pH for the labelling was determined experimentally using the method given below.

#### Method

A series of test-tubes were prepared, each containing 2.5ml of colloidal gold solution. The pH of the solutions were adjusted with 0.2M HCl to produce a range of pH values from pH5.1 - 9.4. An aliquot (0.5ml) of protein (0.125mg/ml) was added to each tube and the tubes were left to stand at room temperature (21°C) for 10 minutes. An aliquot (0.5ml) of 10% NaCl was then added to each tube, which was then shaken and left to stand at room temperature for 2 hours. The tubes were then examined for flocculation using a spectrophotometer (LKB) at 580nm. A graph was plotted of absorbance against pH. The optimum pH was found to be between pH6 - 7.5.

GRAPH TO SHOW OPTIMUM pH FOR IgG ADSORBANCE



## APPENDIX VI

### Calculation of optimal amount of protein (IgG) required to coat the colloidal gold particles (18nm)

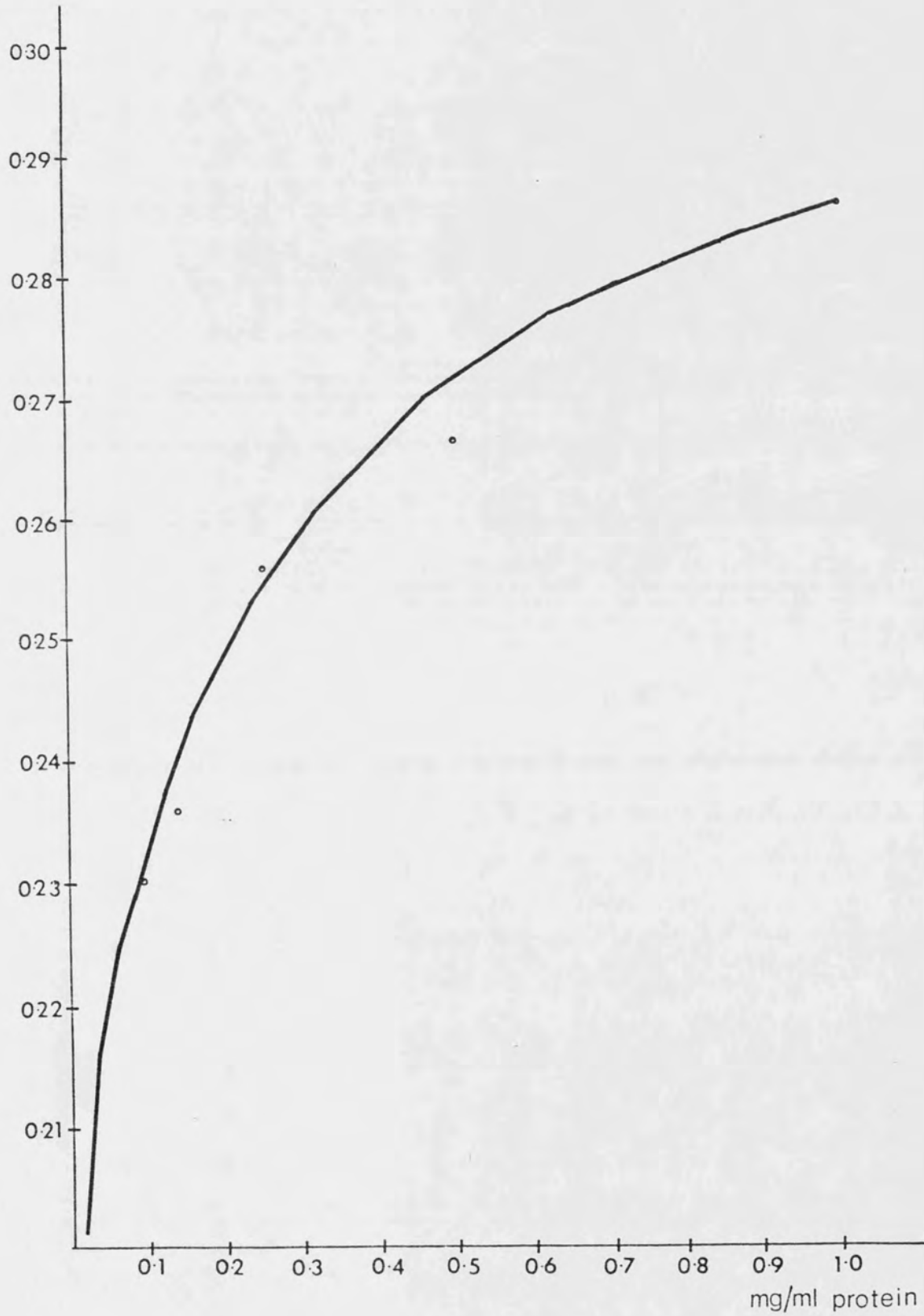
The amount of protein required to stabilize a colloidal gold solution was determined experimentally as given below.

#### Method

A series of tubes were prepared, each containing 2.5ml of colloidal gold solution at pH 7.0. A range of concentrations of IgG solution (in distilled water) were prepared. An aliquot (0.5ml) of each protein concentration was added to the colloidal gold series. The tubes were then shaken to mix the solution and left to stand at room temperature (21°C) for 10 minutes. An aliquot (0.5ml) of 10% NaCl solution was added to each tube which was shaken and left to stand at room temperature for 2 hours. The tubes were then examined for flocculation spectrophotometrically, using an LKB spectrophotometer at wavelength 580nm. A graph was plotted of absorbance against protein concentration. The optimal concentration of protein was found to be 0.125mg/ml IgG.

GRAPH TO SHOW OPTIMUM AMOUNT OF IgG REQUIRED TO COAT 18nm GOLD PARTICLES.

Absorbance



## APPENDIX VII

### Calculation of concentration of colloidal gold probe

The concentration of the gold probe in terms of the particles of gold per ml was calculated using the method given below.

#### Method

An aliquot (2  $\mu$ l) of 0.091 $\mu$ m diameter latex particles (Agar aids) was dried onto a formvar coated electron microscopy grid. 2 $\mu$ l of the gold probe were then dried down onto the same grid and examined in a Jeol 100CX electron microscope. A series of electron micrographs were taken and the ratio of gold particles to latex particles was calculated.

Since the concentration of the latex particles is known to be  $1.37 \times 10^{12}$  /ml the concentration of the gold probe can be calculated.

2 $\mu$ l of latex solution contains  $2.74 \times 10^9$  particles.

However since the latex solution was diluted by 100% before use, 2 $\mu$ l actually contained  $1.37 \times 10^9$  particles.

The ratio of gold to latex was found to be 3 : 1.

Therefore, the concentration of gold particles is approximately  $3 \times 0.685 \times 10^9$  or  $4.11 \times 10^9$  particles in 2 $\mu$ l or  $2.056 \times 10^{12}$  particles /ml.

## APPENDIX VIII

### Method used for replication of the surface of the placental tissue.

Small pieces of placental villi were critically point dried as for scanning microscopy. The dried specimens were mounted on freshly cleaved mica with doublesided tape, and shadowed with platinum at an angle of  $45^{\circ}$ . The tissue was then coated with a layer of carbon approximately 10nm thick. In order to remove the platinum/carbon replica from the tissue the mica was scored with a razor blade and the replica floated off onto a water surface. The replica was then cleaned by passing through a series of solutions listed in the table below.

SOLUTION	TIME
70% sulphuric acid	30 - 60 minutes
distilled water	rinse
concentrated sodium hypochlorite	30 minutes
distilled water	rinse
distilled water	rinse

After cleaning, the replica was mounted on an electron microscope and examined in a Jeol 100CX transmission electron microscope.

## APPENDIX IX

### Method of culturing human placental cells

Pieces of freshly delivered placental tissue were washed several times in Hanks buffer to remove excess blood. The villi were then finely chopped using scissors and fine forceps. The tissue was transferred to a conical flask containing 50ml of 0.25% trypsin solution (Gibco) and left until the suspension became cloudy (about 30 minutes). The trypsin solution was decanted from the flask using a sterile pasteur pipette, and the tissue resuspended in 25ml of fresh trypsin solution. After about 30 minutes the number of cells present in the solution was assessed using a haemocytometer ( $5 \times 10^5$  cells are needed for successful culture). The digestion reaction was stopped by addition of excess culture medium and the resultant solution placed into test tubes and centrifuged for 5 minutes at 3,000 rpm. The supernatant was removed and the cells resuspended in fresh culture medium. This was then dispensed into 10ml culture flasks (Falcon). The cultures were gassed daily with 5% O<sub>2</sub>; 95% CO<sub>2</sub> and incubated at 37°C.

The culture medium was RPM 1640 (Flow), with 10% fetal calf serum (Gibco), and 100 units penicillin 100 units streptomycin (Gibco) per ml.

This method of culture was unsuccessful in maintaining the cells for long periods. The successful method is given on page 29.

APPENDIX X

Processing schedule for examination of cultured cells by  
Transmission Electron Microscopy

Cells were fixed in 3% glutaraldehyde in phosphate buffer then processed as shown below:

SOLUTION	TIME
2% OsO <sub>4</sub> in 0.1m phosphate buffer (pH 7.4)	60 minutes
30% Alcohol in distilled water	3 minutes
50% Alcohol in distilled water	3 minutes
70% Alcohol in distilled water	3 minutes
90% Alcohol in distilled water	3 minutes
100% Alcohol	3 minutes
100% Alcohol dried over ammonium sulphate.	4 changes of 30 minutes
Epon resin (Agar aids)	overnight
Old resin drained from tissue culture flask using heat. Fresh resin added and left overnight.	minimum of 8 hours.
Drain tissue culture flask localise cells. Cure..	60°C for 36 hours.

## APPENDIX XI

### Method for culturing BeWo cells obtained from Professor Page-Faulk

#### The culture method

The culture medium for these cells was RPM1640, with Hepes and Glutamine (Flow Laboratories). 10% fetal calf serum (FCS) was added to this and a Penicillin/Streptomycin mixture (Flow Laboratories) 50 units of penicillin and 50 $\mu$ g of streptomycin per ml of culture medium. The cells were fed every day by replacing the culture medium and subcultured every 3 days.

#### The subculture method

The medium was poured off the cells and the flask washed with sterile phosphate buffered saline. 2-3ml of trypsin/versene solution was added to the flask, to cover the cell layer and the cells reincubated for 10-15 minutes until the cells began to lift off the base of the tissue culture flask. (The trypsin/versene solution consisted of three solutions: Solution A - 8g NaCl (BDH), 0.4g KCl (BDH), 0.58g NaHCO<sub>3</sub> (BDH), and 1g glucose (BDH) made up to 100ml and millipore filtered. Solution B - 2% EDTA disodium salt (Sigma), millipore filtered. Solution C - 4% trypsin (Sigma), millipore filtered. A working solution of 0.4% trypsin/0.2% versene was made up by mixing together 10ml each of stock solutions A,B and C with 70ml of sterile distilled water (pH7.2 -7.4). The digestion reaction was stopped by the addition of culture medium containing 20% FCS, and the resulting mixture centrifuged to concentrate the cells. The supernatant was discarded and the cell pellet resuspended in culture medium with 10% FCS and antibiotics and dispensed into 2 or 3 new culture flasks (Falcon).

## APPENDIX XII

### Method to test different fetal calf serum samples

Several different fetal calf sera were tested to find the one which promoted optimum growth of the BeWo cells. This was accomplished by preparing a series of culture media each containing a different fetal calf serum at a concentration of 15%.

BeWo cells were cultured in limbro wells (Gibco) using the different fetal calf serum culture medium mixtures according to the method used in section 3.3.(i). Growth was assessed by counting the BeWo cells after culturing for one week. The fetal calf serum used in the culture showing most growth was selected as the most suitable for culture of BeWo cells and used in subsequent cultures.

## APPENDIX XIII

### Procedure for freezing cells

The culture medium was removed from the flask and 1-2ml of trypsin-EDTA (Gibco) added, and placed at 37°C for a few minutes, until the cells began to detach from the base of the flask. The digestion was stopped by the addition of culture medium and the cells transferred to a sterile centrifuge tube, and the number of cells in the tube was assessed using a haemocytometer. ( $2 \times 10^6$  cells are required for successful freezing.) The cells were spun at 3,000 rpm for 5 minutes in a Gallenkamp bench centrifuge and the supernatant discarded. The cells were resuspended in 1ml of cold 10% DMSO (Sigma) in 50% Ham's F12 medium and 40% FCS. The cells were then transferred to a freezing vial (Nunc) and frozen slowly by placing on ice (0°C) for 6 hr. (Slow freezing ensures that the cells freeze at the same rate on both the inside and outside of the cell). They were then transferred to an insulated box and put into a -70°C freezer for 24 hours and finally transferred to and stored in liquid nitrogen. (Thawing of the cells was accomplished quickly to avoid the formation of ice crystals and consequent rupture of the cells).

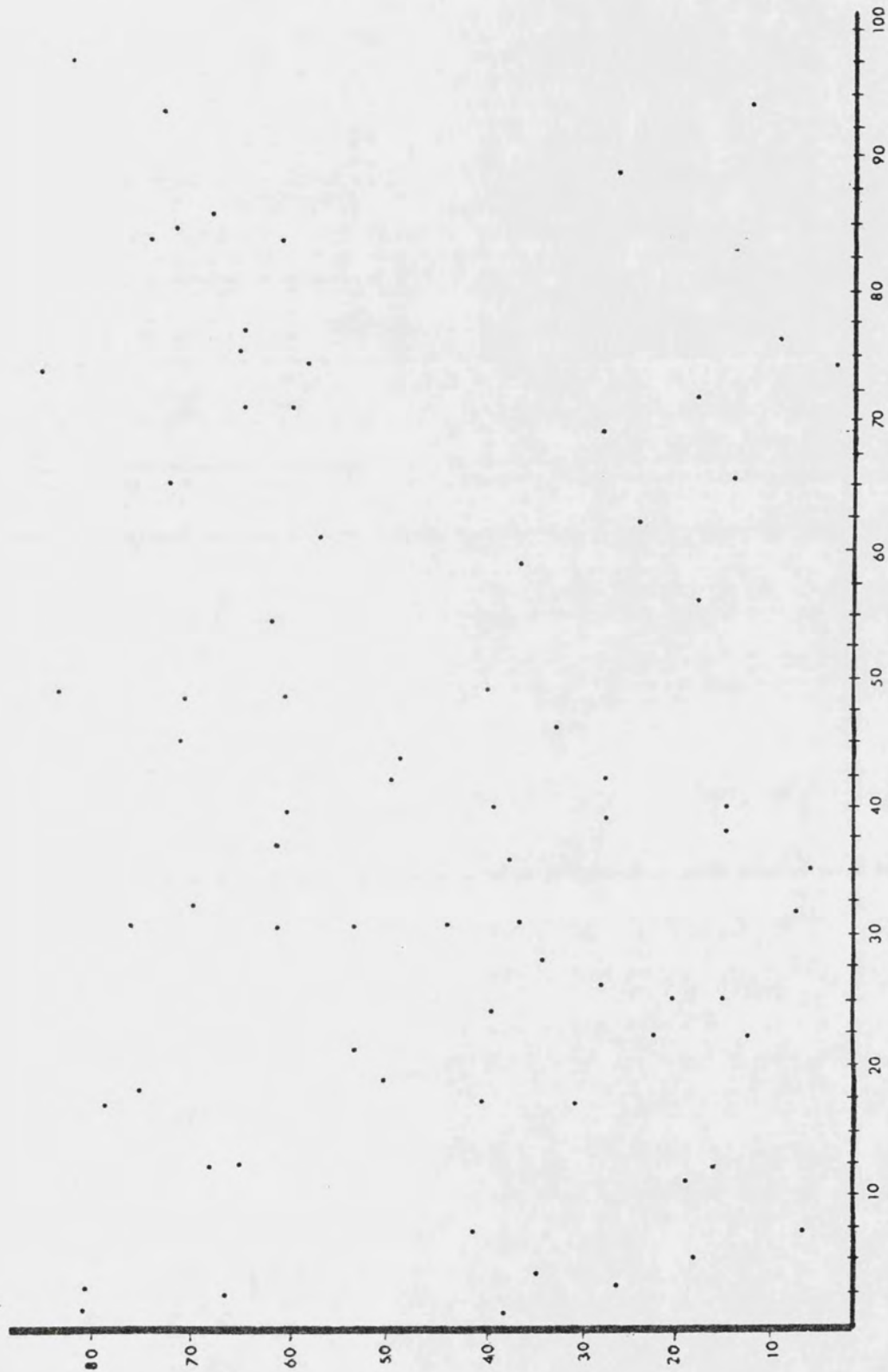
APPENDIX XIV.

Counting method used to assess the amount of radioactivity in the perfused tissue.

Photomicrographs were prepared from the experimental and control autoradiographs by systematic sampling using the vernier scale on the photomicroscope stage and moving it a constant amount for each micrograph.

The photomicrographs were then divided up into epithelial tissue, stromal tissue and background, and counts made of the number of silver grains over each area. These were compared to values obtained from control photographs using the Students t-test.

EXAMPLE OF PATTERN OF DOTS GENERATED FROM RANDOM NUMBER TABLES  
(APPENDIX XVI) - THE PATTERN WAS TRACED ON TO AN ACETATE SHEET  
AND USED AS DESCRIBED IN APPENDIX XV



## APPENDIX XV

### Method of analysis of distribution of silver grains over syncytial vesicles.

A random population of dots was prepared on transparent acetate sheets by generating pairs of random numbers from random tables and plotting them as coordinates on ordinate and abscissa on the acetate sheets, (see over).

Photomicrographs were examined for each of the control and experimental autoradiographs. The number of silver grains lying over vesicles in the epithelium was counted and expressed as a percentage of the total number of silver grains lying over the epithelium. The acetate sheets were then placed over the same photomicrograph until there were the same number of dots overlying the epithelium as there was silver grains. The number of dots overlying vesicles in the epithelium was then counted and expressed as a percentage of the total number of dots. In this way two sets of figures - % silver grains over vesicles in the epithelium and % dots over vesicles in the epithelium - were produced for the experimental and the control photomicrographs.

Appendix XVI - Random Number Table

16 15	57 04	81 71	17 45	53 29	73 46	42 78	77 63	62 58	60 59
98 63	89 52	77 43	61 08	63 90	20 38	42 71	55 70	04 81	05 50
01 03	09 35	02 54	51 95	52 75	58 29	24 23	25 19	89 97	91 29
29 07	16 34	49 22	52 06	89 34	17 11	05 91	24 38	55 06	83 59
72 61	80 54	70 99	24 64	11 33	83 65	27 23	40 37	64 58	40 53
71 11	41 02	79 37	00 45	98 54	52 89	26 24	40 13	60 38	08 86
61 03	66 28	76 82	11 18	61 90	50 63	70 57	32 06	39 95	75 94
81 89	42 34	00 49	97 53	33 16	26 91	57 58	42 48	51 05	48 27
12 24	90 84	22 16	26 95	54 11	01 96	58 81	57 97	80 98	72 81
14 28	33 43	01 32	53 39	19 54	56 57	23 58	24 37	77 35	20 97
55 41	17 89	87 04	28 32	12 45	50 03	91 08	69 24	84 44	42 83
07 59	56 87	68 73	77 64	75 19	05 51	11 64	31 75	49 35	95 60
27 59	15 53	19 68	95 47	25 69	11 90	26 19	07 40	83 59	90 95
95 53	45 52	27 55	86 81	16 29	37 60	39 35	05 24	49 00	29 07
12 95	72 72	81 84	36 58	05 10	70 50	31 04	12 67	74 01	72 90
35 23	06 68	52 50	29 55	92 28	23 83	64 27	80 00	84 53	97 97
86 33	95 73	80 92	25 49	54 50	91 21	06 62	73 91	35 05	21 37
02 82	96 23	16 46	15 51	60 31	55 27	84 14	71 58	94 71	48 35
44 46	54 96	32 58	43 22	40 17	43 25	33 31	26 26	59 34	59 00
08 77	07 19	94 46	17 51	03 73	99 89	28 44	16 87	56 16	56 09
61 59	37 08	08 45	56 75	29 48	23 07	70 79	03 80	96 81	79 68
67 70	18 01	67 19	29 49	58 67	05 56	27 24	20 70	45 31	04 32
23 09	08 79	16 73	00 32	86 74	78 55	55 72	56 54	76 07	53 73
89 10	26 39	74 58	59 55	87 11	74 05	49 45	31 94	85 66	66 97
84 95	66 42	90 74	13 71	00 71	24 41	67 62	38 92	39 26	30 29
52 14	49 02	10 31	28 15	51 01	19 09	97 94	52 43	22 21	17 66
89 55	31 41	37 87	28 15	62 48	01 84	46 05	03 39	94 10	76 21
65 94	05 03	06 63	34 72	73 17	65 24	00 65	75 78	23 97	13 04
13 03	15 75	02 83	48 26	53 77	62 96	56 52	28 26	12 15	75 53
03 13	33 57	16 71	60 27	15 18	39 33	37 01	05 86	25 14	15 41
10 04	00 95	85 04	32 80	19 01	81 03	29 29	80 04	21 52	14 76
23 94	57 28	60 43	42 25	26 48	43 13	34 68	39 22	74 85	03 25
35 63	42 50	90 74	33 17	58 77	83 36	76 22	00 89	61 55	13 17
42 85	03 36	45 33	60 77	72 92	10 76	22 55	11 00	37 60	47 73
67 26	92 87	09 96	85 37	82 61	39 01	70 05	12 66	17 39	99 34
91 93	05 56	35 76	97 35	19 37	14 66	07 57	24 41	06 90	07 72
37 14	73 35	34 01	07 94	78 28	90 33	71 56	63 77	89 24	24 28
07 40	50 58	04 93	42 97	20 42	64 68	48 35	04 38	28 28	36 94
92 18	09 46	91 99	17 41	28 60	67 94	26 54	63 70	84 73	76 61
00 49	95 43	39 67	62 40	41 31	92 28	49 57	15 55	11 81	41 89
08 59	41 41	33 59	43 28	14 51	02 71	24 45	41 57	22 11	79 79
67 03	19 54	30 33	54 68	27 93	39 35	62 51	35 55	40 99	46 19
21 97	48 06	96 41	21 25	29 03	57 71	96 49	51 74	98 90	21 52
65 05	27 45	70 93	27 39	64 37	01 63	21 03	43 78	18 74	77 07
52 70	03 20	84 96	14 37	51 05	63 99	81 02	84 56	17 78	48 45
52 88	29 93	58 21	71 05	65 58	79 08	86 37	98 76	70 45	66 23
54 16	39 40	98 57	02 05	65 15	73 23	51 51	75 06	38 13	51 68
95 22	18 59	54 57	41 22	72 35	81 24	14 94	24 04	42 26	92 14
93 10	27 94	90 45	39 33	50 26	88 46	90 57	40 47	71 63	62 59
19 20	85 20	15 67	78 03	32 23	50 59	24 83	64 99	18 00	78 50

Each digit is an independent sample from a population in which the digits 0 to 9 are equally likely, that is each has a probability of  $\frac{1}{10}$ .

## APPENDIX XVII

### Method used to demonstrate sequestration of gold particles into CB'S of BeWo cells

#### Examination of the distribution of gold particles.

#### To show that gold particles are sequestered into large vesicles (CB'S)

The area occupied by vesicles on each photograph was determined using a MOP electronic planimeter (Kontron-Messgerate). The number of particles contained in each vesicle was also computed so that a final figure of number of particles per unit of vesicle was obtained. Vesicles which did not contain any gold were also included. The number of gold particles in the cytoplasm was also computed in the same way. Vesicles to be measured were determined by the following set of criteria: (i) Vesicles must be greater than 100nm in diameter. This excludes most micropinocytic vesicles but includes capping sections through the large vesicles which were found to contain the gold particles. (ii) The vesicles have no cristae. This excludes mitochondria from the counts. (iii) Vesicles have a definite membrane. (iv) They contain light to moderately dense material. This excludes vesicles containing secretory materials. (v) In cases where the gold was found to be lying across a membrane due to an accuracy error, i.e. failure to tilt the specimen at the time of photographing to ascertain if the particles were inside the limiting membrane, a line was projected continuing the membrane, and the gold which was lying outside this line was counted as being in the cytoplasm and the particles which were contained within the line were counted as being inside the vesicle.

The number of particles in the cytoplasm were computed in the same way. Data was prepared for both the Au(18)-IgG incubations and the Au(18) only incubations. This data was compared statistically (see Appendix XVII (1) using the Mann-Whitney U-test and a significant difference was found (p 0.01)

To examine if there was a difference between the number of particles contained in vesicles in the Au(18)-IgG and Au(18) only incubations.

The data for number of particles contained per unit area of vesicle for the Au(18)-IgG and the Au(18) incubations collected above were compared statistically using the Mann-Whitney U-test. No significant difference was found between the two sets of data. (Appendix XVII (ii) ).

APPENDIX XVII (1)

Association of gold particles with vesicular structures.

AO = Overnight incubation with gold only.

IO = Overnight incubation with gold-IgG probe.

NP in  $1\text{mm}^2$  of V = Number of particles in  $1\text{mm}^2$  of vesicular tissue.

NP in  $1\text{mm}^2$  of NVT = Number of particles in  $1\text{mm}^2$  of non-vesicular tissue.

$n_1$  = Number of cases in larger sample

$n_2$  = Number of cases in smaller sample

AO incubation			
NP in $1\text{mm}^2$ V	Rank	NP in $1\text{mm}^2$ NVT	Rank
74.1	43	0.17	15
2.3	28.5	0	6
24.7	38	0	6
9.6	36	1.26	24
39.8	39	0.11	12
59.8	41	4.6	34
66.4	42	0.45	18
13.6	37	0	6
3.1	32	1.89	26
75.8	44	2.6	30
4.3	40	2.1	27
0	6	1.24	23
0	6	4.66	35
1.0	20	0	6
0.37	16.5	0	6
2.76	31	0	6
1.1	21.5	0	6
1.6	25	0	6
2.3	28.5	0	6
1.1	21.5	0.37	16.5
0.69	19	0.13	13
3.5	33	0.16	14
	$R_2 = 648.5$		$R_1 = 341.5$

Test if there is a difference between NP in 1mm<sup>2</sup> of V and NP in 1mm<sup>2</sup> of NVT.

Using Man-Whitney U-Test:

$$U = \frac{n_1 n_2 + n_1 (n_1 + 1)}{2} - R_1$$

Where  $n_1 = 22$ ;  $n_2 = 22$ ;  $R_1 = 341.5$

$$U = \frac{(22 \times 22) + 22(22 + 1)}{2} - 341.5$$

$$U = 484 + 253 - 341.5$$

$$U = 395.5$$

Substitute in z equation:

$$z = \frac{U - \frac{n_1 n_2}{2}}{\sqrt{\frac{(n_1)(n_2)(n_1 + n_2 + 1)}{12}}}$$

$$z = \frac{395.5 - 242}{\sqrt{1815}}$$

$$z = \frac{153.5}{42.6}$$

$$z = 3.6$$

Significant  $p < 0.01$

IO incubation			
NP in 1mm <sup>2</sup> V	Rank	NP in 1mm <sup>2</sup> NVT	Rank
38.6	90	0	16.5
16.5	77	0	16.5
22.4	79	0	16.5
6.3	64	0.14	37
32.0	85	0	16.5
1.5	52.5	0.11	34
25.0	81	0	16.5
0	16.5	0.38	43
33.6	87	0	16.5
1.5	52.5	0	16.5
10.0	72	0	16.5
30.0	84	0.1	33
3.9	59.5	0.18	38
8.7	69.5	0	16.5
2.6	57	0	16.5
9.5	71	0	16.5
4.6	62	5.3	63
0.42	44	0.12	35
46.4	92	0	16.5
18.6	78	0	16.5
76.9	97	0.31	42
35.4	88	1.33	50
0.7	46	0	16.5
1.64	54	0	16.5
3.9	59.5	0	16.5
1.7	55	0	16.5
28.3	83	1.43	51
33.0	86	0	16.5
15.7	76	0	16.5
6.4	65	0	16.5
7.7	67	0	16.5
47.6	93	0	16.5
14.4	74.5	0	16.5
11.0	73	0.3	41
53.0	94.5	4.0	61
37.4	89	0.6	45
119.0	98	0.22	40
0	16.5	0.86	47
28.0	82	0.21	39
8.25	68	0	16.5
2.9	58	0	16.5
14.4	74.5	0	16.5
23.0	80	0	16.5
8.7	69.5	0	16.5
1.13	49	0.127	56
6.5	66	0	16.5
42.0	91	1.76	56
53.0	94.5	0	16.5
49.7	93	0.95	48

$R_1 = 1333$

Test if there is a difference between NP in 1mm<sup>2</sup> of V and NP in 1mm<sup>2</sup> of NVT.

$$n_1 = 49; n_2 = 49; R_1 = 1333$$

Using Man-Whitney U-Test:

$$\begin{aligned} U &= \frac{(49 \times 49) + 49(50)}{2} - 1333 \\ &= 2401 + 1125 - 1333 \\ &= 2193 \end{aligned}$$

Substitute in z equation:

$$z = \frac{2193 - \frac{49 \times 49}{2}}{\sqrt{\frac{49 \times 49 (49 + 49 + 1)}{12}}}$$

$$z = \frac{2193 - 1200.5}{\sqrt{19808.25}}$$

$$z = \frac{992.5}{140.74}$$

$$z = 7.05$$

Significant  $p < 0.01$

APPENDIX XVII (ii)

Test if there is a difference between NP in 1mm<sup>2</sup> V incubated with Au<sub>(18)</sub>-IgG and NP in 1mm<sup>2</sup> V incubated with Au<sub>(18)</sub> only.

Using Man-Whitney U-Test:

$$n_1 = 22; n_2 = 49; R_1 = 676$$

$$U = \frac{(22 \times 49) + \frac{22(23)}{2} - 676}{2}$$

$$U = 1078 + 253 - 676$$

$$U = 655$$

Substitute in z equation:

$$z = \frac{655 - \frac{22 \times 49}{2}}{\sqrt{\frac{22 \times 49 (22 + 49 + 1)}{12}}}$$

$$z = \frac{116}{\sqrt{6468}}$$

$$z = \frac{116}{80.42}$$

$$z = 1.442$$

Not significant at  $p < 0.01$

IO		AO	
NP in 1mm <sup>2</sup> V	Rank	NP in 1mm <sup>2</sup> V	Rank
38.6	57	74.1	68
16.5	43	2.3	18.5
22.4	45	24.7	47
6.3	28	9.6	36
32.0	52	39.8	58
1.5	13.5	59.8	66
25.0	48	66.4	67
0	2.5	13.6	39
33.6	54	3.1	23
1.5	13.5	75.8	69
10.0	37	41.3	59
30.0	51	0	2.5
3.9	25.5	0	2.5
8.7	33.5	1.0	9
2.6	20	0.37	5
9.5	35	1.1	10.5
4.6	27	2.76	21
0.42	6	1.6	15
46.4	61	2.3	18.5
18.6	44	1.1	10.5
76.9	70	0.69	7
35.4	55	3.5	24
0.7	8		
1.64	16		
3.9	25.5		
1.7	17		
28.3	50		
33.0	53		
15.7	42		
6.4	29		
7.7	31		
47.6	62		
14.4	40.5		
11.0	38		
53.0	65		
37.4	56		
119.0	71		
0	2.5		
28.0	49		
8.25	32		
2.9	22		
14.4	40.5		
23.0	46		
8.7	33.5		
1.13	12		
6.5	30		
42.0	60		
53.0	64		
49.7	63		
	R <sub>2</sub> = 1877		R <sub>1</sub> = 676

IO		AO	
NP in 1mm <sup>2</sup> NVT	Rank	NP in 1mm <sup>2</sup> NVT	Rank
0	20	0.17	48
0	20	0	20
0	20	0	20
0.14	46	1.26	61
0	20	0.11	41.5
0.11	41.5	4.6	69
0	20	0.45	56
0.38	55	0	20
0	20	1.89	65
0	20	2.6	67
0	20	2.1	66
0.1	40	1.24	60
0.18	49	4.66	69
0	20	0	20
0	20	0	20
0	20	0	20
5.3	71	0	20
0	20	0	20
0.12	43	0	20
0	20	0.37	54
0.31	53	0.13	45
1.33	62	0.16	47
0	20		
0	20		
0	20		
0	20		
1.43	43		
0	20		
0	20		
0	20		
0	20		
0	20		
0	20		
0.3	52		
4.0	68		
0.6	57		
0.22	51		
0.86	58		
0.21	50		
0	20		
0	20		
0	20		
0	20		
0	20		
0.127	44		
0	20		
1.76	64		
0	20		
0.95	59		

$R_2 = 1877$

$R_1 = 928.5$

Test if there is a difference between NP in 1mm<sup>2</sup> NVT incubated with Au<sub>(18)</sub>-IgG and NP in 1mm<sup>2</sup> NVT incubated with Au<sub>(18)</sub> only.

Using Man-Whitney U-Test:

$$n_1 = 22; n_2 = 49; R_1 = 928.5$$

$$U = (22 \times 49) + \frac{22(23)}{2} - 928.5$$

$$U = 1078 + 253 - 928.5$$

$$U = 402.5$$

Substitute in equation z:

$$z = \frac{402.5 - \frac{22 \times 49}{2}}{\sqrt{\frac{22 \times 49 (22 + 49 + 1)}{12}}}$$

$$z = \frac{-136.7}{\sqrt{6468}}$$

$$z = \frac{-136.5}{80.42}$$

$$z = -1.697$$

Not significant  $p < 0.01$

APPENDIX XVIII

Calculation of concentration of IgG in a coated vesicle

Calculation of IgG concentration inside a coated vesicle.

$$\begin{aligned} \text{C.V. size range} &= 500 - 1000 \text{ \AA} \text{ ext. diameter.} \\ &= 750 \text{ \AA} \text{ average ext. diameter.} \\ &= 550 \text{ \AA} \text{ internal diameter.} \\ &= 0.00000275 \text{ cm radius.} \end{aligned}$$

$$\begin{aligned} \text{Average volume} &= \frac{4}{3} \times 3.142 \times (0.00000275)^3 \text{ cm}^3 \\ &= 4.188790204 \times 2.0796875 \times 10^{-17} \text{ cm}^3 \\ &= 8.7113746 \times 10^{-17} \text{ cm}^3 \end{aligned}$$

But Pearse (1983) calculates average coated vesicle contains 4 IgG molecules.

$$1 \text{ IgG molecule occupies } 2.1778436 \times 10^{-17} \text{ cm}^3$$

$$1 \text{ cm}^3 \text{ of CV lumen contains } \frac{1}{2.1778436} \times 10^{-17} \text{ IgG.}$$

Now  $6.025 \times 10^{23}$  molecules of IgG weigh 160,000g

$$1 \text{ molecule weighs } \frac{160,000}{6.025 \times 10^{23}}$$

$$1 \text{ cm}^3 \text{ of CV lumen contains } \frac{1}{2.1778436} \times 10^{-17} \times \frac{160,000}{6.025 \times 10^{23}} \text{ g}$$

$$\begin{aligned} &= \frac{160,000}{13121508.02} = 0.01219372 \text{ g / cm}^3 \\ &= 12.19372 \text{ mg / ml.} \end{aligned}$$

BIBLIOGRAPHY

- Adinolfi, M. (1975)  
The Human placenta as a filter for cells and plasma proteins.  
In: Immunobiology of trophoblast. Clinical and experimental  
Immunoreproduction 1.  
Edwards. R.G; Howe C.W.S; Johnson M.H.  
C.U.P. London N.Y. Melbourne. p193
- Aladjem, S., Lueck, J., Harris, J., Wynn. R. (1975)  
Culture of human placenta.  
In: Proceedings of the sixteenth Chilean Congress of obstetrics  
and Gynecology. Campodonico, I  
Santiago; Chile. p.25
- Aladjem, S., Lueck, J., Tsai, A. (1980)  
A method for prolonged in vitro culture of normal human term  
trophoblast.  
Federation of the American Society of Experimental Biology 39 506
- Allansmith, M, McClennan, B.H., Butterworth, M., Moloney, J.R.(1968)  
The development of immunological levels in man.  
J. Pediat. 72 276-289
- Allen, R.D., David, G.B., Normarski, G. (1969)  
The Zeiss - Normarski differential interference equipment for  
transmitted light microscopy.  
Zeitschrift für Wissenschaftliche-mikroskopie und mikroskopische  
Technik 69 193-221
- Alvarez, H. (1964)  
Morphology and physiopathology of the human placenta. 1. Studies  
of morphology and development of chorionic villi by phase contrast  
microscopy.  
Obstet. Gynecol. 23 813-825
- Anderson, T.F. (1950)  
The use of critical point phenomena in preparing specimens for  
the electron microscope.  
J. Appl. Phys. 21 724
- Anderson, R.G.W., Goldstein, J.L., Brown, M.S., (1976)  
Localisation of low-density lipoprotein receptors on plasma membrane  
of normal human fibroblasts and their absence in cells from a  
familial hypercholesterolemia homozygote.  
Proc. Nat'l. Acad. Sci. U.S.A. 73 2434-2438
- Anderson, R.G.W., Goldstein, J.L., Brown, M.S. (1977)  
A mutation that impairs the ability of lipoprotein receptors to  
localise in coated pits on the cell surface of human fibroblasts.  
Nature, Lond. 270 695-699
- Anderson, R.G.W., Vasile, E., Mello, R.J., Brown, M.S., Goldstein,  
J.L., (1978)  
Immunocytochemical visualisation of coated pits and vesicles in  
human fibroblasts: relation to low density lipoprotein receptor  
distribution.  
Cell. 15 919-933

- Anderson, R.G.W., Brown, M.S., Goldstein, J.L. (1981)  
Inefficient internalization of receptor - bound low density lipoprotein in human carcinoma A-431 cells.  
J.Cell. Biol. 88 441-452
- Baker, B.L., Hook, J.J. and Severinghaus, A.E., (1944)  
The cytological structure of the human chorionic villus and decidua parietalis.  
Am. J. Anat. 74 291-326
- Balfour, A. and Jones, E.A. (1976)  
The binding of IgG to human placental membranes in maternofetal transmission of immunoglobulins.  
Hemmings W.A.: C.U.P. Cambridge p.61-72
- Bangham, D.R., Hobbs, K.R. and Terry, R.J. (1958)  
Selective placental transfer of serum proteins in rhesus.  
Lancet. ii, 351-354
- Barr, M., Glenny, A.T. and Randall, K.J. (1949)  
Concentration of diphtheria antitoxin in cord blood and rate of loss in babies.  
Lancet. 2 324-326
- Bauer, H., Horisberger, M., Bush, D.A. and Sigarlakie, E. (1972)  
Mannan as a major component of the bud scar of Saccharomyces cerevisiae.  
Arch. Mikrobiol. 85 202-8
- Bauer, H., Farr, D.R. and Horisberger, M. (1974)  
Ultrastructural localisation of cell wall teichoic acids in Streptococcus faecalis by means of concanavalin A.  
Arch Mikrobiol. 97 17-26
- Becker, V. and Bleyl, V. (1961)  
Placentarzotte bei Schwangerschaftstoxicose und fetaler Erythroblastose im fluorescenzmikroskopischen Bilde.  
Virchows Arch. Pathol. Anat. Physiol. 334 516-527
- Blackburn, W.R. and Vinijchaikul, K. (1969)  
The pancreas in Kwashiorkor. An electron microscopic study.  
Lab. Invest. 20 305-318
- Bliel, J.D. and Bretscher, M.S. (1982)  
Transferrinreceptor and its recycling in HeLa cells.  
E.M.B.O. (Eur. Mol. Biol. Organ.) 1 (3) 351-355
- Blitz, A.L., Fine, R.E. and Toselli, P.A. (1977)  
Evidence that coated vesicles isolated from brain are calcium sequestering organelles resembling sarcoplasmic reticulum.  
J.Cell. Biol. 75 135-147

- Booth, A.G. and Wilson, M.J. (1981)  
Human placental coated vesicles contain receptor - bound transferrin.  
Biochem. J. 196 355-362
- Boyd, J.D and Hugnes, F.W. (1954)  
Observations on human chorionic villi using the electron microscopy.  
J. Anat. 88 356-362
- Boyd, J.D. and Hamilton, W.J. (1966)  
Electron microscopic observations on the cytotrophoblast contribution to the syncythium in the human placenta.  
J.Anat. 100 535-548
- Boyd, J.D. and Hamilton, W.J. (1967)  
Development and structure of human placenta from the end of the third month of gestation.  
J.Obstet. Gynecol. Br.Commonw. 74 161-226
- Boyd, J.D., Boyd, C.A.R. and Hamilton, W.J. (1968a)  
Observations on the vacuolar structure of the human syncytiotrophoblast.  
Z.Zellforsch. Mikrosk. Anat. 88 57-79
- Boyd, J.D., Hamilton, W.J. and Boyd, C.A.R. (1968b).  
The surface of the syncytium of the human chorionic villus.  
J.Anat. 102 553-563
- Boyd, J.D. and Hamilton, W.J. (1970)  
The Human Placenta.  
W.Hoffer and Sons. Cambridge.
- Brambell, F.W.R., Brierley, J., Halliday, R. and Hemmings, W. A;(1954)  
Transfer of passive immunity from mother to young.  
Lancet 1 964-965
- Brambell, F.W.R. (1966)  
Transmission of immunity from mother to young and catabolism of immunoglobulins.  
Lancet. ii 1087
- Brambell, F.W.R. (1970)  
The transmission of passive immunity from mother to young  
North Holland Publ. Co. Amsterdam.
- Burgess, J. and Linstead, P.J. (1977)  
Membrane mobility and the Concanvilin A binding system of the plasmalemma of higher plant protoplasts.  
Planta (Berl) 136 253-260
- Caro, L.G. and Van Tubergen, R.P. (1962)  
High Resolution Autoradiography.  
J.Cell. Biol. 15 173-199
- Carpenter, G., King, L. and Cohen, S. (1979)  
Rapid enhancement of protein phosphorylation in A-431 cell membrane preparations by epidermal growth factor.  
J.Biol. Chem. 254 4884-4891

- Carter, J.E. (1964)  
Morphological evidence of syncytial formation from the  
cytotrophoblast.  
J.Obstet. Gynecol. 23. 647-656
- Challier, J.C., Schneider, H. and Dancis, J. (1976)  
In vitro perfusion of the human placenta.  
Am.J. Obstet. Gynecol. 126 261-265
- Chandra, R.K. (1976)  
Levels of IgG, IgM and tetanus antitoxin in paired maternal  
and fetal sera: Findings in healthy pregnancy and placental  
insufficiency.  
In: Maternofetal transmission of Immunoglobulins.  
Hemmings. W.A.: Camb. University Press. Cambridge. p.77-87
- Clint, J.M., Wakely, J. and Ockleford, C.D. (1979)  
Differentiated regions of the human placental cell surface  
associated with the attachment of chorionic villi, phagocytosis of  
maternal erythrocytes and syncytiotrophoblast repair.  
Proc. R. Soc. London. Ser. B. 204 345-353
- Dancis, J., Lind, J., Oratz, M., Smolens, J. and Vara, P. (1961)  
Placental transfer of proteins in human gestation.  
Am. J. Obstet. Gynecol. 82 167-171
- Das, M. (1980)  
Mitogenic hormone-induced intracellular message: Assay and  
partial characterisation of an activator of DNA replication  
induced by epidermal growth factor.  
Proc. Nat'l. Acad. Sci. USA. 77 112-116
- Dearden, L. and Ockleford, C.D. (1983)  
Structure of human trophoblast: correlation with function.  
In: Biology of Trophoblast.  
Loke, Y.W. and Whyte, A.  
Elsevier. Amsterdam. New York. Oxford. p.69-110
- Dempsey, E.W. and Luse, S.A. (1971)  
Regional specialization in the syncytial trophoblast of early  
human placentae.  
J.Anat. 108 545-561
- Dickson, R.B., Nicolas, J., Willingham, M.C., Pastan, I. (1981)  
Internalisation of  $\alpha_2$  macroglobulin in receptosomes. Studies with  
monovalent markers.  
Expt'l. Cell Res. 132(2) 488-93
- Edelman, G.M., Cunningham, B.A., Gall, W.E., Gottlieb, P.D.,  
Rutishauser, U. and Waxdal, M.J. (1969)  
The covalent structure of an entire G immunoglobulin molecule.  
Proc. Nat. Acad. Sci. 63 78-85
- Enders, A.C. (1965)  
A comparative study of the fine structure of the trophoblast  
in several haemochorial placentae.  
Am. J. Anat. 116. 29-67

Fan, J., Carpentier, J., Gorden, P., Van Obberghen, E., Blackett, N., Grunfeld, C. and Orci, L. (1982)

Receptor - mediated endocytosis of insulin: Role of microvilli, coated pits and coated vesicles.

Proc. Nat. Acad. Sci. USA 79 7788-7791

Faulk, W.P. and Taylor, G.M. (1971)

An immunocolloid method for the electron microscope.

Immunochemistry 8 1081-1083

Favard, P. and Carasso, N. (1973)

The preparation and observation of thick biological sections in the high voltage electron microscope.

J. Microscopy 97 59-81

Fawcett, D.W. (1965)

Surface specialisations of absorbing cells.

J. Histochem. Cytochem 13 75-91

Fox, H. and Agrofojo-Blanco, A. (1974)

Scanning electron microscopy of the human placenta in normal and abnormal pregnancies.

Eur. J. Obstet. Gynecol. Reprod. Biol. 4 45-50

Fox, H. (1965)

The significance of villous syncytial knots in the human placenta.

Obstet. Gynecol. Br. Commonw. 72 347-355

Fox, H. (1967)

The incidence and significance of vasculosyncytial membranes in the human placenta.

J. Obstet. Gynecol. Br. Commonw. 74 28-33

Fox, H. (1978a)

In: Major problems in Pathology. The Pathology of the human placenta Vol 7. Saunders. London p.1-37

Fox, H. (1978b)

Placental structure.

In: Scientific basis of obstetrics and gynaecology. 2nd ed.

R.R. Macdonald. Churchill Livingstone. Edinburgh. p.28-59

Franke, W.W. and Schinko, W. (1969)

Nuclear shape in muscle cells.

J. Cell Biol. 42 326-331

Frens, G. (1973)

Controlled nucleation for the regulation of the particle size in monodisperse gold suspensions.

Nature Phys. Sci. 241 20-22

Friend, D.S. and Farquhar, M.G. (1967)

Functions of coated vesicles during protein absorption in rat vas deferens.

J. Cell. Biol. 35 357-376

- Galton, M. (1962)  
DNA content of placental nuclei.  
J.Cell. Biol. 13 183-203
- Garland, J.M., Archibald, A.D. and Baddiley, J. (1975)  
An electron microscopic study of localisation of teichoic acid and its contribution to staining reactions in walls of streptococcus faecalis.  
J.General. Microbiol. 89 73-86
- Geoghegan, W.D. and Ackerman, G.A. (1977)  
Adsorption of horseradish peroxidase, ovomucoid and anti-immunoglobulin to colloidal gold for indirect detection of concanavalin A, wheat germ agglutinin and goat anti-human immunoglobulin on cell surfaces at the electron microscopic level: a new method-theory and application.  
J. Histchem. Cytochem. 25. 1187-1200
- Geoghegan, W.D., Scillian, J.J. and Ackerman, G.A. (1978)  
The detection of human B lymphocytes by both light and electron microscopy utilizing colloidal gold labelled anti-immunoglobulin.  
Immunol. Communications 7 (1) 1-12
- Geoghegan, W., Ambegankar, S. and Calvanico, W.J. (1980)  
Passive gold agglutination. An alternative to passive haemagglutination.  
J.Immunol. Methods. 34 11-22
- Gerber, H., Horisberger, M. and Bauer, H. (1973)  
Immunosorbent for the isolation of specific antibodies against mannan localisation of antigens in yeast cell walls.  
Infect. Immun. 7 487-492
- Getzowa, S. and Sadowsky, A. (1950)  
On the structure of the human placenta with full term and immature fetus, living or dead.  
J.Obstet. Gynecol. Br. Emp. 57 388-396
- Gey, G.O., Seegar, G.E. and Hellman, L.M. (1938)  
The production of a Gonadotropic Substance (Prolan) by placental cells in tissue culture.  
Science 88 306-307
- Ghadially, F.N. (1975)  
Ultrastructural Pathology of the cell - A text and atlas of physiological and pathological alterations in Cell Fine Structure.  
Butterworths. London & Boston.
- Gitlin, D., Kumate, J., Urrusti, J., and Morales, C. (1964a)  
The selectivity of the human placenta in the transfer of plasma proteins from mother to fetus.  
J.Clin. Invest. 43 1938-1951

- Gitlin, D., Kumate, J., Urrusti, J. and Morales, C. (1964b)  
 Selective and directional transfer of 7S and globulin across  
 the human placenta.  
*Nature (Lond)* 203 86-87
- Gitlin, J.D., and Gitlin, D. (1974)  
 Protein binding by specific receptors on human placenta and  
 suckling murine placenta in relation to protein transport across  
 these tissues.  
*J.Clin. Invest.* 54 1155-1166
- Gitlin, J.D., and Gitlin, D. (1976)  
 Protein binding by cell membranes and the selective transfer of  
 proteins from mother to young across tissue barriers.  
 In: *Maternofetal transmission of Immunoglobulins.*  
 Hemmings, W.A. Cambridge. Cambridge University Press. p.113-119
- Grey, A.M. and Kungel, H.G. (1964)  
 H chain subgroups of myeloma proteins and normal 7S gamma globulin.  
*J.Exp. Med.* 120 253-263
- Goerke, R.J., McKean, C.M., Margolis, A.J., Glendening, M.B. and  
 Page, E.W. (1961)  
 Studies of the isolated perfused human placenta. I methods and  
 organ responses.  
*Am.J. Obstet. Gynecol.* 81 1132-1139
- Goldstein, J.L., Anderson, R.G.W. and Brown, M.S. (1979)  
 Coated pits, coated vesicles and receptor - mediated endocytosis  
*Nature* 279 679-684
- Good, R.A. and Zak, S.J. (1956)  
 Disturbances in gamma-globulin synthesis as 'experiments of  
 nature'.  
*Pediatrics* 18 109-149
- Goodman, S.L., Hodges, G.M. and Livingston, D.C. (1980)  
 A review of the colloidal gold marker system.  
 In: *Scanning Electron Microscopy 1980/II*  
 Johari, O. Sem. inc. AMF. O'Hare. Chicago. p.133-146
- Goodman, S.L., Hodges, G.M., Trejdosiewicz, L.K. and Livingston,  
 D.C.(1981)  
 Colloidal gold markers and probes for routine application in  
 microscopy.  
*J. Microscopy* 123 (2) 201-213
- Hay, F.C., Hull, M.S. and Topping, G. (1971)  
 The transfer of human IgG subclasses from mother to fetus  
*Clinical and Experimental Immunology* 9 355-8
- Haigler, H.J. McKanna, J. and Cohn, S. (1979)  
 Direct visualisation of the binding and internalisation of a  
 ferritin conjugate of epidermal growth factor in human carcinoma  
 cells. A-431  
*J.Cell Biol.* 81 382-395

- Hemmings, W.A. and Williams, E.W. (1976)  
The attachment of IgG to cell components of transporting membranes.  
In: *Maternofetal Transmission of Immunoglobulins.*  
Hemmings, W.A. Cambridge University Press. Cambridge.  
p 91-111.
- Hertz, R. (1961)  
Choriocarcinoma of women maintained in serial passage in hamster and rat.  
Proceedings of the Society for Experimental Biology and Medicine  
102 77
- Heuser, J. (1980)  
Three dimensional visualisation of coated vesicle formation in fibroblasts.  
J.Cell. Biol. 84 560-583
- Horisberger, M., Rosset, J., Bauer, H. (1975)  
Colloidal gold granules as markers for cell surface receptors in the scanning electron microscope.  
Experientia 31 1147-1149
- Horisberger, M. and Rosset, J. (1977)  
Colloidal gold, a useful marker for transmission and scanning electron microscopy.  
Histochem. Cytochem. 25(4) 295-305
- Horisberger, M. and Vonlanthen, M. (1977)  
Localisation of mannan and chitin on thin sections of budding yeast with gold markers.  
Arch. Microbiol. 115 1-7
- Horisberger, M. and Vonlanthen, M. (1978)  
Simultaneous localisation of a hepatic binding protein specific for galactose and of galactose containing receptors on rat hepatocytes.  
J. Histochem. Cytochem. 26 960-966
- Horisberger, M., Vonlanthen, M., and Rosset, J.(1978a)  
Localisation of  $\alpha$ -galactomannan and wheat germ agglutinin receptor in Schizosaccharomyces pombe.  
Arch. Microbiol. 119 107-111
- Horisberger, M., Farr, D.R. and Vonlanthen, M. (1978b)  
Ultrastructural localisation of  $\beta$ -D-galactan in the nuclei of the myxomycete Physarum polycephalum.  
Biochem. Biophys. Acta. 542 308-314
- Horisberger, M. (1979)  
Evaluation of colloidal gold as a cytochemical marker for transmission and scanning electron microscopy.  
Biol. Cellulaire 36 253-258
- Horisberger, M. and Vonlanthen, M. (1979)  
Multiple marking of cell surface receptors by gold granules: Simultaneous localisation of three lectin receptors on human erythrocytes.  
J. Microscopy 115 97-102

- Hormann, G. (1966)  
 Über die sogenannten septen, inseln, Zysten, Furchen und die  
 Randzone der menschlichen Plazenta.  
 Z.Geburtsch. Gynakol. 165 125-134
- Huxham, I.M. and Beck, F. (1981)  
 Receptor mediated coated vesicle transport of rat IgG across the  
 11.5 day in vitro rat yolk sac endoderm.  
 Cell. Biol. Int. Reports 5 (12) 1073-1081
- Huxham, I.M. (1982)  
 Yolk-sac receptors: their association with coated vesicles and  
 transport of specific proteins in vitro in the early post-  
 implantation rat conceptus.  
 Ph.D. thesis: University of Leicester.
- Jenkinson, E.J., Billington, W.D. and Elson, J. (1976)  
 Detection of receptors for immunoglobulin on human placenta by  
 E.A. rosette formation,  
 Clin. Exp. Immunol. 23 456-461
- Jirgensons, B. and Straumanis, M.E. (1964)  
 A short text of colloidal Chemistry. 2nd ed. Pergamon Press.  
 London
- Johnson, P.M., Brown, P.J. (1981)  
 Fc $\gamma$  receptor in the human placenta.  
 Placenta 2 (4) 355-370
- Johnson, P.M., Brown, P.J., and Slade, M.B. (1982)  
 Identification of syncytiotrophoblast - associated IgG in term  
 human placentae.  
 J.Reproductive Immunol. 4 (1) 1-9
- Jones, C.P.J and Fox, H. (1977)  
 Syncytial knots and intervillous bridges in the human placenta  
 J.Anat. 124 275-286
- Jones, G.E.S., Gey, G.O. and Gey, M.K. (1943)  
 Hormone production by placental cells maintained in continuous  
 culture.  
 Bull. John Hopkins Hospital 72 26-38
- Jones, E.A. and Waldmann, T.A. (1972)  
 The mechanism of intestinal uptake and transcellular transport  
 of IgG in the neonatal rat.  
 J.Clin. Invest. 51 2916-2927
- Kanaseki, T. and Kadota, K. (1969)  
 The 'vesicle in a basket' - A morphological study of the coated vesicle  
 isolated from nerve endings of guinea-pig brain with special reference  
 to mechanisms of membrane movement.  
 J.Cell. Biol. 42 202-220

Kastschenko, N. (1885)

Das menschliche chorionepithel und dessen Kollagen bei der Histogenese der Placenta. Arch. Anat. Physiol. Leipzig. Jahr. 451-480

Keen, J.H., Willingham, M.C. and Pastan, I.H. (1979)

Clathrin - coated vesicles: isolation, dissociation and factor - dependent reassociation of clathrin baskets. Cell 16 303-312

Kempe, C.H. and Benenson, A.S. (1953)

Vaccinia. Passive immunity in newborn infants. I. Placental transmission of antibodies. II Response to vaccination. J. Pediat. 43 525-531

Kessel, R.G. (1968)

Annulate lamellae. J. Ultrastruct. Res. Supp 10.

King, B.F. and Enders, A.C. (1970)

Protein absorption and transport by the guinea pig visceral yolk-sac placenta. Am. J. Anat. 129 261-289

King, B.F. (1977)

Invitro absorption of peroxidase - conjugated IgG by human placental villi. Anat. Rec. 187 624-625

Kohler, P.F. and Farr, R.S. (1966)

Elevation of cord over maternal IgG immunoglobulins. Nature. 210. 1070-1

Krantz, K.E., Panos, T.C. and Evans, J. (1962)

Physiology of the maternal - fetal relationship through the extracorpeal circulation of the human placenta. Am. J. Obstet. Gynec. 83 1214-1228

Lane, B.P. (1955)

Alterations in the cytological detail of intestinal smooth muscle cells in various stages of contractions. J. Cell. Biol. 27. 199-213

Lin, C.T. (1980)

Immunoelectron microscopic localisation of immunoglobulin G in human placenta. J. Histochem. Cytochem. 28 (4) 339-346

Loke, Y.W. (1978)

Immunology and immunopathology of the human fetal - maternal interaction. Elsevier. North Holland.

Loke, Y.W. and Borland, R. (1970)

Immunofluorescent localisation of chorionic gonadotrophin in monolayer cultures of human trophoblast cells. Nature 228 561-562.

Lozinski, P. (1911)

I. Wissenschaftliche mitteilungen 1. Über die Malpighischen Gefäße der Myrmeleonidenlarven als Spinnrüben. Zool Anz 38 401-429

- Ludwig, H. (1974)  
 Surface structure of the human placenta.  
 In: *The Placenta: Biological and Clinical aspects*. Michissi. K.S.  
 and Hafez.  
 Springfield. Illinois. Charles C. Thomas. p.40-64
- Lueck, J. and Aladjem, S. (1980)  
 Time lapse study of normal human trophoblast in vitro.  
 Am.J. Obstetrics. & Gynecology 138 288-292
- Lutzner, M.A. and Jordan, H.W. (1968)  
 The ultrastructure of an abnormal cell in Sezary's syndrome.  
 Blood 31 719 - 726
- Mahadevan, S. and Tappel, A.L. (1968a)  
 Lysosomal lipases of rat liver and kidney.  
 J.Biol. Chem. 243 2849-2854
- Mahadevan, S. and Tappel, A.L. (1968b)  
 Hydrolysis of higher fatty acid esters of p-nitrophenol by rat  
 liver and kidney lysosomes.  
 Archs. Biochem. Biophys. 126 945-953
- Mantyljarvi, R. , Hirvonen, T. and Toivanen, P. (1970)  
 Maternal antibodies in human meonatal sera.  
 Immunol. 18 449-451
- Marsh, M. and Helenius, A. (1981)  
 Adsorptive endocytosis of Semliki Forest virus.  
 J.Mol. Biol. 142 439-454
- Martin, B.J. and Spicer, S.S. (1973)  
 Multivesicular bodies and related structures of the syncytiotropho-  
 blast of human term placenta.  
 Anat. Rec. 175 15-36
- Matre, R., Tonder, O. and Endresen, C. (1975)  
 Fc receptors in human placenta.  
 Scand. J. Immunol. 4 741-745
- Matre, R. (1977)  
 Similarities of Fc receptors on trophoblasts and placental  
 endothelial cells.  
 Scand. J.Immunol.6 953-958
- McNabb, T., Koh, T.Y., Dorrington, K.J. and Painter, R.H. (1976)  
 Structure and function of immunoglobulin domains V.Binding of  
 immunoglobulin G and fragments to placental membrane preparations.  
 J.Immunol. 117 882-887
- Maxfield, F. R., Schlessinger, J., Schechter, Y., Pastan, I. and  
 Willingham, M.C. (1978)  
 Collection of insulin, E.G.F. and  $\alpha$ 2 macroglobulin in the same  
 patches on the surface of cultured fibroblasts and common  
 internalisation.  
 Cell 14 805-810

- Merriam, R.W. (1962)  
Some dynamic aspects of the nuclear envelope.  
*J.Cell. Biol.* 12 79-90
- Midgley, A.R. Jr. and Pierce, G.R. Jr. (1962)  
Immunohistochemical localisation of human chorionic gonadotrophin  
*J.Exp. Med.* 115 289-294
- Moskalewski, S., Ptak, W., Czarnik, Z. (1975)  
Demonstration of cells with IgG receptors in human placenta.  
*Biol. Neonate* 26 268-273
- Doxon, L.A., Wild, A.E. and Slade, B.S. (1976)  
Localisation of proteins in coated micropinocytic vesicles during  
transport across rabbit yolk-sac endoderm.  
*Cell and Tissue Res.* 171 175-193
- Neill, J.M., Gaspari, E.L., Richardson, L.V., and Sugg, J.Y (1932)  
Diphtheria antibodies transmitted from mother to child.  
*J. Immunol* 22 117-124
- Nesbitt, R.E. Jr., Rice, P.A., Rourke, J.E., Tores, V.F. and  
Souchay, A.M. (1970)  
Perfusion studies using the human placenta.  
*Gynecol. Invest.* 1 185-196
- Niezgodka, M., Mikulska, J., Ugorski, M. , Boratynski, J. and  
Lisowski, J. (1980)  
Human placenta membrane receptor for IgG-1. Studies on the  
properties and solubilisation of the receptor.  
*Molecular Immunology.* 18 163-172
- Ockleford, C.D. (1976)  
A three dimensional reconstruction of the polygonal pattern on  
placental coated vesicle membranes.  
*J.Cell. Sci.* 21 83-91
- Ockleford, C.D., Whyte, A. and Bowyer, D.E. (1977)  
Variation in volume of coated vesicles isolated from human  
placenta.  
*Cell. Biol. Int. Reports.* 1 137-146
- Ockleford, C.D. and Menon, G. (1977)  
Differentiated regions of human placental cell surface associated  
with exchange of materials between maternal and fetal blood: A  
new organelle and the binding of iron.  
*J. Cell.Sci.* 25 279-291
- Ockleford, C.D. and Whyte, A. (1977)  
Differentiated regions of human placental cell surface associated  
with exchange of materials between maternal and fetal blood:  
coated vesicles.  
*J.Cell. Sci.* 25 293-312

- Ockleford, C.D., White, A. and Bowyer, D.E. (1977)  
Negative staining of coated vesicles.  
*Micron* 8 233-235
- Ockleford, C.D. and Clint, J.M. (1980)  
The uptake of IgG by human placental chorionic villi: A  
correlated autoradiographic and wide aperture counting study.  
*Placenta* 1 91-111
- Ockleford, C.D., Wakely, J. and Badley, R.A., (1981)  
Morphogenesis of human placental chorionic villi; cytoskeletal,  
syncytioskeletal and extracellular matrix proteins.  
*Proc. R. Soc. Lond. B.* 212 305-316
- Ockleford, C.D., (1982)  
Coated vesicles. In: *electron microscopy of proteins.* R.Harris.  
Academic Press. New York and London p 255-299
- Ockleford, C.D., Dearden, L. (1983)  
The acquisition of immunity by the fetus.  
In: *Immunological aspects of reproduction in mammals.*  
D.B. Crichton. Butterworths. In press.
- Ockleford, C.D., Dearden, L. and Badley, R.A. (1983/4)  
Syncytioskeletons in choriocarcinoma in culture.  
*J.Cell. Sci.* In Press.
- Ogra, S.S., Weintraub, D and Ogra, P.L. (1977)  
Immunological aspects of human colostrum and milk. III fate and  
absorption of cellular and soluble components via the gastroint-  
estinal tract of the newborn.  
*J. Immunol.* 119 245-8
- Okudaira, Y., Hashimoto, T., Hamanaka, N. and Yoshinare, S. (1971)  
Electron microscopic study on the trophoblast cell column of human  
placenta.  
*J. Electron. Microsc.* (Tokyo) 20 (2) 93-106
- Osborn, J.J., Dancis, J., and Julia, J.F. (1952)  
Studies on the immunology of the newborn infant. II Interference  
with active immunization by passive transplacental circulating  
antibody.  
*Pediatrics* 10 328-334
- Pattillo, R.A. and Gey, G.O. (1968)  
Establishment of cell line of human hormone synthesizing  
trophoblastic cells *in vitro*.  
*Cancer Research* 28 1231-1236
- Pearse, B.M.F. (1976)  
Clathrin: a unique protein associated with intracellular transfer  
of membrane by coated vesicles.  
*Proc. Nat. Acad. Sci. USA.* 73 1255-1259

- Pearse, B.M.F. (1978)  
On the structural and functional components of coated vesicles.  
J.Mol. Biol. 126 803-812
- Pearse, B.M.F. (1980)  
Coated vesicles. Trends.  
Biochem. Sci. 111 131-134
- Pearse, B.M.F. (1982)  
Coated vesicles from human placenta carry ferritin, transferrin  
and Immunoglobulin G.  
Proc. Nat. Acad. Sci. USA Biol. Sci. 79 (2) 451-455
- Penfold, L., Drury, R., Simmonds, K. and Hytten, F.E. (1981)  
Studies of a single placental cotyledon in vitro I. The  
preparation and its viability.  
Placenta 2 149-154
- Petersen, O.W. and Van Deurs, B. (1983)  
Serial section analysis of coated pits and vesicles involved  
in absorptive pinocytosis in cultured fibroblasts.  
J.Cell. Biol. 96 277-281
- Pierce, G.B.Jr., and Midgely, A.R.Jr. (1963)  
Origin and function of human syncytium giant cells.  
Am.J.Pathol. 43 153-173
- Pilch, P., Shia, M., Benson, R.J. and Fine, R. (1983)  
Coated vesicles participate in receptor - mediated endocytosis  
of insulin.  
J.Cell. Biol. 96 133-138
- Porter, R.R. (1960)  
The chemical structure of gamma globulin and antibodies and its  
relation to theories of antibody formation  
In: Mechanisms of antibody formation. A symposium Holub and  
Jaroskova. Academic Press. p 208-210.
- Reynolds, E.S. (1963)  
The use of leadcitrate at high pH, as an electron opaque stain  
in electron microscopy.  
J.Cell Biol. 17 208-212
- Rhodin, J.A.G. and Terzakis, J. (1962).  
The ultrastructure of the human full term placenta.  
J. Ultrast. Res. 6 88-106
- Rhodin, J.A.G. (1963)  
An atlas of ultrastructure.  
Saunders Philadelphia. Pa. p.14.
- Richart, R. (1961)  
Studies of placental morphogenesis. 1. Radioautographic studies  
of human placenta utilizing tritiated thymidine.  
Proc. Soc. Exp. Biol. Med. (New York) 106 829-831

- Rodewald, R. (1976)  
 Intestinal transport of peroxidase - conjugated IgG fragments  
 in the neonatal rat.  
 In: Maternofetal transmission of Immunoglobulins. Hemmings  
 W.A. Cambridge University Press. Cambridge. p137-153
- Rodewald, R. (1980)  
 Immunoglobulin transmission in mammalian young and the in -  
 volvement of coated vesicles.  
 In: Coated vesicles. C.D. Ockleford and A. Whyte.  
 Cambridge. Cambridge University Press p69-101
- Romano, E.L. and Romano, M. (1977)  
 Staphylococcal protein A bound to colloidal gold: a useful  
 reagent to label antigen - antibody sites in electron microscopy.  
 Immunochem. 14 711-715
- Roth, T.F. and Porter, K.R. (1964)  
 Yolk protein uptake in oocyte of mosquito, Aedes aegypti.  
 J.Cell Biol 20 313-332
- Roth, J. and Binder, M. (1978)  
 Colloidal gold, ferritin and peroxidase as markers for electron  
 microscopic double labellinglectin technique.  
 J. Histochem. Cytochem. 26 163-169
- Roth, J., Bendayan, M. and Orci, L. (1978)  
 Ultrastructural localisation of intracellular antigens by the  
 use of protein A - gold complex.  
 J. Histochem. Cytochem. 26 1074-1081
- Ryan, K.J. (1959)  
 Metabolism of C-16 oxygenated steroids by human placenta.  
 The formation of estriol.  
 J. Biol. Chem. 234. 2006-2008
- Salazar, H. and Gonzalez - Angulo, A. (1967)  
 The fine structure of human chorionic villi and placental  
 transfer of iron in late pregnancy.  
 Am. J. Obstet. Gynecol. 87 851-865
- Salisbury, J.L., Condeelis, J.S., Maihle, N.J., Satir, P. (1981)  
 Calmodulin localisation during capping and receptor mediated  
 endocytosis.  
 Nature 294 163-166
- Schlessinger, J. (1980)  
 The mechanism and role of hormone induced clustering of membrane  
 receptors.  
 T.I.B.S. 5 210-214
- Schneider, H., Panigel, M. and Dancis, J. (1972)  
 Transfer across the perfused human placenta of antipyrine, sodium,  
 and leucine.  
 Am. J. Obstet. Gynecol. 114 (6) 822-828

- Schwab, M.E. and Thoenen, H. (1978)  
 Selective binding uptake and retrograde transport of tetanus toxin  
 by nerve terminals in the rat iris. An electron microscope study  
 using colloidal gold as a tracer.  
*J. Cell. Biol.* 77 1-13
- Simons, K., Garoff, H., Helenius, A. (1982)  
 How an animal virus gets into and out of its host cell.  
*Scientific American* 246 (2) 46-54
- Spurr, A.R. (1969)  
 A low viscosity epoxy resin embedding medium for electron microscopy.  
*J. Ultrastructure Res.* 26 31-43
- Steigman, A.J. and Lipton, M. M. (1958)  
 Neonatal immunity II. Poliocidal effect of human amniotic fluids.  
*Proc. Soc. Exp. Biol. Med.* 99 576-579
- Stein, L., Fernandes, J. and Lewandowsk, H. (1974)  
 The Ultrastructure of the normal placenta.  
*J. Am. Osteopath. Assoc.* 73 (6) 463-468
- Strauss, L., Goldenberg, N., Hirota, K and Okydaira, Y. (1965)  
 Structure of human placenta with observations on ultrastructure  
 of the terminal chorionic villus.  
*Birth Defects. Orig. Artic. Ser.* 1 13-26
- Stromberg, K., Azizkhan, J.C. and Speeg, K.V. (1978)  
 Isolation of functional human trophoblast cells and their partial  
 characterisation in primary cell culture.  
*In Vitro* 14 (7) 631-638
- Stromberg, K. (1980)  
 The Human placenta in cell and organ culture.  
 In: *Methods in cell biology* 21B. Academic press.
- Taylor, P.V. and Hancock, K.W. (1973)  
 Viability of human trophoblast in vitro  
*J. Obstet. Gynecol. of Br. Commonw.* 80 834-40
- Ten Broeck, C. and Bauer, J.H. (1923)  
 The transmission of tetanus antitoxin through the placenta.  
*Proc. Soc. Exp. Biol. Med.* 20 399-400
- Terry, W.D. and Fahey, J.L. (1964)  
 Heterogeneity of the H chains of human 7S gamma-globulin. In:  
 48th Annual Meeting of the Federation of American Societies for  
 Experimental Biology, Chicago.
- Tighe, J.R., Garrod, P.R. and Curran, R.C. (1967)  
 The trophoblast of human chorionic villus.  
*J. Pathol. Bacteriol.* 93 559-567

- Ungewickell, E. and Branton, D. (1981)  
 Assembly units of clathrin coats.  
 Nature. 289 420-422
- Usategui - Gomez, M. and Stearns, S. (1969)  
 Comparative study of the Rh.D antibody titres of amniotic fluids  
 and corresponding maternal sera in Rh.D sensitised pregnancies.  
 Nature (Lond) 221 82-83
- Virella, G., Nures, M.A., and Tamagnini, G. (1972)  
 Placental transfer of human IgG subclasses. Clinical and Exptl.  
 Immunology 10 475-8
- Wall, D.A., Wilson, G. and Hubbard, A.L. (1980)  
 The galactose-specific recognition system of mammalian liver:  
 the route of ligand internalisation in rat hepatocytes.  
 Cell 21 79-93
- Wang, A.C., Faulk, W.P., Sruckley, M.A. and Fundenberg, H.H. (1970)  
 Chemical differences of adult, foetal and hypogammaglobulinemic  
 IgG. Immunochemistry 7 703-8
- Wasz - Höckert, O., Wager, O., Hautala, T. and Widholm, O. (1956)  
 Transmission of antibodies from mother to fetus. A study of the  
 diphtheria level in the new-born with oesophageal atresia.  
 Ann. Med. Exp. Biol. Fenn. 34 444-446
- Wehland, J., Willingham, M.C., Dickson, R. and Pastan, I. (1981)  
 Microinjection of anti-clathrin antibodies into fibroblasts does  
 not interfere with the receptor - mediated endocytosis of  $\alpha_2$  -  
 macroglobulin.  
 Cell 25 105-119.
- Weiser, H.B. (1949)  
 Inorganic colloidal chemistry.  
 Wiley and Sons. New York p1-444
- Wild, A.E. (1960)  
 Proteins of the liquor amnii. Brit Med. J. 1 802
- Wild, A.E. (1976)  
 Mechanism of protein transport across the rabbit yolk sac endoderm.  
 In: Maternofoetal transmission of Immunoglobulins. Hemmings  
 W.A. Cambridge. University Press Cambridge. p 155-167
- Williams, M.A. (1977)  
 Autoradiography and Immunocytochemistry.  
 In: Practical methods in electron microscopy. A.M. Glauert.  
 North-Holland. Amsterdam. N.Y. Oxford.
- Willingham, M.C., Maxfield, F.R., and Pastan, I (1979)  
 $\alpha_2$  macroglobulin binding to the plasma membrane of cultured  
 cells : diffuse binding followed by clustering in coated regions.  
 J.Cell Biol, 82 614-625

- Willingham, M.C. and Pastan, I. (1980)  
Receptor mediated endocytosis in cultured fibroblasts: The Receptosome. *Eur. J. Cell. Biol.* 22 (1) 203. M604
- Willingham, M.C. and Pastan, I. H. (1981)  
The morphologic pathway of receptor mediated endocytosis in cultured fibroblasts.  
In: Cellular controls in differentiation. C.W. Lloyd and D.A. Rees. Academic Press. p59-78
- Willingham, M.C., Keen, J.H., Pastan, I.H., (1981)  
Ultrastructural immunocytochemical localisation of clathrin in cultured fibroblasts.  
*Expt'l Cell. Res.* 132 329-338
- Wislocki, G.B. and Bennett, H.S., (1943)  
The history and cytology of the human and monkey placenta with special reference to the trophoblast.  
*Am. J. Anat.* 73 335-450
- Wislocki, G.B. and Dempsey, E.W. (1955)  
Electron microscopy of the human placenta.  
*Anat. Rec.* 123 133-149
- Woodward, M.P. and Roth, T.F. (1978)  
Coated vesicles, characterisation, selective dissociation and reassembly.  
*Proc. Nat. Acad. Sci.* 75 4394-4398
- Wynn, R.W. (1975)  
Fine structure of the placenta.  
In: The placenta and its maternal supply line. Gruenwald. P. Medical Technical Publishing Co. Lancaster. p56-79.
- Yasuzumi, G., Nakai, Y., Tsubo, I., Yasuda, M. and Sugioka, T. (1967)  
The fine structure of nuclei as revealed by electron microscopy IV. The intranuclear inclusion formation in Leydig cells of ageing human testis.  
*Expt'l Cell. Res.* 45 261-276
- Yoshida, Y. (1964)  
Ultrastructure and secretory function of the syncytial trophoblast of human placenta in early pregnancy. *Exp. Cell. Res.* 34 305-317
- Zander, J. (1964)  
Progesterone in human blood and tissues. *Nature.* 174 406-407
- Zucker - Franklin, D. (1968)  
Electron microscopic studies of human granulocytes: Structural variations related to function.  
*Semin. Hemat.* 5 109-133

UNIVERSITY OF LEICESTER MEMORANDUM

FROM E. Critchlow, Higher Degrees

DATE 28th November 1983

TO Dr J. Wakely, Anatomy

RE:- LINDA DEARDEN

I am enclosing a copy of the above-named's thesis together with a copy of the notes for the guidance of examiners. I have told Dr Y.W. Loke, the external examiner, that you will be getting in touch with him about the oral examination and have sent him an Examiners' Report form.

I should be grateful if you could return the thesis and abstract to me in due course for transmission to the University Library along with the copy sent to the external examiner.

*EC*

EC/BS

## ABSTRACT

Transport of Immunoglobulin G across the human placenta. by  
Linda Dearden.

It is well known that Immunoglobulin G (IgG) is transported across the human placenta during gestation. However the route of this transport is not clear and the aim of this thesis is to elucidate the transport pathway.

A number of different methods and placental systems were employed to investigate the IgG transport pathway.

1. Human placentae were perfused with a human IgG probe using an isolated cotyledon method.
2. Dissected chorionic villi from both term and first trimester placentae were incubated in culture medium containing a human IgG probe.
3. Human placental cells were cultured and incubated with a human IgG probe.
4. Choriocarcinoma cells (BeWo) were cultured and incubated with a human IgG probe.

The IgG transport process was investigated at the light microscope level using tritiated IgG, and at the electron microscope level using colloidal gold particles coated with IgG. From these investigations new evidence was discovered concerning the transport of IgG across the human placenta.

In addition an extensive morphological study of the BeWo cells has provided much new information. There are clear indications in the structure of these cells, first of transformed state and secondly of their origin from trophoblast tissue.

Observations are presented of the in vitro differentiation of cultured cells towards the villous state of the parent tissue. Cytoplasmic characteristics and mutual positioning of these cells was noted which were similar to those of cytotrophoblast and syncytiotrophoblast in vivo. Bulbous projections were also noted in the culture cells both attached to the tissue and floating in the culture medium. These features may be related to the budding off and deportation of trophoblast in vivo.

TRANSPORT OF IMMUNOGLOBULIN G  
ACROSS THE HUMAN PLACENTA

LINDA DEARDEN



Ph.D.

1983



Thesis  
1.6.1984

FIGURES.



The following abbreviations and meanings are used consistently throughout the illustrations which follow.

bm	=	basement membrane
C	=	cytotrophoblast cell
CN	=	cytotrophoblast nucleus
CV	=	coated vesicle
D	=	desmosome
en	=	endothelial cell
er	=	endoplasmic reticulum
Fc	=	Fetal capillary
G	=	Golgi
g	=	granule
jnv	=	juxtannuclear vacuole
L	=	lipid
m	=	mitochondria
mv	=	microvillus
mvb	=	multivesicular body
N	=	nucleus
Nu	=	Nucleolus
r	=	ribosomes
rbc	=	red blood cell
S	=	syncytiotrophoblast
SN	=	syncytiotrophoblast nucleus
St	=	Stroma
V	=	Vacuole
vs	=	vesicle





FIG 1 This table shows the main organs responsible for immunoglobulin G transport to the young in a number of animals, both before and after birth.

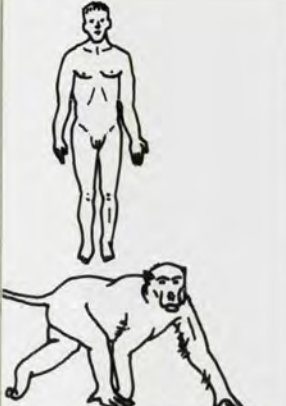
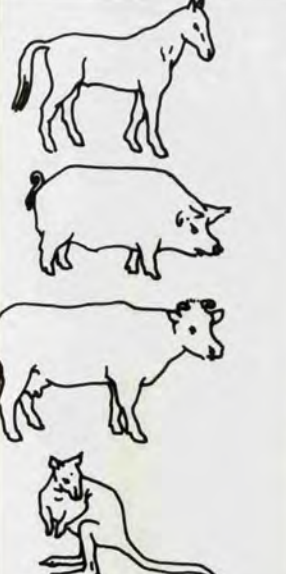
	<b>Before Birth</b>	<b>After Birth</b>
	chorioallantoic placenta  chorioallantoic placenta	
	yolk sac  yolk sac  yolk sac  yolk sac	neonatal small intestine   neonatal small intestine
		neonatal small intestine  neonatal small intestine  neonatal small intestine  neonatal small intestine





FIG 2 Schematic diagram showing the possible routes for immunoglobulin transport a) via amniotic swallowing (long arrows). b) via the placenta (broken arrows). The fetus is in the breach position not the normal head down one.

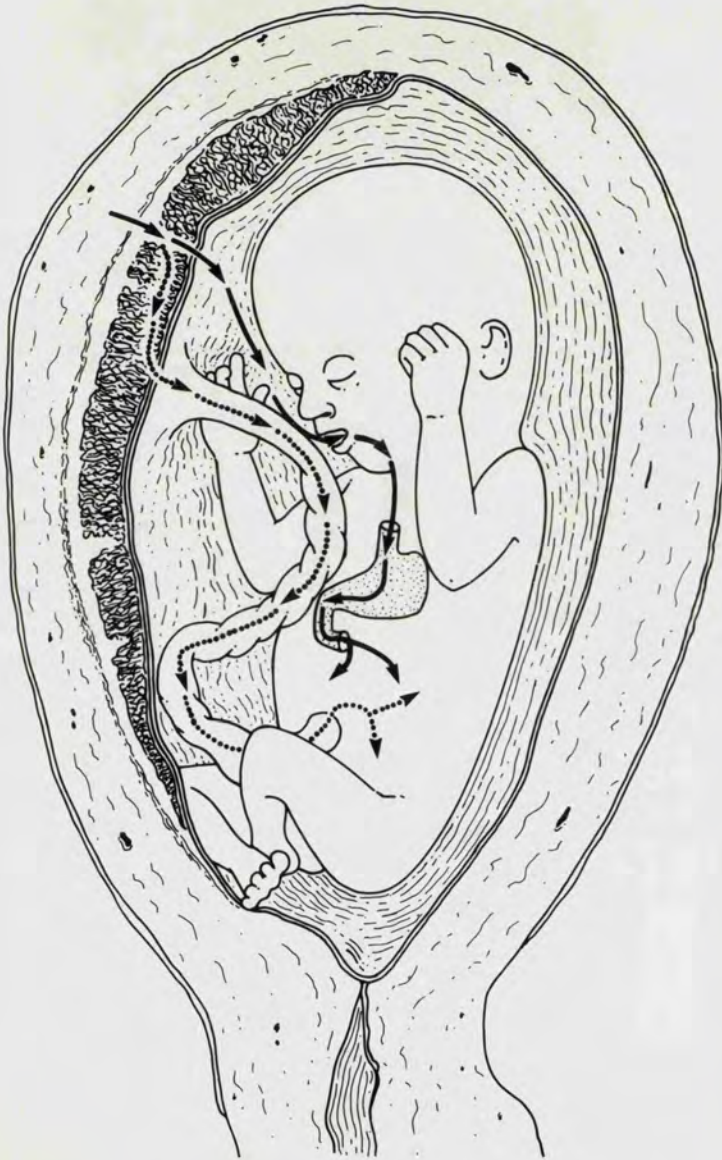






FIG. 3 Photograph of the perfusion apparatus used  
in the experiments.

FIG. 4 Diagram of perfusion apparatus.

THE FETAL "CIRCUIT"

A = Fetal Reservoir  
B = Flow meter 1  
C = Heat exchanger  
D = Peristaltic pump  
E = Sampling taps  
F = Nylon microcannulae  
G = Flow meter 2  
H = Mercury manometer  
I = Gas cylinder 40% O<sub>2</sub>; 5% CO<sub>2</sub>; 55% N<sub>2</sub>

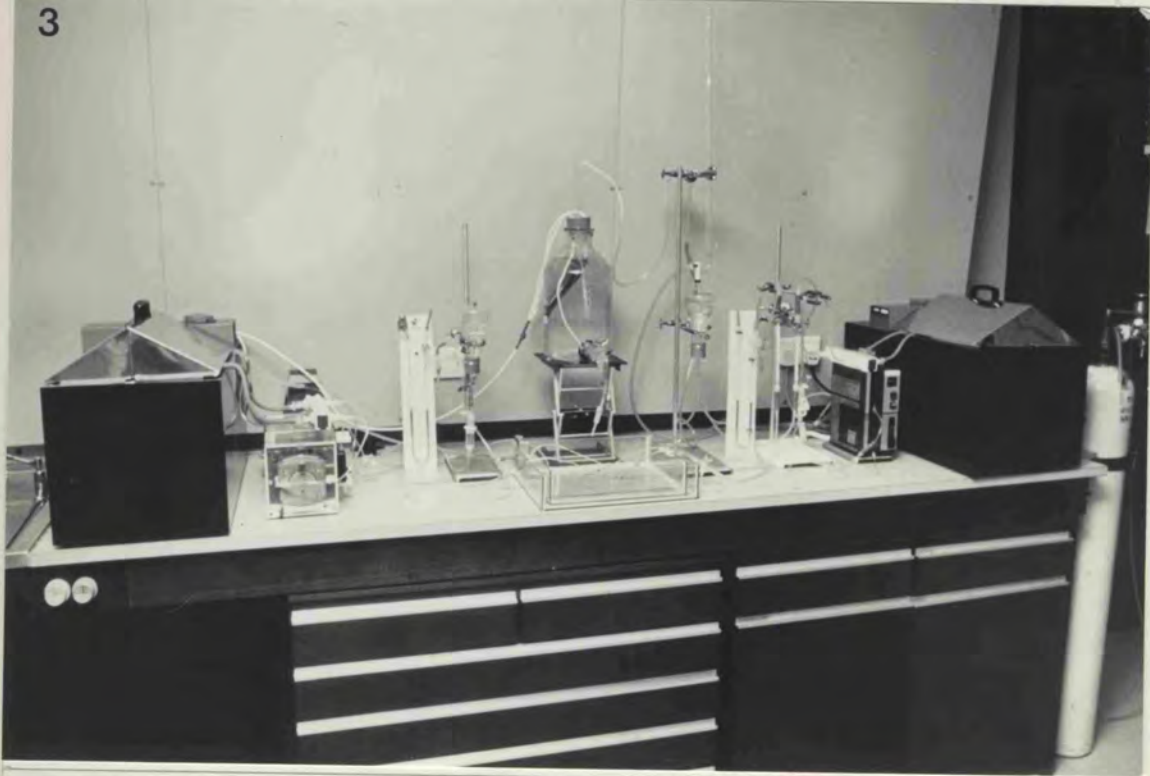
THE MATERNAL "CIRCUIT"

J = Maternal reservoir  
K = Heat exchanger  
L = Pump  
M = Mercury manometer  
N = Flow meter  
O = Glass microcannula  
P = Gas cylinder 95% O<sub>2</sub> 5% CO<sub>2</sub>

THE PLACENTA AREA

Q = Reservoir of buffer  
R = Thermostat Heater  
S = Spray to keep placenta moist  
T = Dish in which placenta was contained

3



4

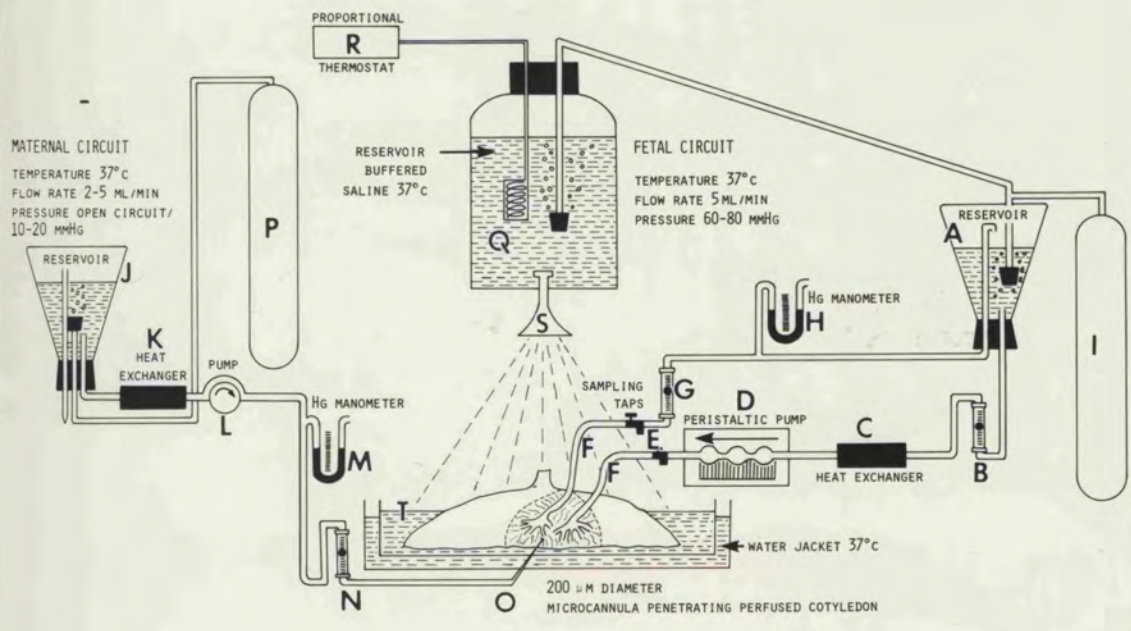


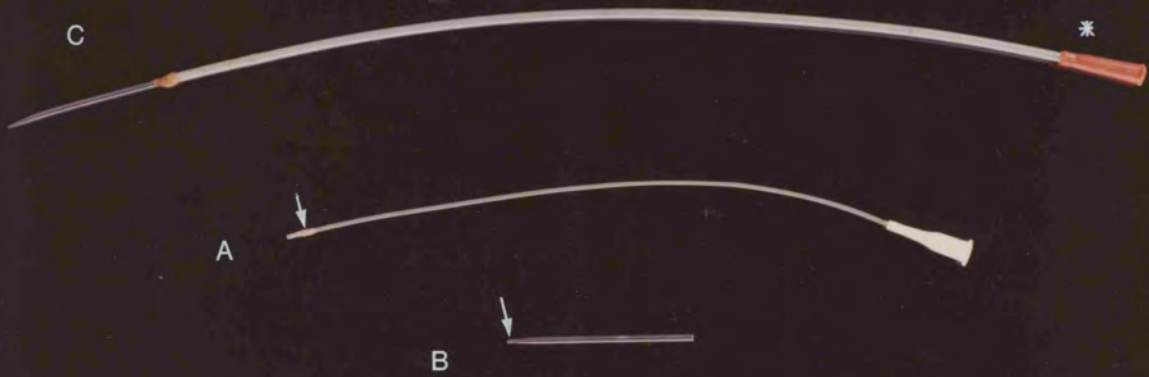
FIG 5 (A) nylon microcannula used in the fetal 'circuit' of the perfusion apparatus. Note 'lip' of Araldite close to the tip (arrow)

(B) Glass microcannula used in maternal 'circuit' of the perfusion apparatus. Note 'lip' of Araldite (arrow) to prevent it pulling out of the tissue.

(C) Glass microcannula Araldited into position in a nylon cannula. The fitting at the opposite end enables it to be attached easily into the perfusion apparatus (\*)

FIG 6 Perfused placenta, maternal side uppermost showing paled cotyledon (arrow)

5



6

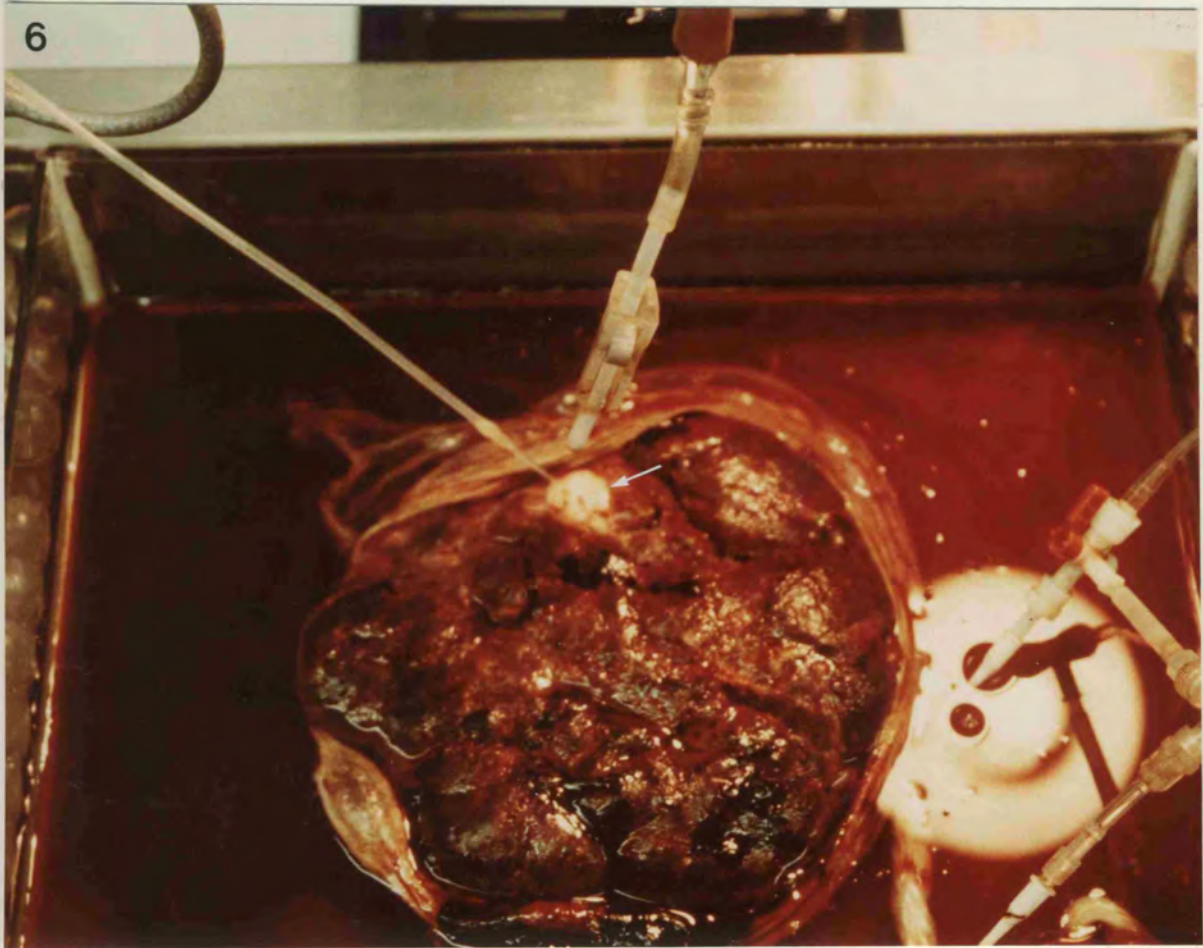


FIG 7 Diagram of a perfused cotyledon. For clarity the chorionic villous tree is simplified in structure, (see Fig 17 for the actual appearance) and the cotyledonary vessels are represented as being dissected away from the chorionic plate.

Microcannula from maternal "circuit"  
containing probe

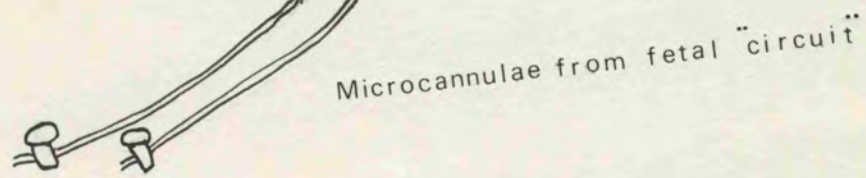
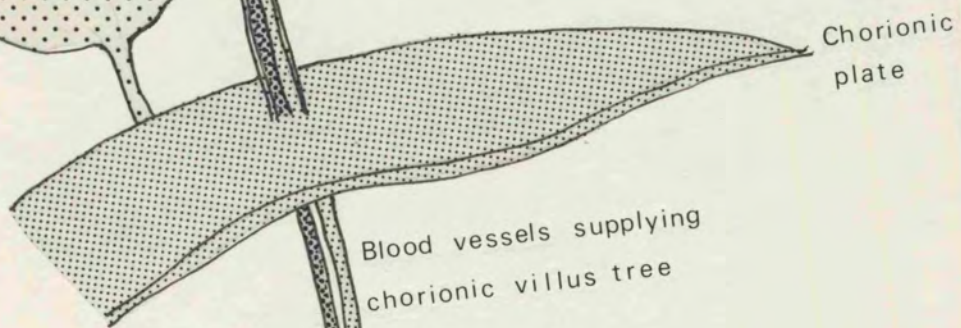
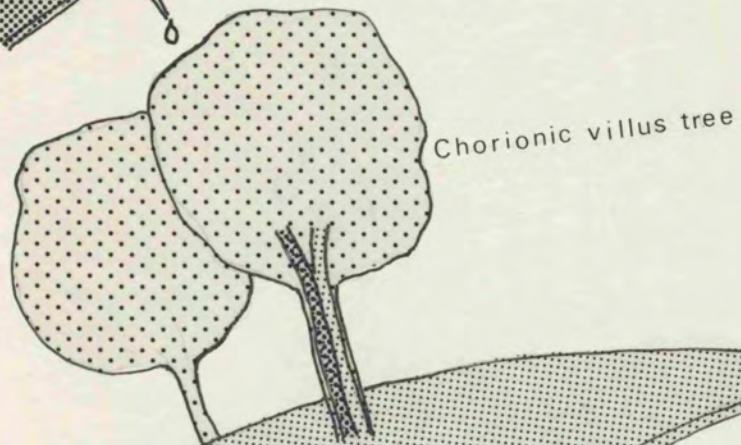
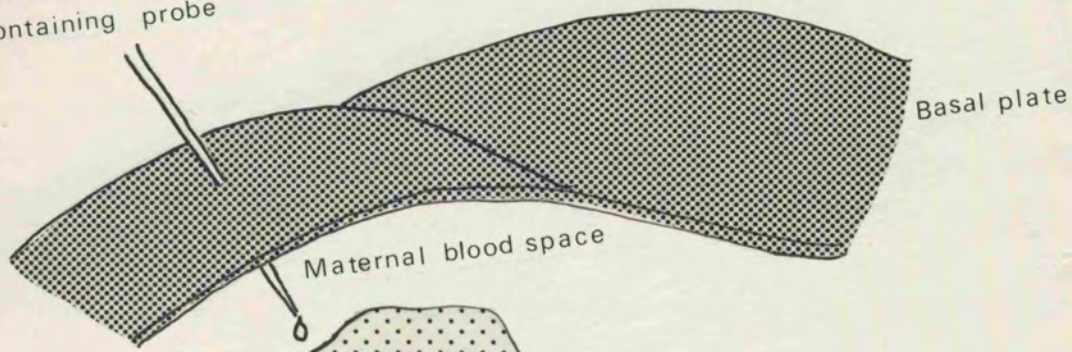


Fig 7

FIG 8 Transmission electron micrograph showing 18nm particles of colloidal gold. (A drop of the colloidal gold preparation was dried down onto a formvar coated electron microscope grid and viewed in a Jeol 100CX transmission electron microscope.)

The particles of gold are highly electron dense and very uniform in appearance. These two characteristics make them easily identifiable.

FIG 9 Electron micrograph of a 2 $\mu$ l drop of colloidal-gold preparation and a 2 $\mu$ l drop of latex spheres of known diameter (0.9 $\mu$ m -Agar aids), dried down onto a formvar coated electron microscope grid. The ratio of gold particles to latex spheres was calculated and an estimate made of the concentration of the gold-preparation.

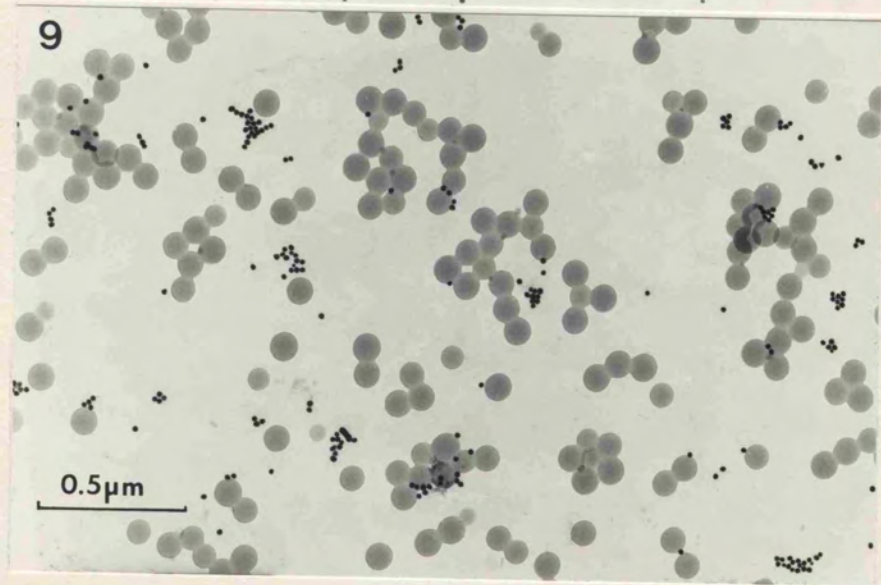
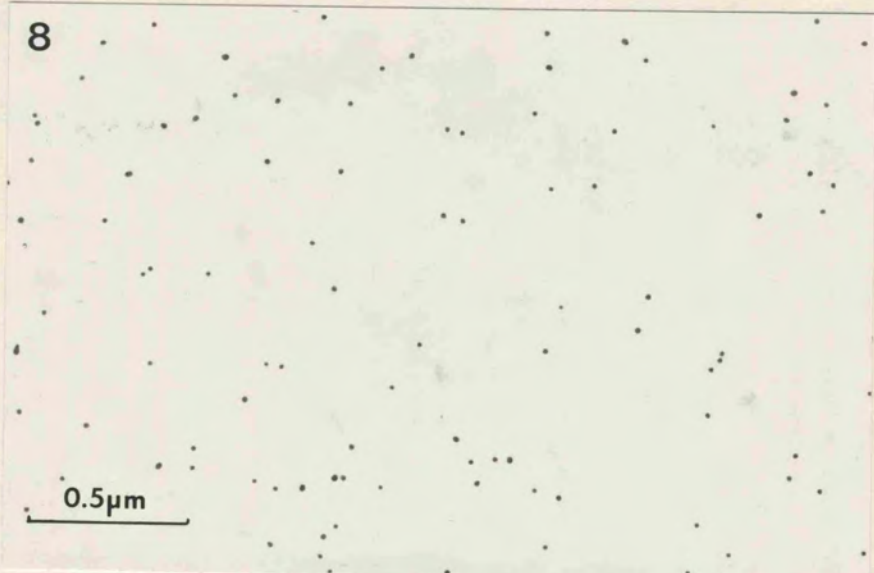


FIG 10 Increase in temperature of the culture medium after the placental cell cultures were transferred from ice (2°C) to the incubator (37°C) and warmed for 60 minutes.

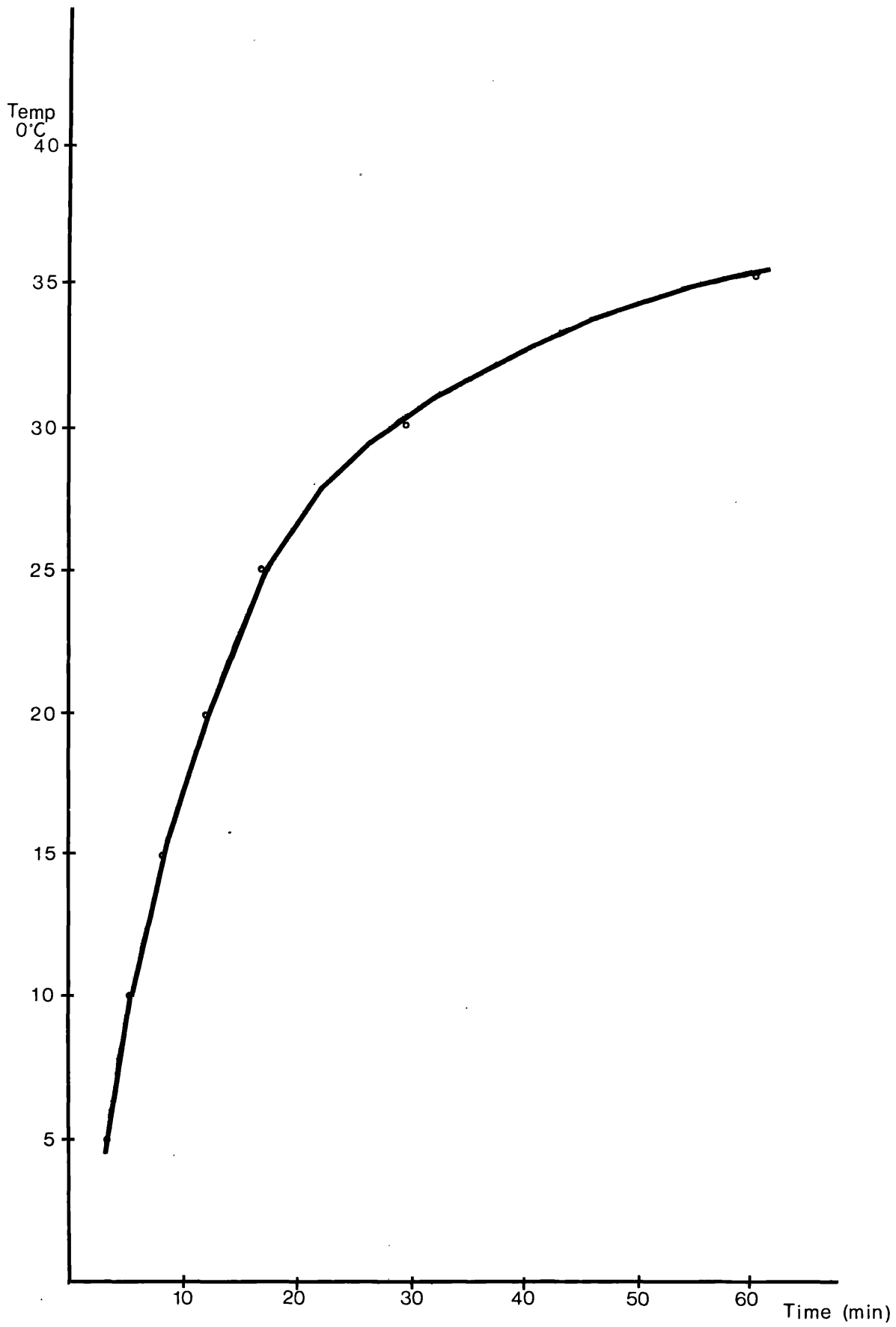


Fig 10

FIG 11 Curve showing the increase in temperature in culture medium when BeWo cells are transferred from incubations at 2°C to 37°C and warmed for 30 minutes before fixation. (The temperature was recorded for 60 minutes).

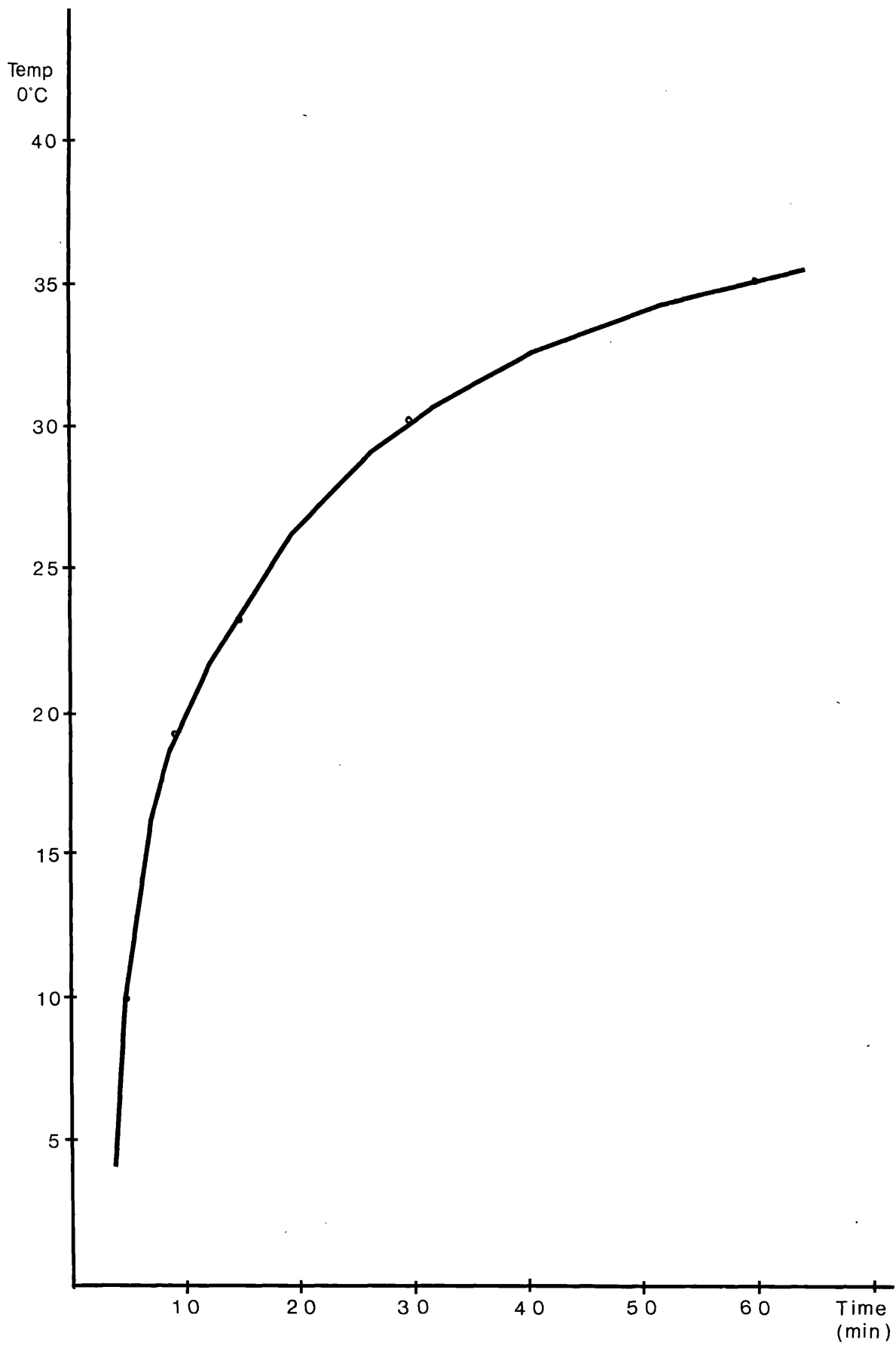


Fig 11

FIG 12 Photograph of a normal human term placenta - fetal side. The membranes (arrows) and umbilical cord (Uc) are clearly visible and the blood vessels (bv) can be seen radiating out from the point of attachment of the umbilical cord.

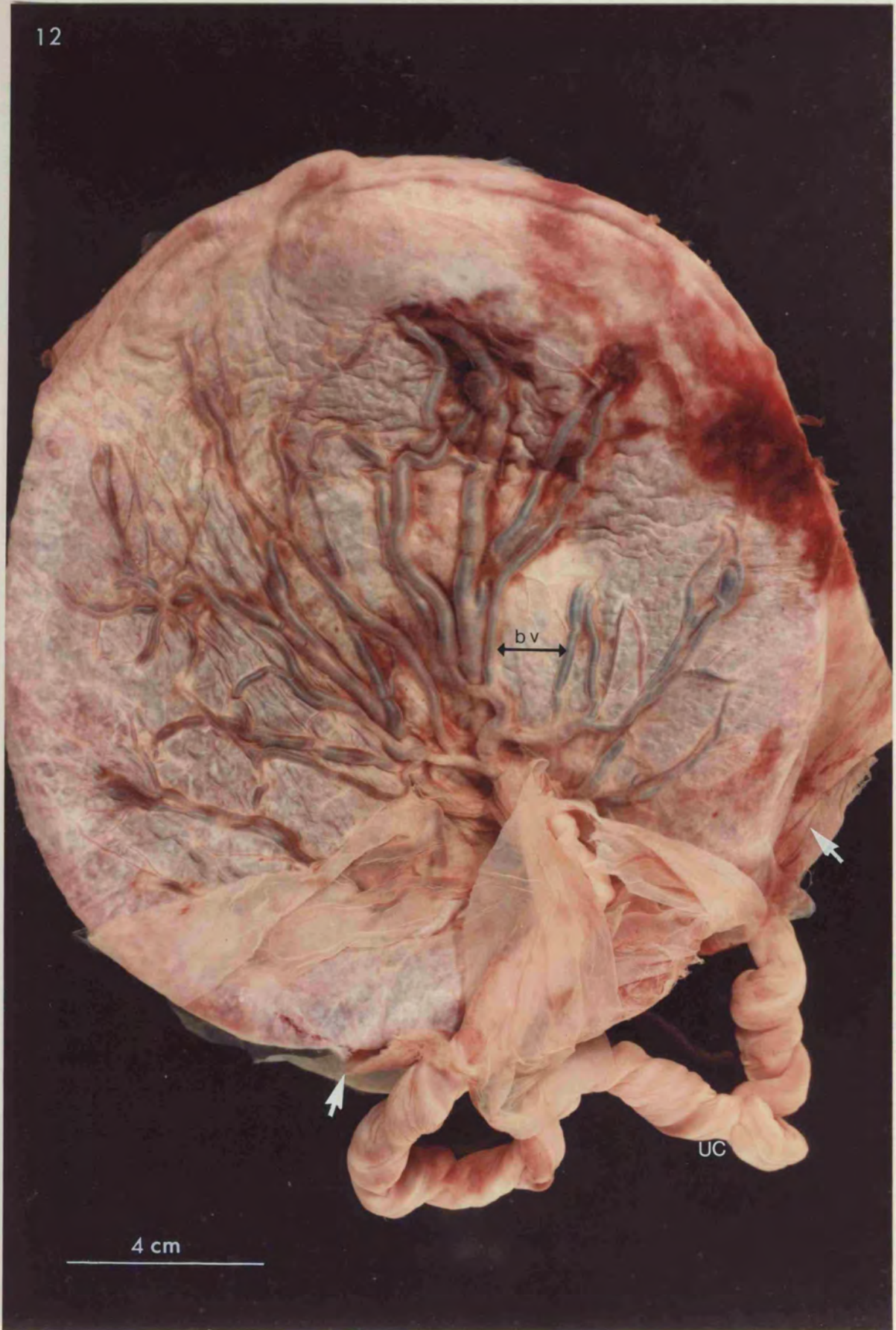


FIG 13 Photograph showing details of the blood vessels (arrows) on the chorionic plate (fetal aspect) of the placenta.

A thin transparent membrane - the chorion - covers this side of the placenta. The folds of this can be seen (arrowhead).

13

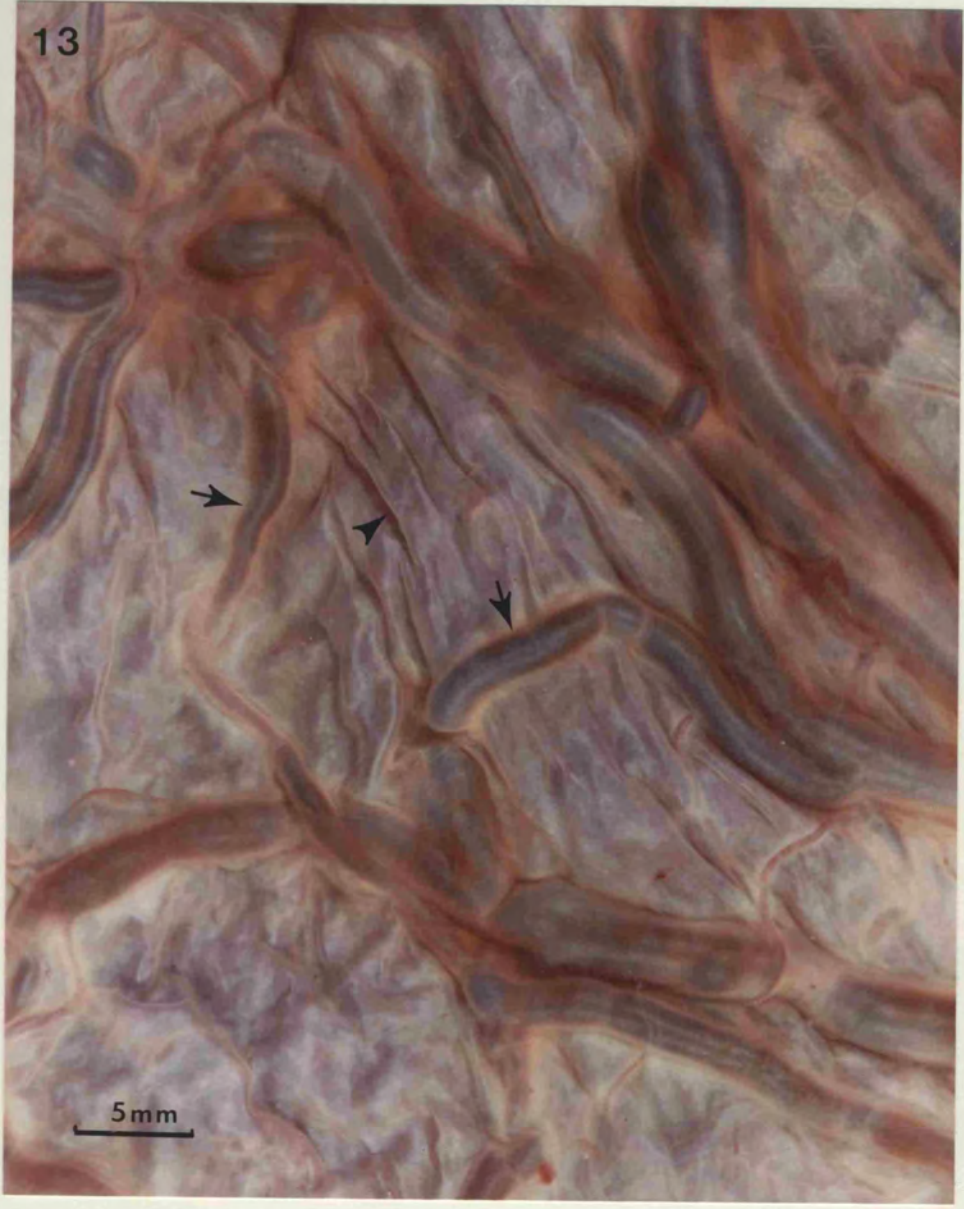


FIG 15 Photograph showing details of the basal plate. The fine pale membraneous abscission layer can be seen (arrow). During the perfusion studies the microcannula penetrates this layer.



FIG 16 Diagrammatic representation of the structure of the human placenta.

- A Whole placenta showing
  - a. umbilical cord
  - b. fetal surface
  - c. maternal surface
- B Highly simplified cross-section diagram through a whole placenta showing the internal structure of the placenta
  - d. cotyledon
  - e. chorionic villus tree
  - f. basal plate
  - g. chorionic plate
  - h. vessels supplying the chorionic villi - these would normally lie flat across the placental surface but for clarity in the diagram they are represented as having been dissected away from the surface.
- C Diagrammatic representation of the structure of the chorionic tree.
  - j. stem villus
  - k. intermediate villus
  - l. terminal villus
  - m. blood capillaries derived from the cotyledonary vessels.

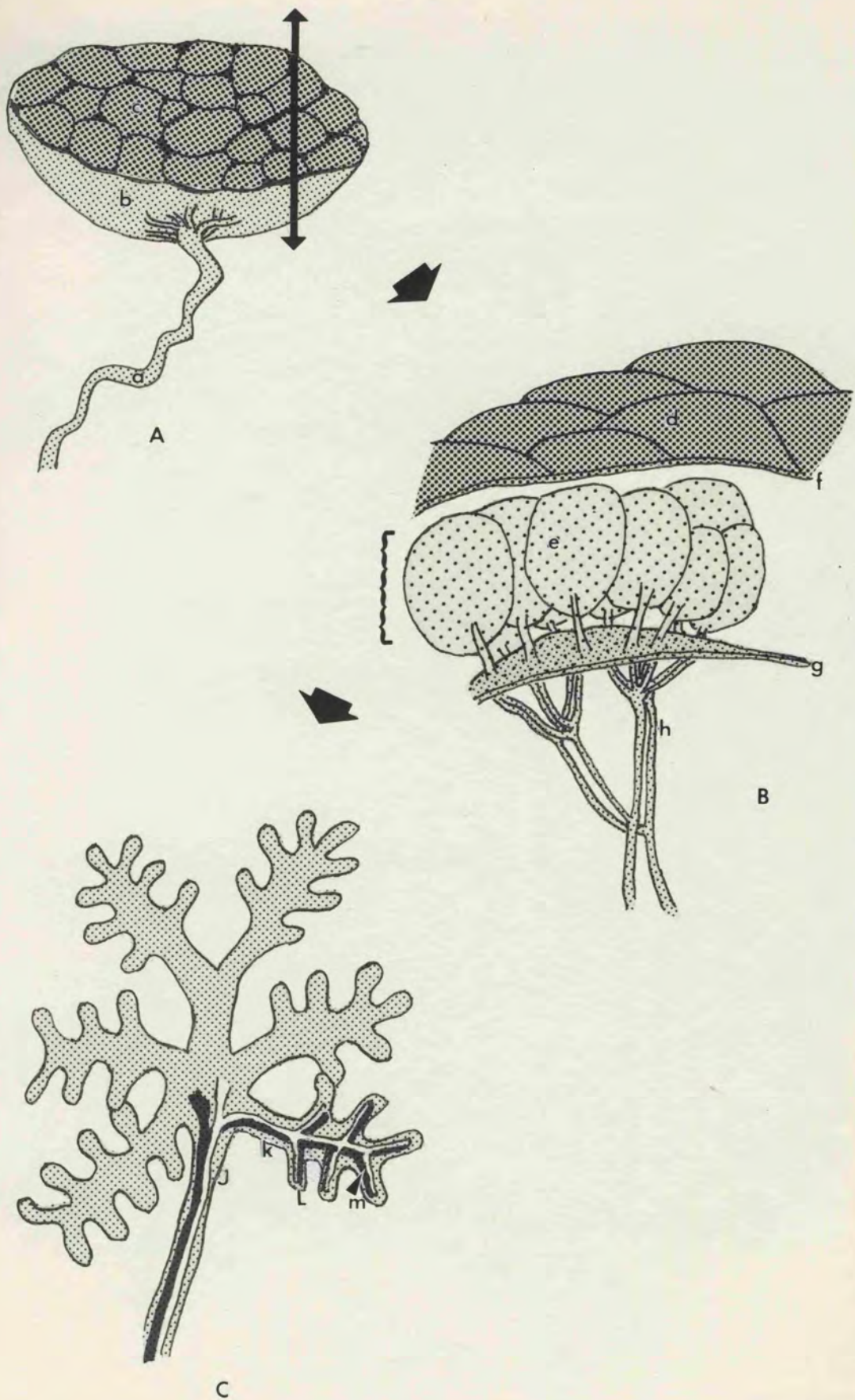


Fig 16

FIG 17 Optical section through the chorionic villi of normal term placenta using Nomarski differential interference contrast (DIC) microscopy. This photomicrograph shows the branching nature of the chorionic villi of normal placenta.

FIG 18 Optical section through the chorionic villi of normal term placenta using Nomarski(DIC) microscopy. The outline of a blood vessel can be seen within the chorionic villus (arrowhead)

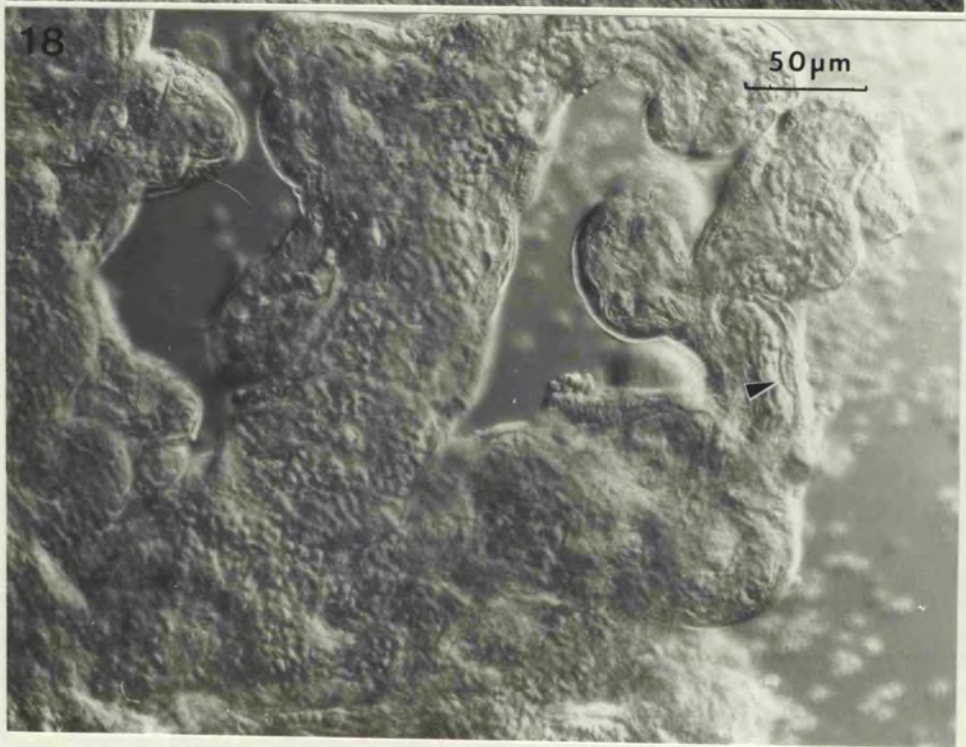
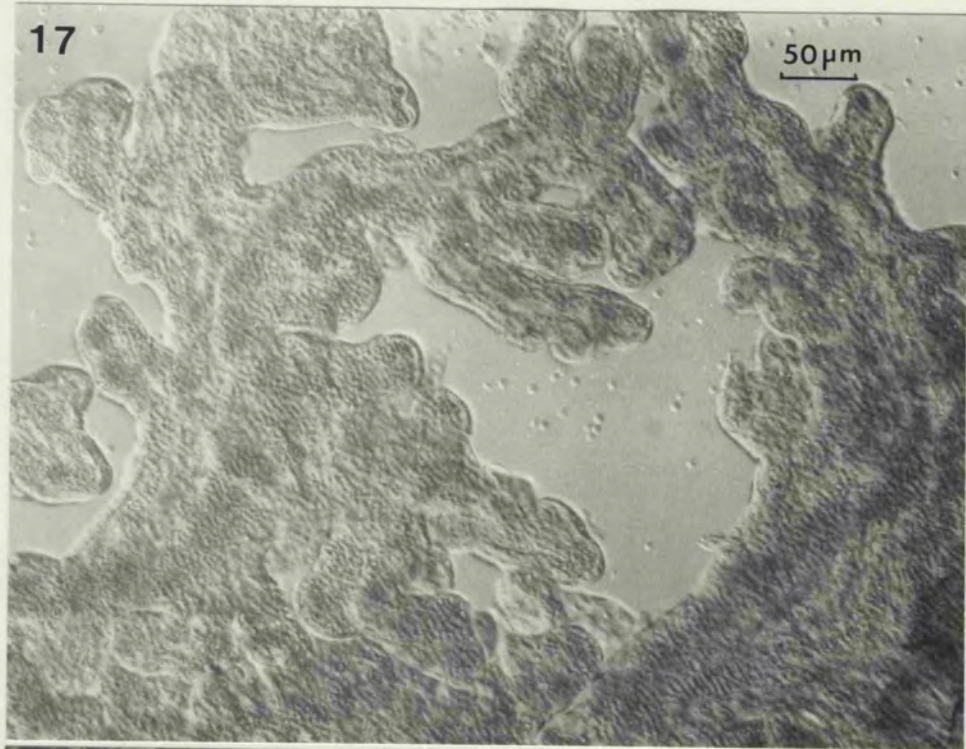


FIG 19 Light micrograph of thick (0.5 $\mu$ m) section of resin embedded term placental tissue stained with 1% toluidine blue in 1% borax. The darkly staining syncytiotrophoblast layer (s) is clearly visible, as are large numbers of dark syncytial nuclei (SN). The microvillous border on the surface of the syncytiotrophoblast is just visible (mv - arrow). A few cytotrophoblast cells can be seen below the syncytiotrophoblast. Stromal tissue (St) is present in the centre of the section.

FIG 20 Higher power micrograph of term placenta. In this micrograph there are very few cytotrophoblast cells present, and the syncytiotrophoblast appears to be in direct contact with the stroma (arrowhead). In fact electron microscopic examination shows the syncytiotrophoblast is in contact with the basement membrane (see Fig 24).

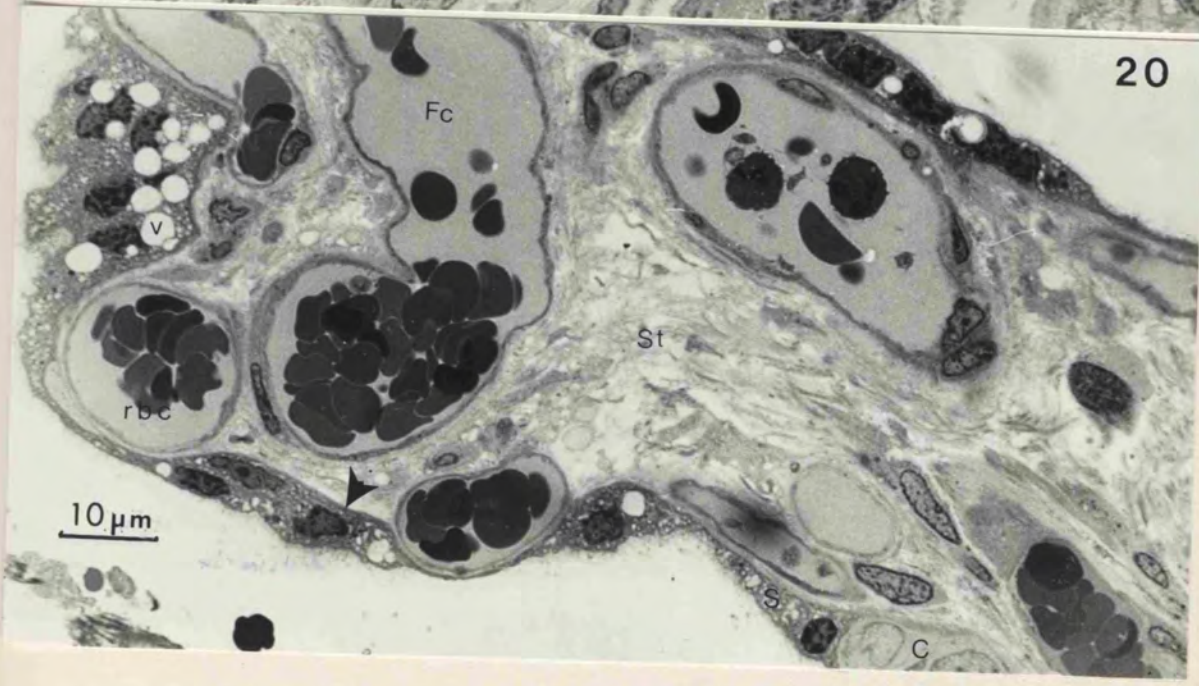


FIG 21 Scanning electron micrograph of term placenta showing the branching organisation of the placental tissue. Each branch is a villus (arrow).

FIG 22 Scanning electron micrograph of term placenta showing the numerous microvilli (arrow) which cover the surface of each individual villus.

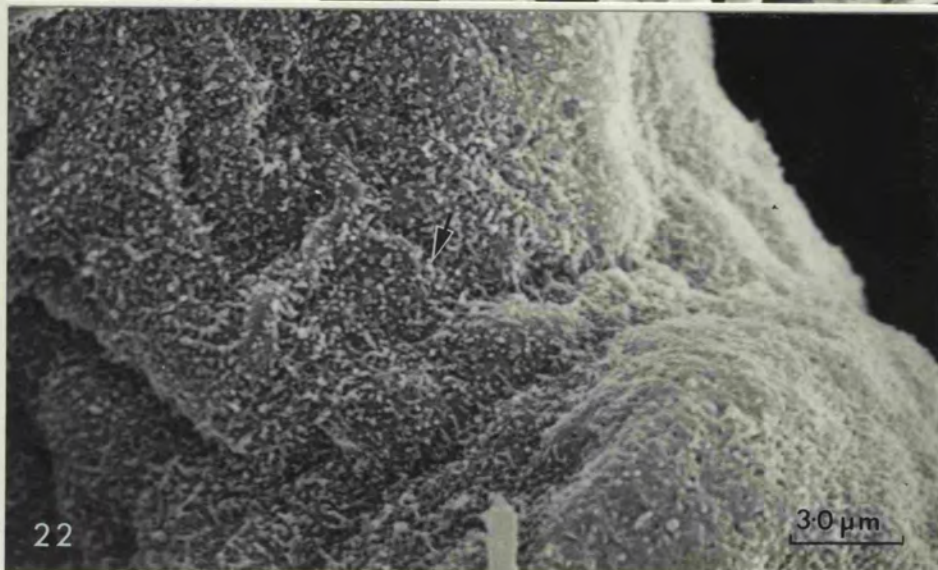


FIG 23 - 26 Transmission electron micrographs of term placental tissue stained with 10% methanolic uranyl acetate and Reynolds lead citrate.

FIG 23. The syncytiotrophoblast layer (S) can be seen in this micrograph. It appears as a thin electron-dense layer with a microvillous border (mv) on its surface. A syncytial nucleus is visible (SN). Beneath the syncytiotrophoblast are three cytotrophoblast cells (C). They are clearly distinguishable by their characteristic electron-lucent appearance.

FIG 24 Low power micrograph showing the general organisation of a villus of term placental tissue. In many areas the syncytiotrophoblast is in direct contact with the basement membrane. Fetal capillaries (Fc) can be seen within the stroma.

FIG 25 High power micrograph of part of Fig 24 showing the highly vesiculated appearance of the syncytiotrophoblast. A fetal capillary can be seen close to the basement membrane.

FIG 26 Invaginations of membrane are found between the microvilli. Many of these invaginations have a protein coating (arrow)

FIG 27 Coated vesicle (CV) profiles (arrow). One appears to be joined to the surface by a tube-like structure (arrowhead). Fine filaments (f.) are also found in the syncytiotrophoblast.

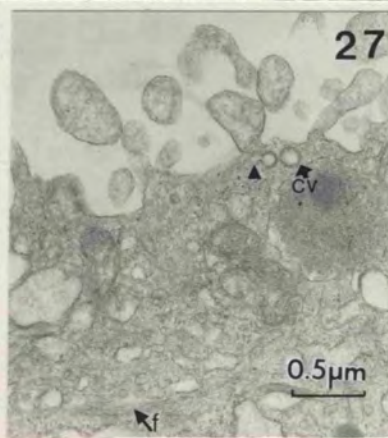
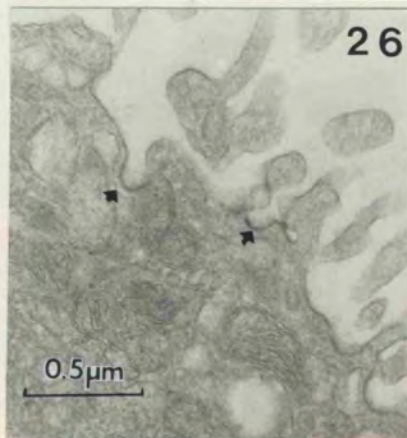
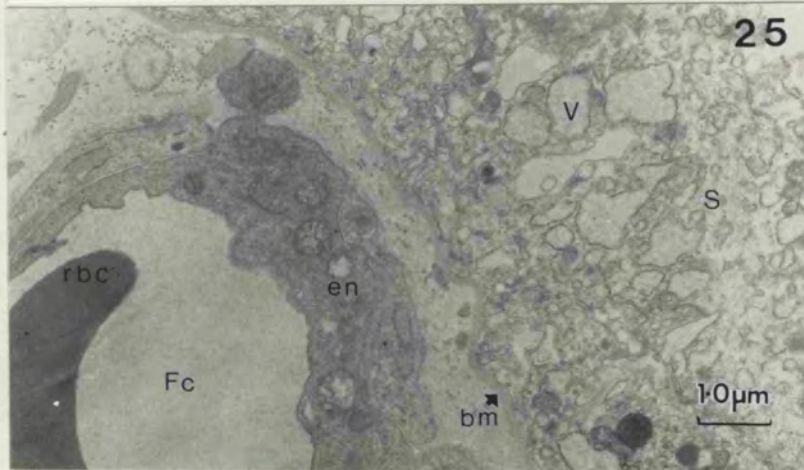
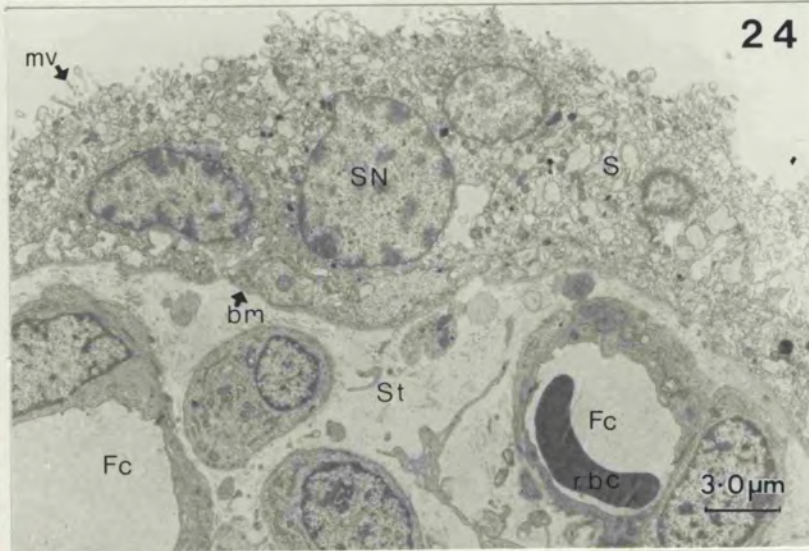
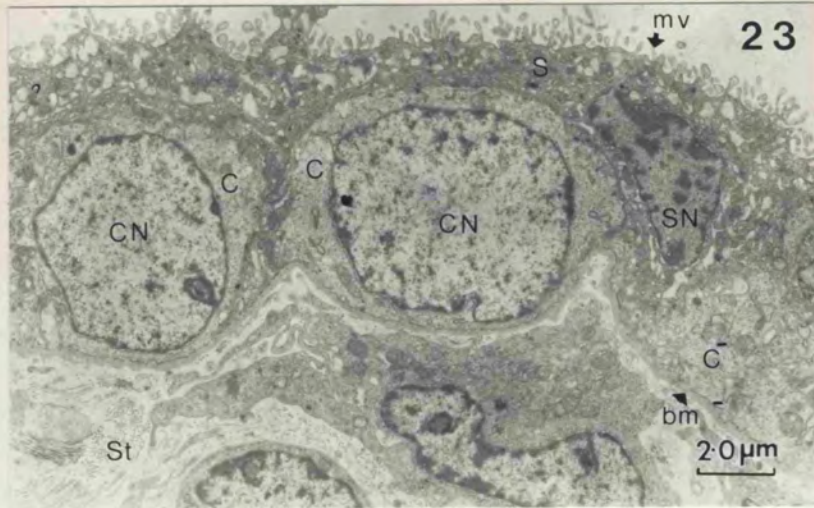


FIG 28 Coated vesicle (arrow) joined to the surface by a tube-like structure (arrowhead).

FIG 29 A Juxtannuclear vacuole (jnv) is visible in this micrograph close to a syncytial nucleus. (SN). Sometimes electron-dense droplets are present which do not appear to be membrane bounded (L)

FIG 30 Electron dense granules (arrowhead) are present in the syncytiotrophoblast.

FIG 31 Desmosomes (arrowhead) are identifiable between the syncytial and cytotrophoblast.

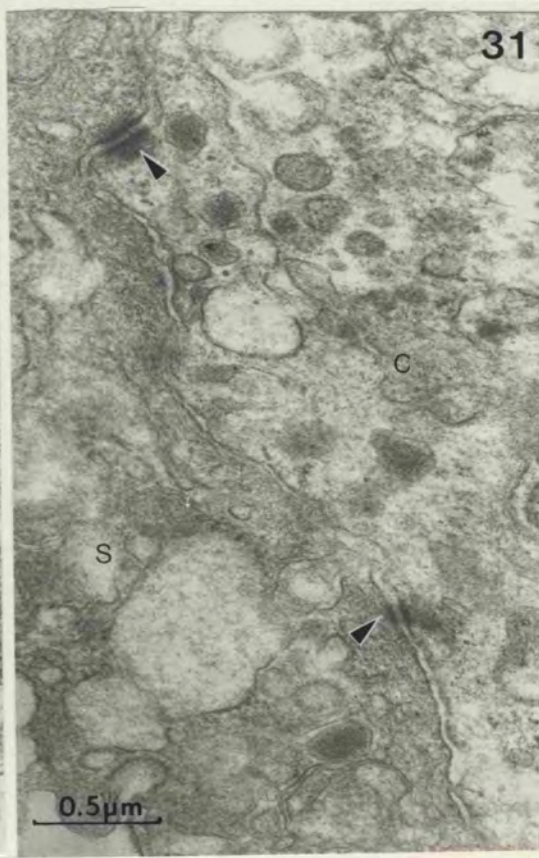
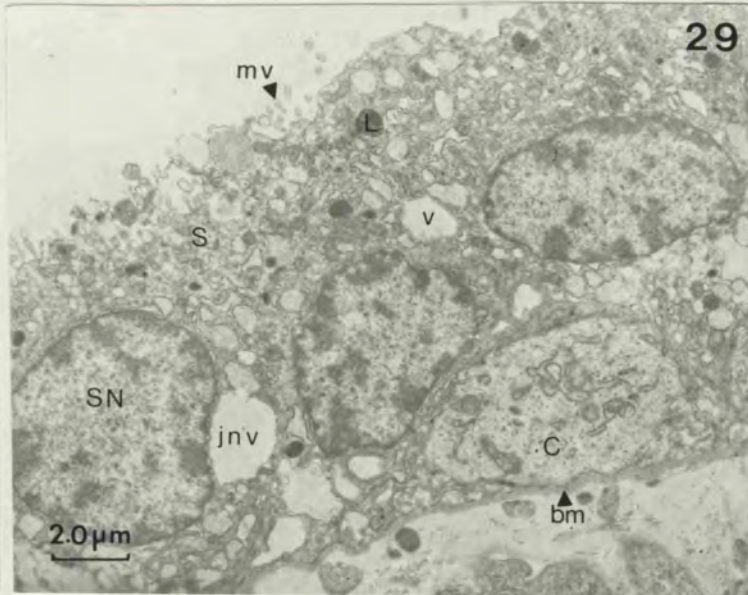
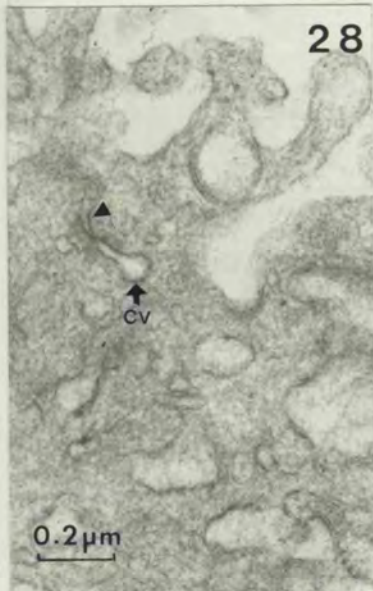


FIG 32-36 Transmission electron micrographs of cytotrophoblast cells showing sparseness of organelles.

FIG 32 & 33

Mitochondria (m) are found, endoplasmic reticulum (er) is present, ribosomes (r) are seen scattered throughout the cytoplasm.

FIG 32 Electron-dense membrane-bounded bodies (arrowhead) are found. Microvilli (mv) can be seen interdigitating with the syncytiotrophoblast (arrow) and a desmosome (D) (arrowhead) is found in this area.

FIG 33 Note the presence of fine filaments (f-arrow)

FIG 34 Golgi (G) is found in the cytotrophoblast cells. (C) often close to the nucleus (CN).

FIG 35 This micrograph shows the presence of a coated vesicle (arrow) in the cytotrophoblast cell (C) close to the basement membrane (bm).

FIG 36 Nucleoli (arrowhead) are found in both syncytial nuclei (SN) and cytotrophoblast nuclei (CN).

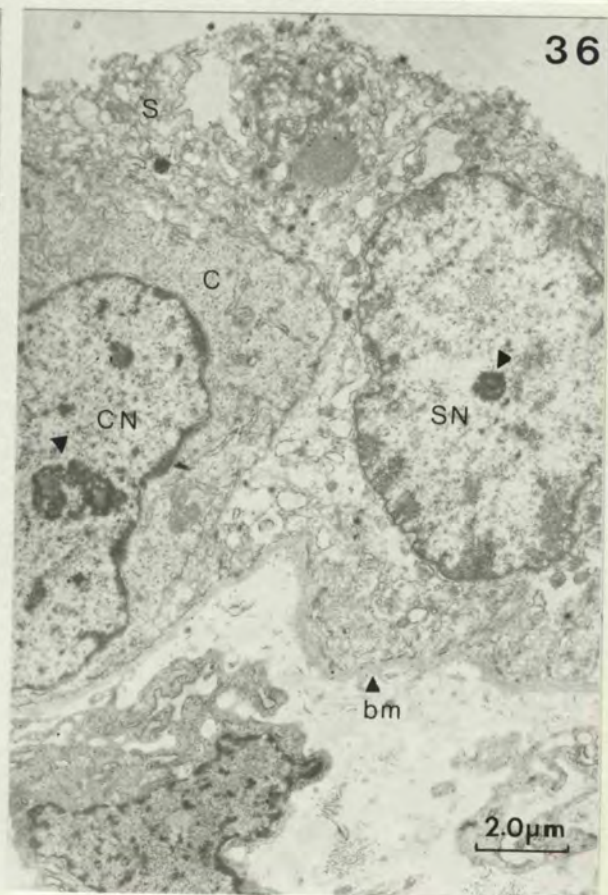
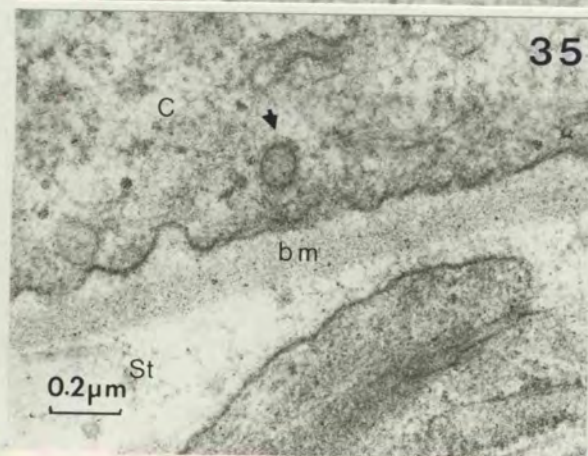
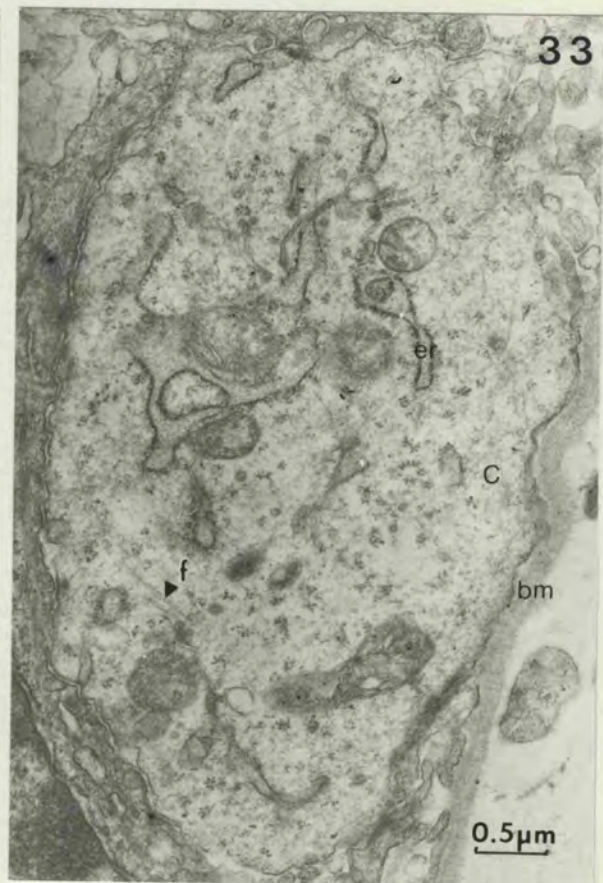
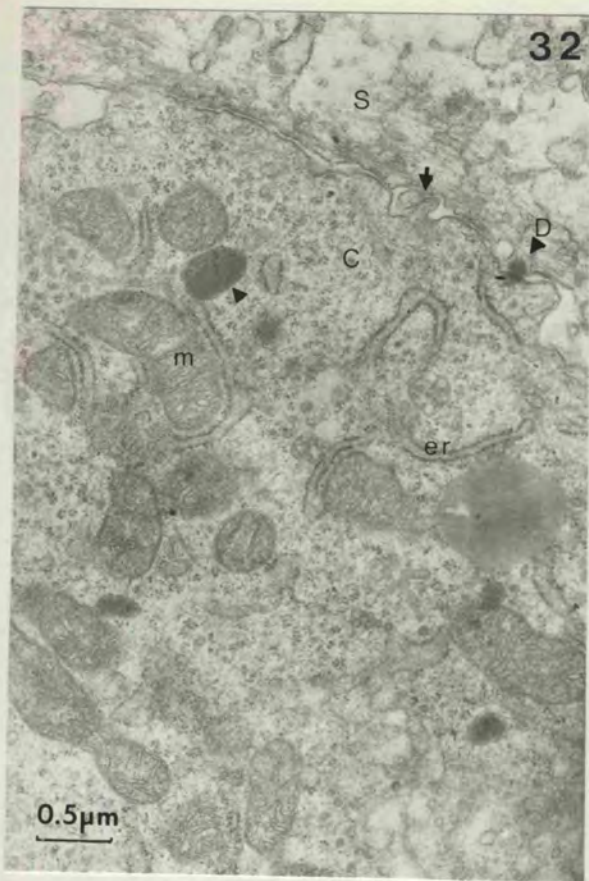


FIG 37 Light micrograph of thick (0.5 $\mu$ m) section of resin embedded first trimester placenta stained with 1% toluidine blue in 1% borax. A complete layer of cytotrophoblast cells (C) is present beneath the syncytiotrophoblast (S). Note the cell of intermediate morphology between cytotrophoblast and syncytiotrophoblast (arrow).

FIG 38 Transmission electron micrograph showing the features of first trimester placenta. Cytotrophoblast cells (C), cytotrophoblast nucleus (CN), syncytiotrophoblast (S); syncytiotrophoblast nucleus (SN). Vesicular structures (vs), Lipid-like droplets (L); Stroma (St), basement membrane (bm). Note the presence of densely staining bodies in the basement membrane (arrow).

FIG 39 Cytotrophoblast cell showing the following organelles: Mitochondria (m), densely staining bodies (db), and endoplasmic reticulum (er).

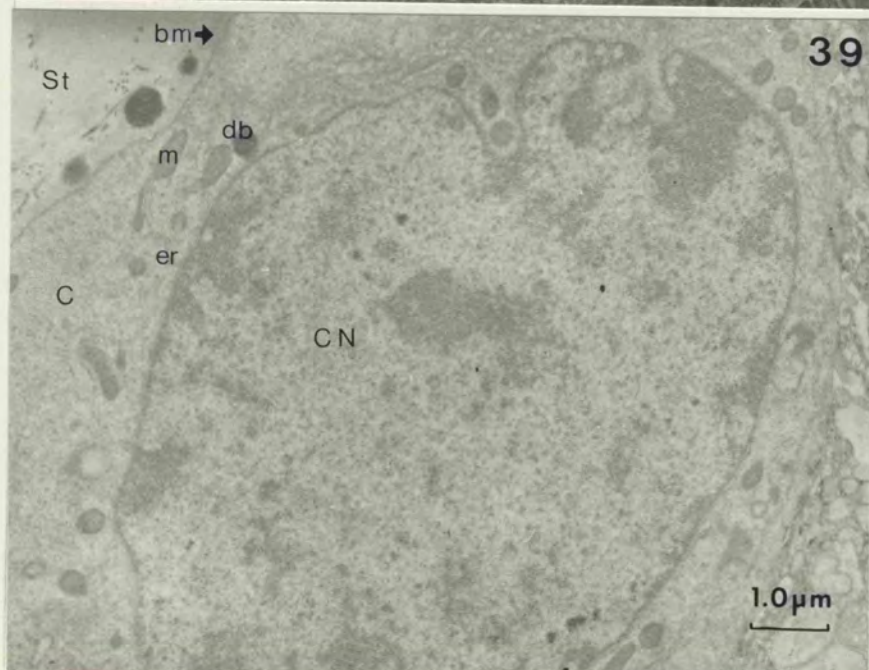
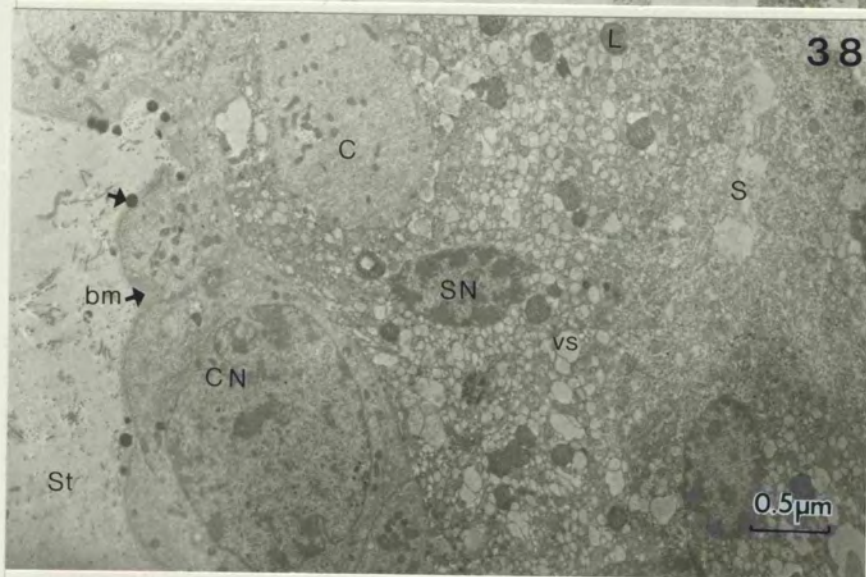
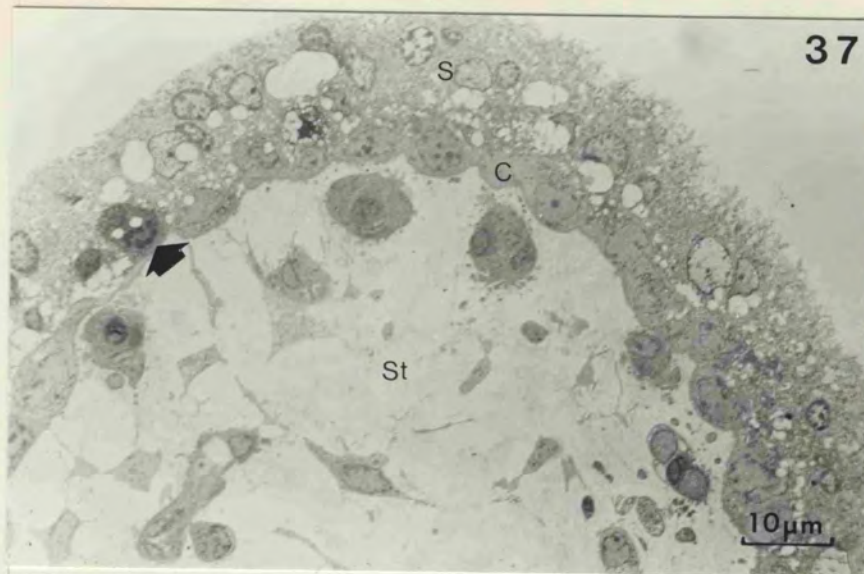


FIG 40 Graphs of increase in radioactivity in samples taken from the venous return of the fetal circuit of the perfusion apparatus against time. The graphs are for each of the successful perfusions and indicate transport of the tritiated IgG probe across the placenta from the maternal 'circuit' to the fetal 'circuit'.

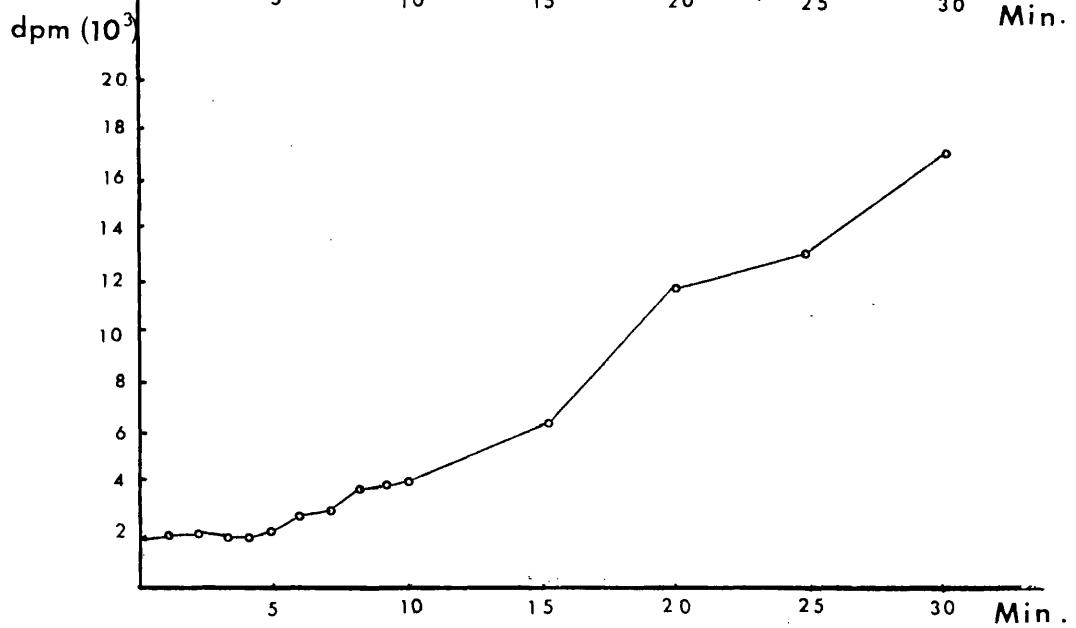
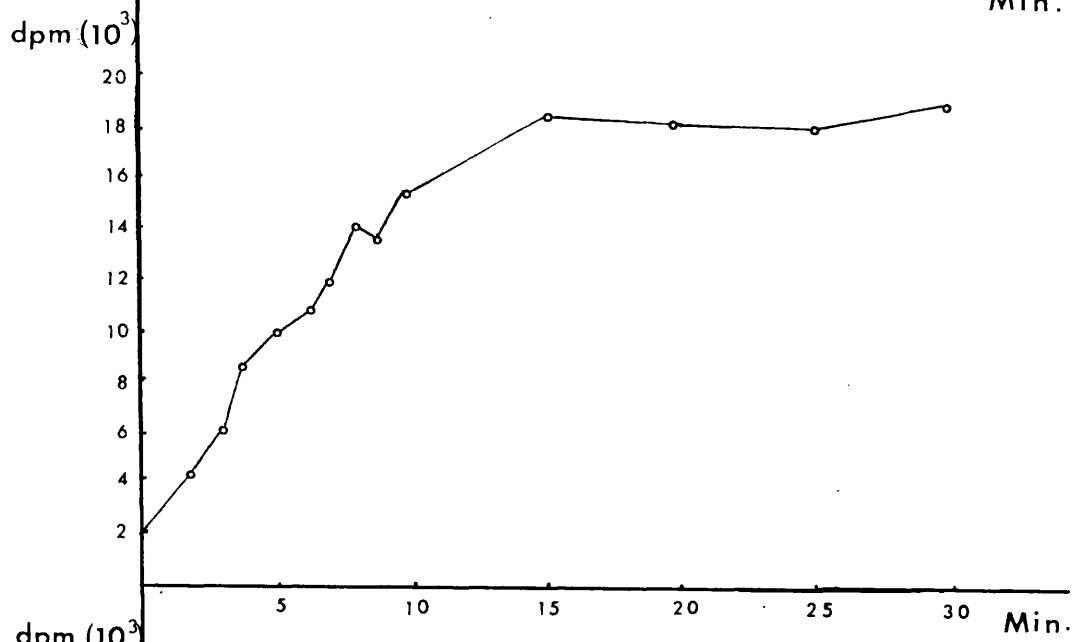
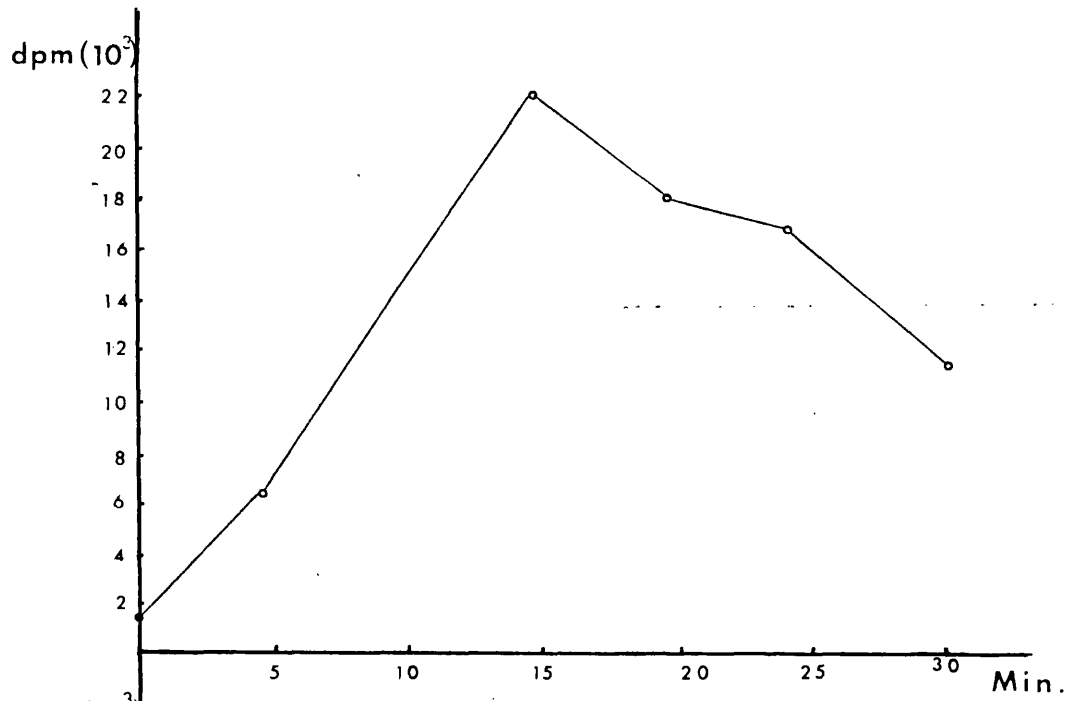


Fig 40

FIG 41 Light microscope autoradiograph of human term placenta perfused with  $^3\text{H}$ -IgG. Silver grains (circled) were found scattered over the epithelium (arrow) and associated with the endothelial cells of the fetal blood capillaries. (arrowhead).

FIG 42 Light microscope autoradiograph of control tissue excised and fixed at delivery. A few silver grains (circled) can be seen scattered randomly over the tissue and these can be attributed to background radiation.

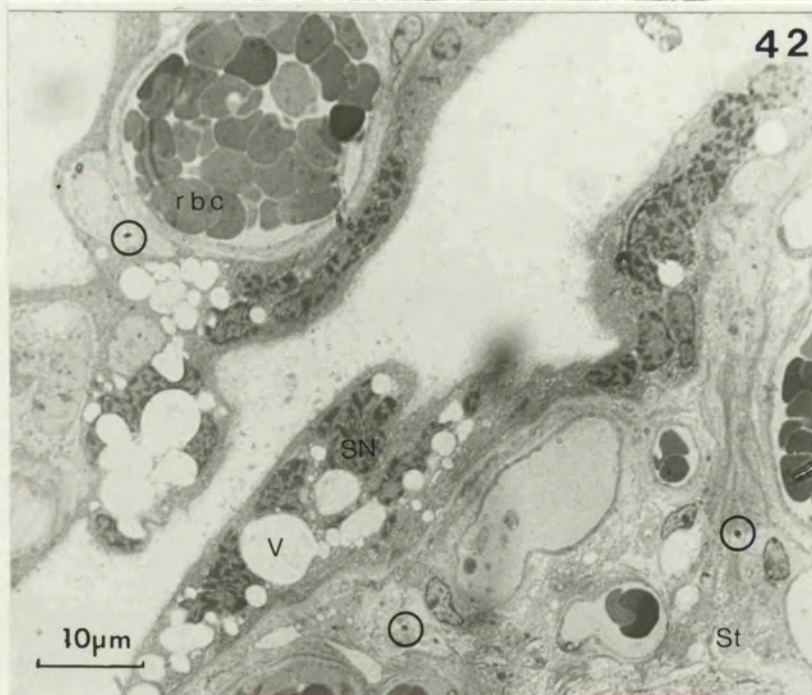
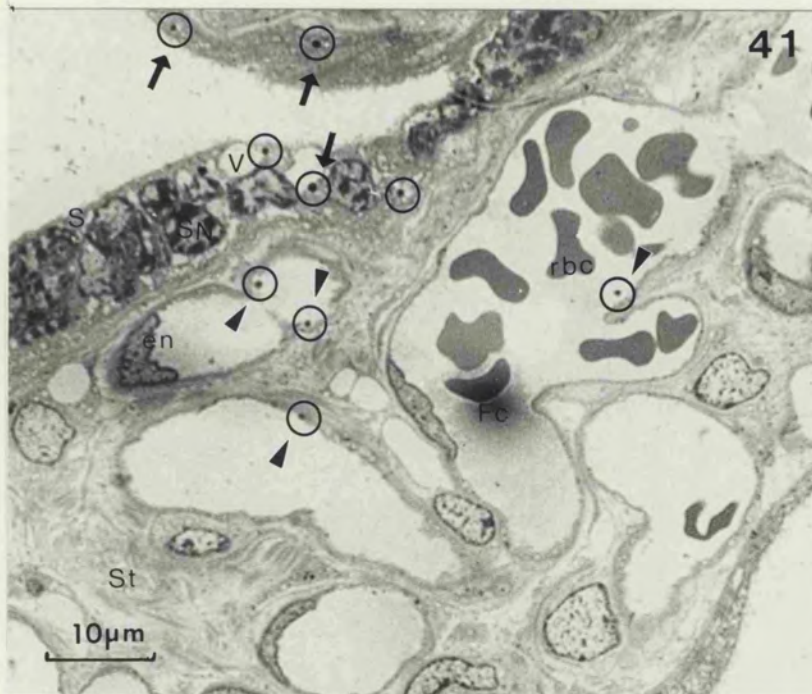


FIG 43 Histograms for each of the three successful perfusions showing amount of radioactivity, expressed as number of silver grains  $\times 10^{-3}$  in  $1\mu^2$  of tissue section.

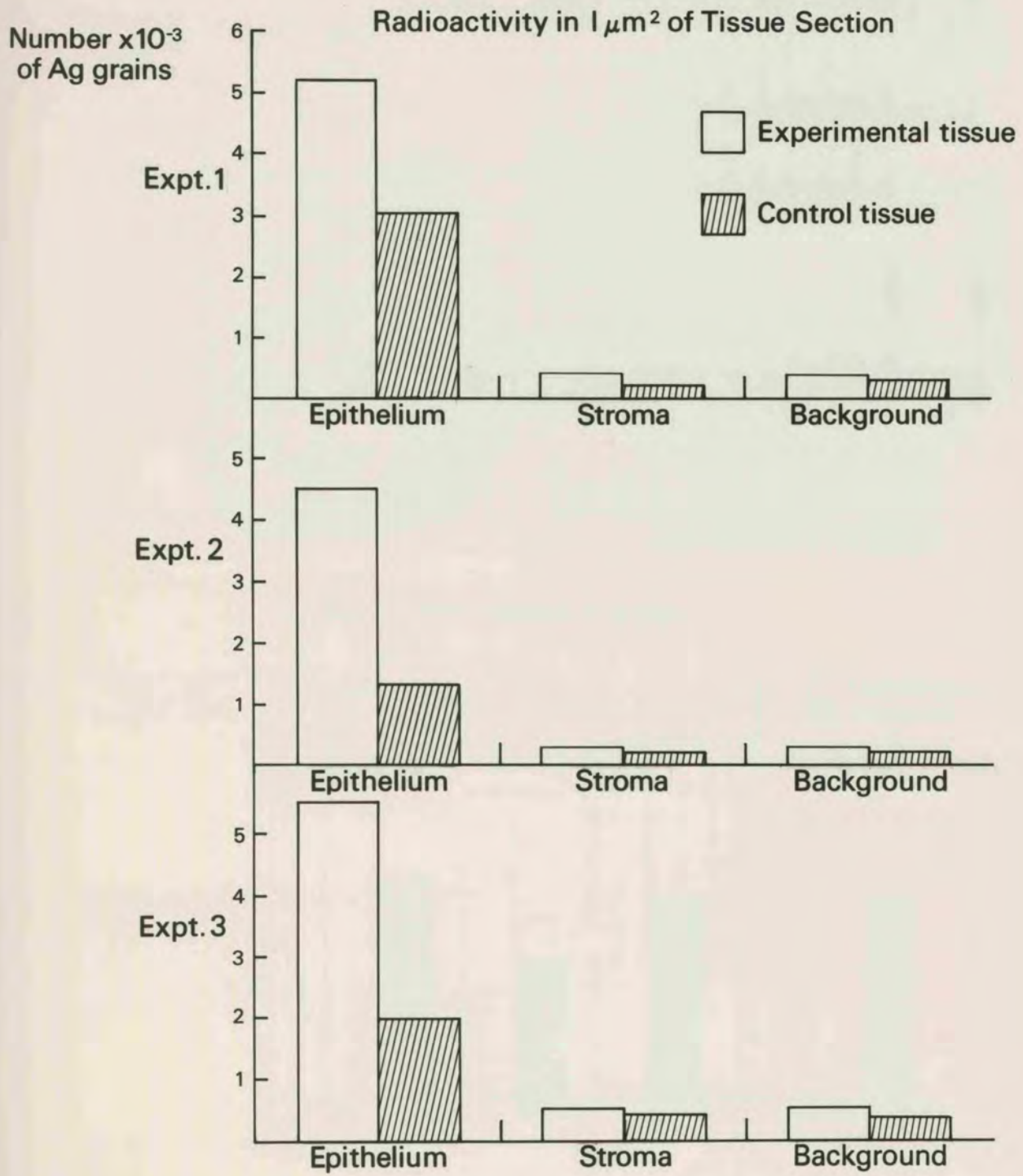


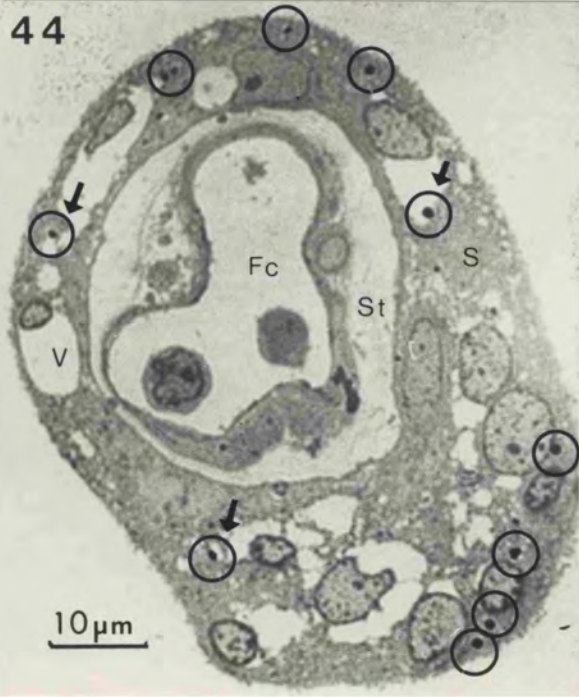
Fig 43

FIG 44 Light microscope autoradiograph showing silver grains (circled) associated with light microscopically visible vesicles in the syncytiotrophoblast (arrow).

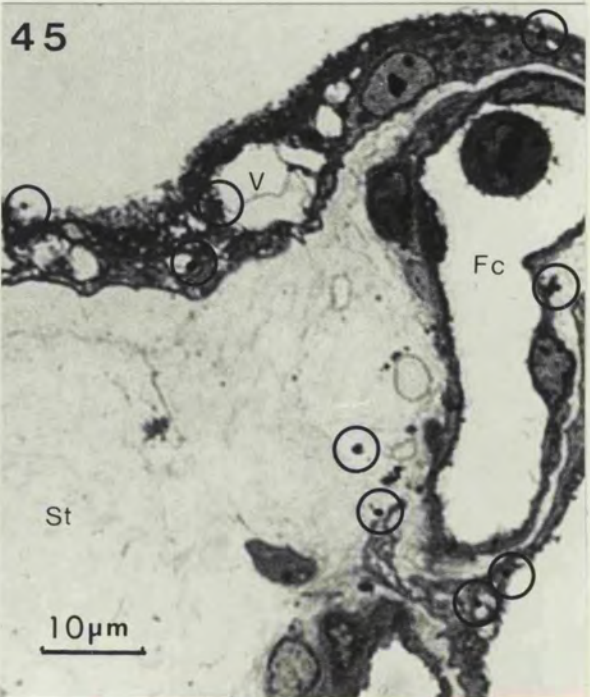
FIG 45 This light microscope autoradiograph shows the variation in morphology of these large light microscopically visible vesicles.

FIG 46 Histogram showing the association of silver grains and random dots with the syncytial vesicles.

44

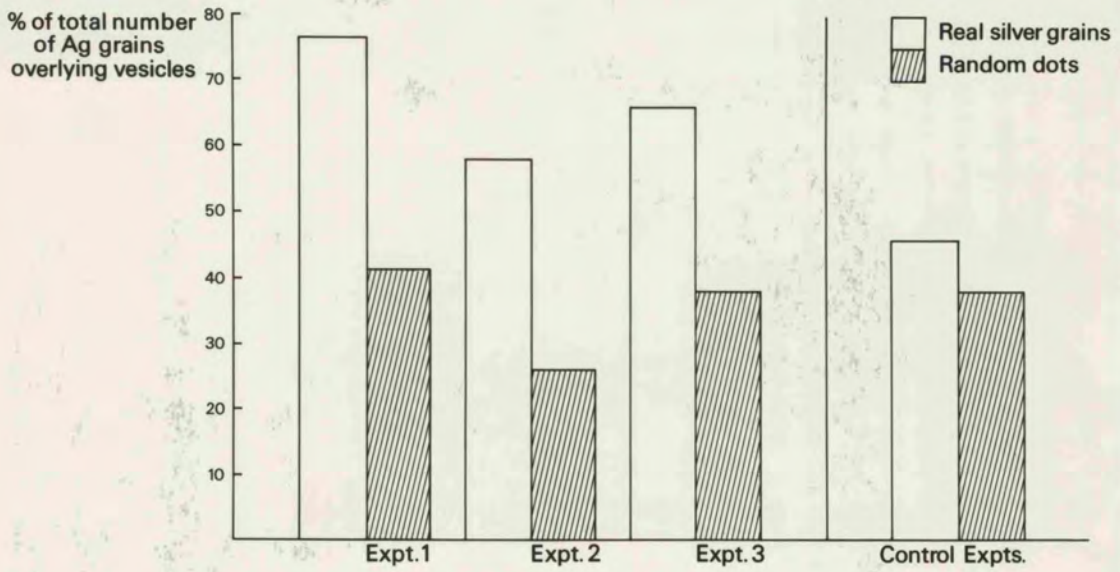


45



46

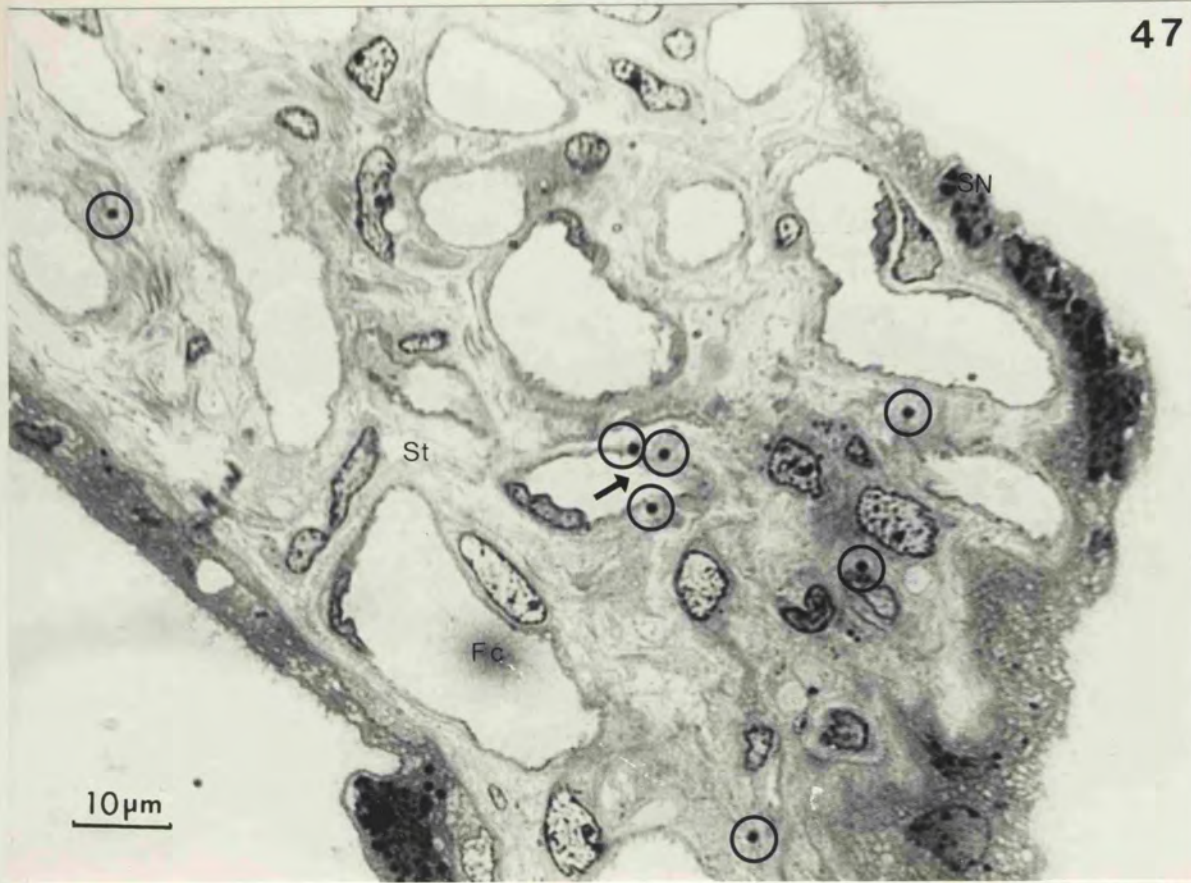
Syncytial Vesicle Association of Ag Grains



---

FIG 47 Light microscope autoradiograph showing silver grains (circled) and their association with the fetal capillary endothelial cell (arrow).

FIG 48 Histogram showing endothelial association of the silver grains.



Endothelial Association of Ag Grains.

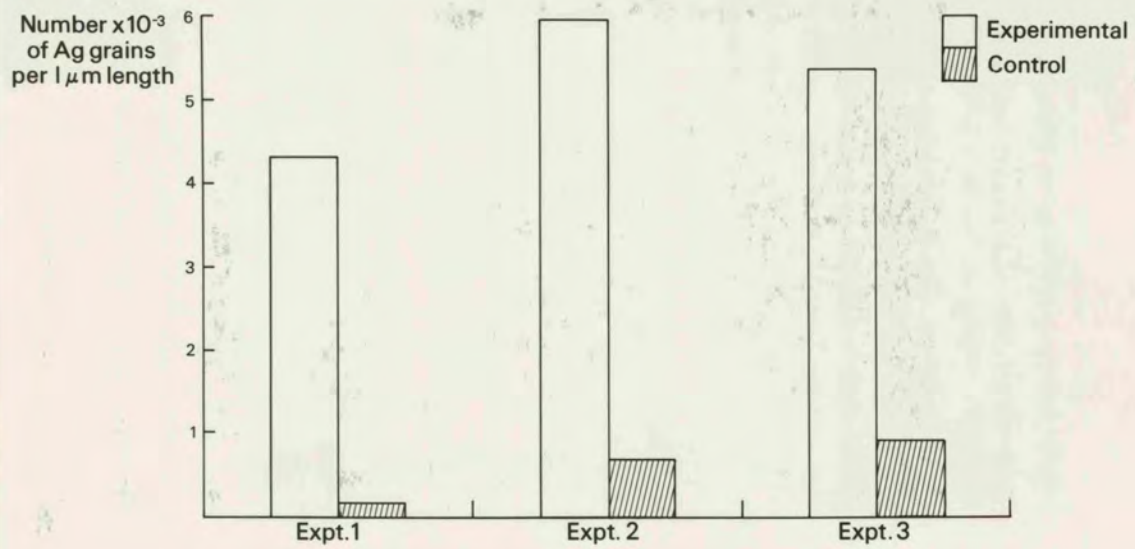


FIG 49 & 50 Transmission electron microscope autoradiographs showing silver grains (circled) apparently associated with vesicles in the syncytiotrophoblast (arrow).

In Fig 49 one silver grain can be seen to be associated with the fetal capillary (arrowhead).

FIG 51 Transmission electron microscope autoradiograph showing silver grains (circled) distributed throughout the stroma. One silver grain can be seen lying close to the fetal capillary endothelial cell (arrow).

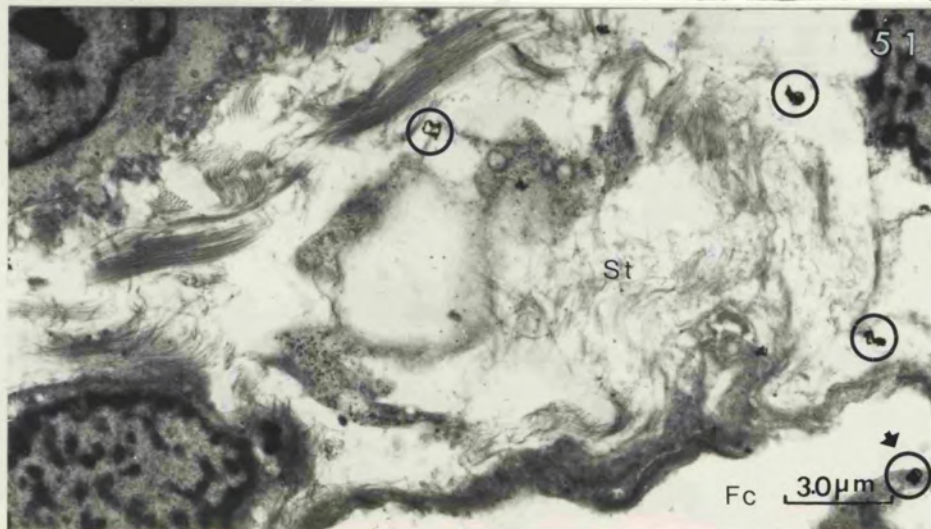
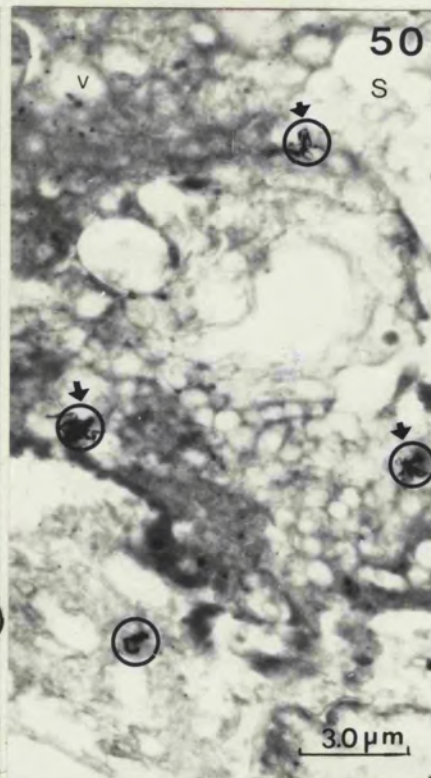
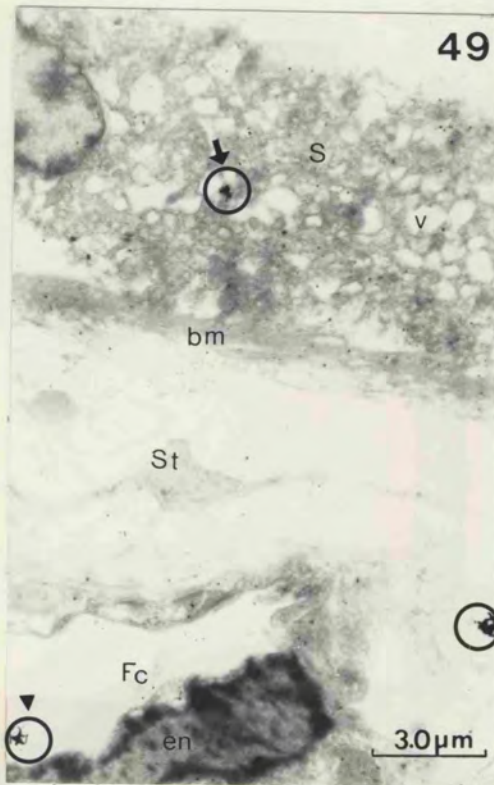


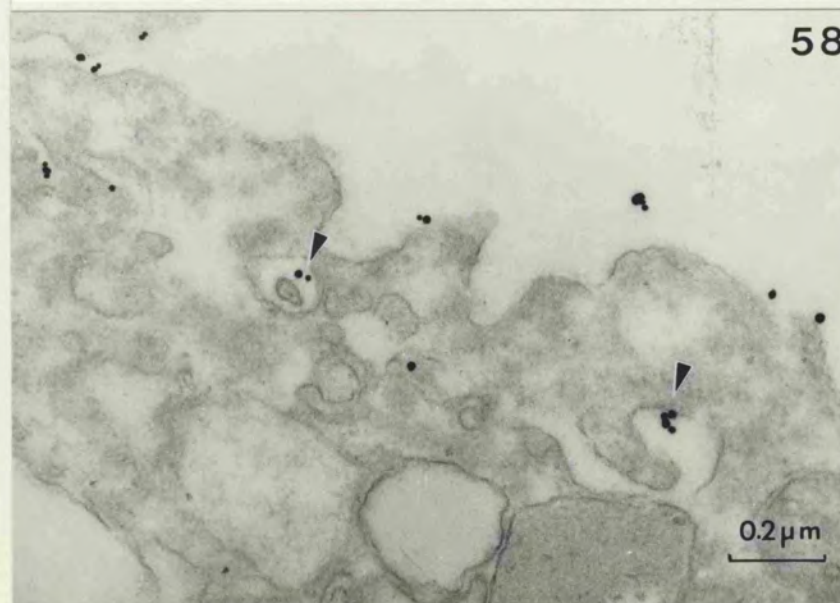
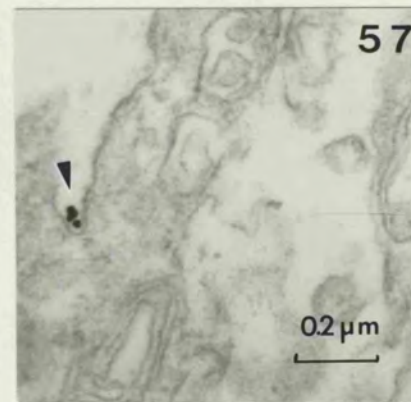
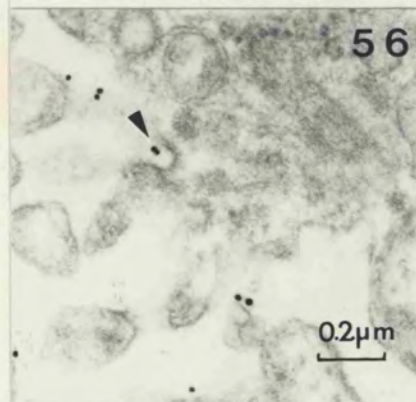
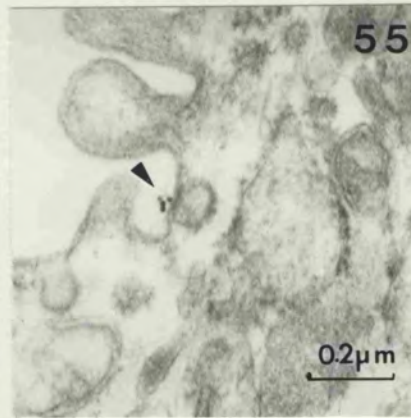
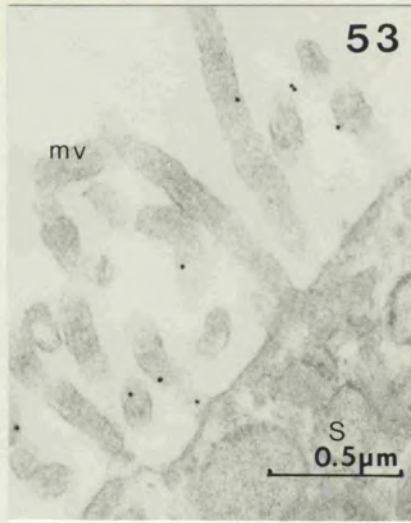
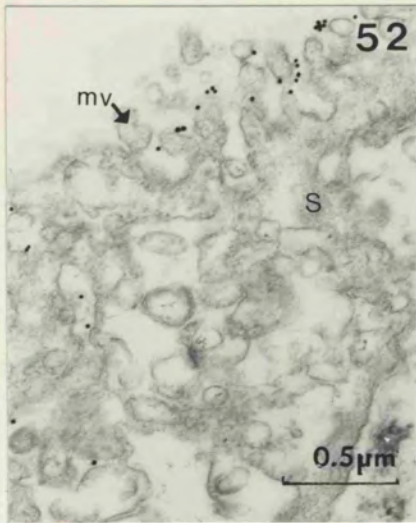
FIG 52-61. Transmission electron micrographs showing term placental tissue perfused with colloidal gold-IgG probe. The gold-IgG particles are clearly visible owing to their highly electron-dense and very uniform appearance.

FIG 52 & 53 Gold-IgG probe was found associated with the microvillous surface (mv) of the tissue.

FIG 54 Gold-IgG probe was found associated with the non-microvillous surface of the tissue (arrowhead).

FIG 55-57 Gold-IgG probe was found associated with coated pits on the surface of the syncytiotrophoblast (arrowheads).

FIG 58 & 59 Gold-IgG probe was found associated with smooth vesicular structures within the syncytiotrophoblast (arrowheads).



---

FIG 60 Gold-IgG probe was found within coated vesicles within the syncytiotrophoblast (arrowhead)

FIG 61 Gold-IgG probe was found:

- (a) lying free in the syncytiotrophoblast
- (b) in the basement membrane
- (c) in the stroma
- (d) associated with the fetal capillary endothelial cell.

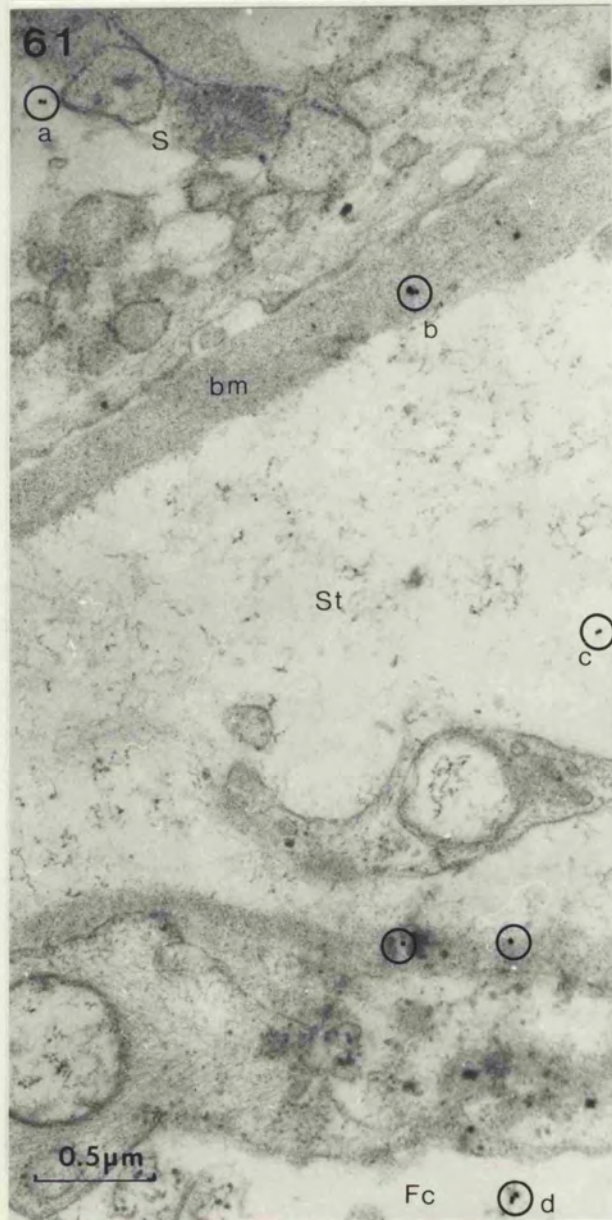
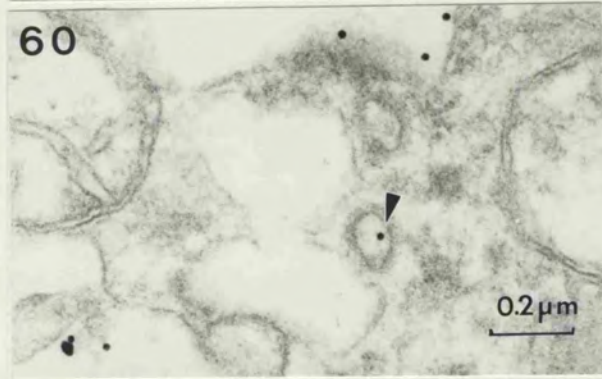
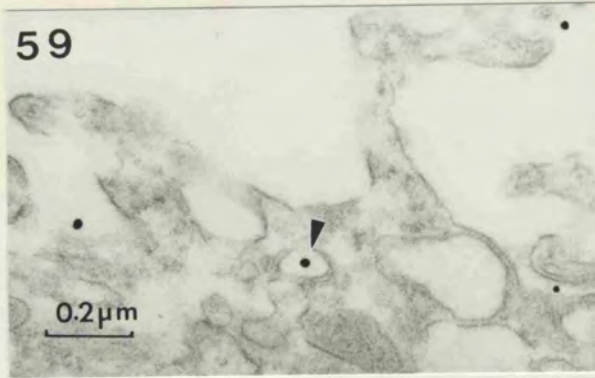


FIG 62-67 Scanning transmission electron microscope (STEM) stereo pair micrographs. When viewed with a stereo-viewer these pictures have a three dimensional image.

FIG 62 & 63 Shows coated pits on the surface of the syncytiotrophoblast.

FIG 64 Shows a vesicular structure close to the basement membrane.

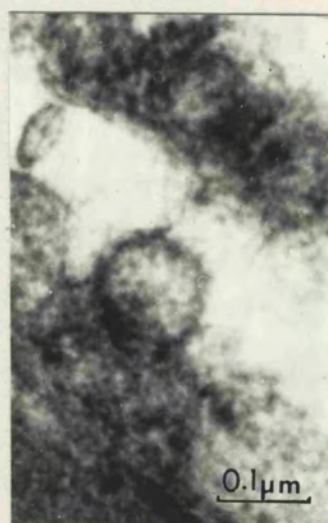
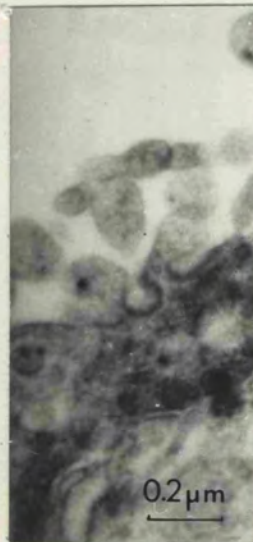
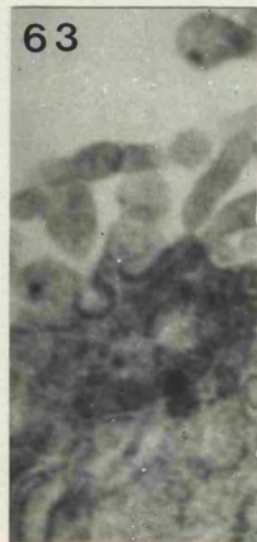
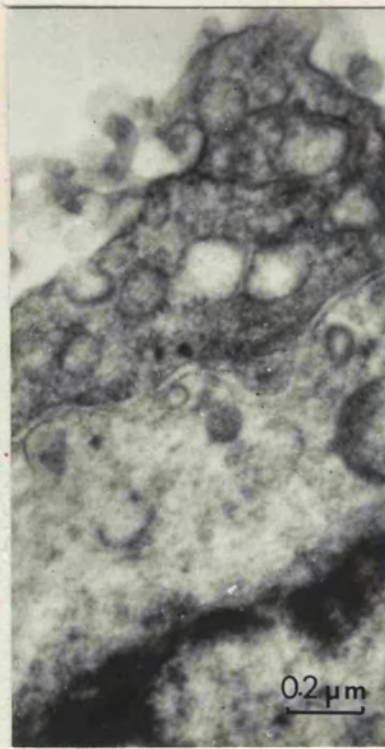
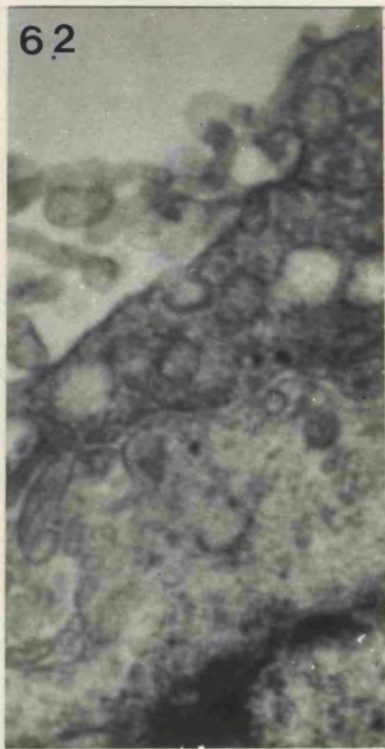


FIG 65 Gold-IgG probe located in a large vesicular structure within the syncytiotrophoblast.

FIG 66 Gold-IgG probe lying apparently free in the syncytiotrophoblast.

FIG 67 Gold-IgG probe associated with the surface microvilli of the syncytiotrophoblast.

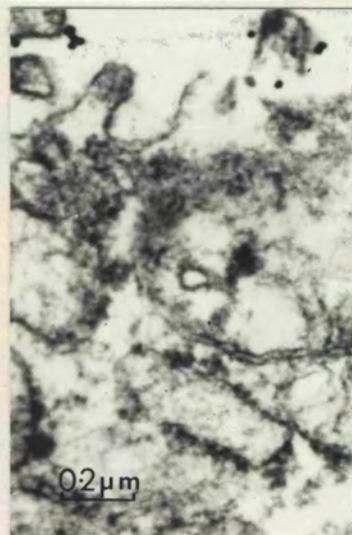
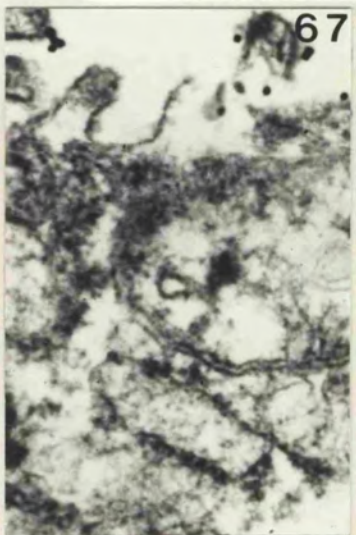
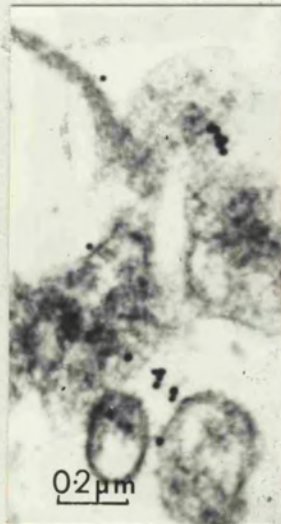
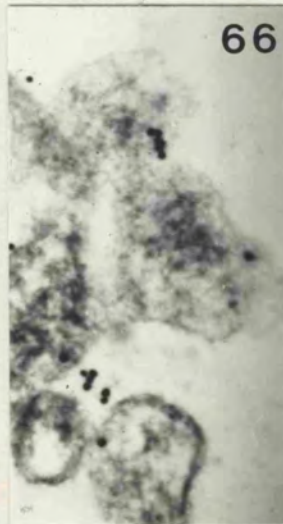
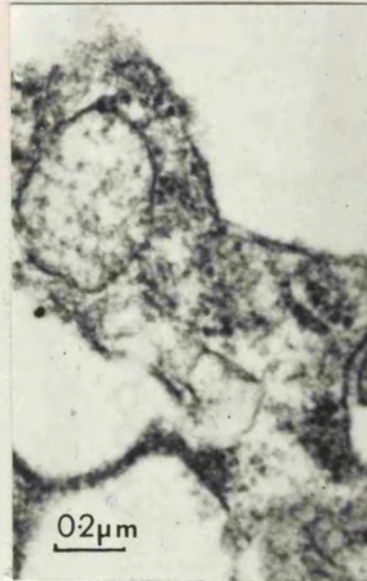
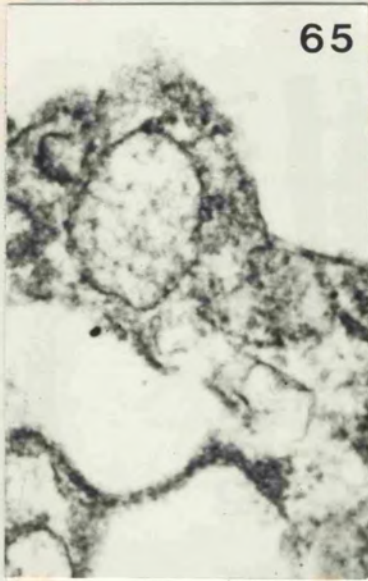


FIG 68 Ouchterlony double diffusion plate showing a pale precipitation line between the tritiated probe (centre well) and the serially diluted anti-IgG serum in the outer wells. The intensity of the precipitation line decreased with decrease in concentration of the anti-IgG (The anti-IgG decreased in concentration from (\*) in an anti-clockwise direction ).

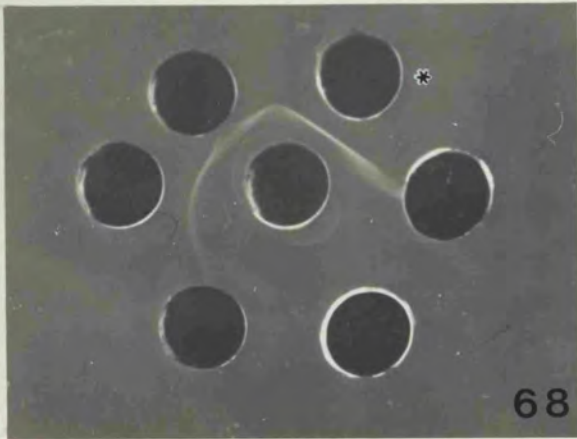
FIG 69 Autoradiograph of the above Ouchterlony plate. The black areas on the plate indicate the location of the tritiated IgG probe.

FIG 70 Transmission electron micrograph of negatively stained gold-IgG particles. A pale halo (arrow) around the central electron dense gold particles indicated the presence of the protein IgG.

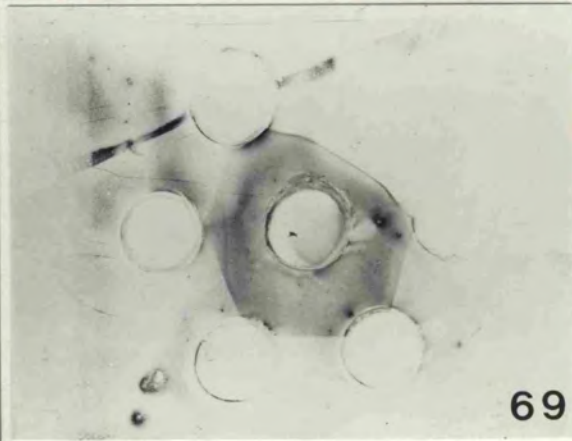
FIG 71 Negatively stained preparation of gold particles only. The pale halo is absent.

FIG 72 Transmission electron micrograph of gold-IgG particles incubated with anti-IgG serum. Clumping of the gold particles indicates precipitation of the IgG on the gold particles by the anti-IgG.

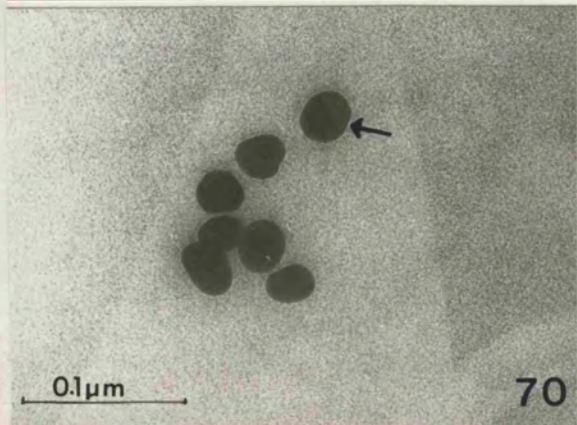
FIG 73 Control preparation of gold particles only incubated with anti-IgG. No precipitation has occurred.



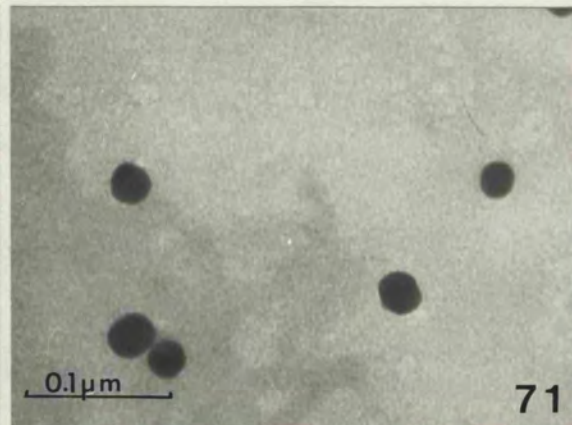
68



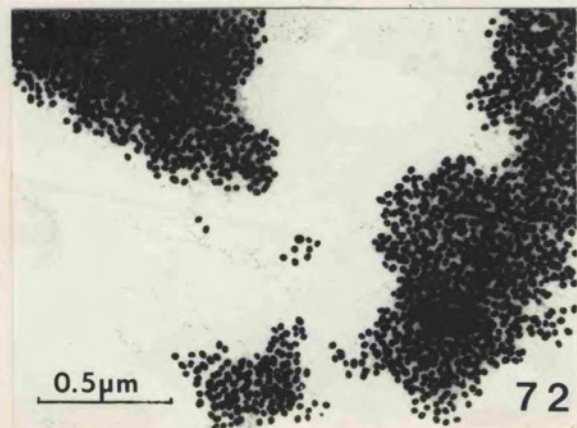
69



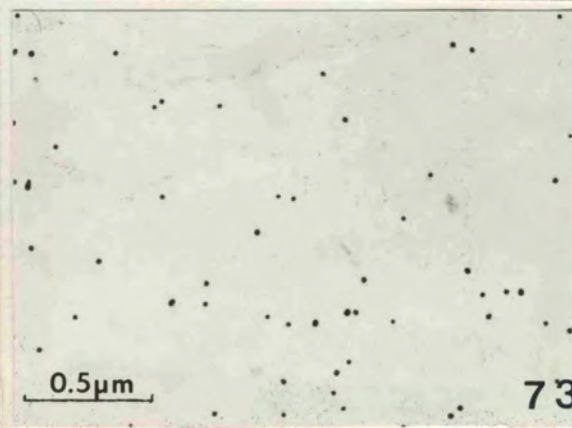
70



71



72



73

FIG 74 Results of incubation of gold-IgG with Sepharose-4B-protein A (a) and gold-IgG with Sepharose 4-B only (b). The Au-IgG probe is retained in the tube shown by the pink colouration, even after extensive washing, indicating that the colloidal gold has IgG attached to it.

FIG 75 Results of incubation of gold particles only with Sepharose-4B-protein A (a) and gold particles only with Sepharose 4B only (b). No pink colour is retained in the tubes after washing indicating an absence of IgG.

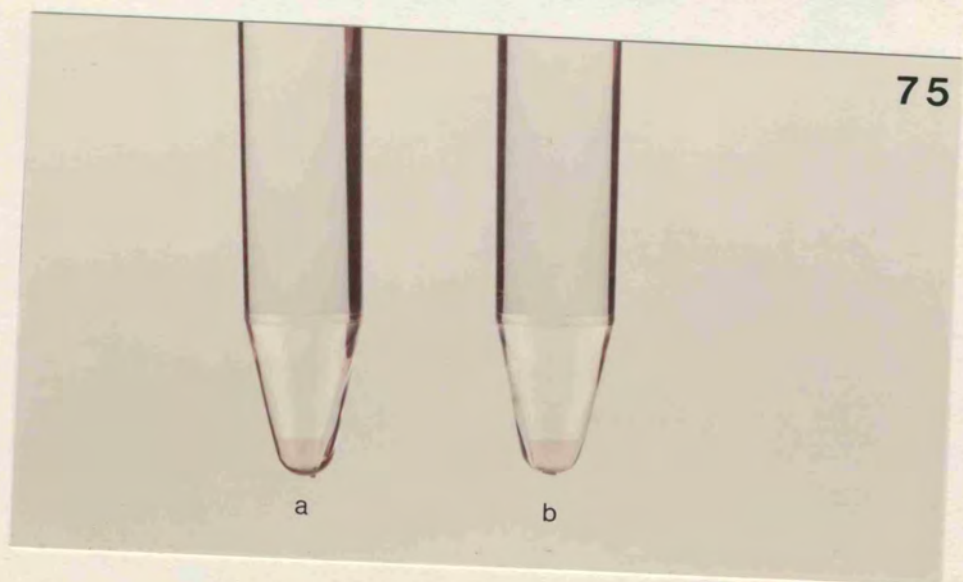
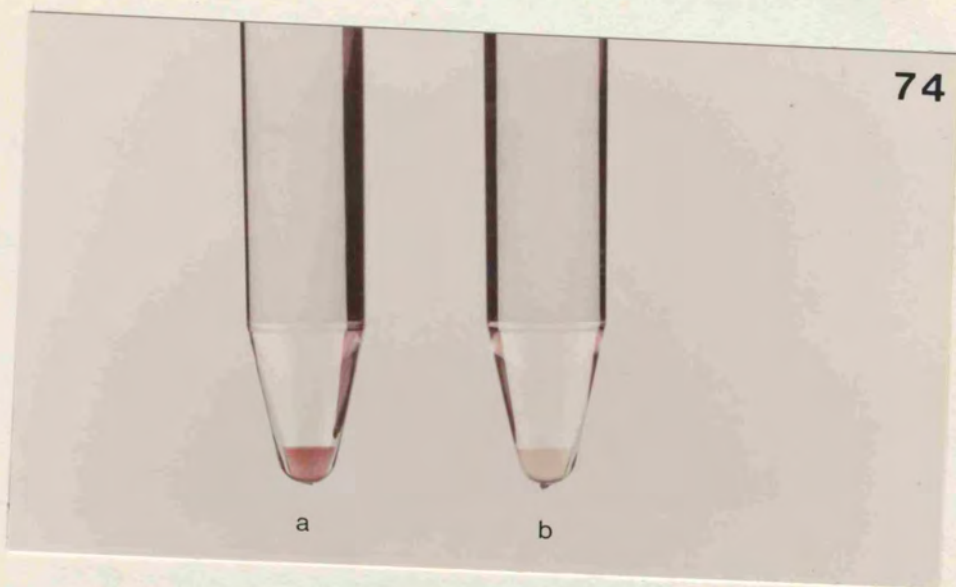


FIG 76 Light microscope autoradiograph of term placental tissue incubated with medium only. A few silver grains (circled) are present randomly distributed over the tissue and these can be attributed to background radiation.

FIG 77 Light microscope autoradiograph of term placenta incubated with tritiated IgG. Silver grains (circled) seen over the tissue associated with the epithelium.

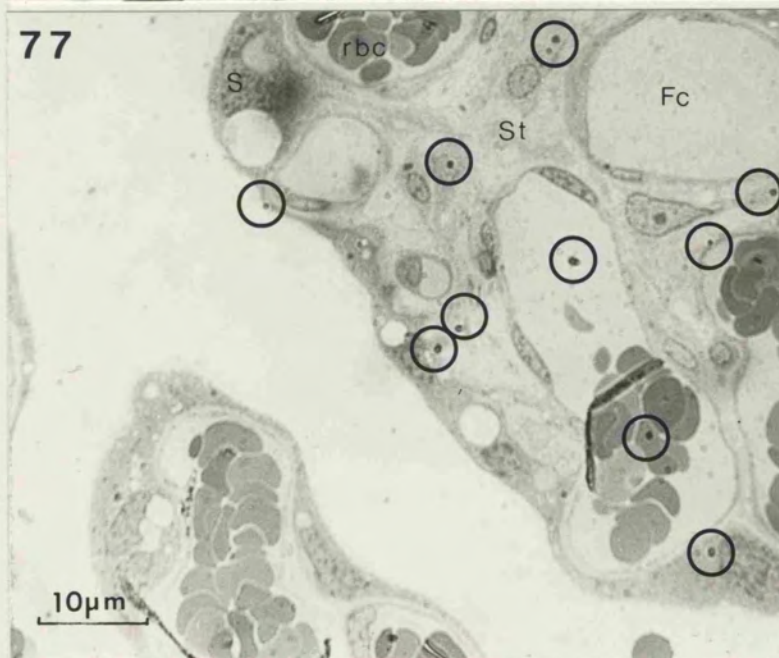
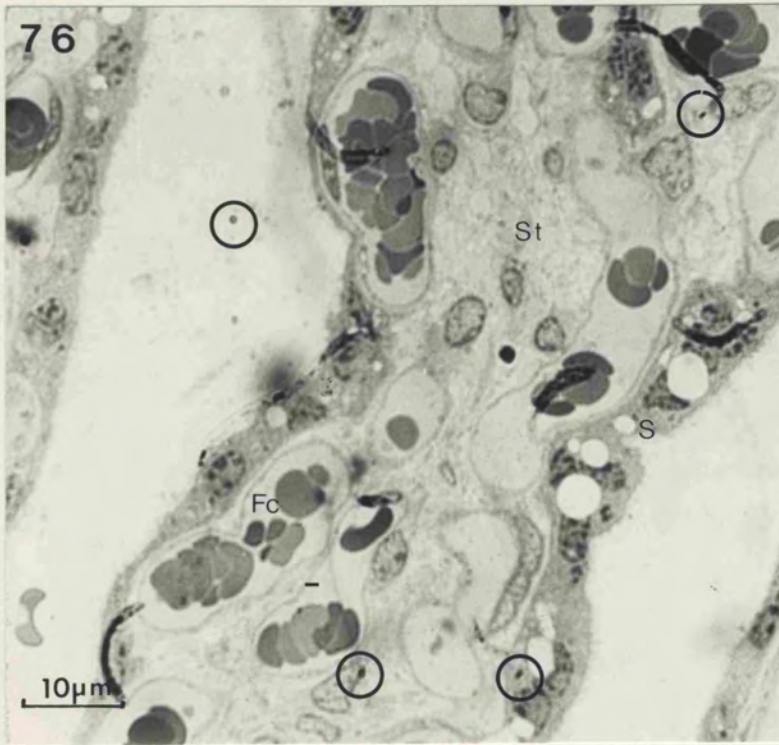


FIG 78-81 Transmission electron micrographs of term placental tissue incubated with Au(18)-IgG at pH4.2.

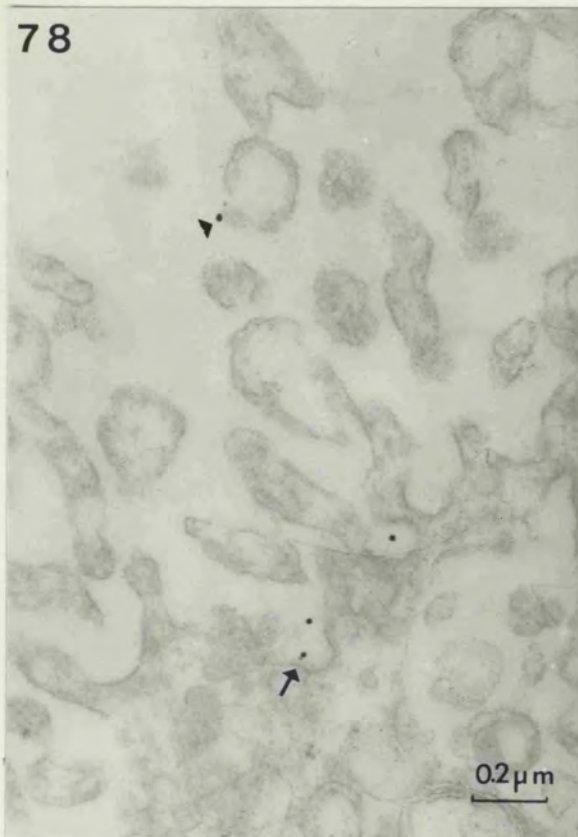
FIG 78 Gold-IgG complexes were found lying close to the microvillar surface of the syncytiotrophoblast and near a coated pit on the surface (arrow).

FIG 79 Gold probe was found in a large vesicle within the syncytiotrophoblast (arrowhead). There appears to be a coated region within the membrane of this vesicle (arrowhead). A gold particle is also seen close the non-microvillar surface of the syncytiotrophoblast (arrow).

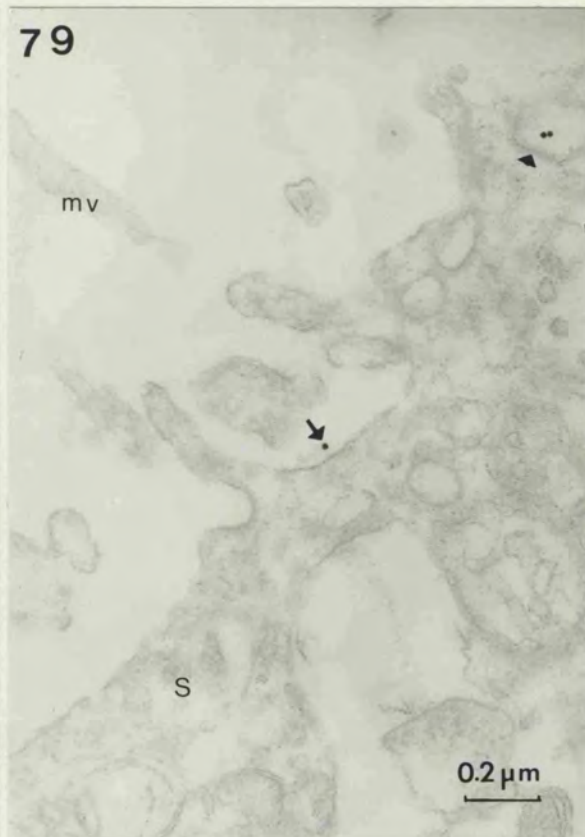
FIG 80 Particles of the gold-probe are found close to a coated region of the surface membrane of the syncytiotrophoblast (arrow).

FIG 81 Particles of gold probe were found lying free in the cytoplasm of the tissue (arrow). One particle of gold probe can be seen lying between two syncytial nuclei (arrowhead).

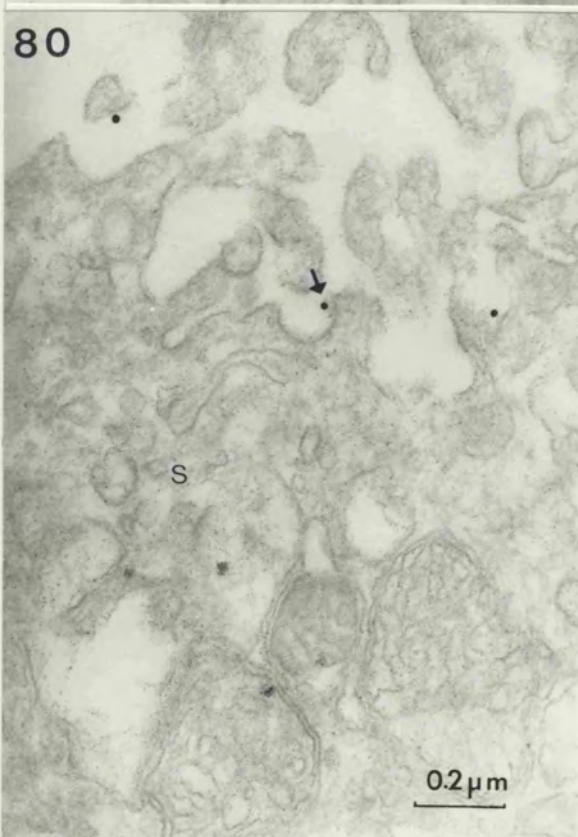
78



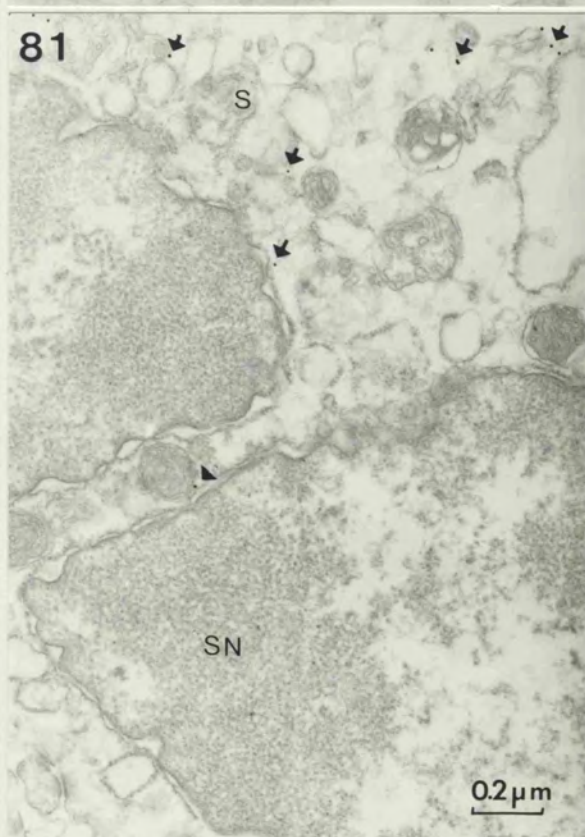
79



80



81



---

FIG 82 - 86 Transmission electromicrographs showing term placenta incubated with Au(18)-IgG pH 7.0 for 30 minutes.

FIG 82 Particles of the gold-IgG probe were found associated with the surface microvilli (arrowheads).

FIG 83 Particles of gold-IgG were found in vesicular structures (arrow) and lying free in the syncytial cytoplasm (arrowhead).

FIG 84 Three particles of probe found associated with a large vesicular structure (arrowheads).

FIG 85 & 86 Particles of Au(18)-IgG probe were found lying free in the syncytiotrophoblast cytoplasm (arrowheads).

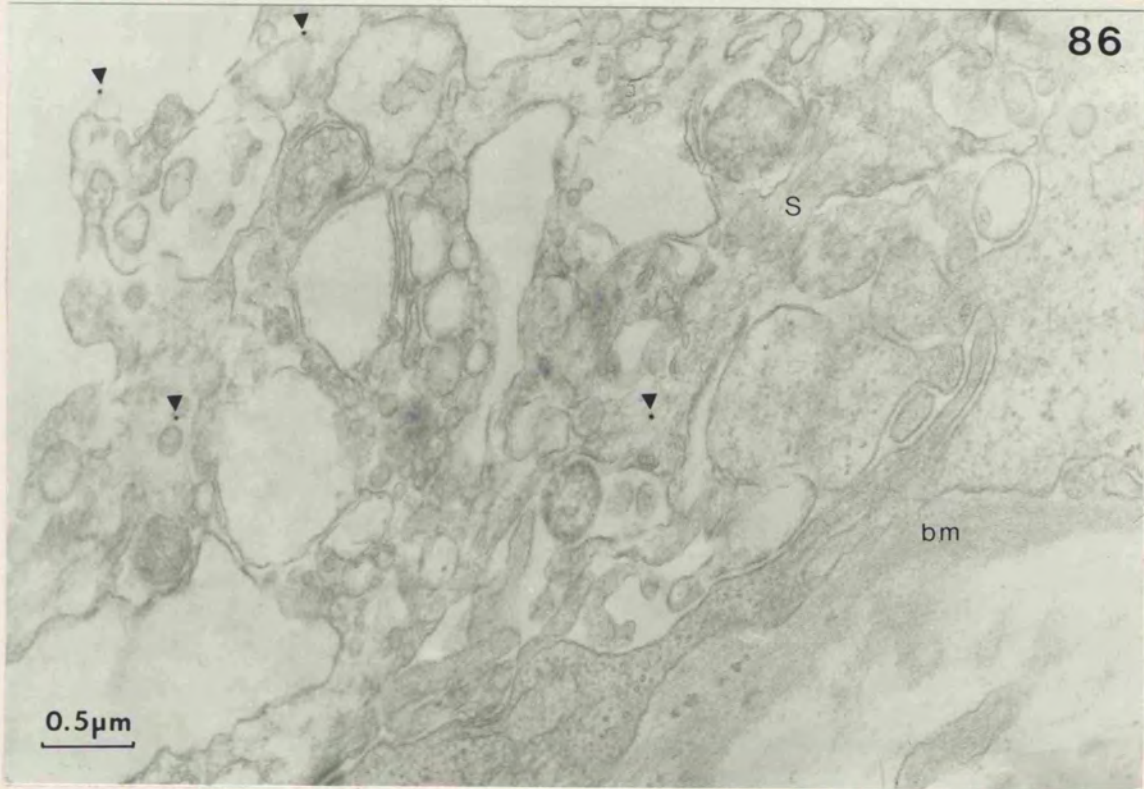
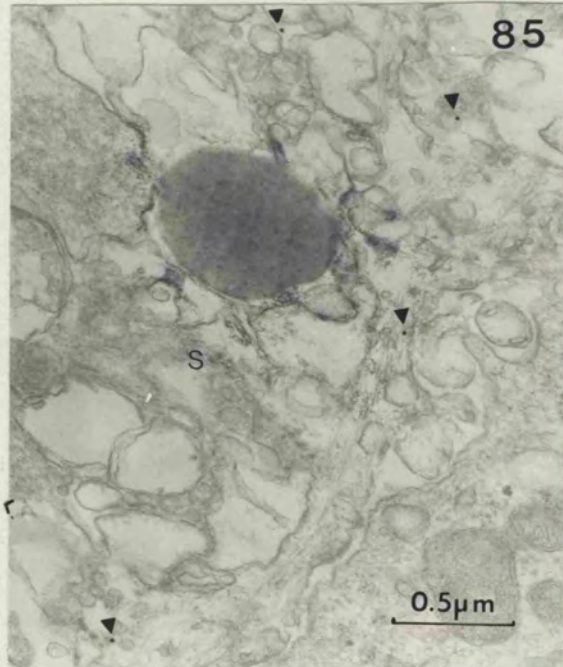
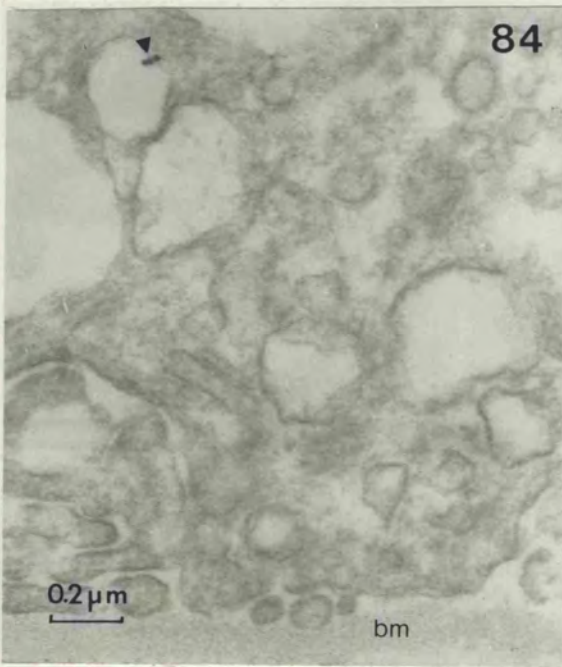
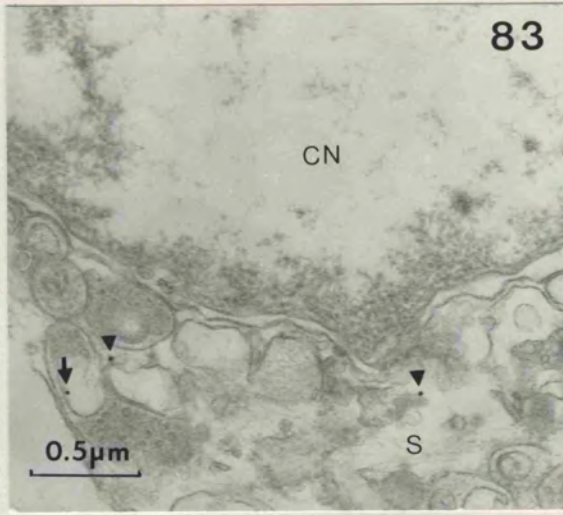
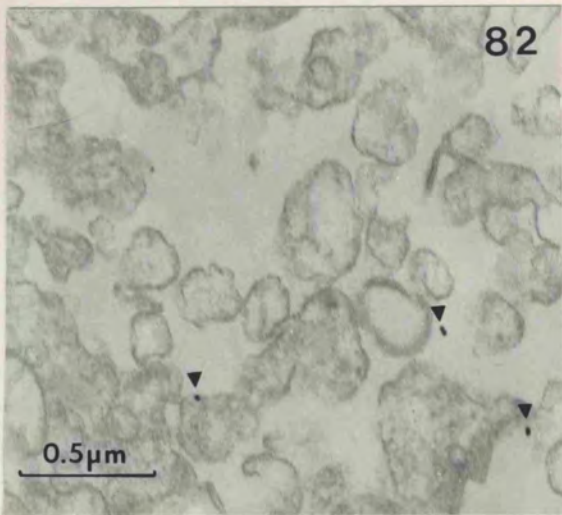


FIG 87-94 Transmission electron micrographs of term placenta incubated with Au(18)-IgG (pH 7.0) for 60 minutes.

FIG 87 Particles of probe were found lying free in the syncytiotrophoblast (arrowhead) close to the cytotrophoblast.

FIG 88 Some particles of gold appeared to be membrane-bounded (arrowhead).

FIG 89 Particles of probe found adjacent to cytotrophoblast cells. (arrowhead).

FIG 90,91 & 92 Particles of probe located close to the basement membrane (arrowhead)

FIG 93 Gold-IgG probe was found enclosed in a large electron-lucent vesicle in the cytotrophoblast cell (arrowhead).

FIG 94 High power micrograph of vesicle in Fig 93 showing gold-IgG particle within (arrowhead).

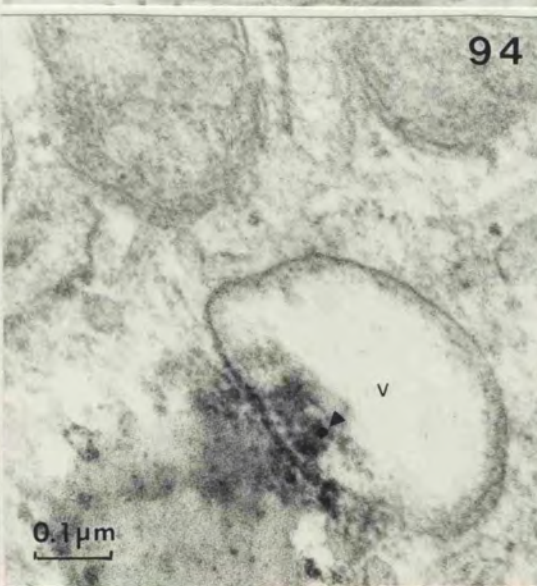
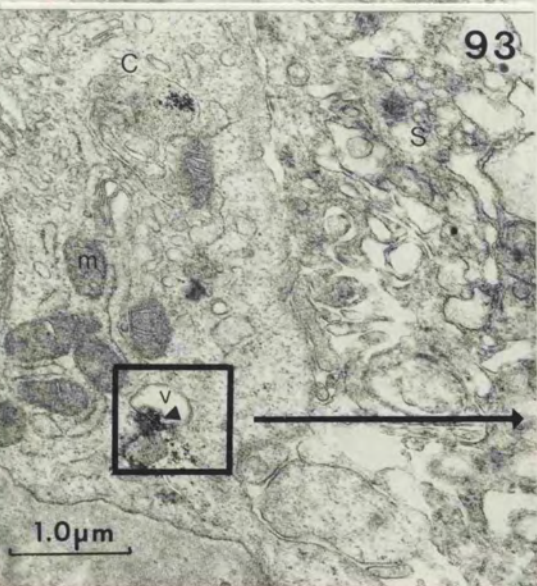
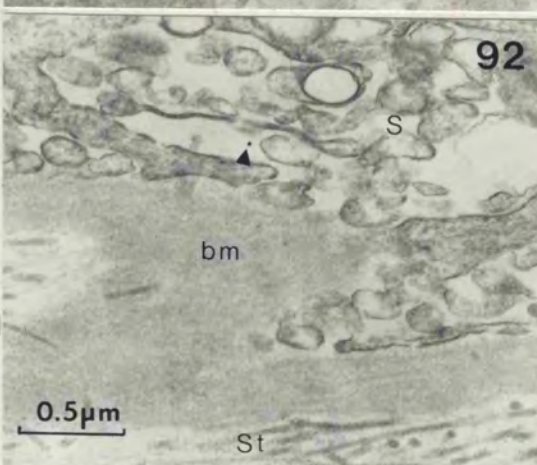
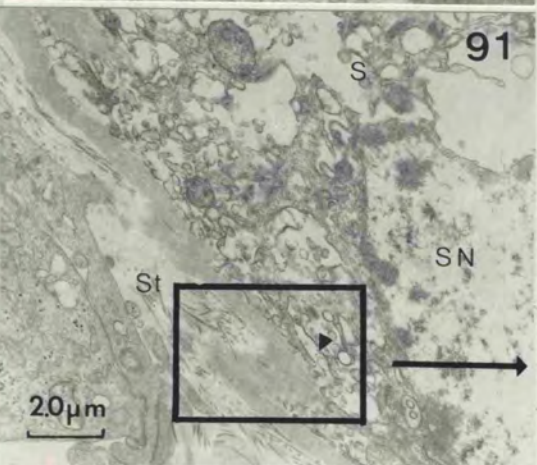
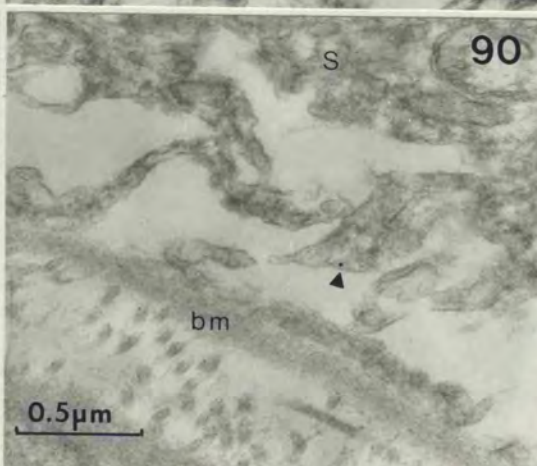
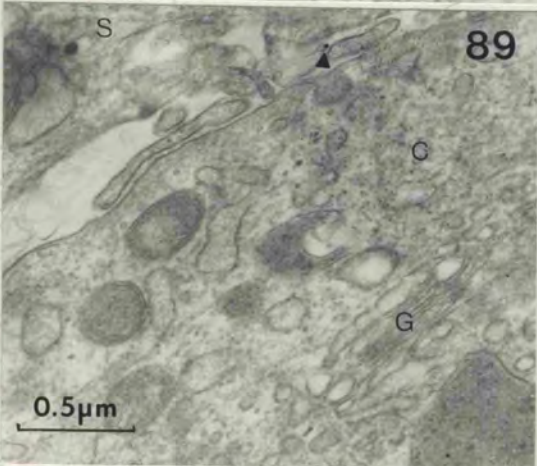
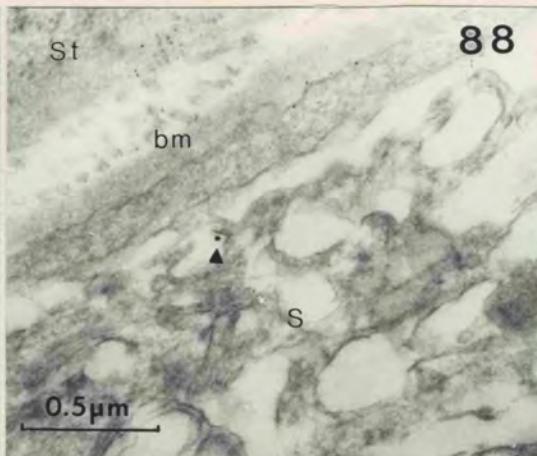
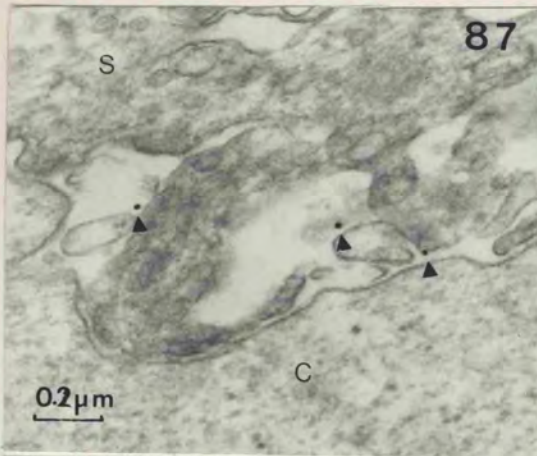
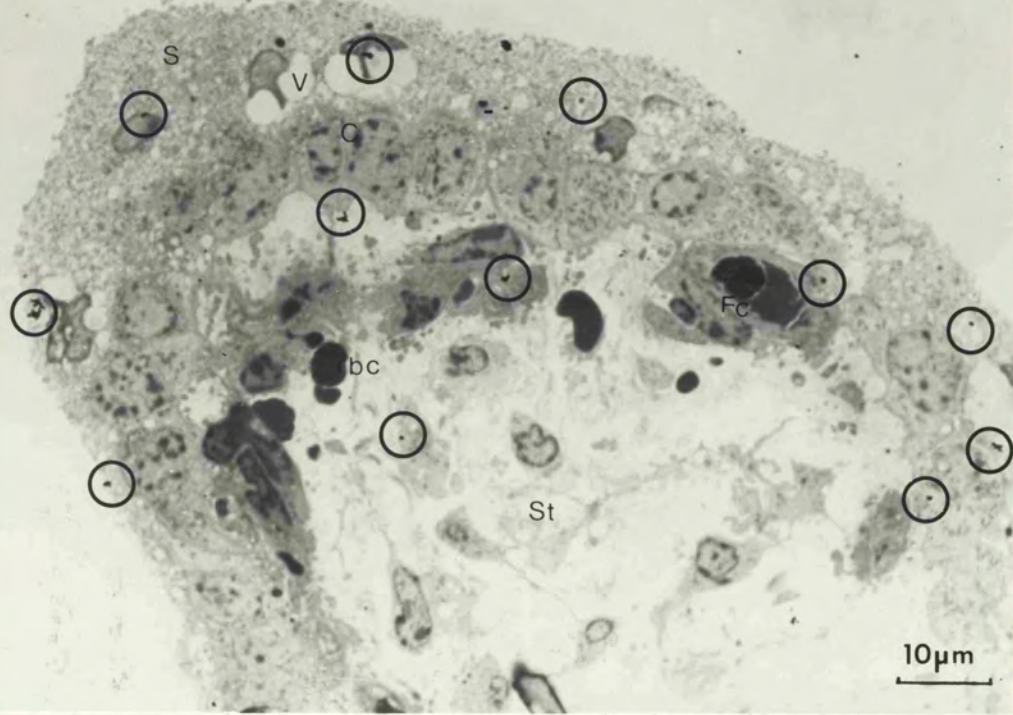


FIG 95 Light microscope autoradiograph of first trimester placenta incubated with tritiated IgG, showing silver grains (circled) distributed over the tissue.

FIG 96 Control tissue incubated in medium only. Silver grains (circled) can be seen distributed randomly over the tissue and can be attributed to background radiation. Note in both Fig 95 & 96 there is a complete layer of cytotrophoblast cells present beneath the syncytiotrophoblast characteristic of first trimester placenta.

95



96

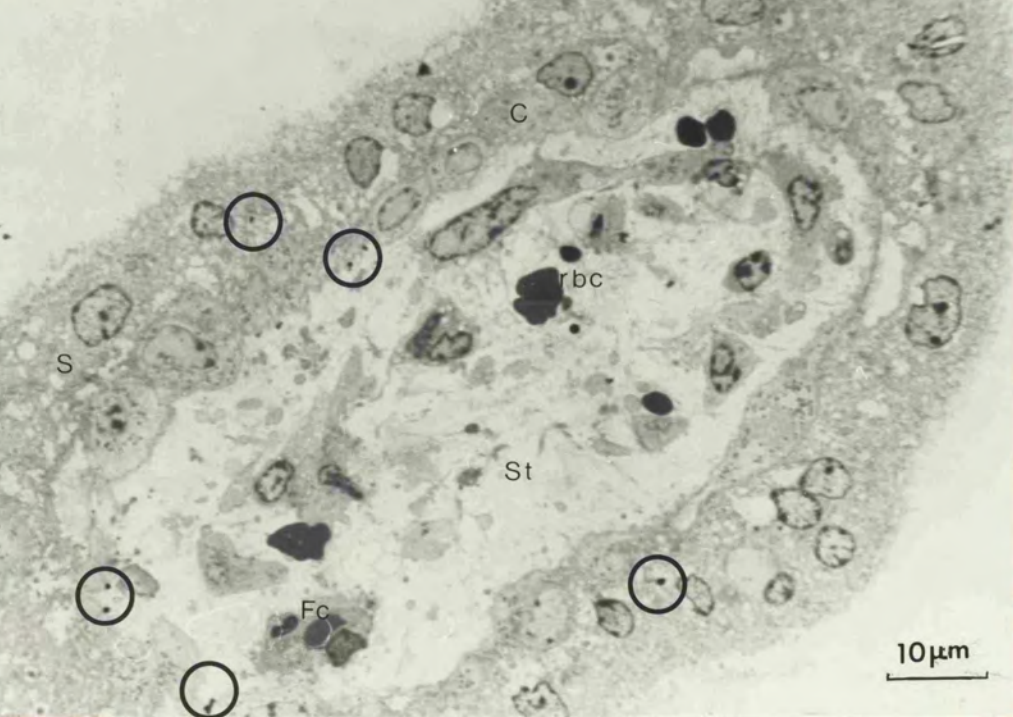


FIG 97 - 99 Transmission electron micrographs of first trimester placenta incubated with Au(18)-IgG.

FIG 97 Particles of probe associated with the syncytiotrophoblast (arrow).

FIG 98 A particle of IgG-gold probe was located near the basement membrane (arrow).

FIG 99 Particles of probe (arrow) enclosed within a vesicular structure (vs) in a cytotrophoblast cell (C).

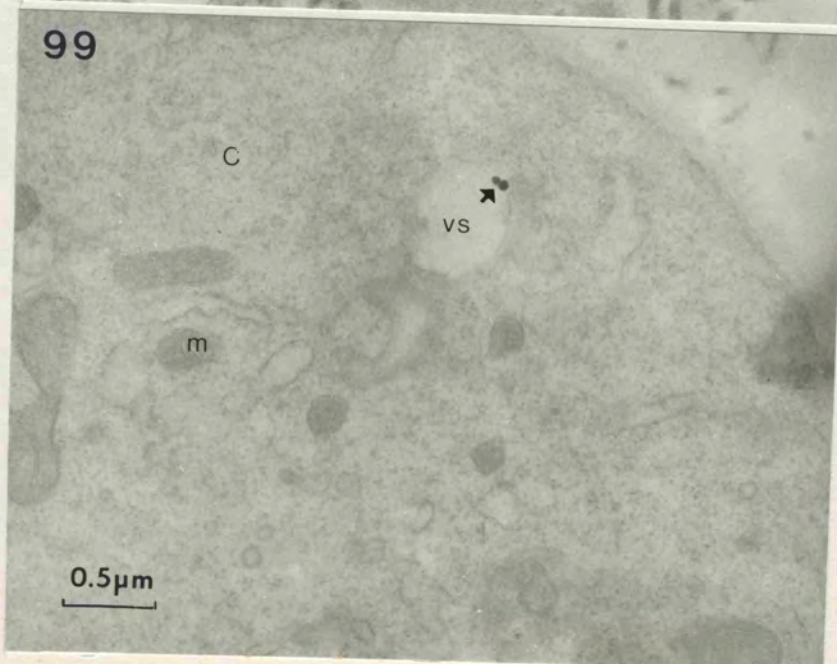
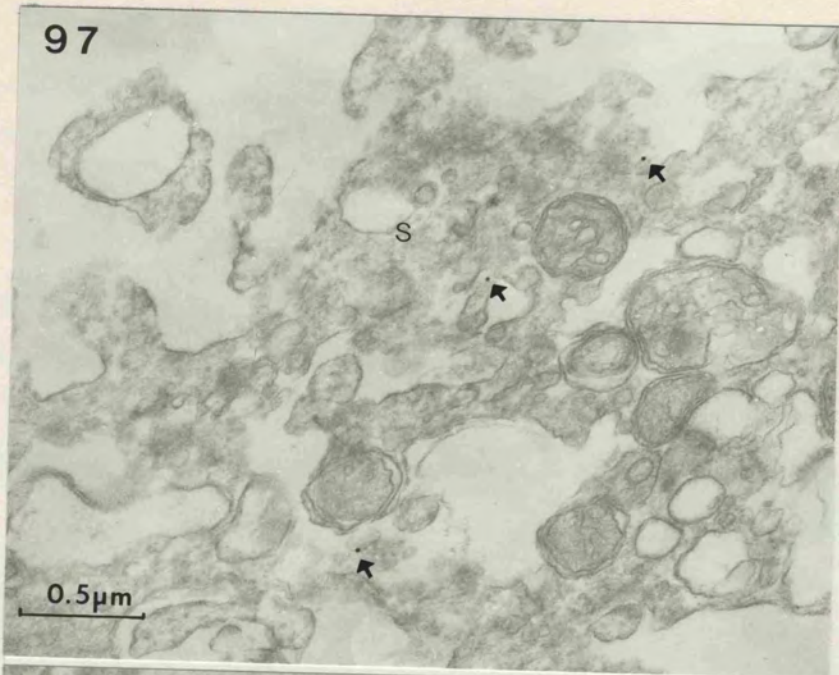


FIG 100 Low power light micrograph of normal human placental cells in tissue culture after 5 weeks. The characteristic central tissue clump (A) has individual cells on its edges (arrows).

(It is important to note that the optical quality of this particular photograph is poor because this is a thick piece of tissue embedded in epoxy resin which has been sheared from the base of the culture flask).

FIG 101 Light micrograph of a thick 0.5 $\mu$ m section of resin embedded human placental tissue culture cells stained with 1% toluidine blue. This section passes through the central mass of the tissue clump and it can be seen to be composed of both light and darker staining cells. Very densely staining bodies (arrow) are present.

FIG 102 This micrograph shows a section through the edge of the tissue clump. The surface microvilli are just visible on the edge of a electron-dense staining cell (arrow)

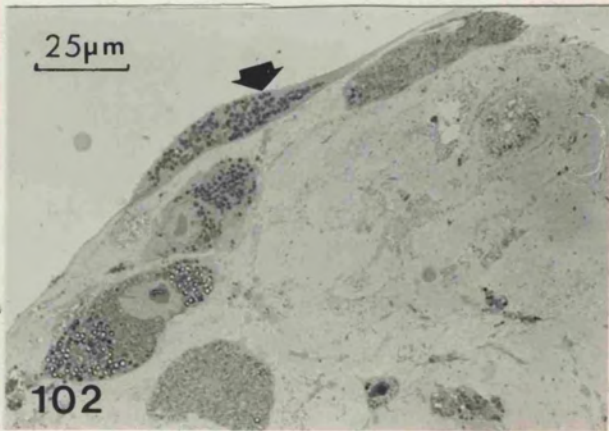
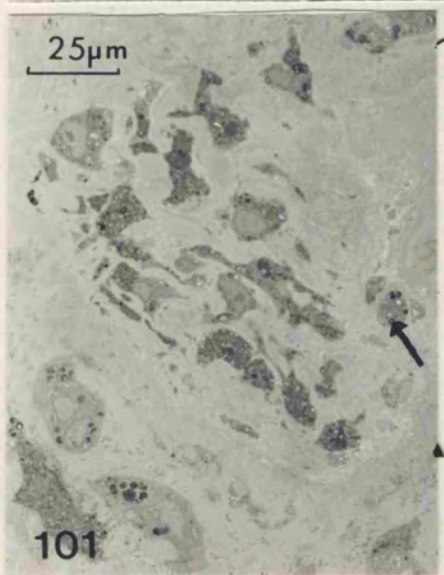
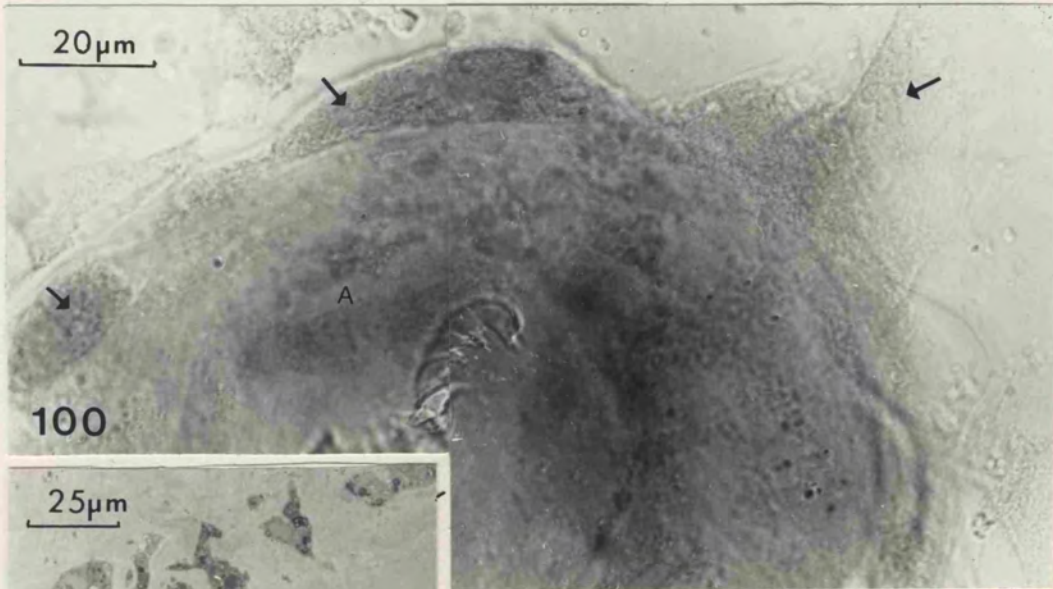


FIG 103-106 Nomarski light micrographs of normal placental cells cultured for 5 weeks.

FIG 103(i) & (ii) Villus-like structures can be seen around the edge of the tissue clump (arrow). Fine filaments (arrowhead) and bulbous swellings can also be seen (open arrow) by focusing at different levels.

FIG 104 Several villus-like structures are present in this photomicrograph (arrow)

FIG 105 (i) & (ii) Photomicrographs taken at different levels of the same area of tissue. A very long villous structure is visible (arrow).

FIG 106 (i) & (ii) Photomicrographs taken at different levels of the same area of tissue. A bulbous structure joined to the surface by a fine filament can be seen (arrow) as well as other villous (arrowhead) and filamentous structures (open arrow).

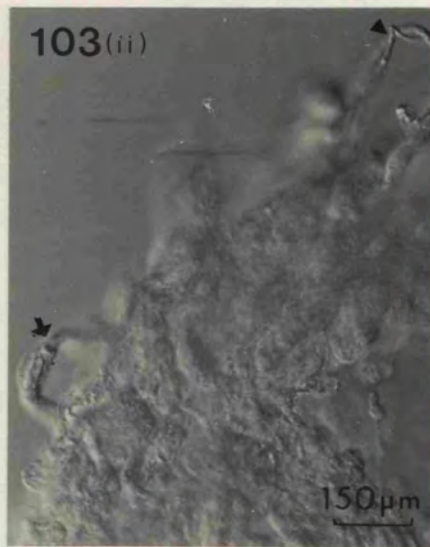
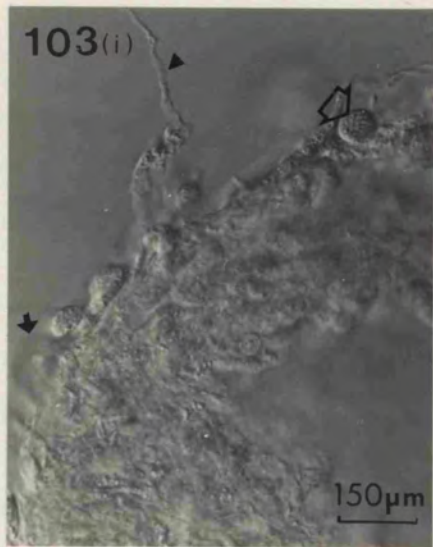


FIG 107 Light micrographs and transmission electron micrographs of different regions of the tissue clump of a human placental cell culture.

1. Low power light micrograph of thick 0.5 $\mu$ m vertical section of resin embedded tissue clump. The bottom right-hand corner (open arrow) shows where the clump was attached to the base of the cell.

A. Light micrograph of top region of tissue clump. Microvilli are just visible on the surface (arrowhead). Pale staining nuclei can be seen (arrow).

B. Light micrograph of left-hand side of the tissue clump. Microvilli again can be seen on the surface (arrow) and vesicular profiles are also present (arrowhead). Densely staining bodies can also be seen (open arrow)-see also Fig G.

C. High power light micrograph of middle region of tissue clump showing light and dark areas of tissue, very similar to that found in normal placenta.

D. Light micrograph of right-hand side of tissue clump. A difference in staining between the cells on the outside of the clump (arrow) and those on the inside (arrowhead) can be seen, similar to the differential staining seen in normal placental tissue between the epithelial and connective tissue core region.

E. Transmission electron microscopy of this area shows the presence of microvilli on the surface of the cells which are on the outside of the clump (arrow). A coated vesicular structure is present just below the surface (arrowhead).

F. High power light micrograph of basal area of tissue clump. This region is composed of individual cells (arrow) more loosely packed with fibres between them.

G. Transmission electron micrographs showing the presence of darkly staining bodies in the cell cytoplasm (arrow). Microvillar structures can be seen on the surface, and a vesicle is present just below the surface attached to it by a narrow tube (arrowhead).

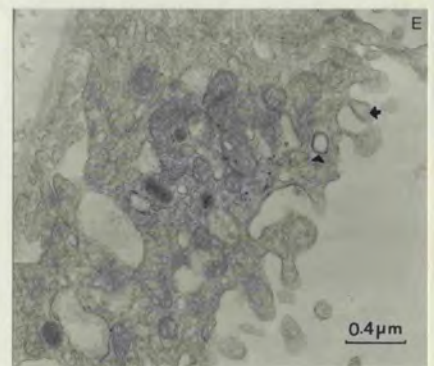
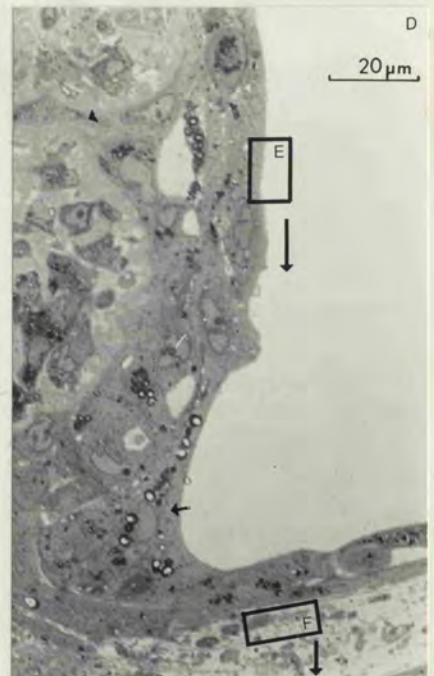
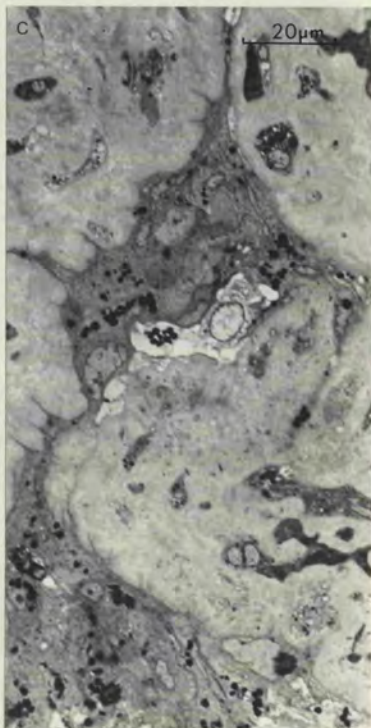
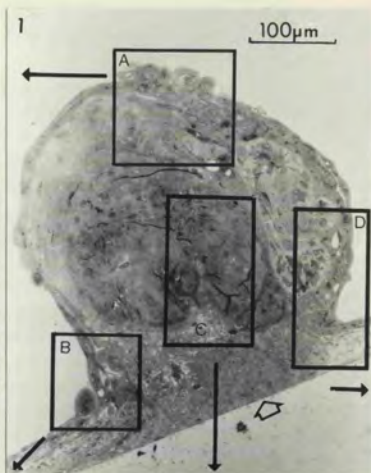
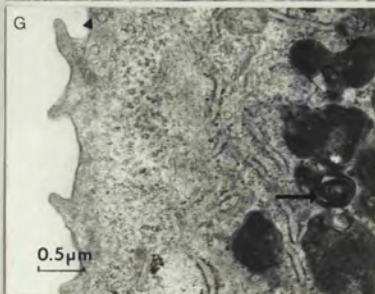
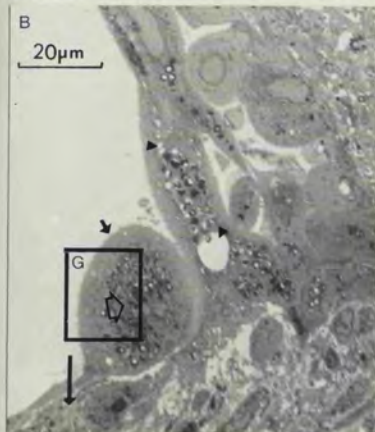
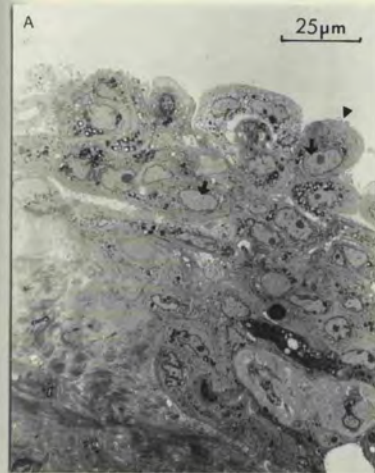


Fig 107

FIG 108 & 109 Transmission electron micrographs through the centre of the tissue clump. Densely staining syncytial-like nuclei are present (SN). A basement membrane can be seen (bm). Two centrioles can be seen (arrows).

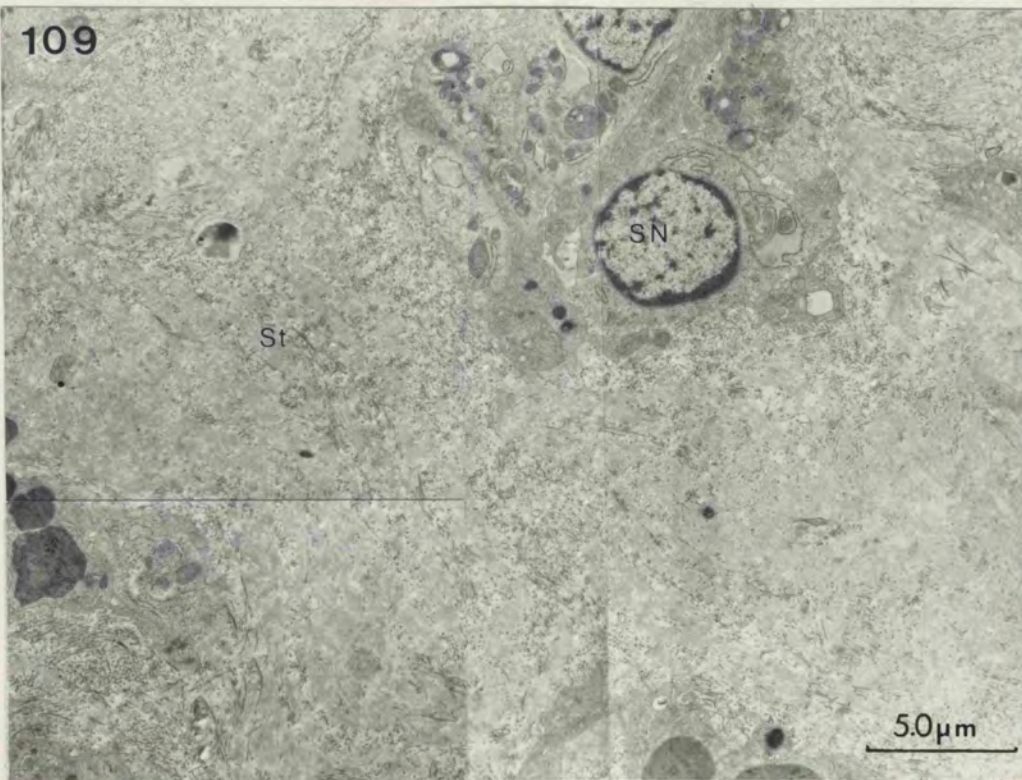
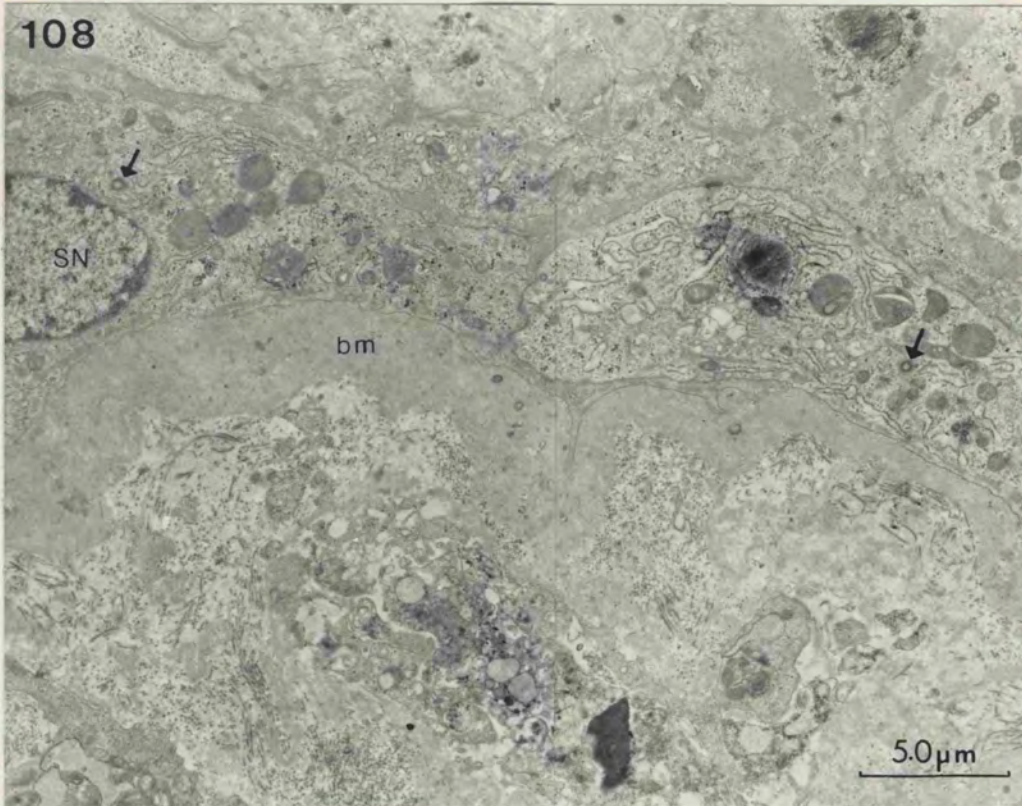


FIG 110 Transmission electron micrograph of cultured human placental cells. All the organelles characteristic of normal placentae are present. Nucleus (N), mitochondria (m), coated vesicle (cv; arrow) microvilli (mv) and fine filaments (arrowhead, f) are found in the cytoplasm. Note that all the organelles lie on the left-hand side of the figure. The cortical layer is clear with numerous fine filaments, possibly forming a syncytioskeletal layer.

FIG 111 Numerous desmosomes can be seen in this transmission electron micrograph (arrows). Interdigitating microvilli can be seen between cells (arrowhead).

FIG 112 Numerous tubular structures can be seen throughout the cell (arrows). Vesicular structures are present (V) and densely-staining droplets can be seen (arrowhead). A nucleolus is present (Nu) within the nucleus (N).

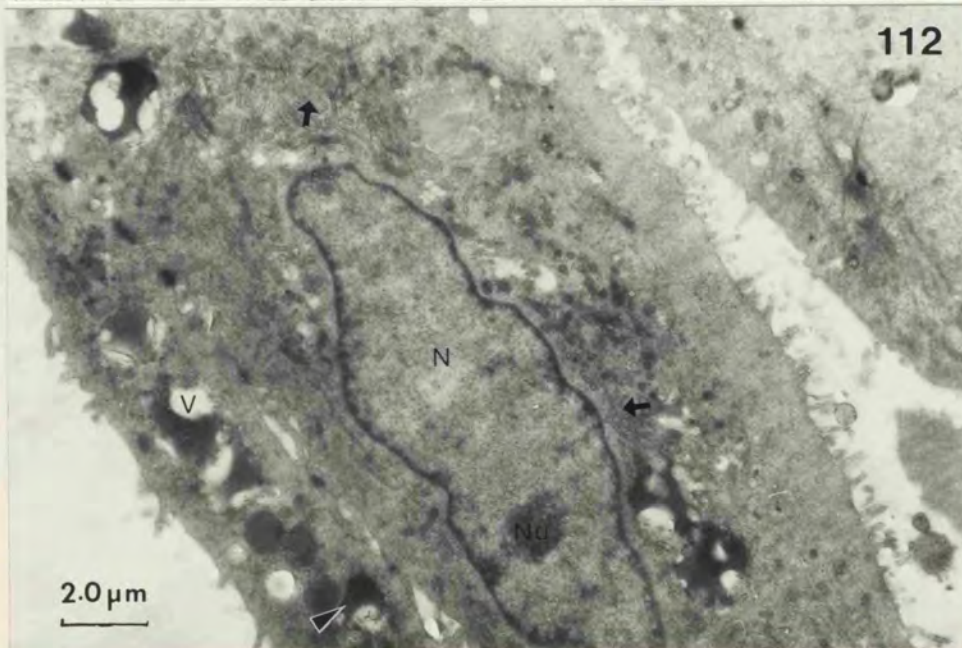
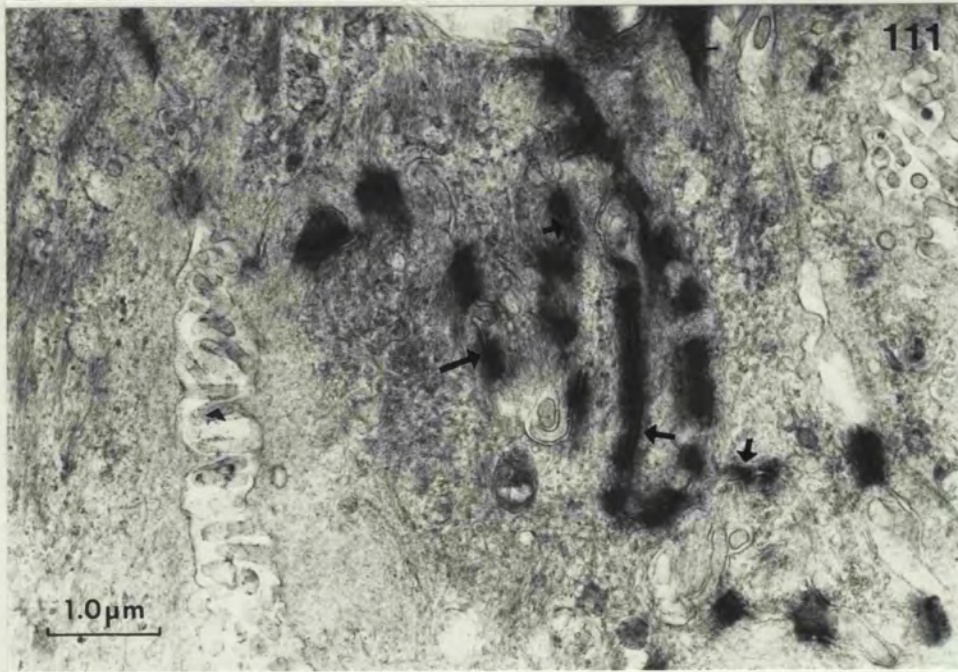
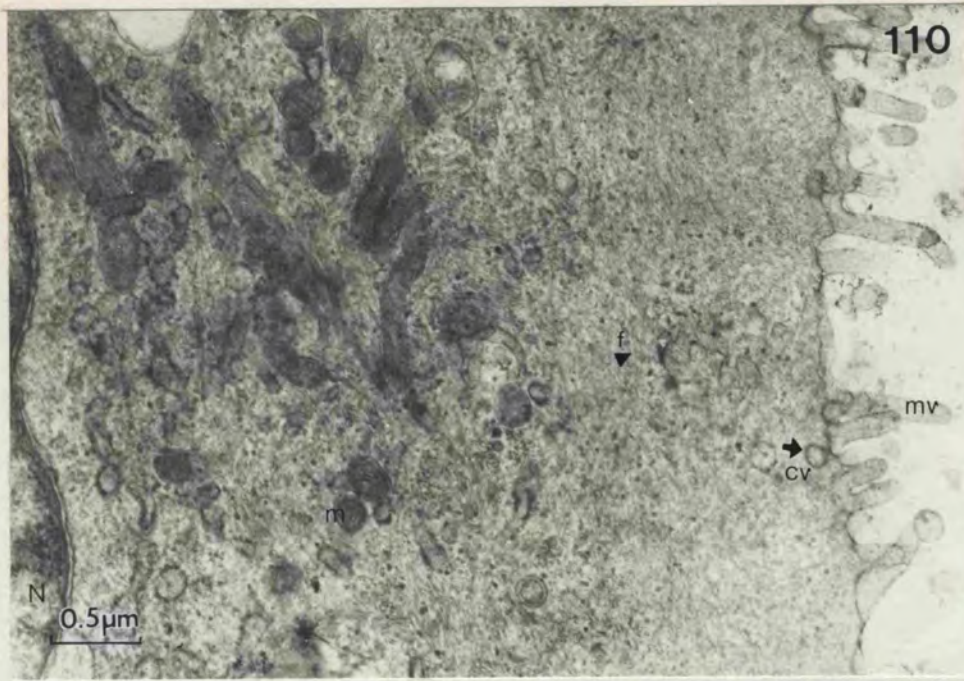


FIG 113 - 116 Transmission electron micrographs showing organelles found in the cytotrophoblast-like cells of the tissue clumps.

FIG 113 Organelles similar to those found in normal placental tissue were present; mitochondria (m), endoplasmic reticulum (er) densely staining droplets (L) vesicular structures (arrowhead) were identified.

FIG 114 Stromal elements were identified in the tissue; fibres similar to collagen fibres were found.

FIG 115 Higher power micrograph of cytotrophoblast-type cell.

FIG 116 Cell found near the edge of the tissue clump, composed mainly of endoplasmic reticulum.

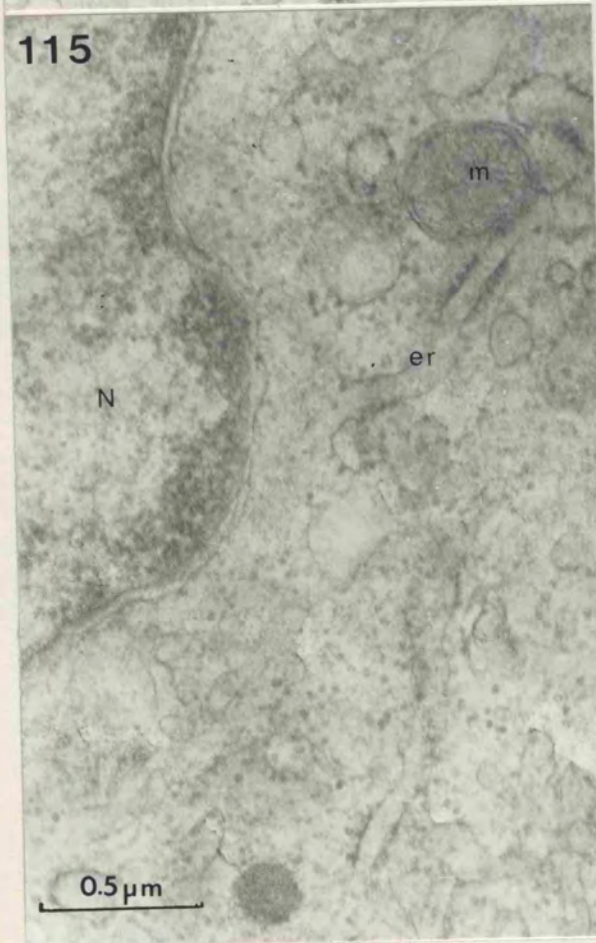
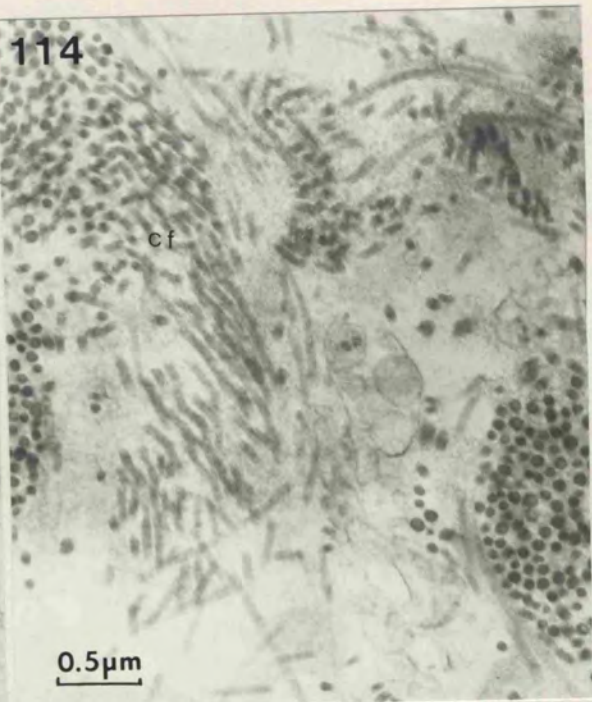
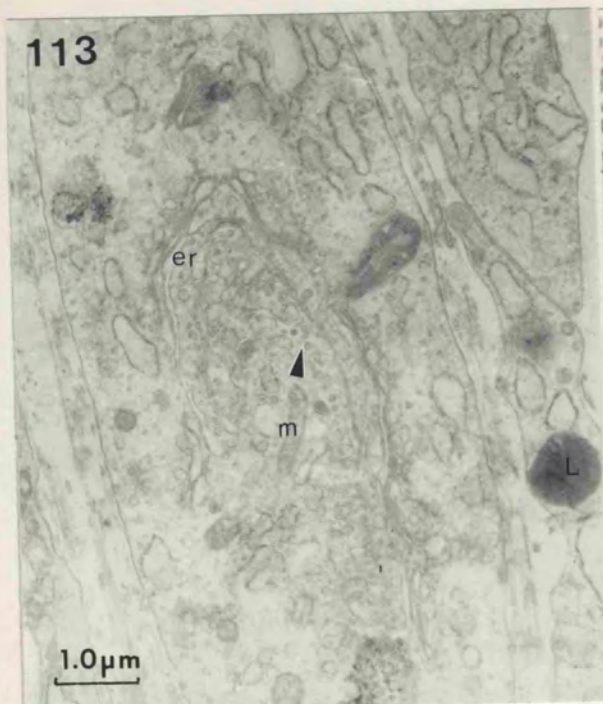


FIG 117 Transmission electron micrograph of villus-like structure found in the cultured placental cells. A large convoluted nucleus (N) is present containing some nucleolar material (Nu). The rest of the tissue is very vacuolar in appearance (V). Some densely-staining lipid-like material is present (L) and mitochondria can be identified (m).

FIG 118 Micrograph showing a different area of the villus-like structure close to the area shown in Fig 117. This tissue is very vacuolated.

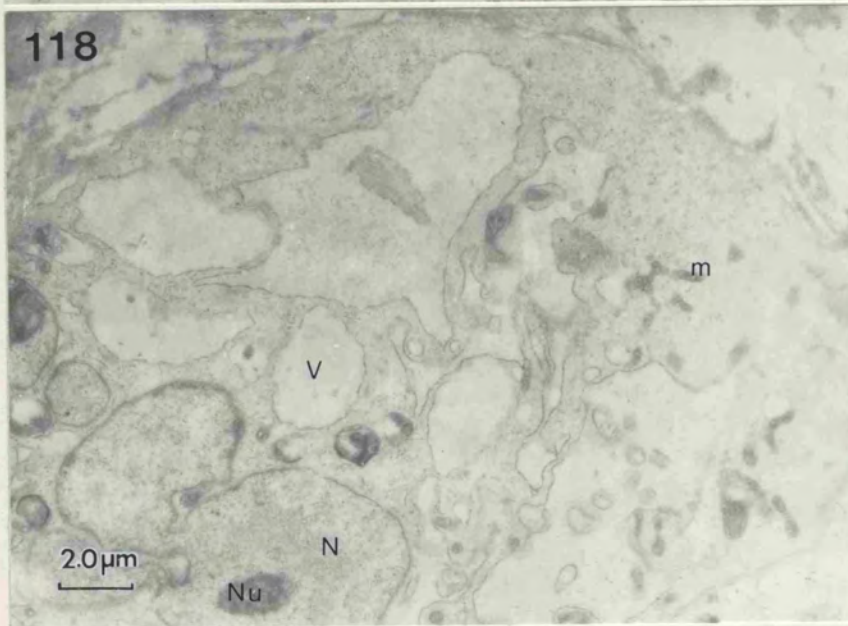
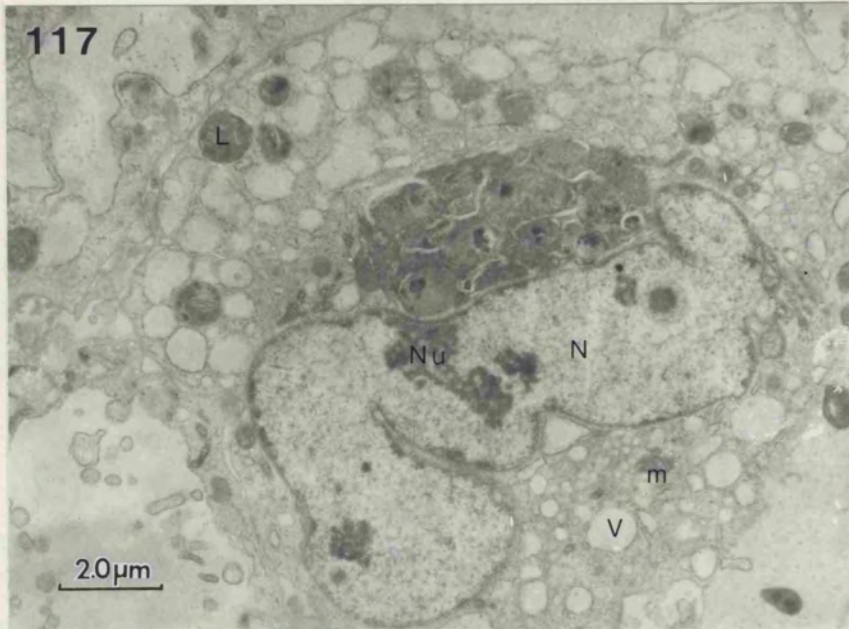


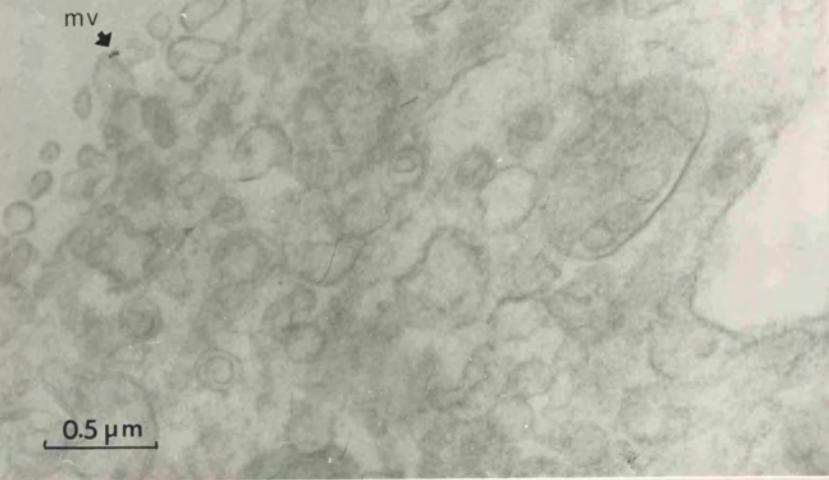
FIG 119 - 121 Transmission electron micrographs of placental tissue culture cells incubated with Au(18)-IgG.

FIG 119 Gold-IgG complexes associated with the surface microvilli (arrow).

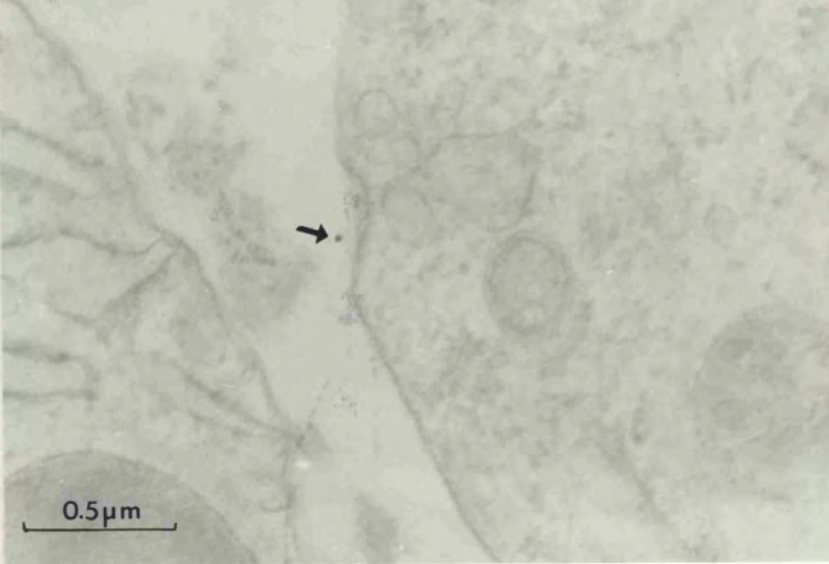
FIG 120 Gold-IgG particle associated with the cell surface close to a coated invagination of the membrane (arrow).

FIG 121 Large vesicular structure in which gold-IgG complex was found.

119



120



121

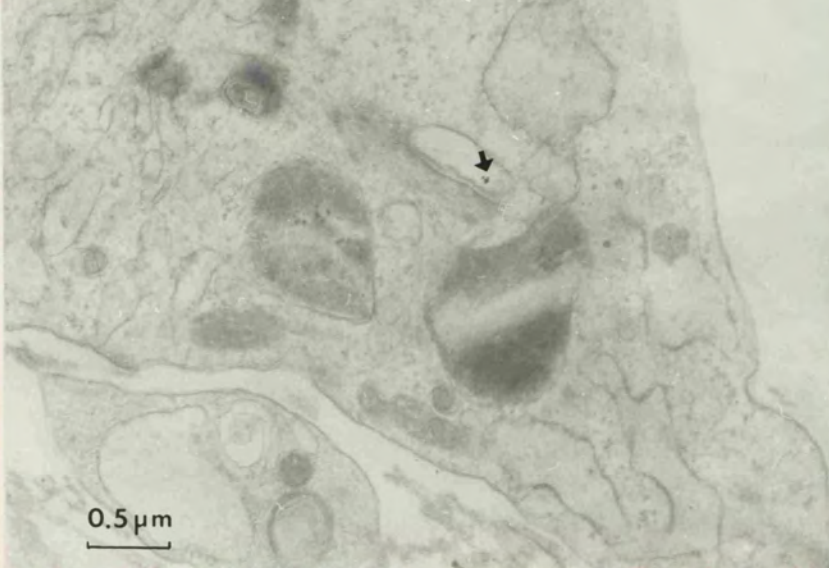


FIG 122 - 129 Nomarski micrographs of BeWo cells.

FIG 122 This BeWo cell appears to have two nuclei (N) and several nucleoli (arrows).

FIG 123 This clump of cells shows that there are several layers present. Compare the edge of the clump (arrow) with the thickness of the centre region (arrowhead).

FIG 124 Filopodial structures can be seen on the edges of the tissue clump (arrow).

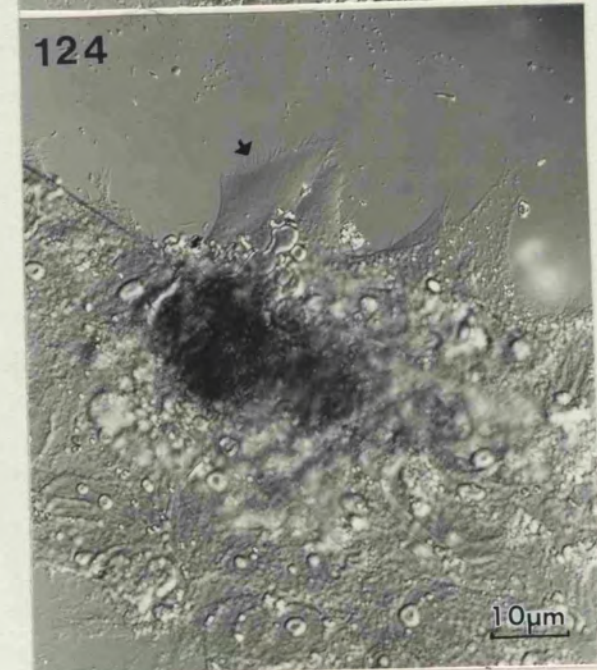
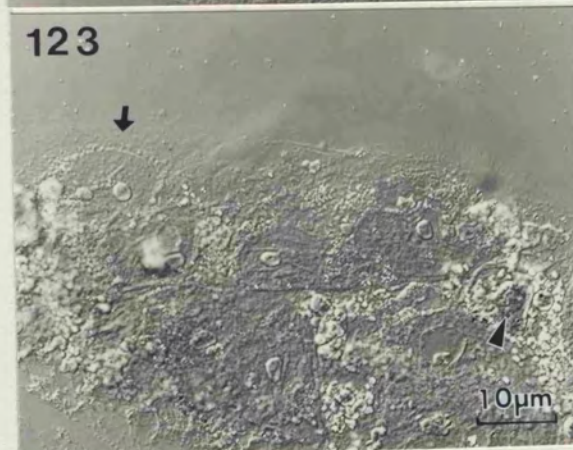
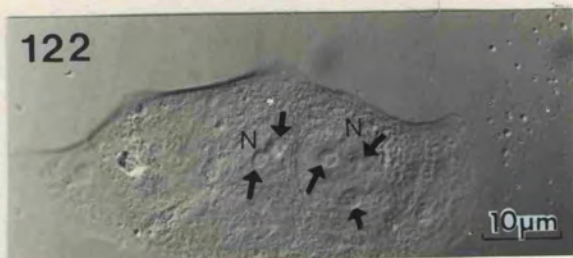
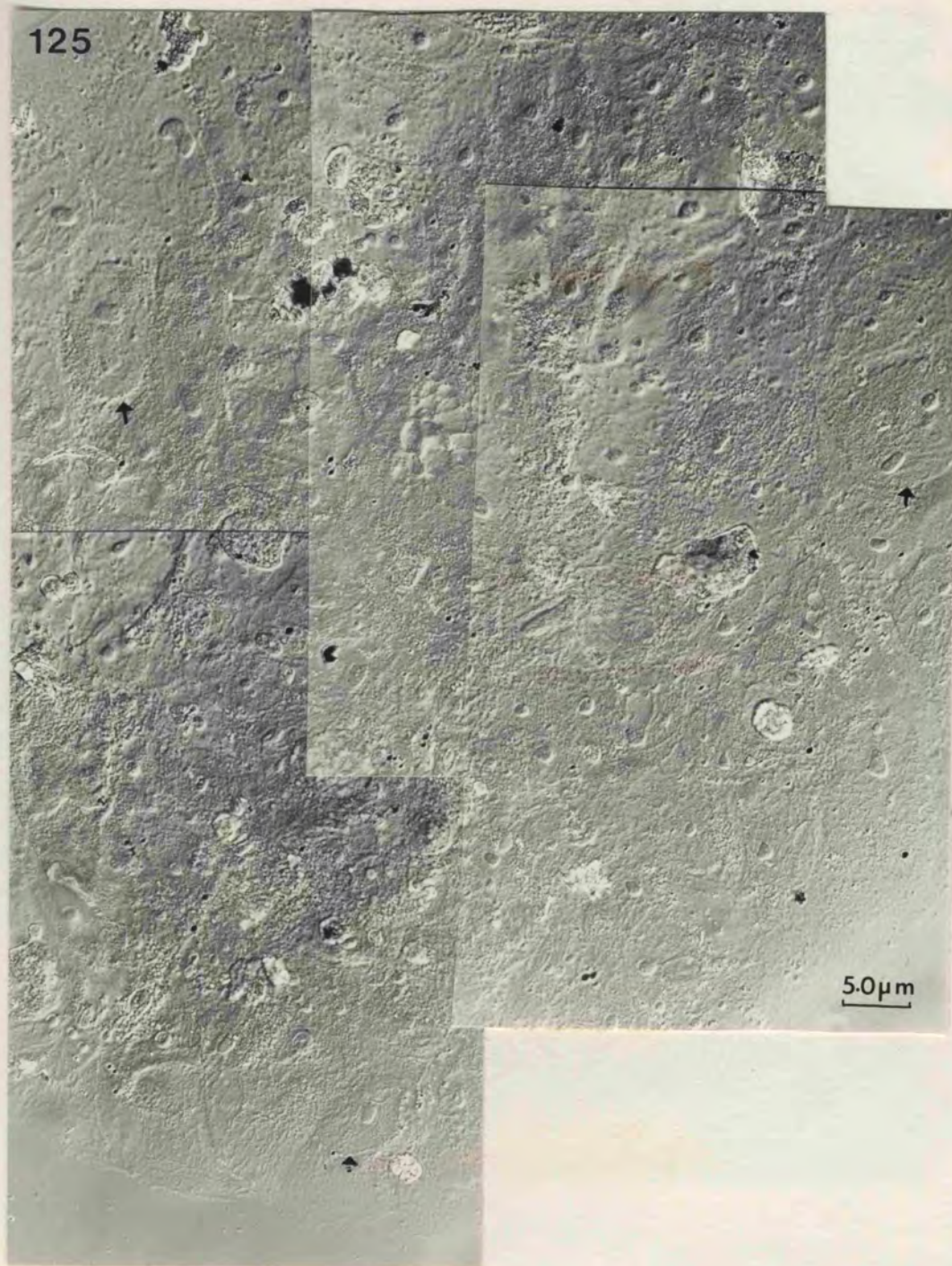


FIG 125 Montage of BeWo cells examined by Nomarski  
Differential Interference Contrast microscopy.  
Some dividing membranes can be seen between  
the cells (arrow).

125



5.0µm

FIG 126 Finger-like outgrowths are visible on the edges of the BeWo cells (arrow).

FIG 127 Higher power light micrograph of the area shown in Fig 126.

FIG 128 Several layers of cells are clearly visible here (arrow ).

FIG 129 (i) & (ii) Upgrowth of a villous-like structure joined to the underlying tissue by a thin filament (arrow).

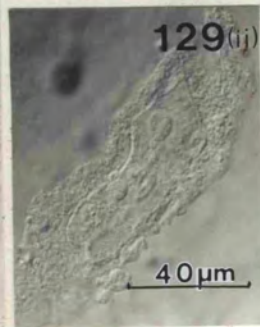
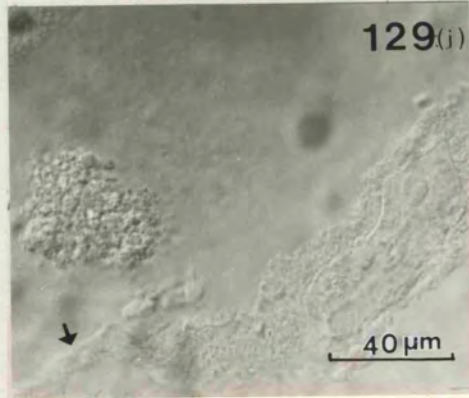
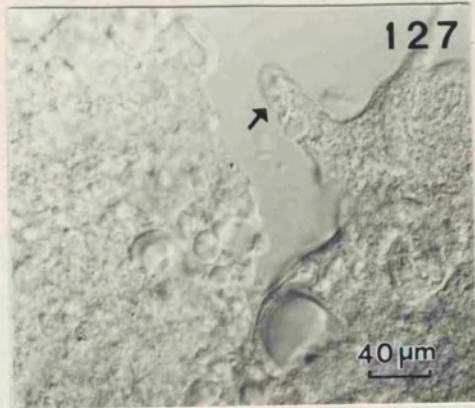


FIG 130 Light micrograph of a 0.5 $\mu$ m section of resin embedded BeWo cells stained with toluidine blue in 1% borax.

The highly convoluted nuclear envelopes are visible (arrow). Some nuclei have more than one nucleoli (arrowhead). Densely staining bodies can be seen (open arrow).

FIG 131 Transmission electron micrograph of BeWo. An upper darker layer (a) and a lower lighter layer (b) is present. This could be two adjacent cells, one over-lying the other.

FIG 132 Transmission electron micrograph of first trimester placenta showing the similarity between this tissue and the BeWo cells.

FIG 133 Transmission electron micrograph showing a pale electron-lucent cell (a) with part of a darker adjacent cell over lying it (b).

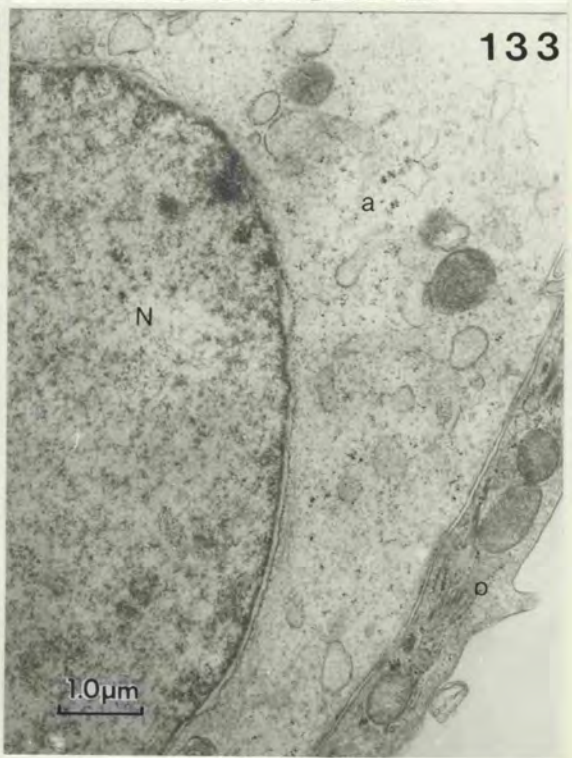
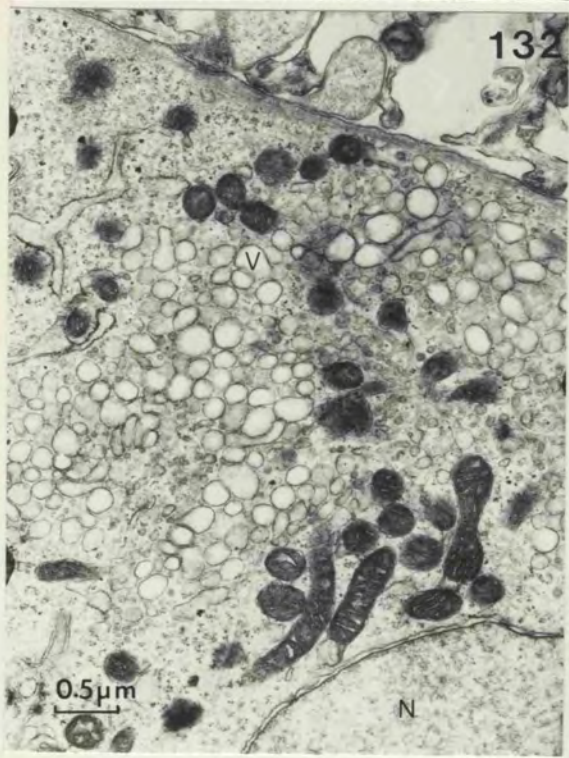
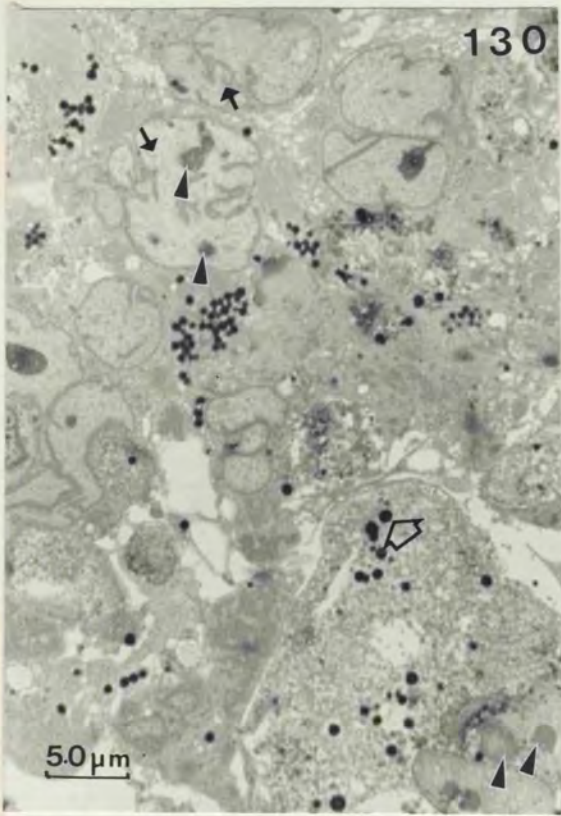


FIG 134 Diagram to show the variation in nuclear shape  
found in the BeWo cells.  
(The tracings were taken from transmission  
electron micrographs of BeWo cells).

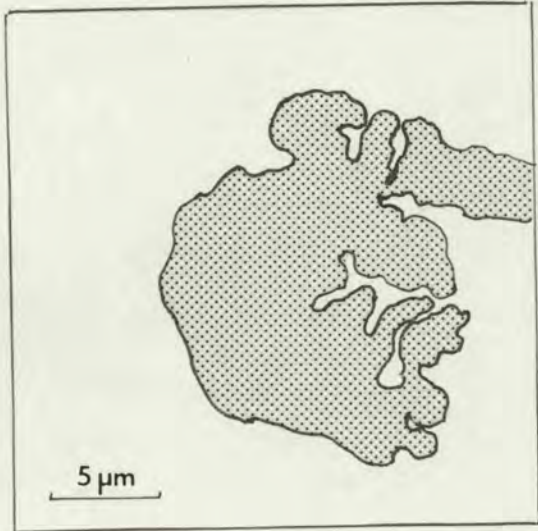
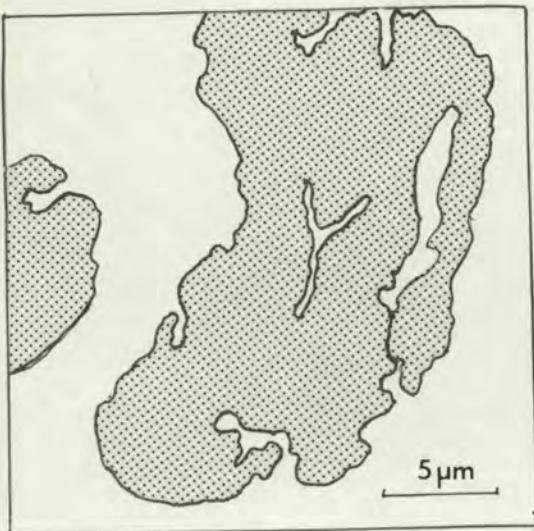
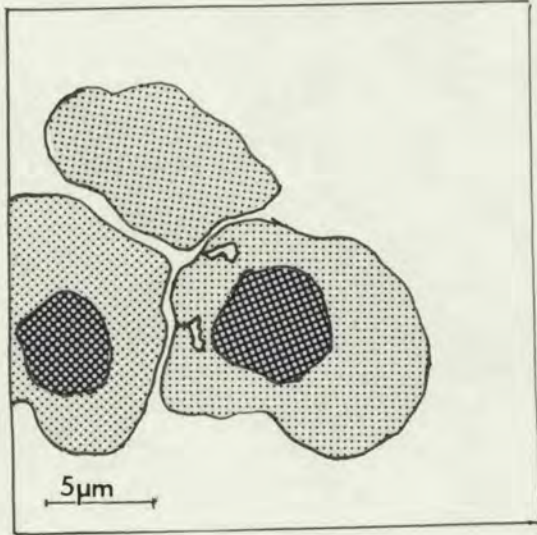
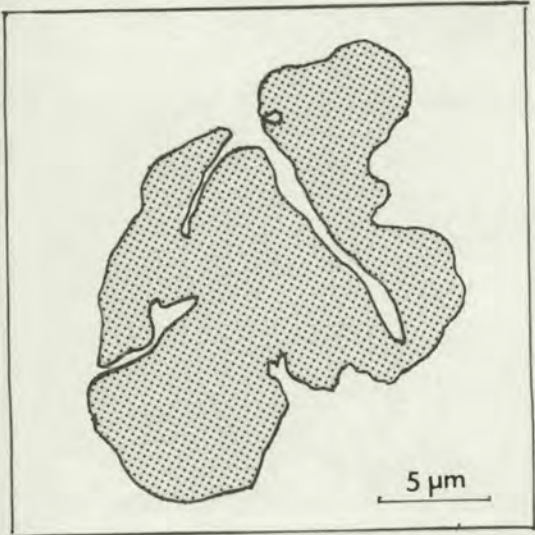
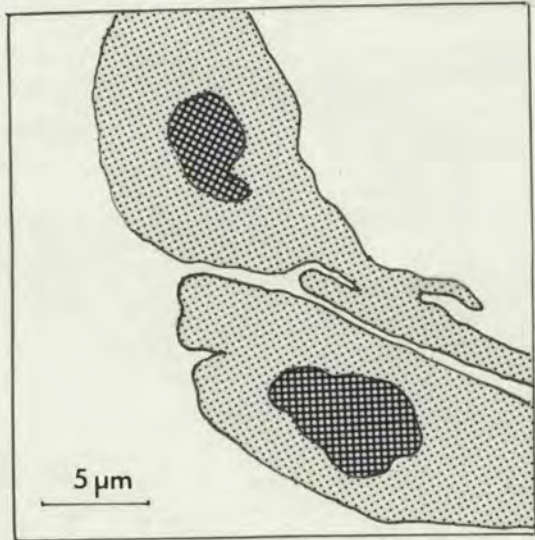
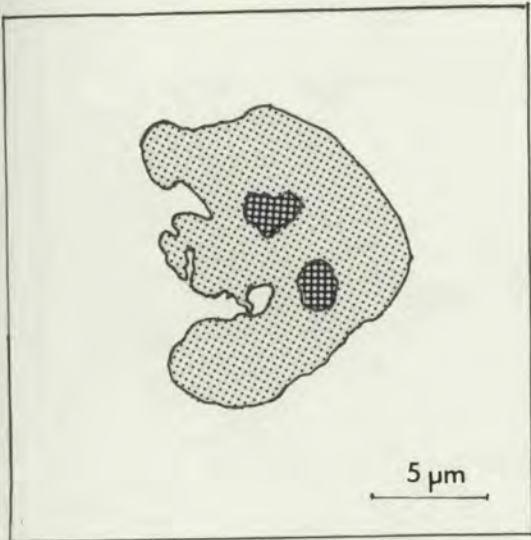


Fig 134

FIG 135 - 138      Transmission electron micrographs of  
BeWo cells.

FIG 135            Highly convoluted nucleus (N)  
containing two nucleoli (Nu)

FIG 136            Nucleolus located close to the nuclear  
envelope (Nu). Note the invaginations  
of the nuclear envelope (arrowhead).

FIG 137            Tangential section through nuclear pores.  
A central dense granule can be seen in  
some profiles (arrow).

FIG 138            Longitudinal section through a nuclear  
pore (arrow)

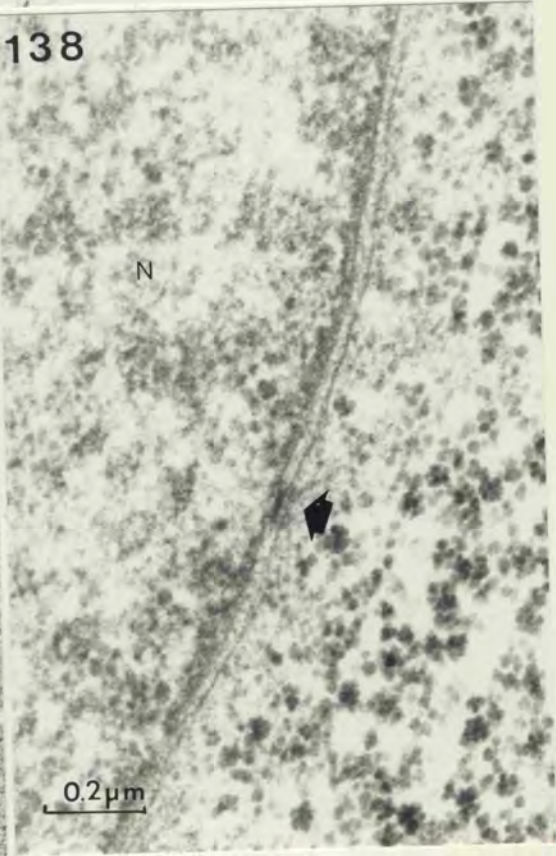
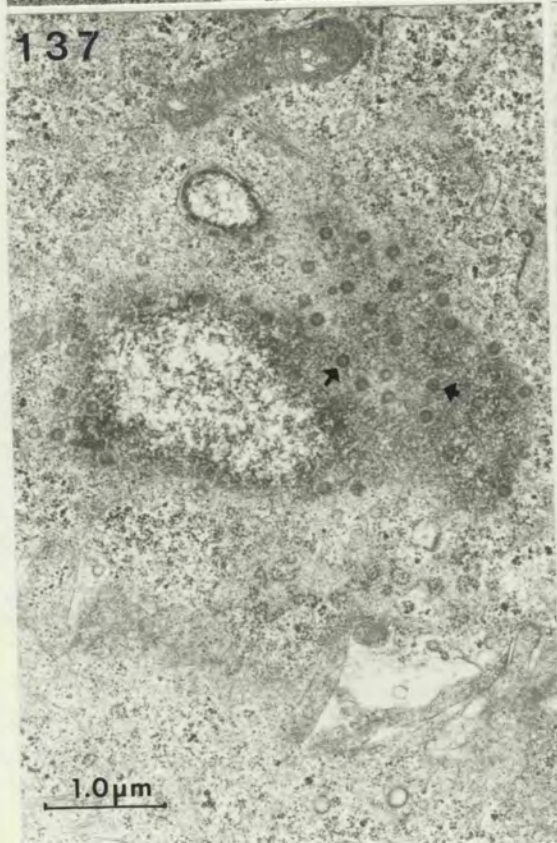
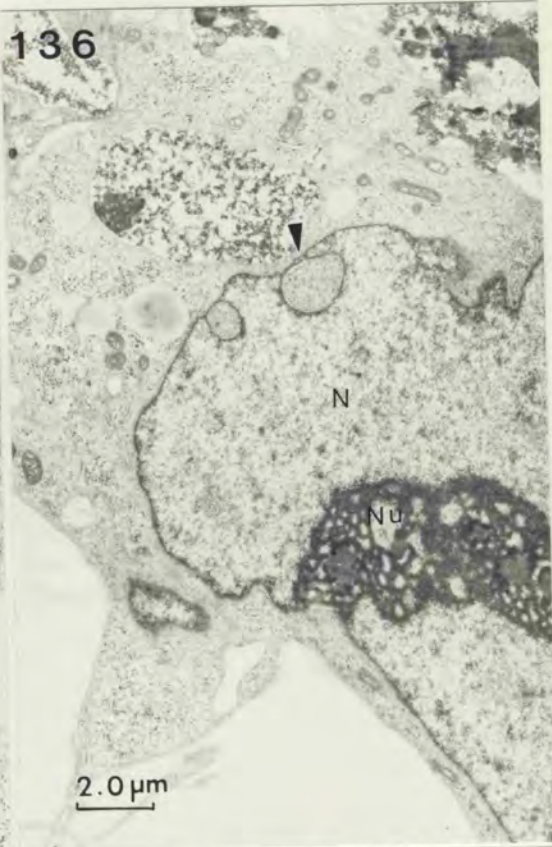
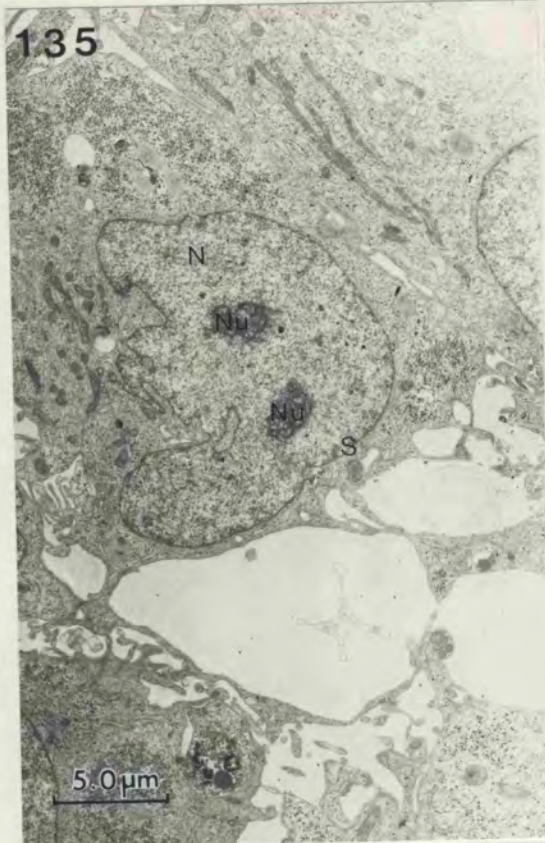


FIG 139 - 141 Transmission electron micrographs of BeWo cells.

FIG 139 Condensed chromatin close to the nuclear envelope of the BeWo cell (arrow)

FIG 140 Filopodial structures on the surface of the BeWo cells. A coated vesicle is present near the base of a filopodial structure (arrowhead).

FIG 141 Microvilli on the surface of the BeWo cells. Fine filaments can be seen within the microvilli (arrow).

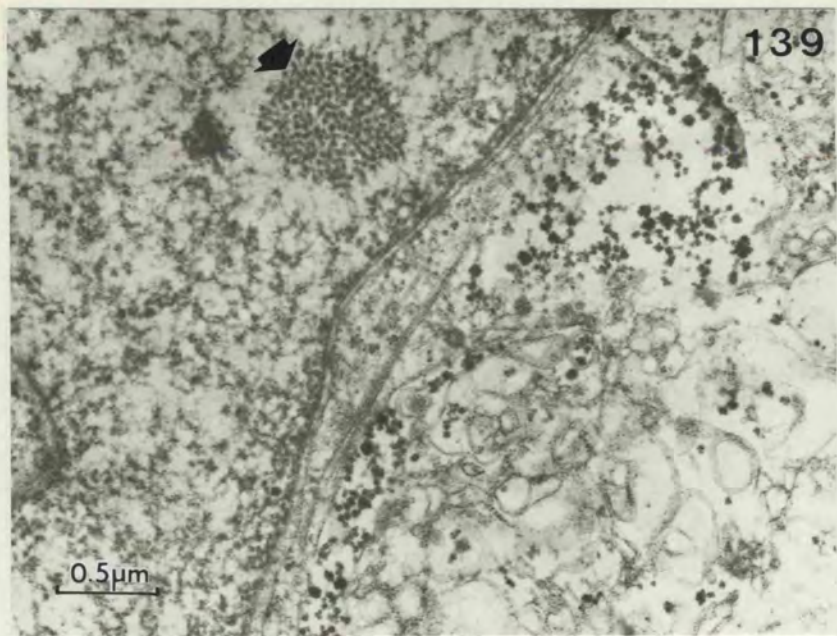


FIG 142-144 Transmission electron micrographs of BeWo cells.

FIG 142 Microvilli are present apparently in the centre of a group of cells (arrow). A large quantity of glycogen is also present (g).

FIG 143 Microtubules were identified within the BeWo cells (arrow). Fine filaments were also present (f).

FIG 144 Centrioles (Ct) were also noted in the BeWo cells. Note the presence of a large number of microtubules near the centrioles (arrow).

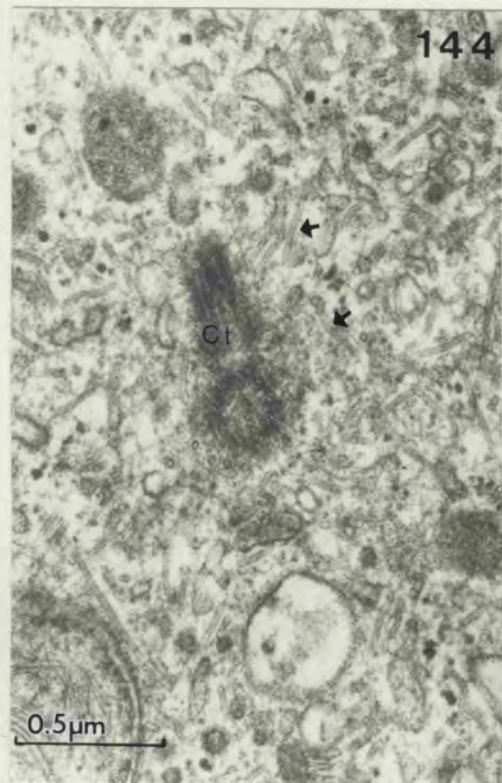
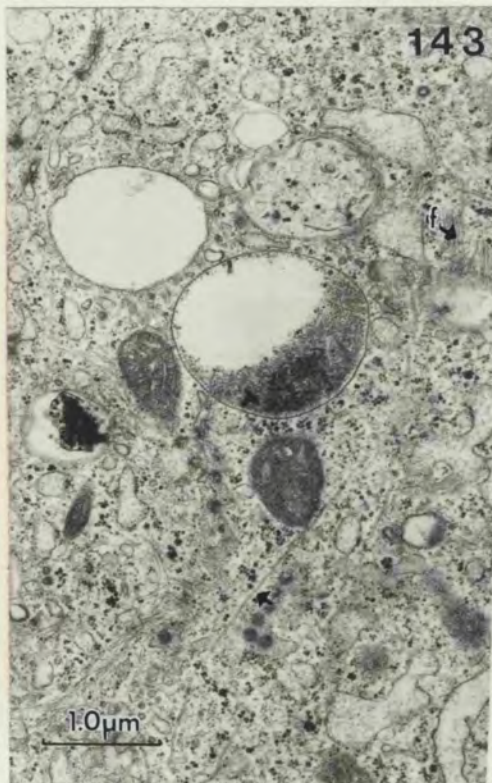
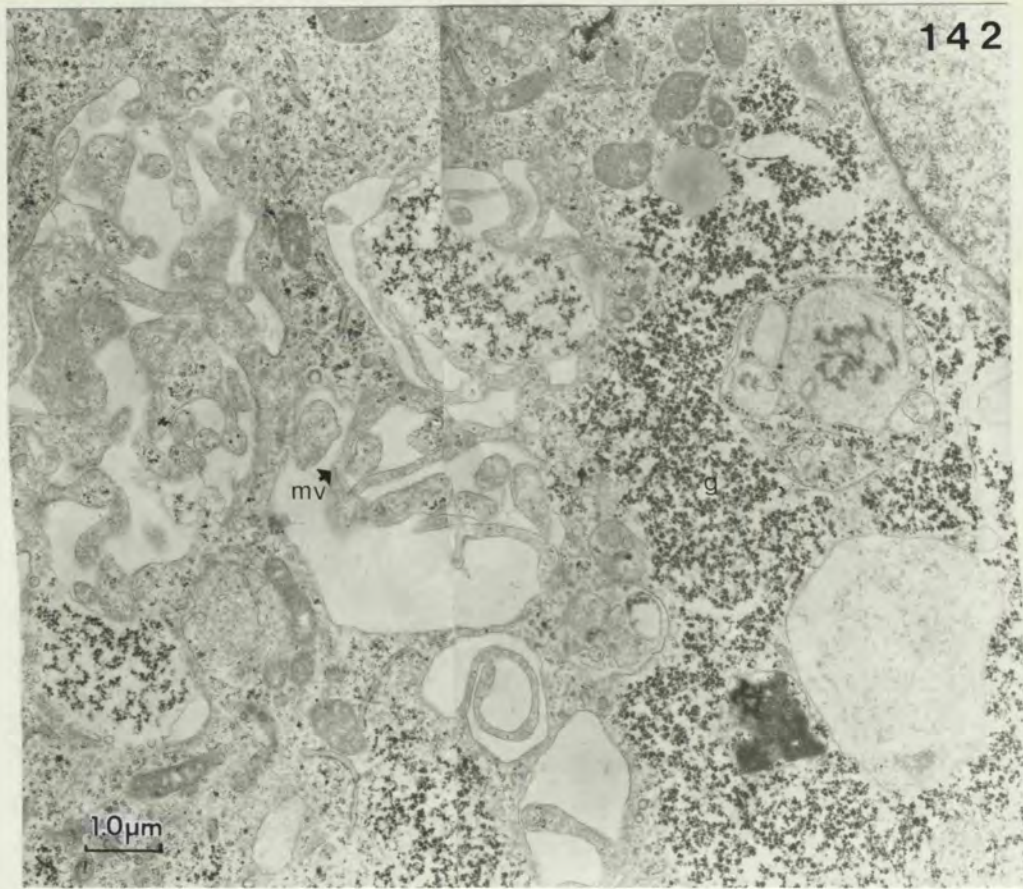


FIG 145 Transmission electron micrograph montage showing features of a BeWo cell.

N = nucleus  
L = Lipid  
Ne = Nuclear envelope  
G = Golgi  
m = mitochondria  
er = endoplasmic reticulum  
mv = microvilli  
mf = microfilaments  
g = glycogen  
V = vacuolar structures  
vs = vesicular structures  
cv = coated vesicle

145

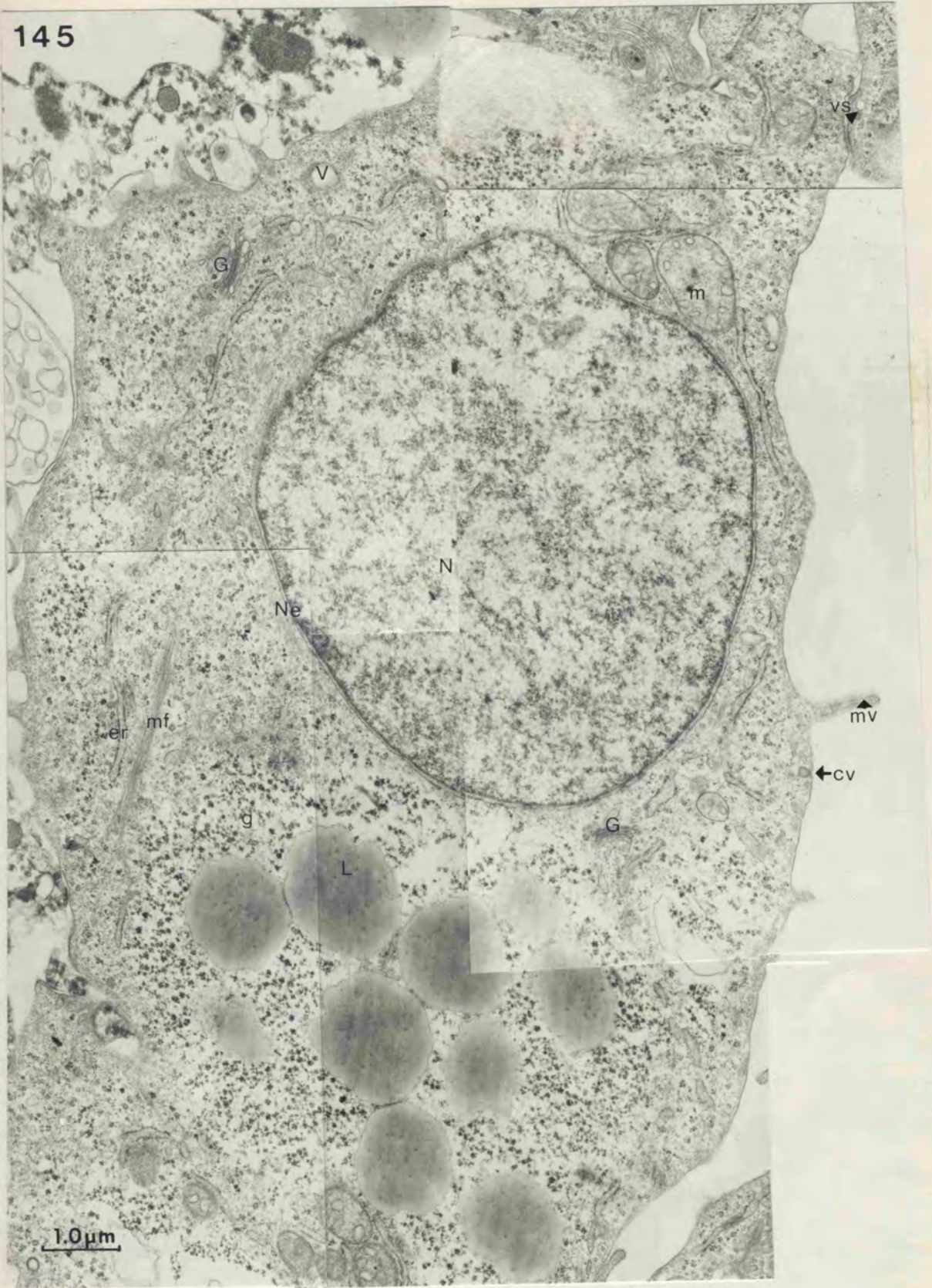


FIG 146 - 151 Transmission electron micrographs of BeWo cells.

FIG 146 Perinuclear cytoplasmic filaments were present in the BeWo cells (arrow).

FIG 147 Cytokeratin filaments (arrow)

FIG 148 & 149 Centriole (Ct) and pericentriolar material (arrow).

FIG 150 Centriole (Ct).

FIG 151 Numerous Golgi (G) were found near the nuclear envelope.

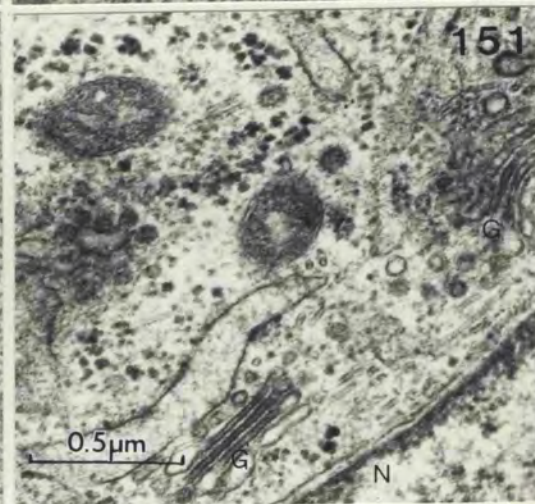
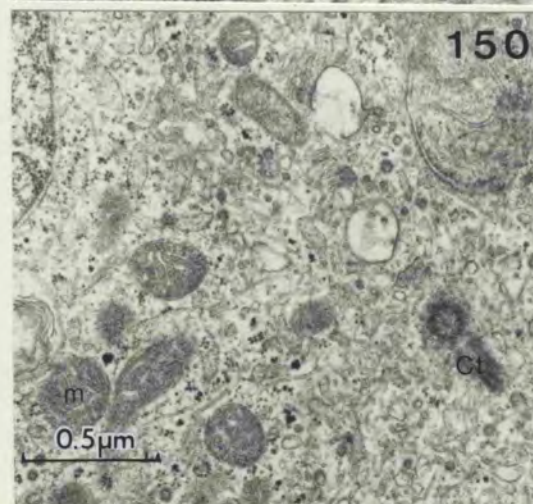
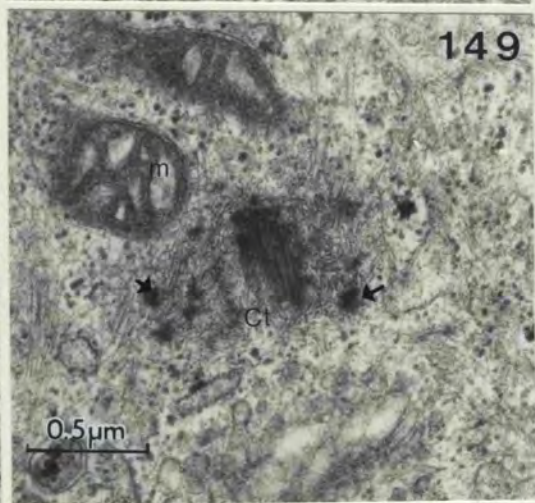
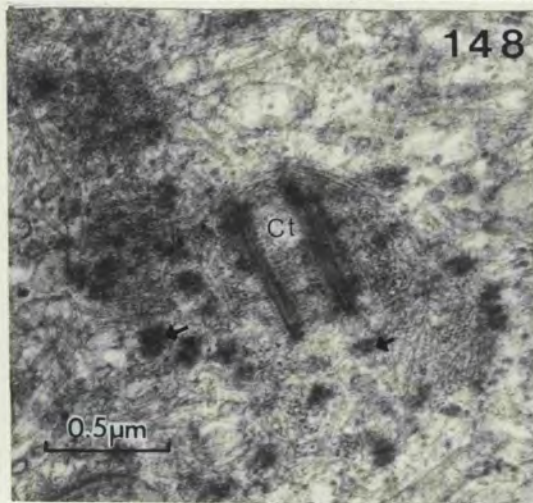
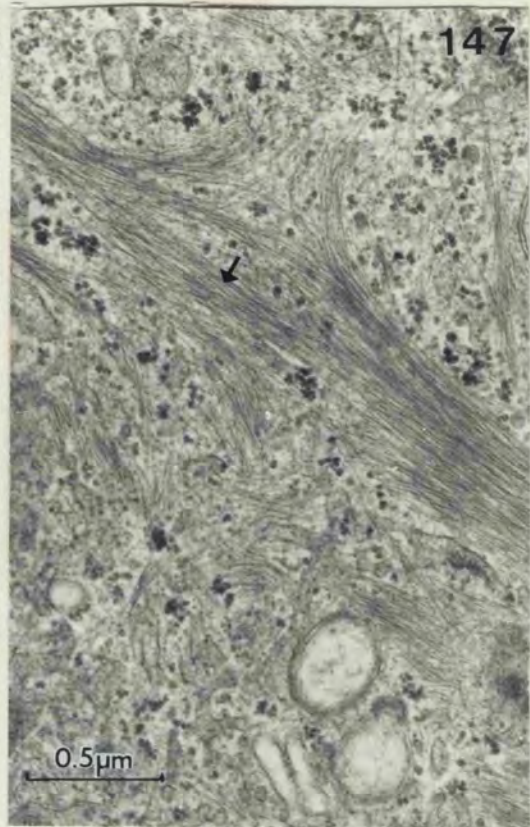
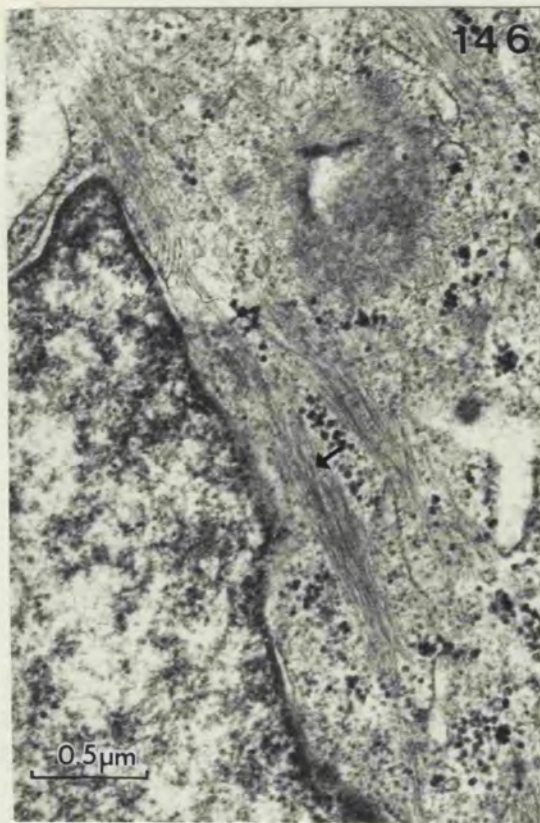


FIG 152 - 155 Transmission electron micrographs of  
BeWo cells.

FIG 152 Groups of mitochondria were often found  
clumped together in the cytoplasm.

FIG 153 & 154 Desmosomes (D) were sometimes found in  
the BeWo cells.

FIG 155 Densely staining droplets were found in  
the cytoplasm. They were not membrane  
bounded and were probably lipid (L).

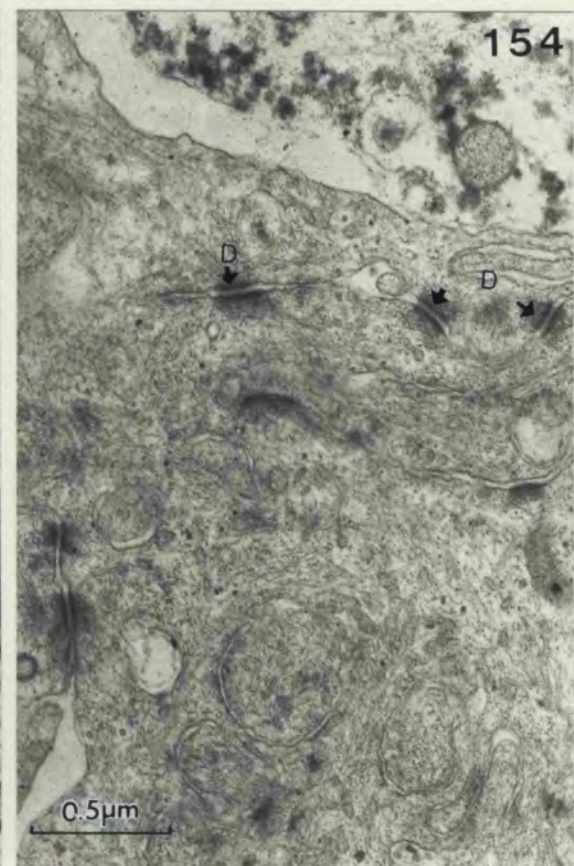
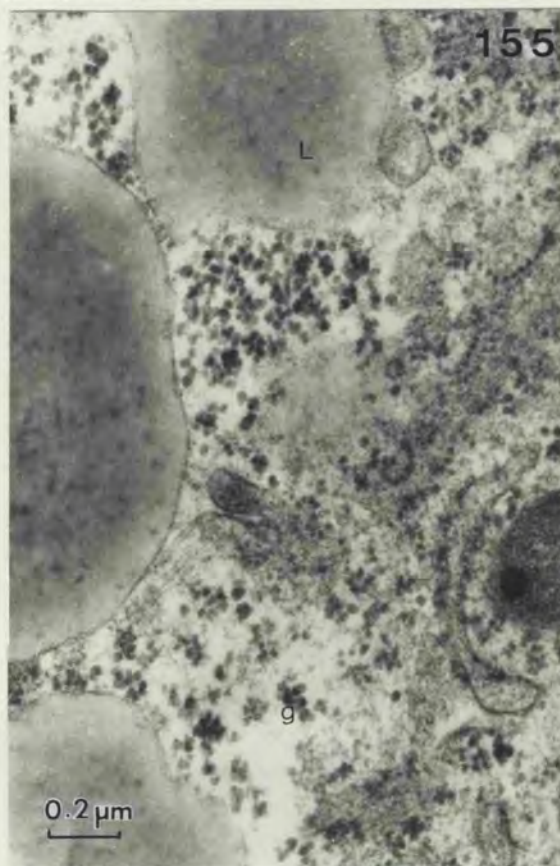
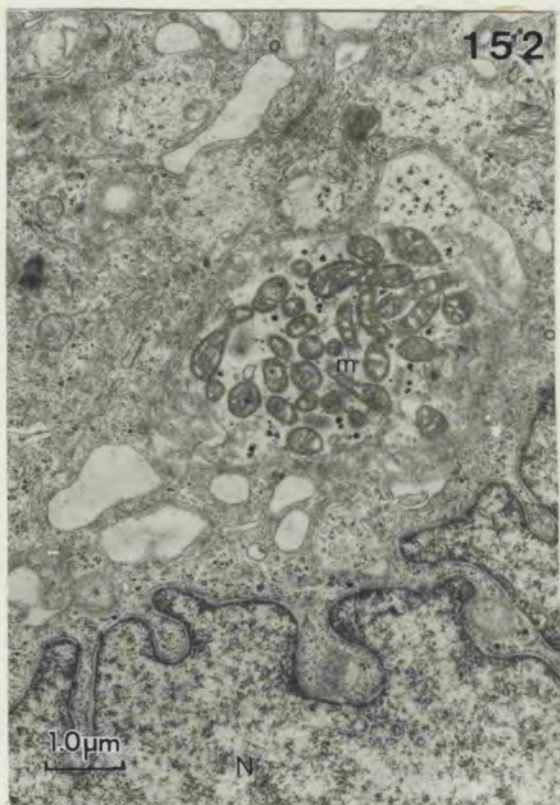
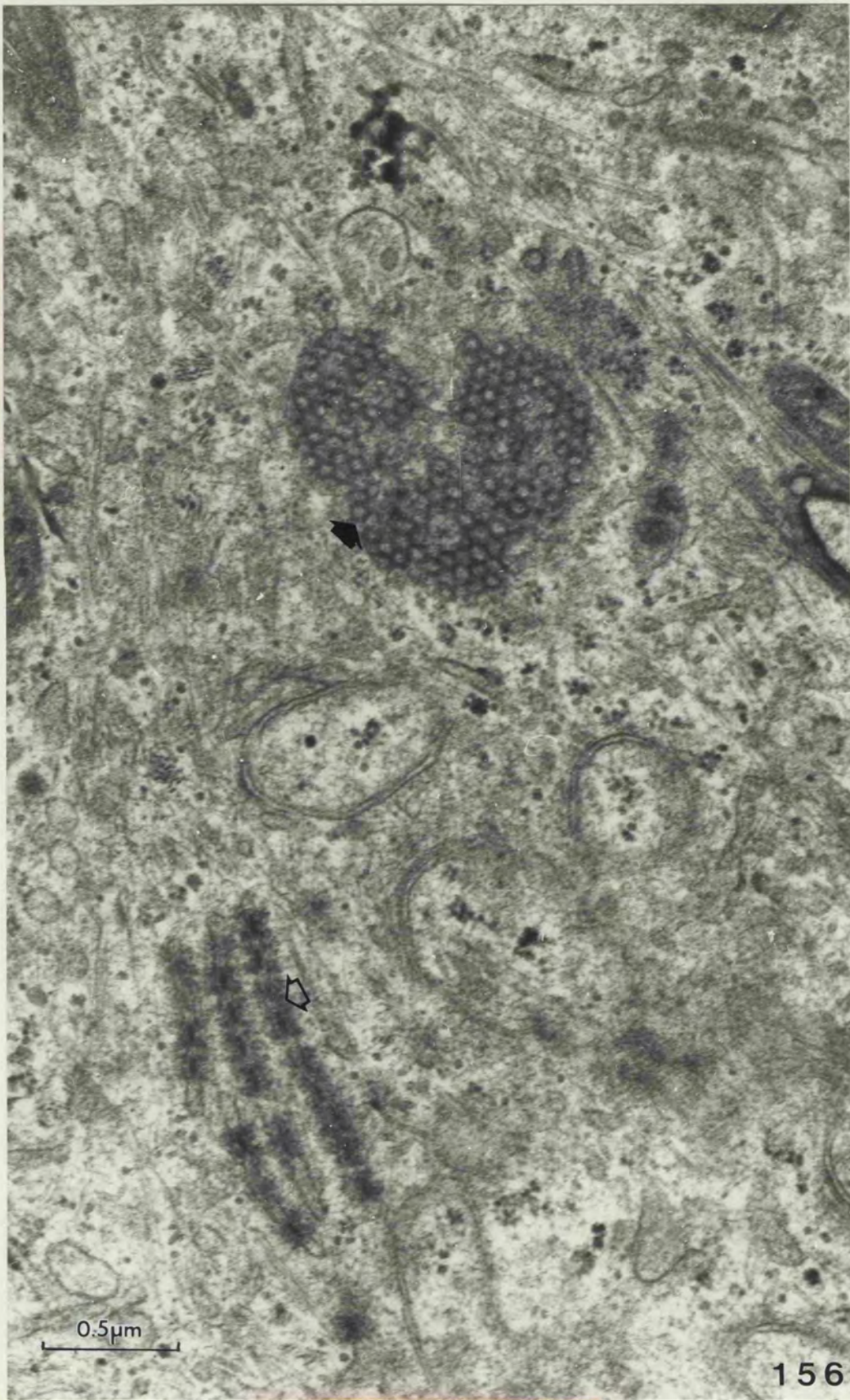
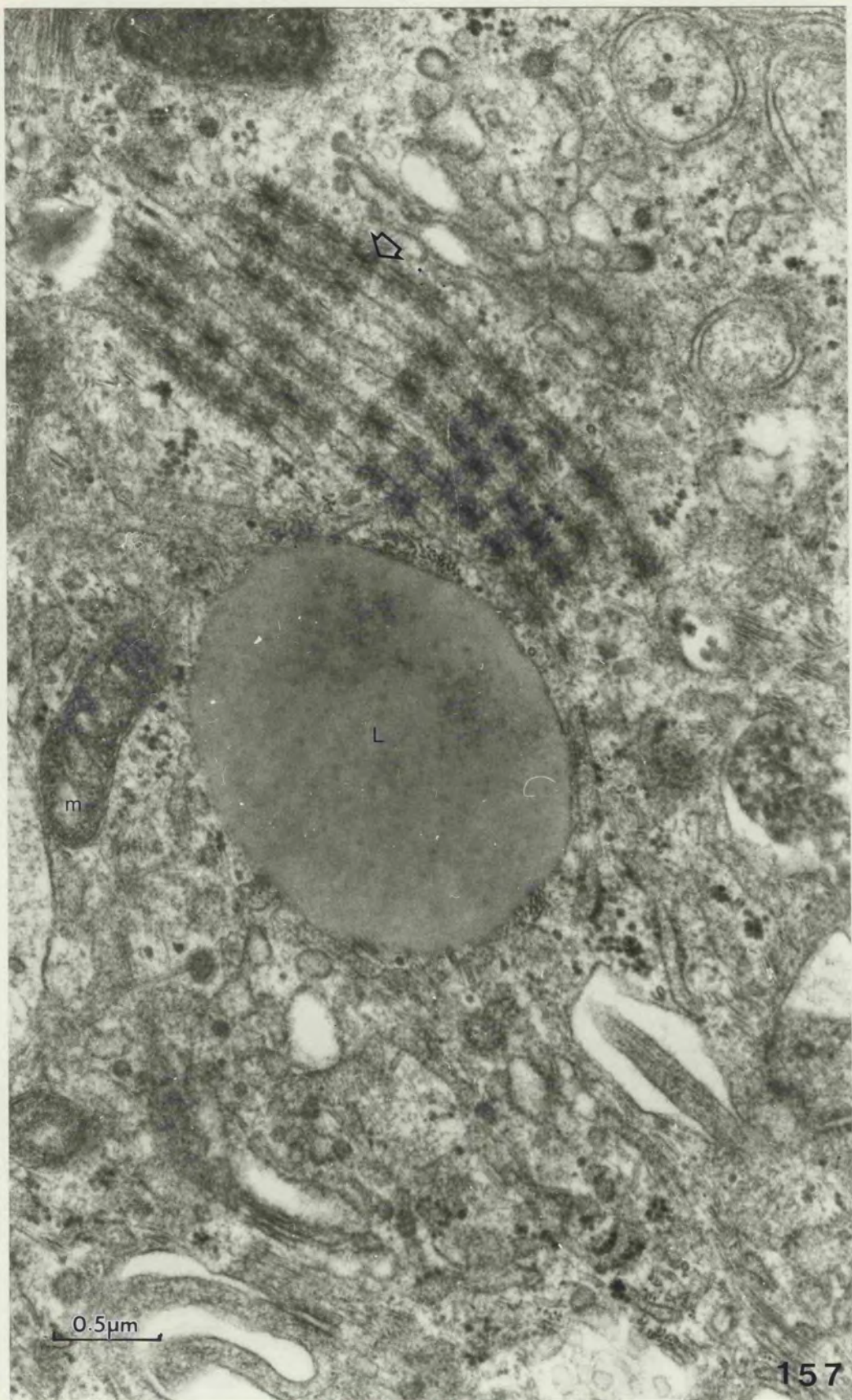
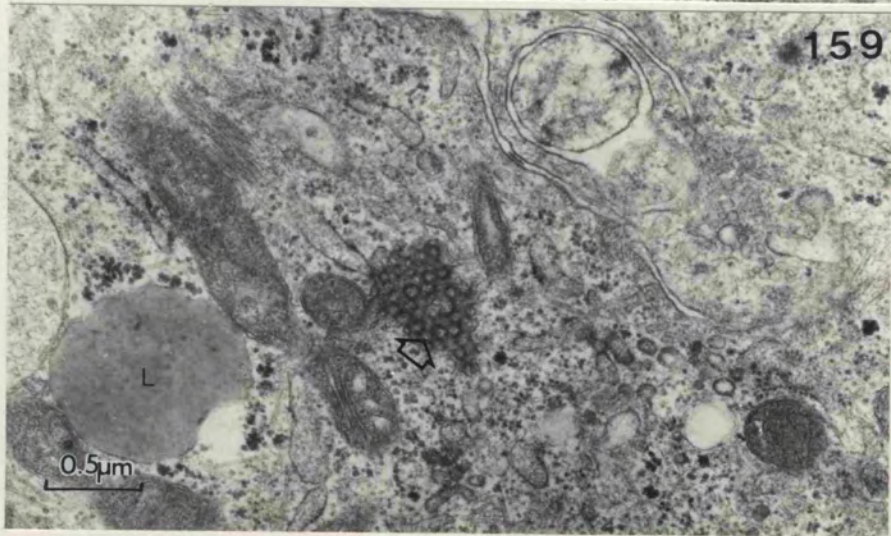
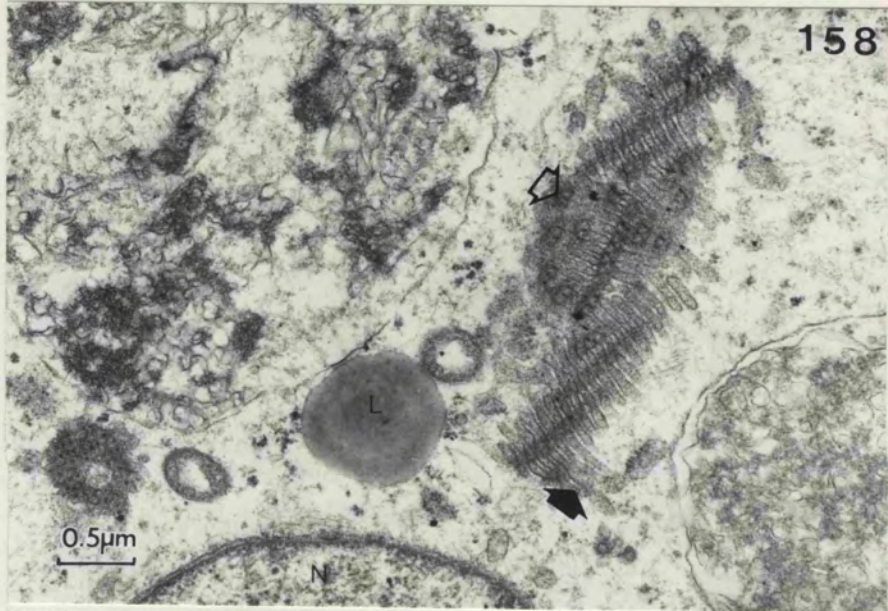


FIG 156 - 159 Annulate lamellae were present in the cytoplasm of the BeWo cells (open arrow). Some profiles showed lamellae cut in transverse section (arrow).







FIGS 160 - 163 Transmission electron micrographs of  
BeWo cells.

FIG 160 Myelin figures were found in the cytoplasm  
(arrow). Note grouping of mitochondria.

FIG 161 Cytoplasmic bodies of variable density (CB).

FIG 162 Endoplasmic reticulum (er).

FIG 163 Multivesicular body (mvb) close to the  
nucleus (N).

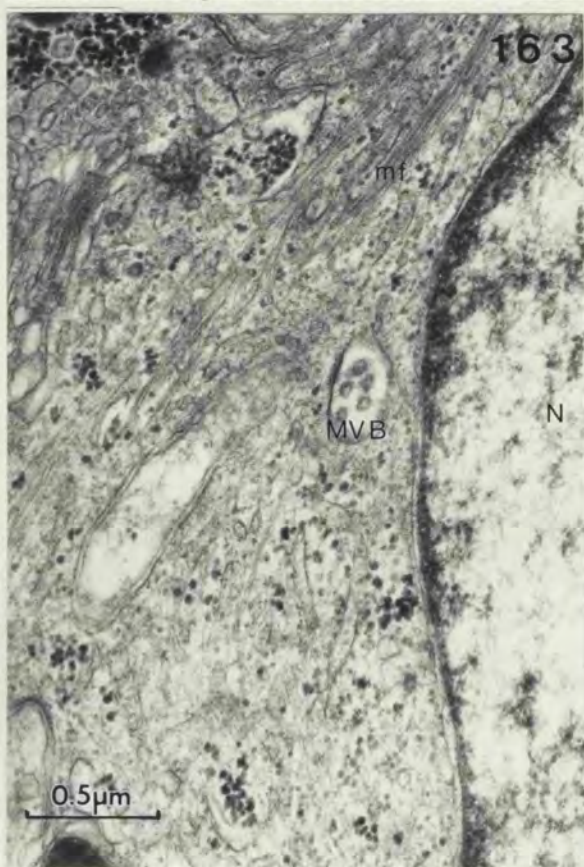
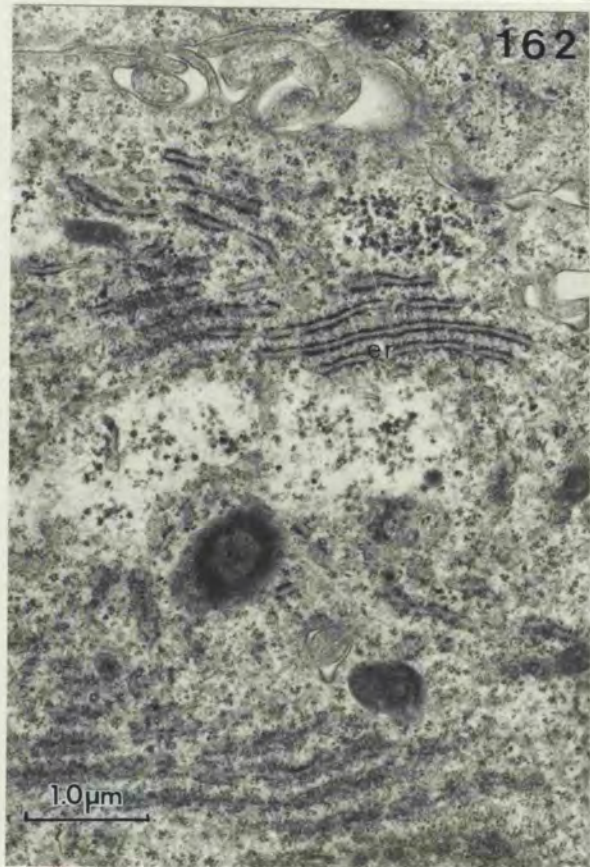
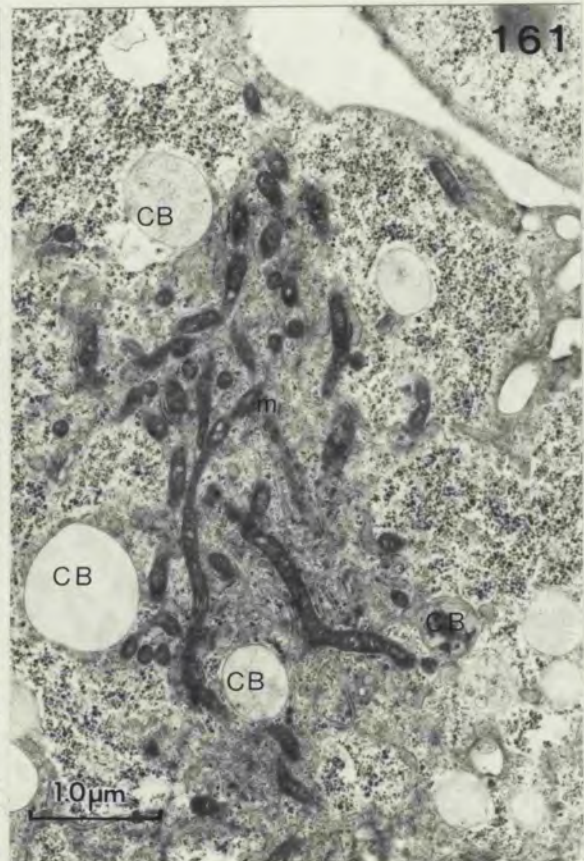
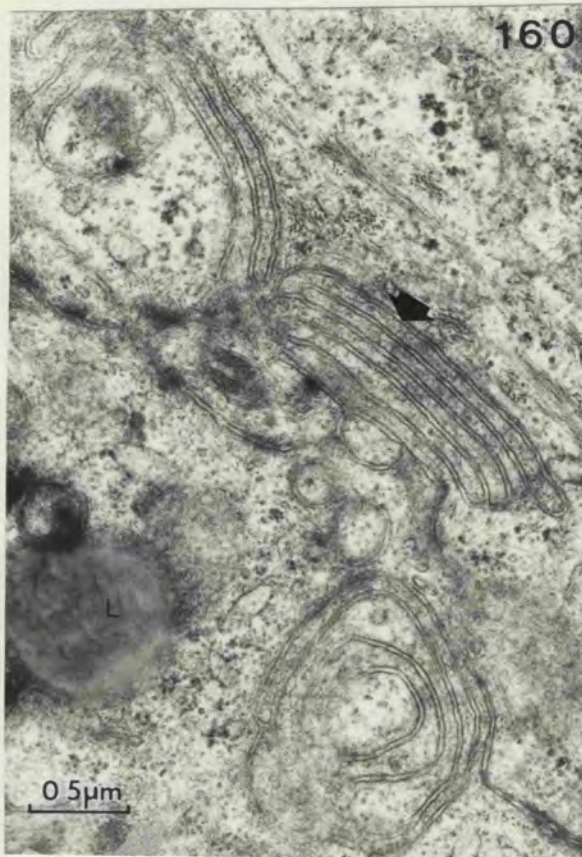


FIG 164 - 172 Transmission electron micrographs of BeWo cells showing the location of coated pits and vesicles.

FIG 164 Coated pit located between adjacent cells (arrow).

FIG 165 Coated pits and vesicles located between adjacent cells (arrows).

FIG 166 Coated pit (arrow) adjacent to a desmosome (D).

FIG 167-170 Coated pit profiles joining larger smooth vesicular structures. Note coated vesicle close to a smooth vesicle in Fig 170 (arrowhead).

FIG 171 Coated vesicle (arrow) surrounded by actin filaments (f).

FIG 172 Coated vesicle (arrow) joined to the surface by a tube-like structure (arrowhead).

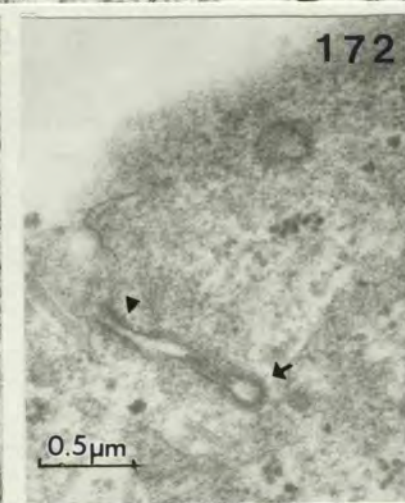
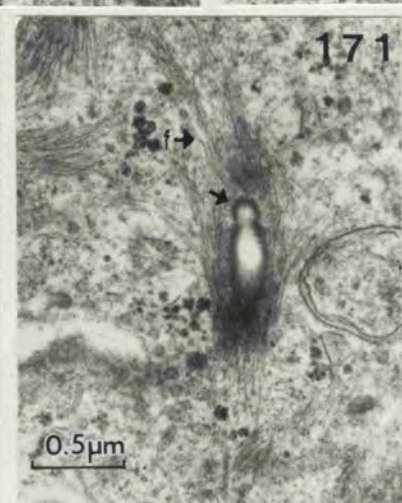
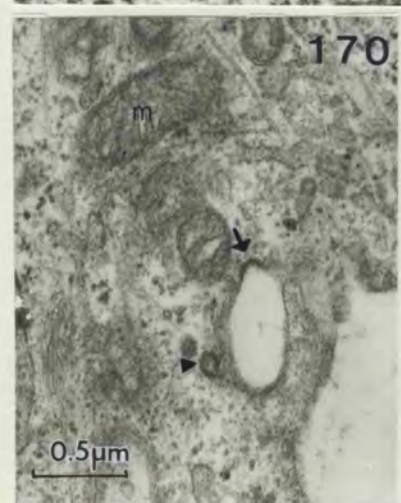
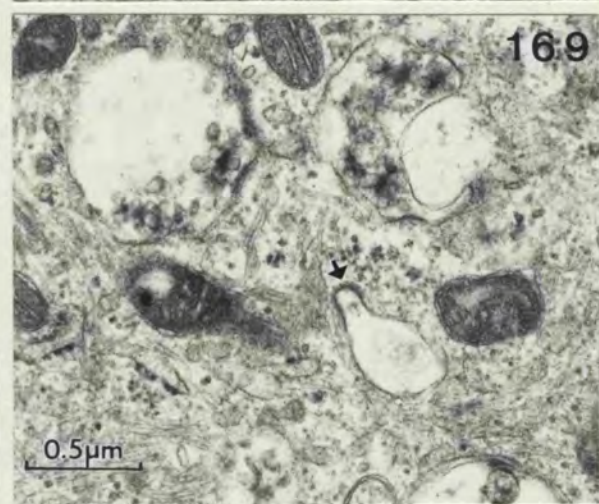
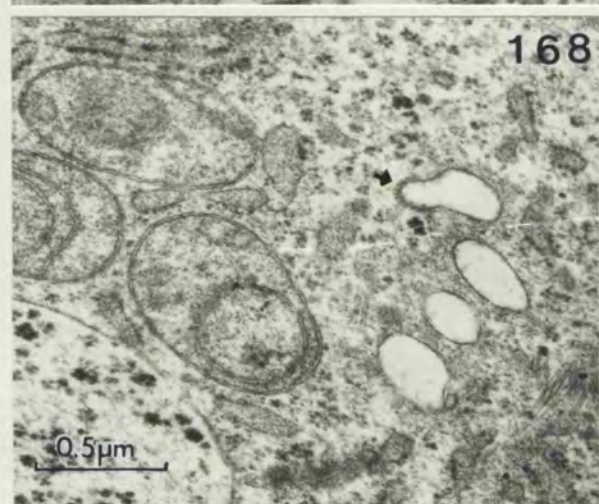
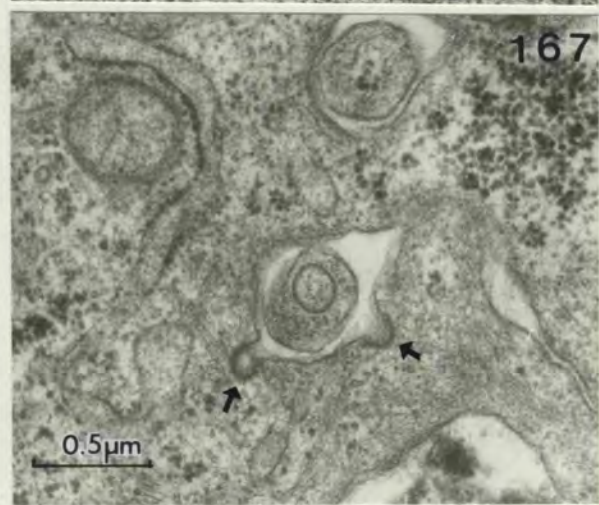
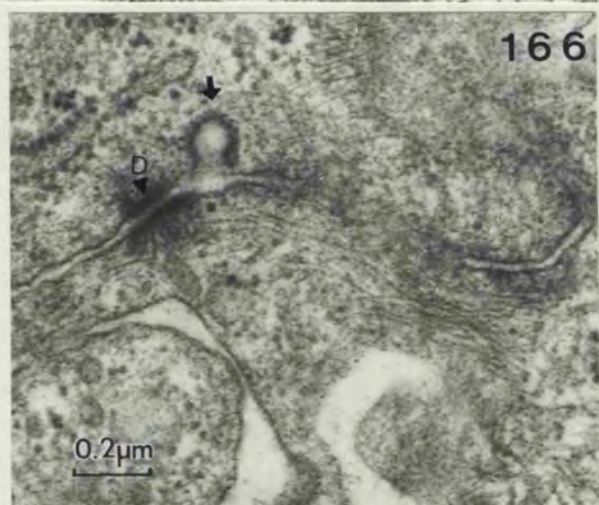
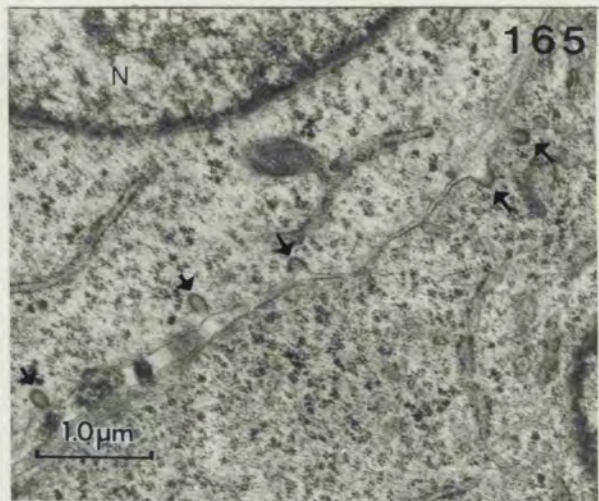
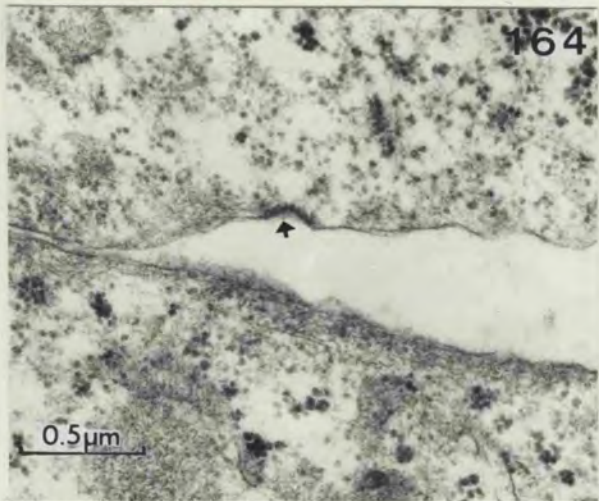


FIG 173 - 175 Transmission electron micrographs of  
tubular structures in the cytoplasm of  
the BeWo cells joined to coated vesicles.

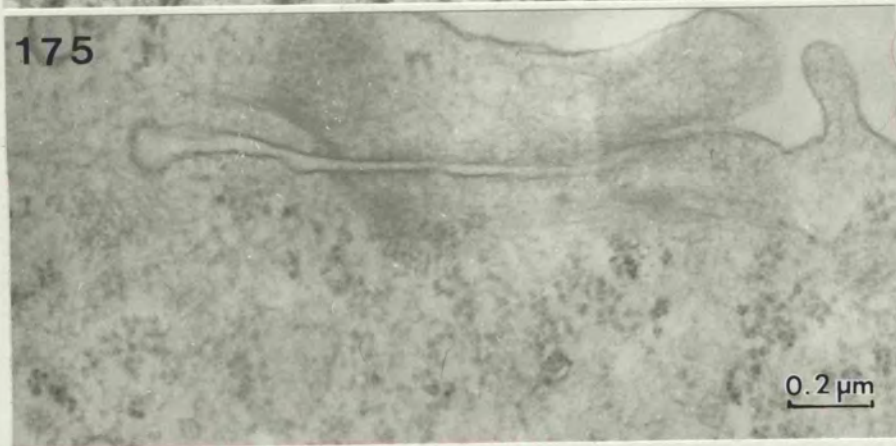
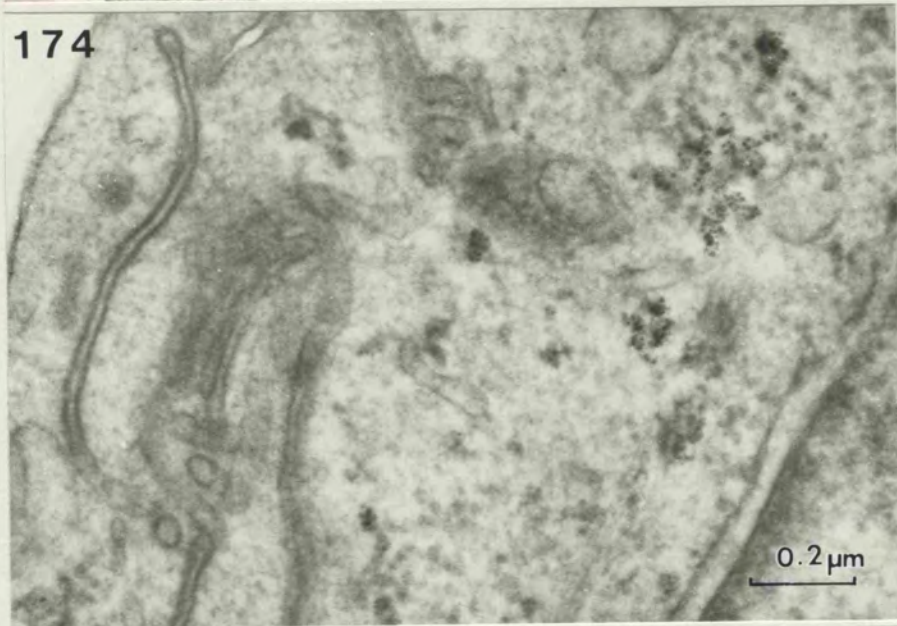
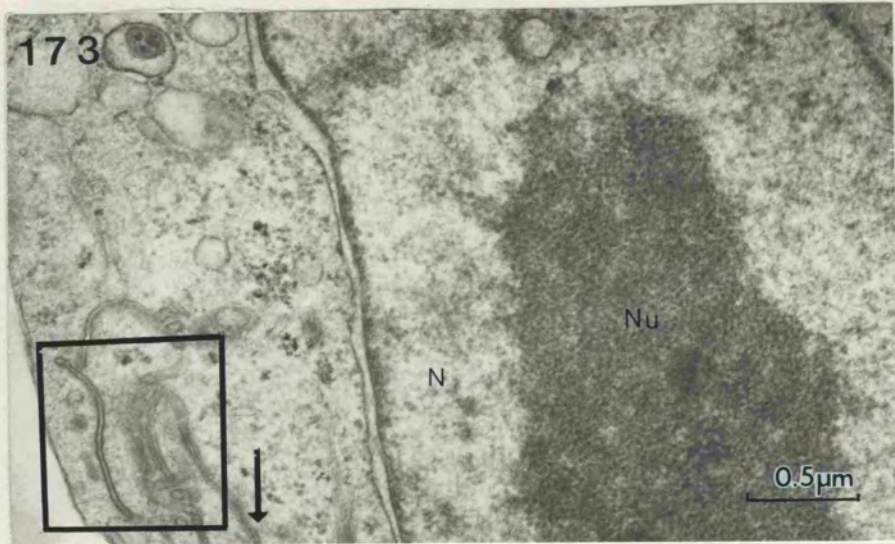


FIG 176 - 180 Transmission electron micrographs of BeWo cells.

FIG 176 Structure on cell surface similar to 'iron-binding' organelle (arrow).

FIG 177 Dead cell. A small area of an adjacent viable cell can be seen in the top right hand corner of the figure.

FIG 178 Tubular structure joining a larger vesicular structure in the cytoplasm of the BeWo cell. This possibly may be a CURL (compartment of uncoupling of receptor and ligand).

FIG 179 Unidentified structure in a BeWo cell.

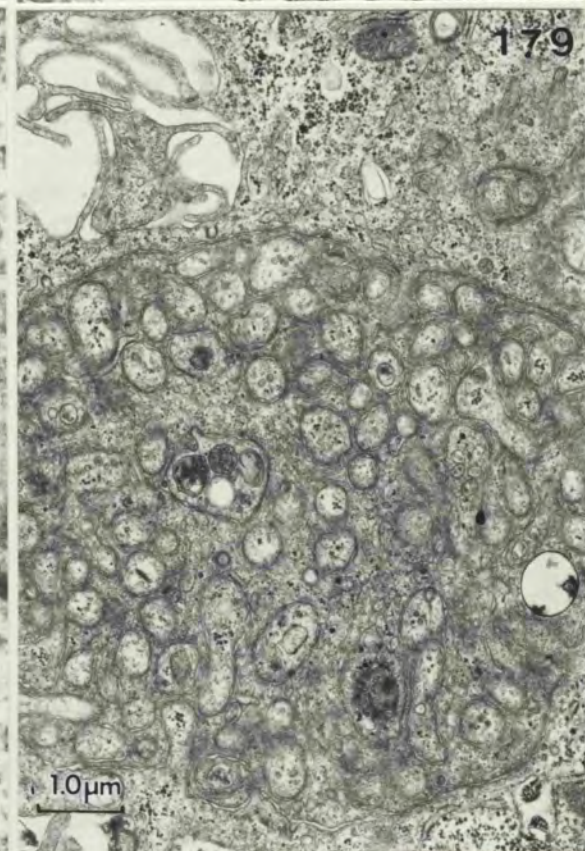
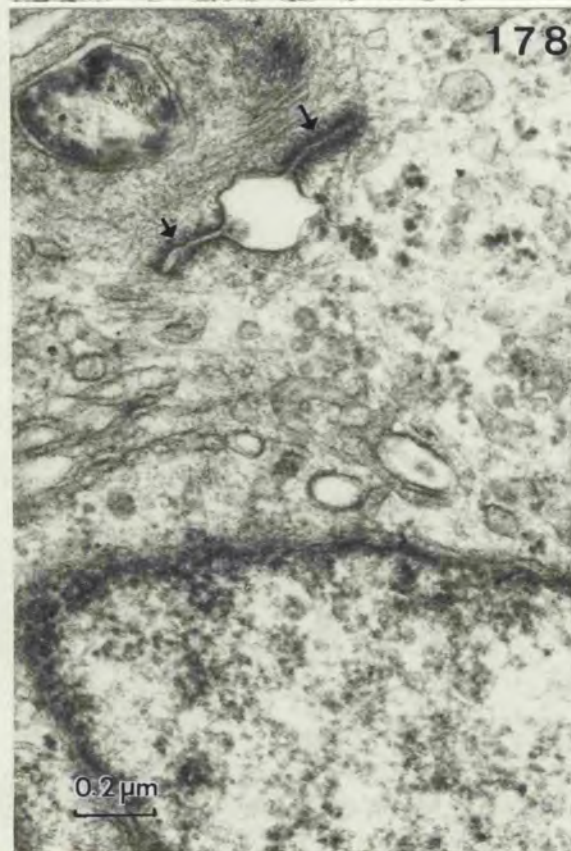
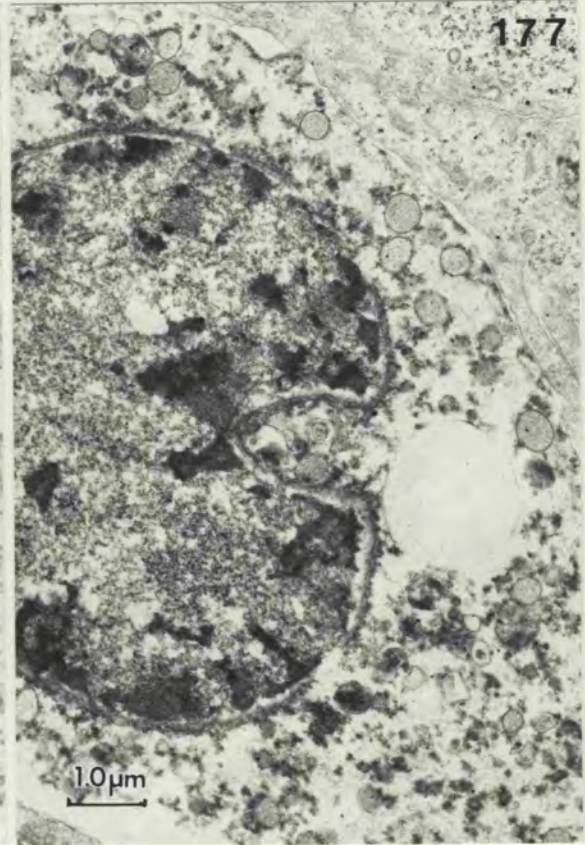
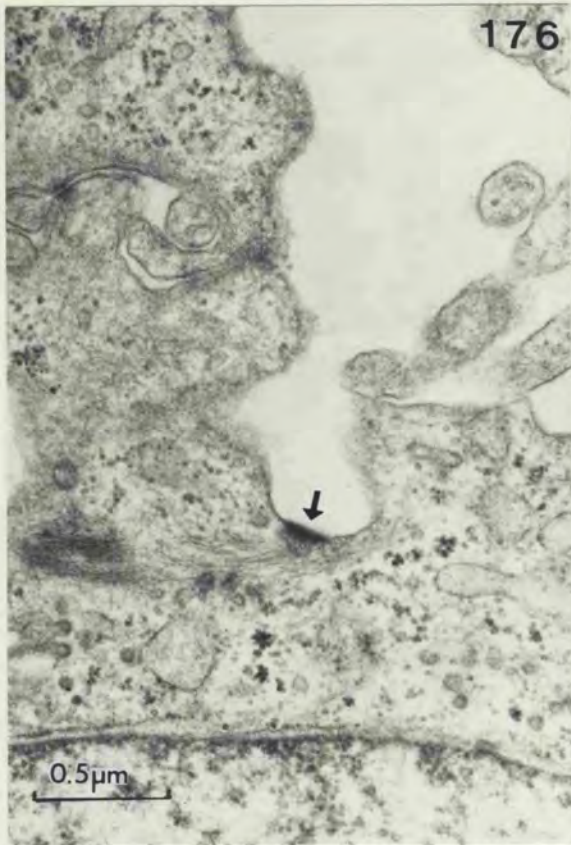


FIG 180 Light micrograph of villus-like upgrowth seen in BeWo cells.

FIG 181 Transmission electron micrograph of villus-like upgrowth showing it to be composed of a number of cells. The cells which were attached to the base of the culture flask (arrow) look more healthy than those above.

Note cell on the right is growing over the paler cell on the left (arrow).

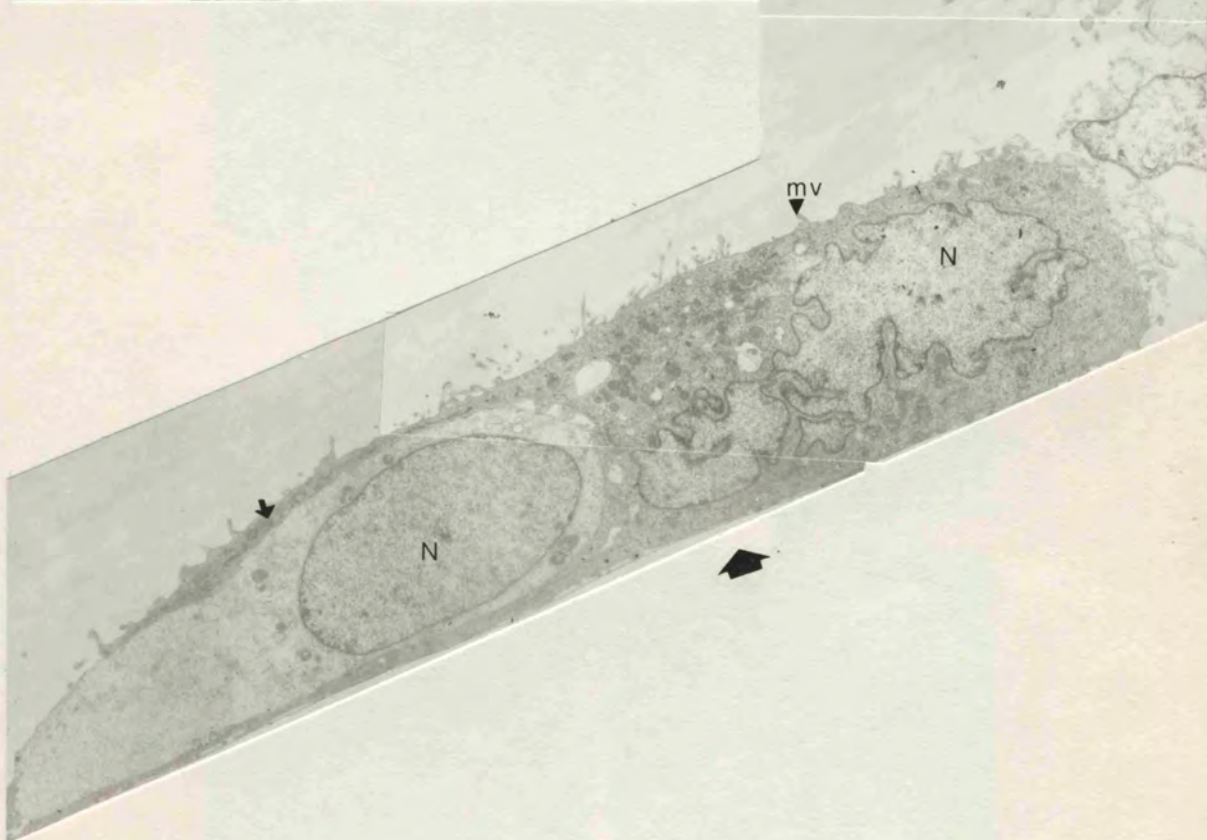
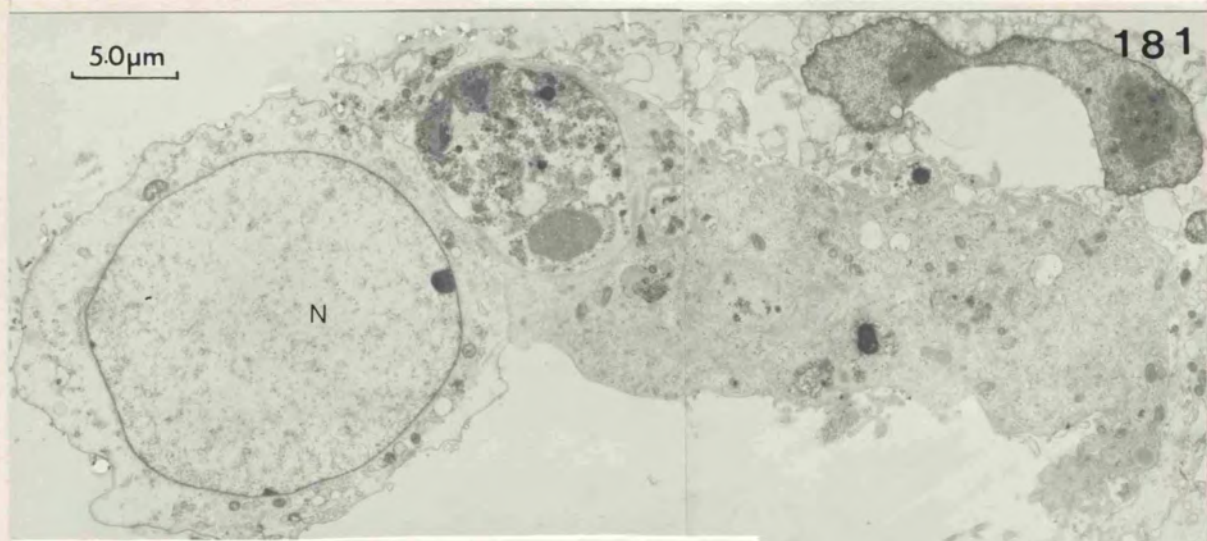


FIG 182 "Cauliflower" shaped outgrowth from BeWo cell. Glycogen (g), lipid (L), mitochondria (m), membrane fragments and various vesicles (vs) are identifiable within the "florets". The cell beneath the outgrowth has a normal appearance. (arrow).

FIG 183 & 184 Higher power micrograph area of interdigitating microvilli between cell and outgrowth.

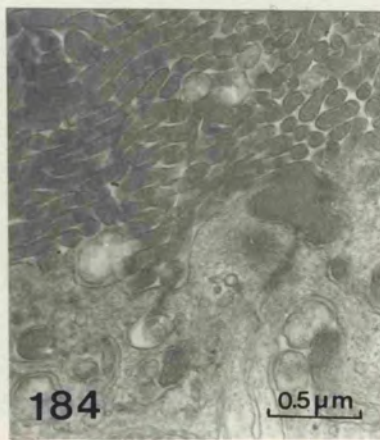
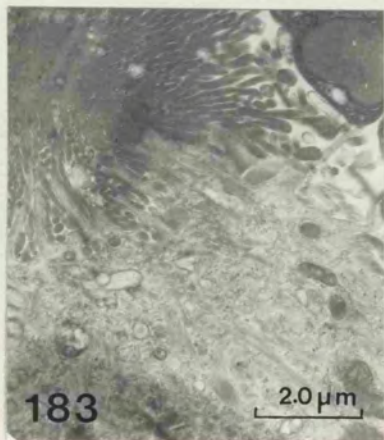
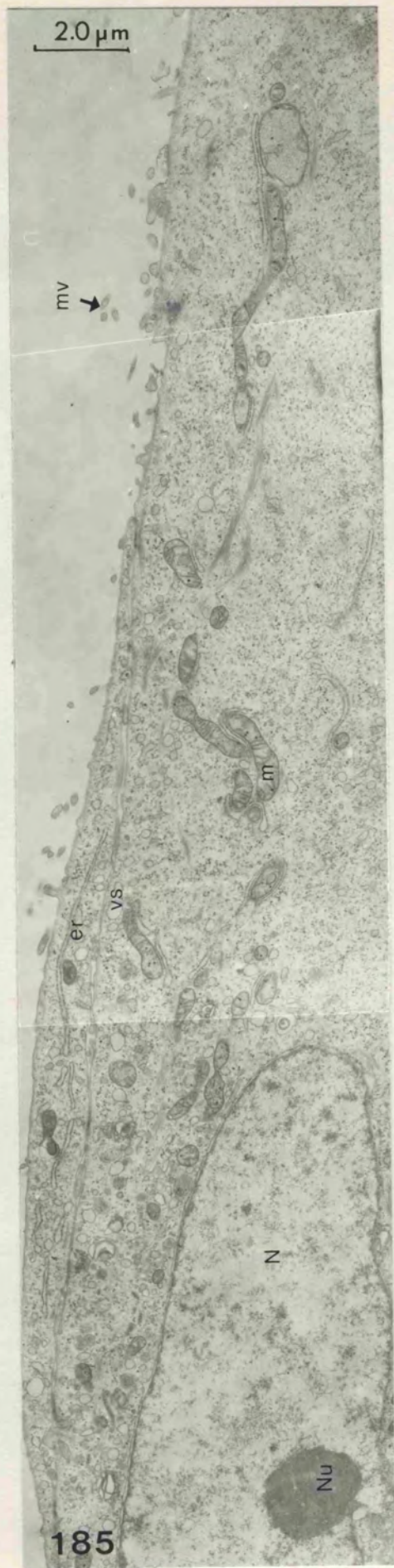


FIG 185 Transmission electron micrograph of a normal  
BeWo cell.

m = mitochondria  
N = nucleus  
vs = vesicles  
er = endoplasmic reticulum  
Nu = nucleolus  
mv = microvilli



185

---

FIG 186 & 187 Transmission electron micrograph of BeWo cells incubated with Au(18)-IgG for 30 minutes.

FIG 186 Shows gold probe located in a coated vesicle (arrow)

FIG 187 Shows gold probe located in large electron-lucent vesicles (arrow). Note the presence of a myelin figure at the bottom right of the micrograph (\*)

FIG 188 In control cells incubated with Au(18) only for 30 minutes gold particles were found in large electron-lucent vesicles (arrow).

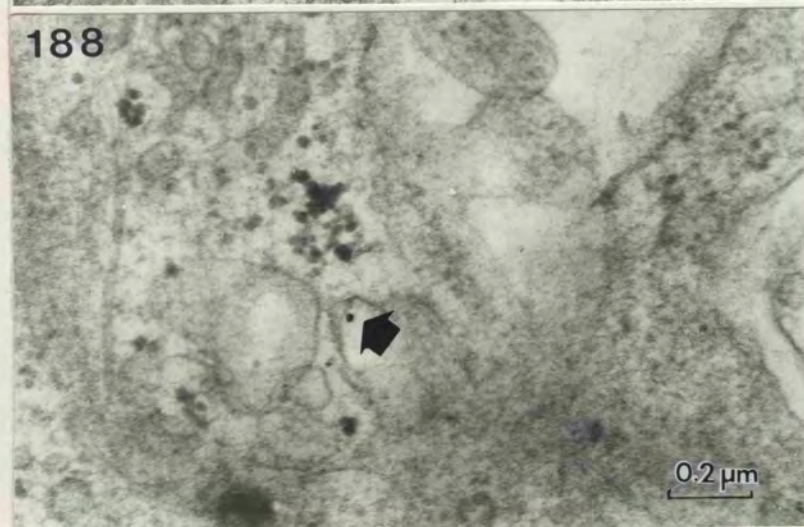
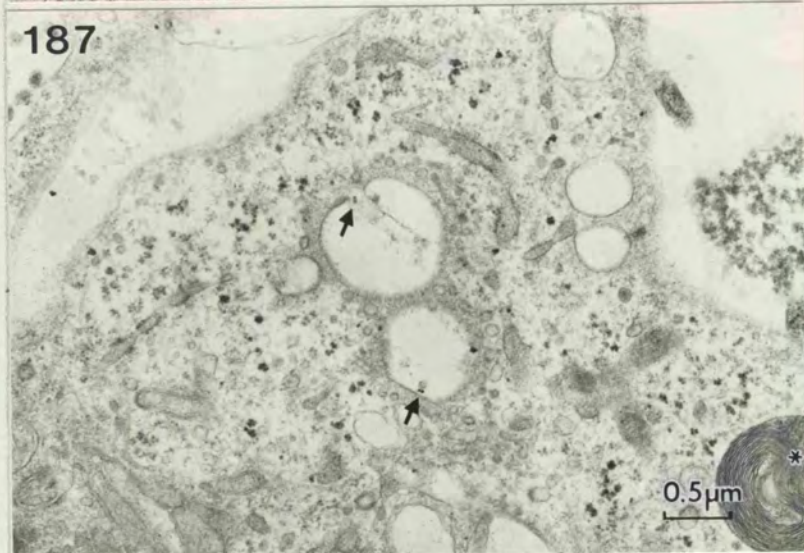
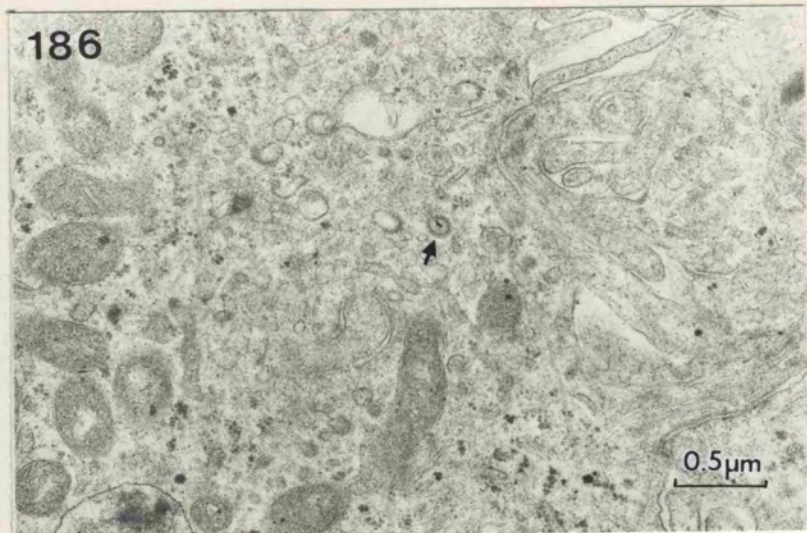


FIG 189 - 194 Transmission electron micrographs of BeWo cells incubated with either Au(18)-IgG (FIGS 189, 191 and 193) or Au(18) only (FIG 190, 192 and 194) for 18 hours.

Gold particles were found:-

(i) in small electron-lucent cytoplasmic bodies - CB (arrow) - FIG 189 and 190. Sometimes these bodies (CB's contained small vesicles (arrowhead) within them, and gold particles (arrow) were found close to the outer surface of these small vesicles. - FIG 191 and 192.

(ii) in large electron-lucent bodies containing smaller vesicles within (arrow). Note coated regions of the membrane of the larger bodies (arrowhead), possibly CURL. - FIG 193 and 194.

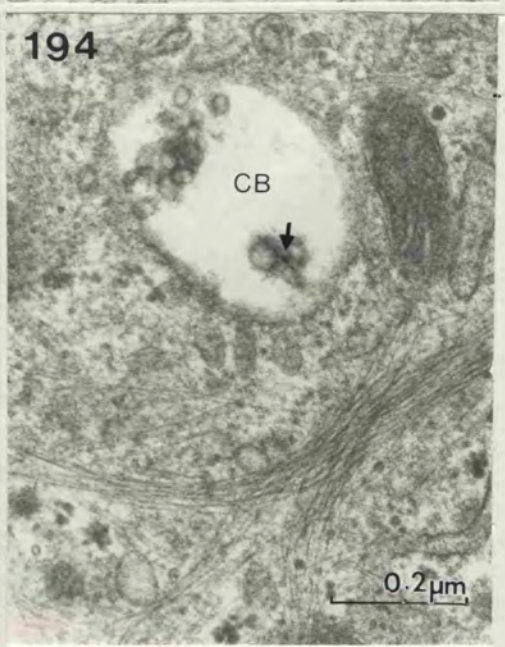
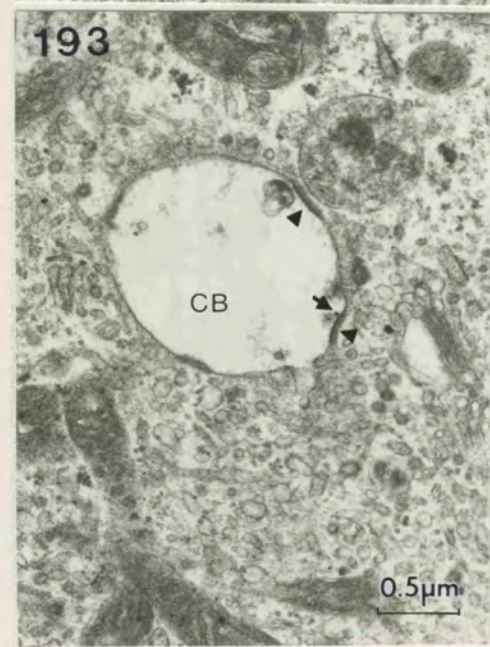
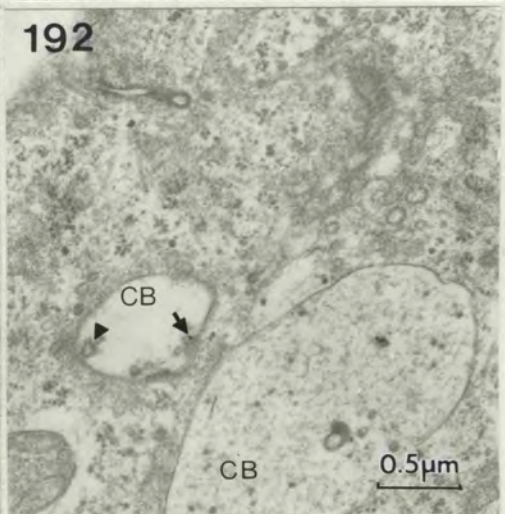
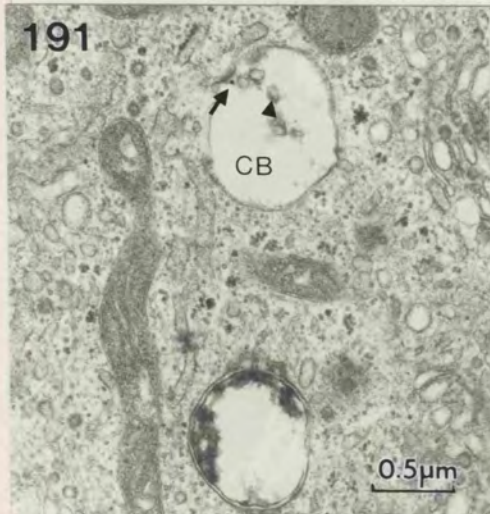
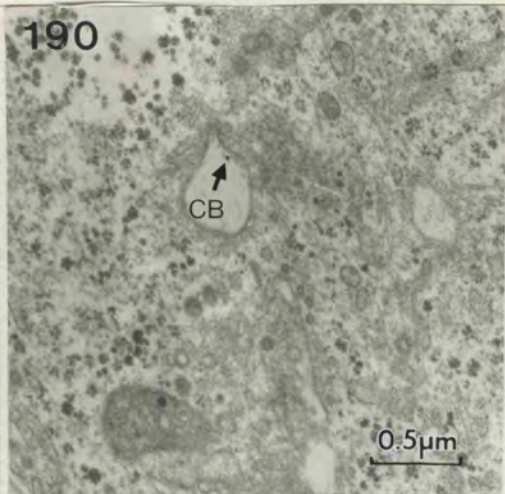
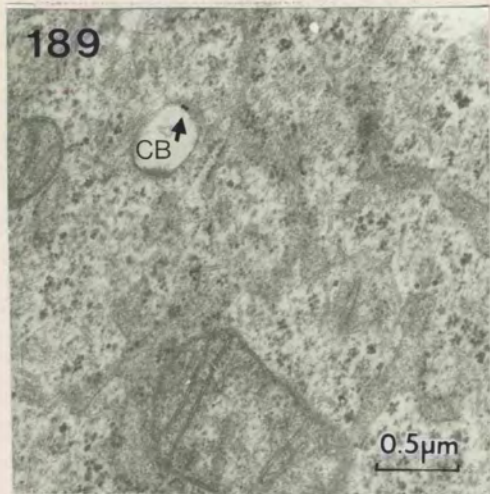


FIG 195-198 Transmission electron micrographs of BeWo cells incubated with either Au(18)-IgG (FIG. 195 & 197) or Au(18) only (FIGS 196 & 198) for 18 hours.

FIGS 195 & 196 Show particles (arrow) located in cytoplasmic bodies (CB) with light electron density.

FIG 195 Shows a cytoplasmic body containing glycogen in addition to the gold probe (open arrow). Note also the coated vesicle profile at the top of this figure (arrow - cv)

FIG 197 & 198 Show gold probe (arrow) in large cytoplasmic bodies with very dense inclusions. Note the presence of microtubules (mt) in Fig 197 and fine filaments (f) in Fig 198.

FIG 198 Some particles of gold were found apparently free in the cytoplasm (open arrow)

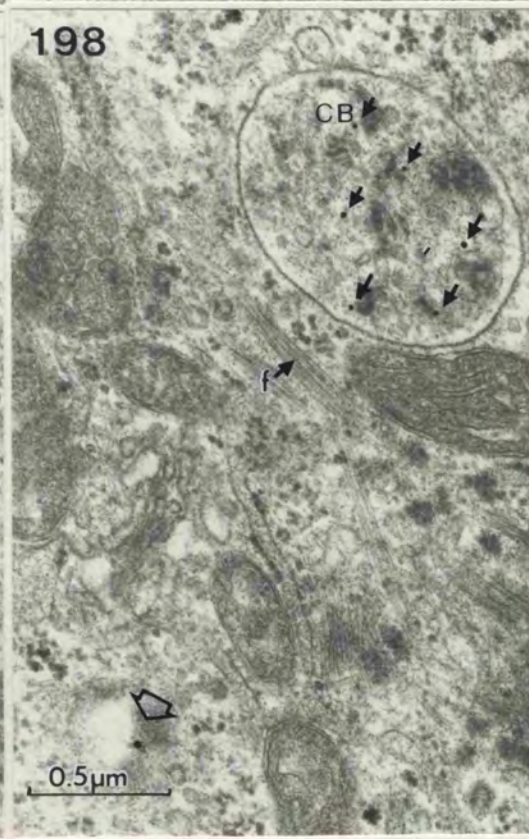
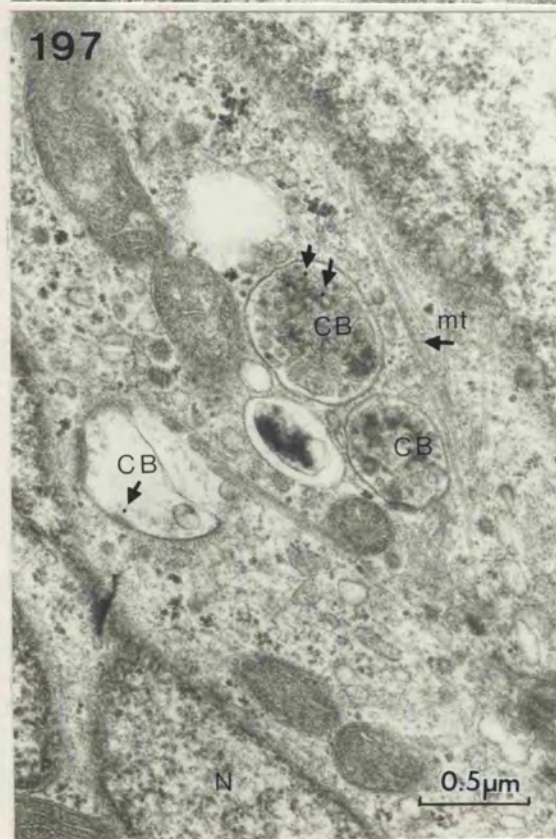
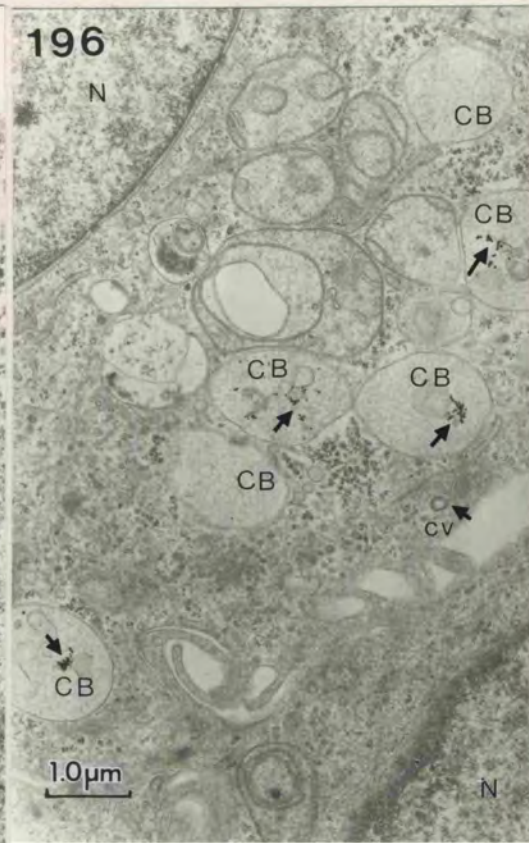
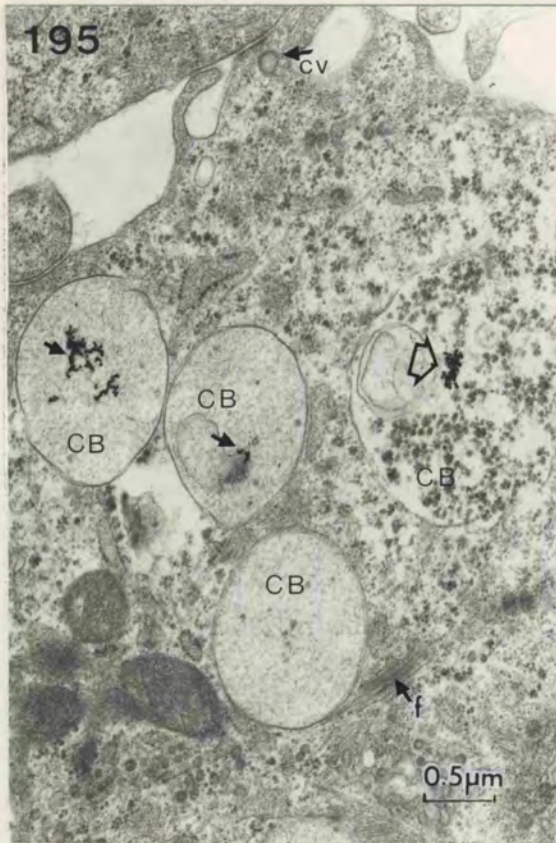


FIG 199 Montage of transmission electron micrograph of BeWo cell showing grouping together of cytoplasmic bodies (CB'S) into clusters. Note that the gold probe Au(18)-IgG is located in groups in the centre of the cytoplasmic bodies (arrow)

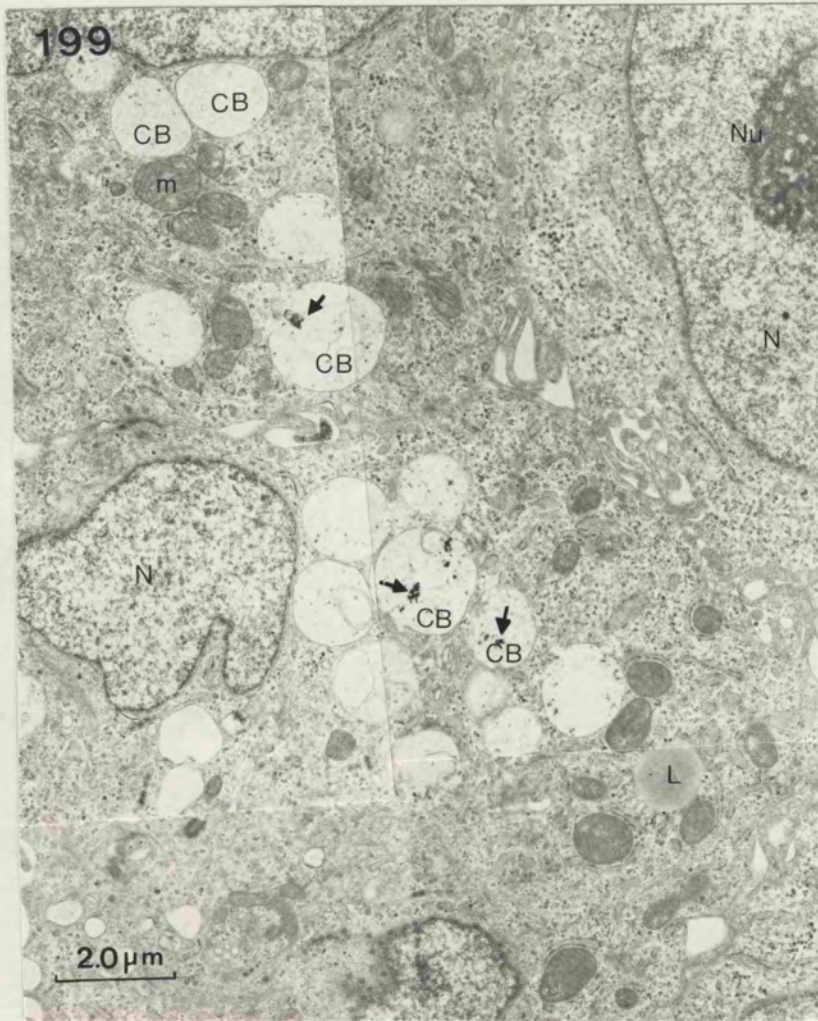


FIG 200 - 206

Transmission electron micrographs of cells incubated with either Au(18)-IgG or Au(18) alone for 4 hours at 2°C then fixed immediately after washing.

In cells incubated with the Au(18)-IgG probe gold particles were found:

- (i) Associated with both the microvillar and non-microvillar cell surface (Fig 200)
- (ii) Associated with small vesicular structures just below the surface of the cell (Fig 202 , arrow)
- (iii) In large smooth membrane vesicles (Fig 204, arrow).
- (iv) In a tube-like structure just below the surface of the cell (Fig 206, arrow).

In cells incubated with Au(18) only, particles of gold were found:

- (i) Associated with the microvillar and non-microvillar cell surface (Fig 201). Note the association of probe with a coated pit (arrow).
- (ii) Associated with a coated pit on the cell surface (Fig 203, arrow)
- (iii) Associated with large smooth membrane vesicles (Fig 205, arrow).

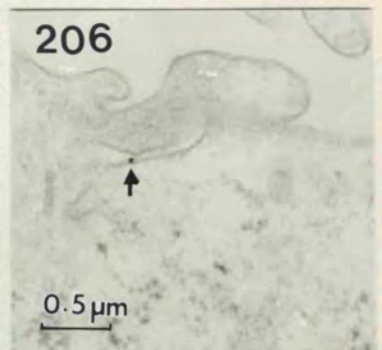
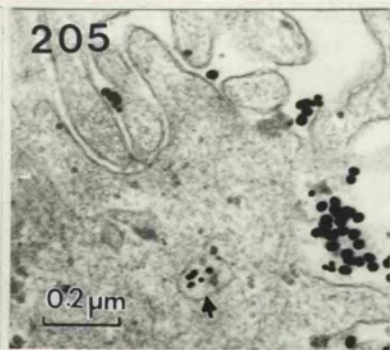
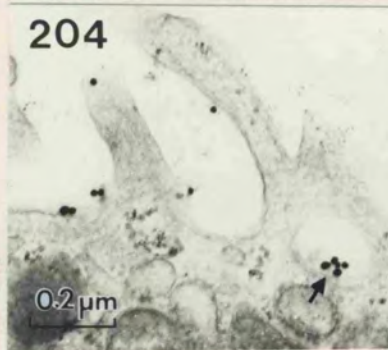
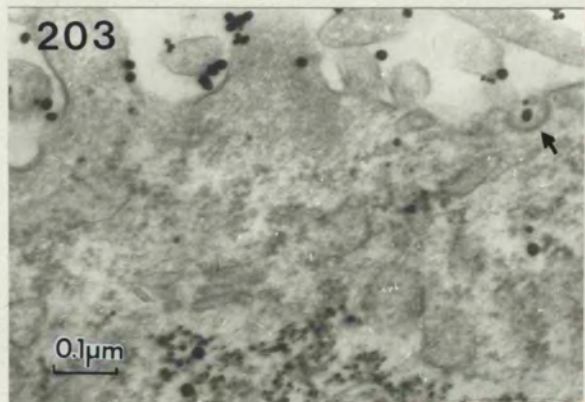
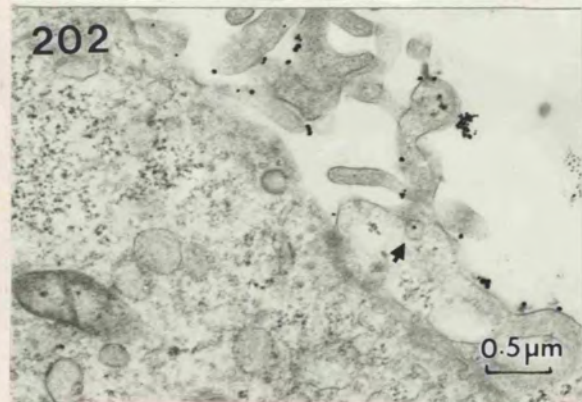
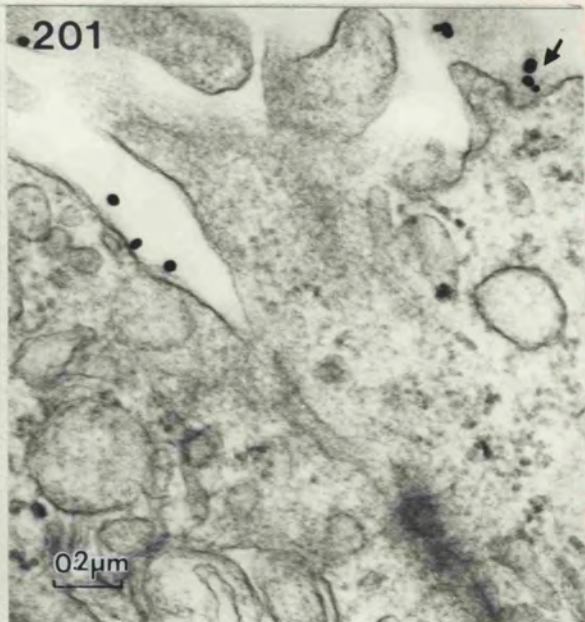
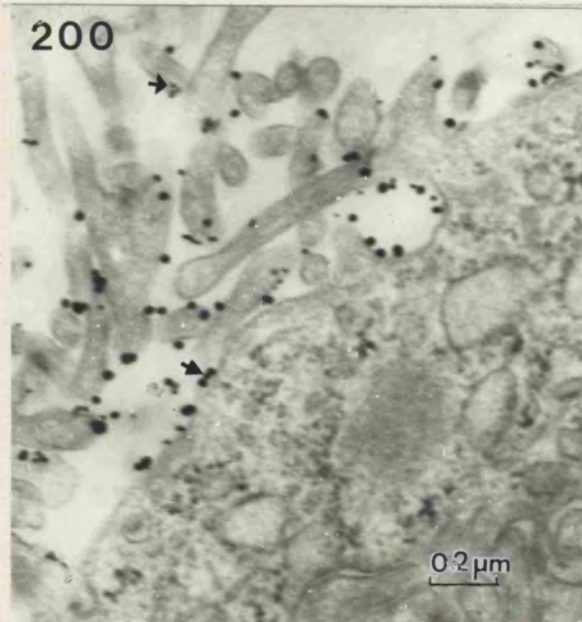
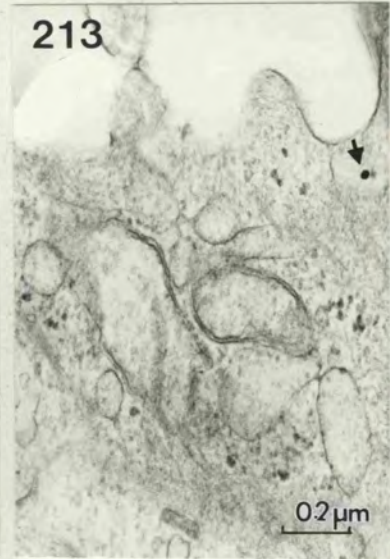
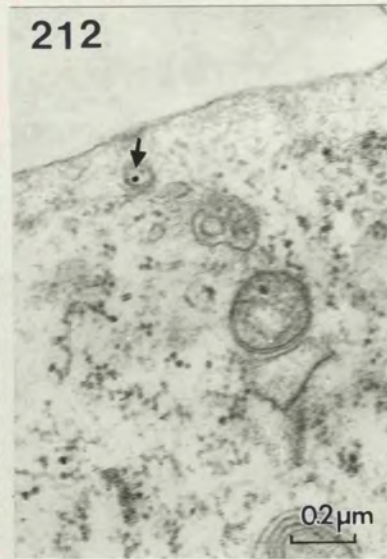
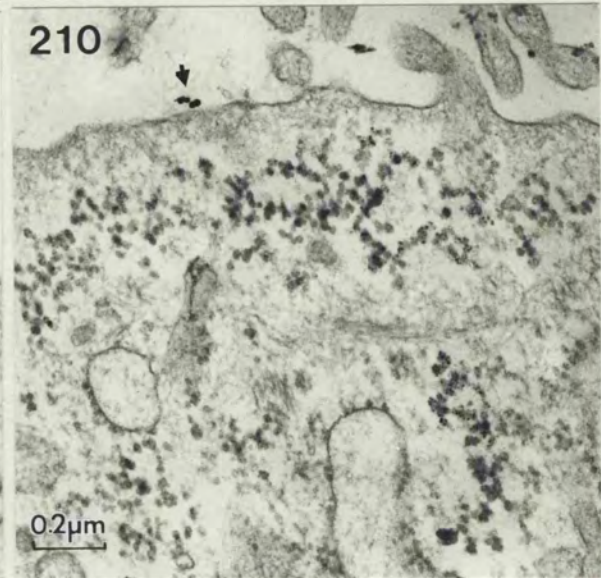
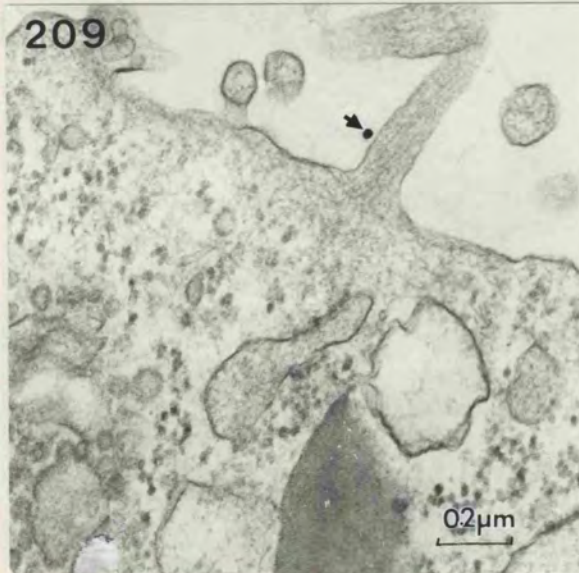
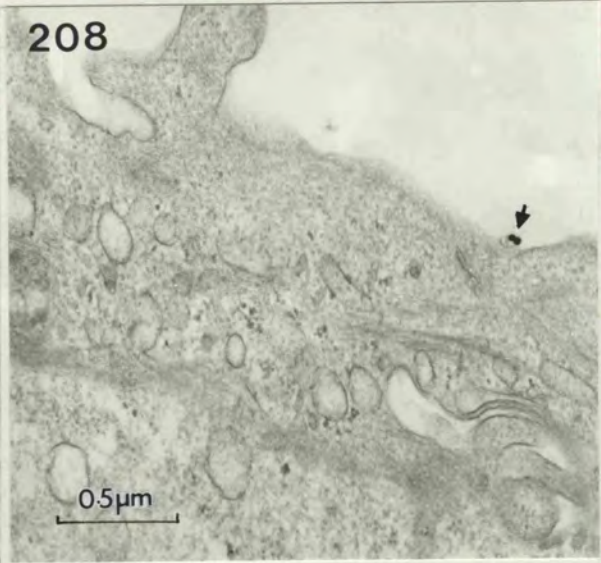
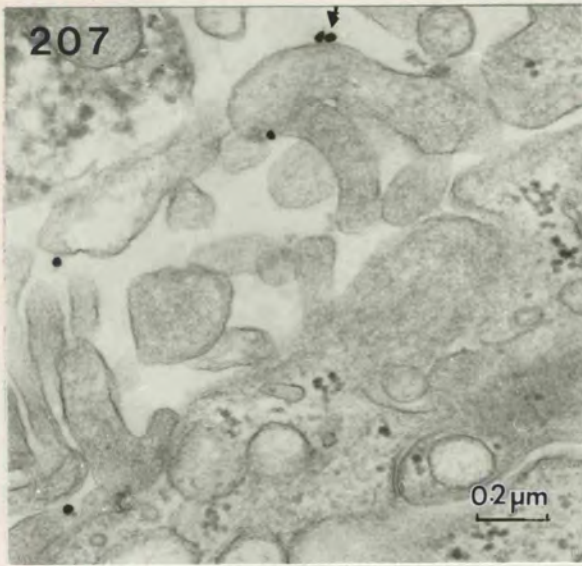


FIG 207-213 Transmission electron micrographs of BeWo cells incubated with either Au(18)-IgG or Au(18) for 4 hours at 2°C then fixed after warming.

FIG 207 & 208 Fixation of cells after 5 minutes warming showed the presence of gold particles associated with the non-microvillar surface of the cell (arrow) in both the Au(18)-IgG incubations (FIG 207) and the Au(18) only incubations (FIG 208)

FIG 209,210,211,212 & 213 Cells fixed after 10 minutes warming showed presence of the probe:  
(i) associated with the cell surface and associated with non-microvillar areas of cell (arrow). FIG 209, 210 show the Au(18)-IgG incubations, FIG 211 shows incubation with Au(18) only.

(ii) Gold particles were found within smooth membrane vesicles (arrows). FIG 212 shows the Au(18)-IgG incubations and FIG 213 the Au(18) only incubation.



- FIG 214 - 217 BeWo cells incubated with Au(18)-IgG and fixed 10 minutes after warming.
- FIG 214 Au(18)-IgG particles were found in coated pits (arrow).
- FIG 215 Au(18)-IgG particles were found in large dense, membrane-bounded vesicular structures (arrow).
- FIG 216 & 217 Au(18)-IgG particles were found lying free in the cytoplasm (circled).
- FIG 218 BeWo cells incubated with Au(18)-IgG and fixed 30 minutes after warming. Au(18)-IgG particles were found associated with the cell surface (arrow).
- FIG 219 BeWo cells incubated with Au(18) alone and fixed 30 minutes after warming. Au(18) particles were found associated with the cell surface (arrow).

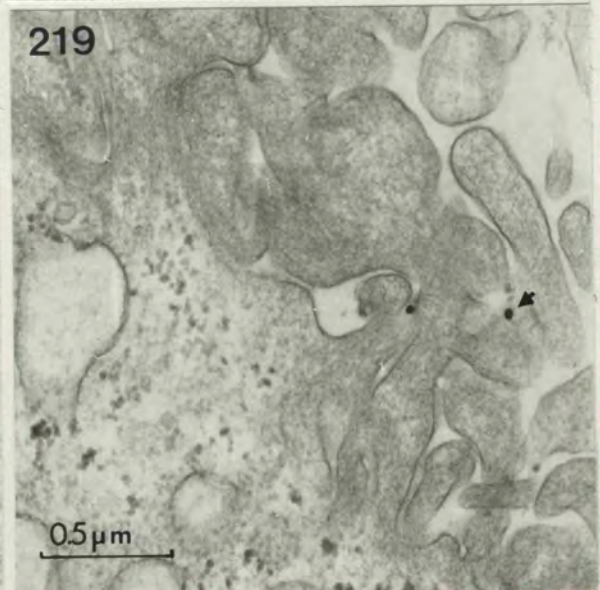
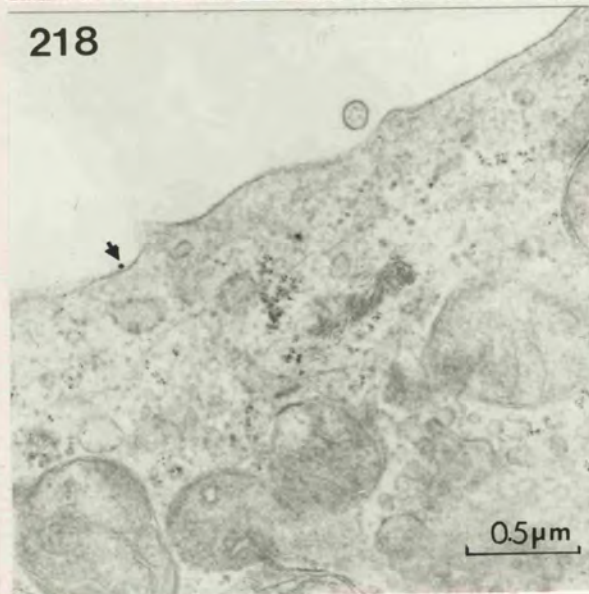
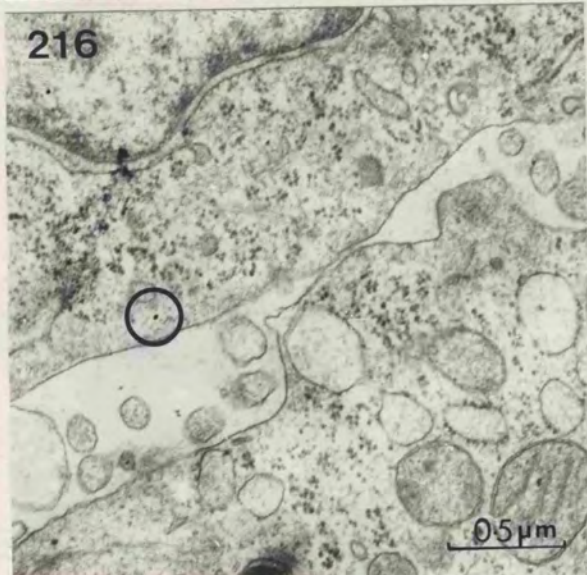
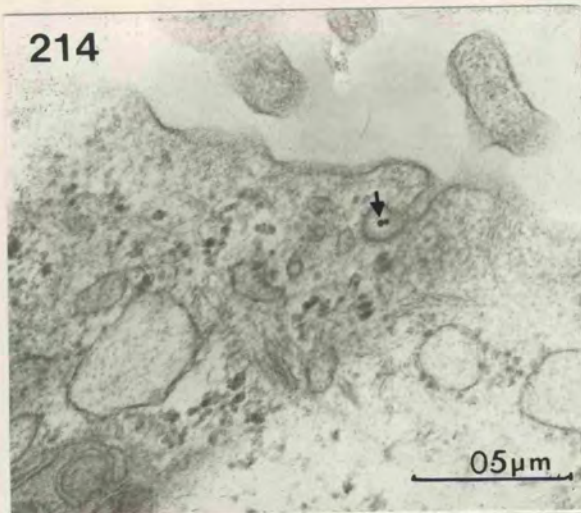


FIG 220 - 223 show results of the BeWo cell incubations with Au(18)-IgG.

FIG 220 Gold-IgG particles were found between the basal microvilli of the cells (circled).

FIG 221 Gold-IgG particles were found lying free within the basal microvilli (circled).

FIG 222 & 223 Gold-IgG particles were found lying free along the basal surface of the cell where it was attached to the plastic culture dish (circled).

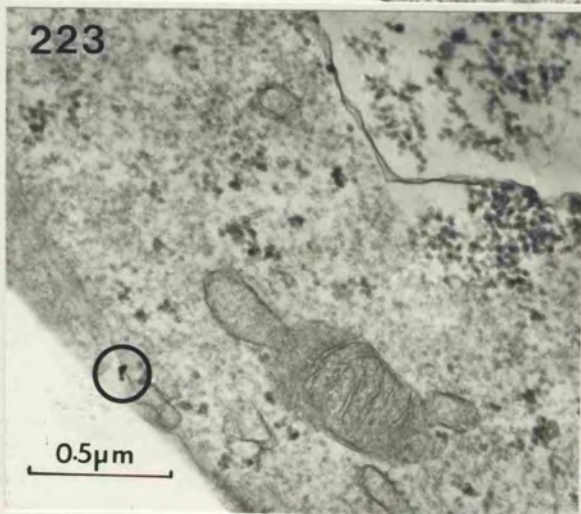
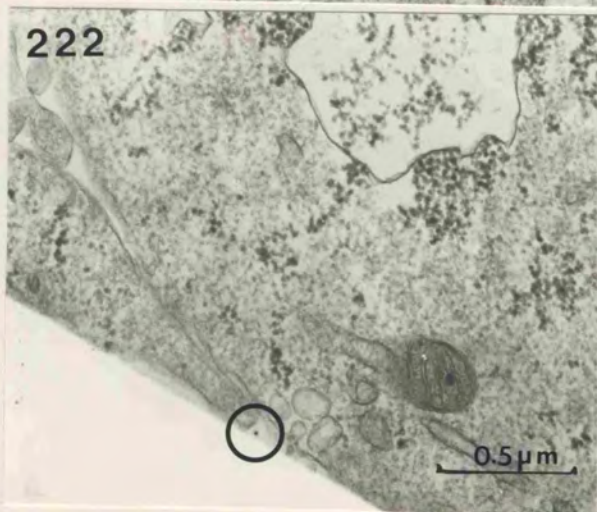
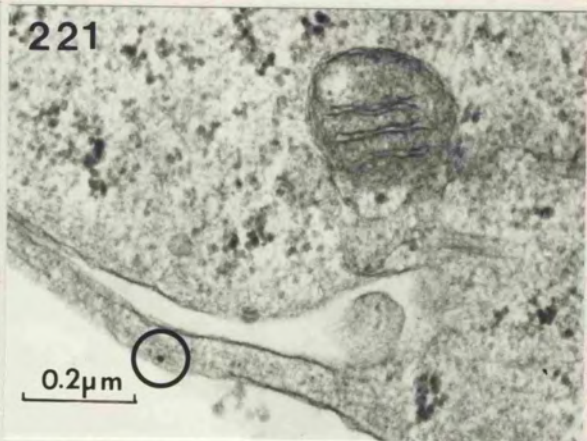
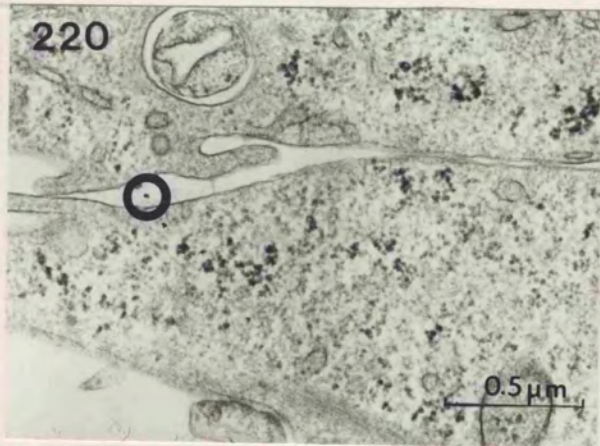


FIG 224 Diagram showing the condensation reaction between N-succinimidyl propionate and the Fab portion of the IgG molecule.

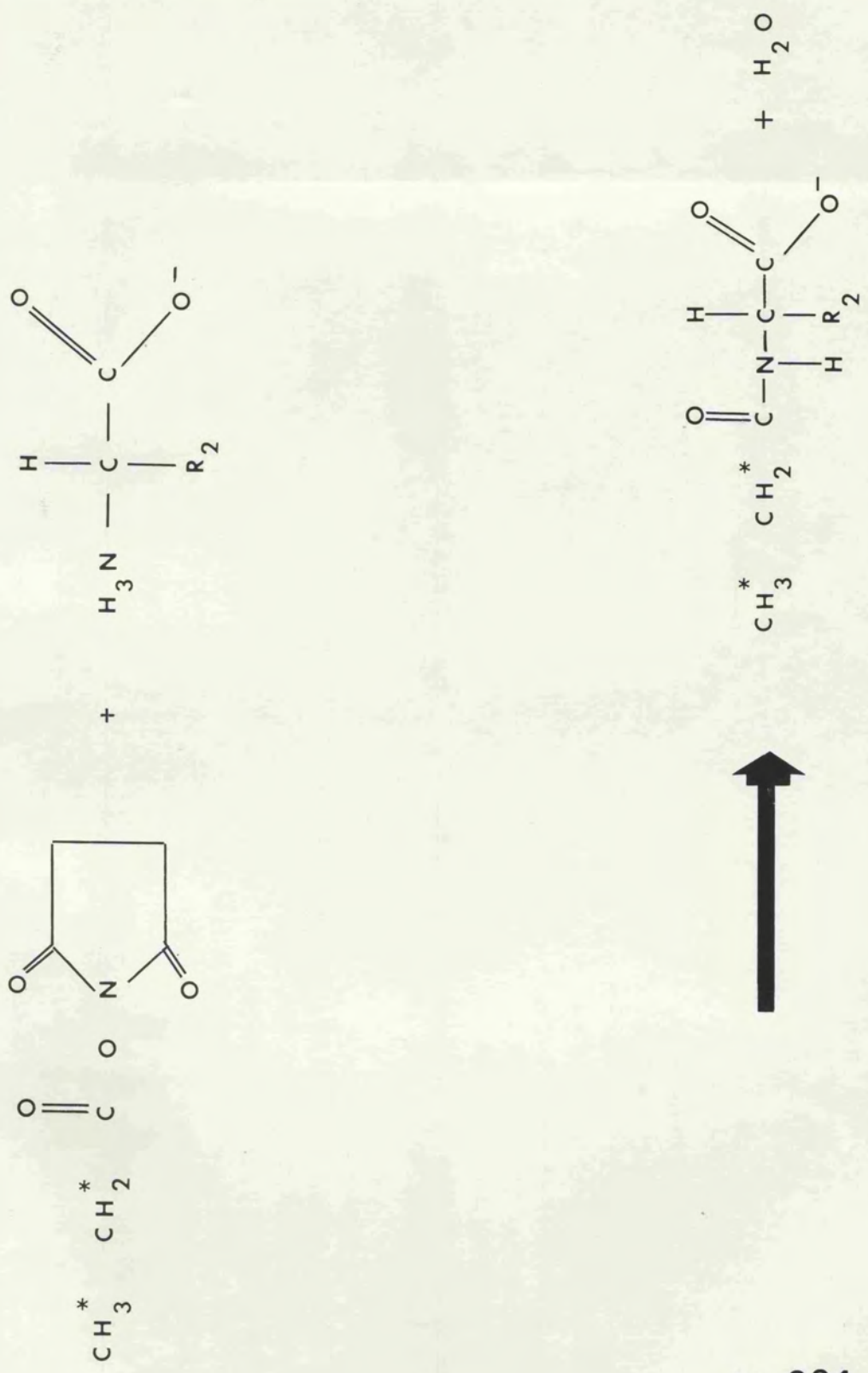


Fig 224

**D.18. Autoradiographic study of IgG transport in the human placenta.** By LINDA DEARDEN and C. D. OCKLEFORD. *Department of Anatomy, The University of Leicester*

Immunoglobulin G (IgG) is transported across the human placenta, but exactly how this is accomplished is unclear.

Apparatus similar to the isolated perfused cotyledon system (Schneider *et al.*, *Am. J. Obstet. Gynec.* **114**, 1972) was employed to study the route of IgG transport across the human placenta. Once the maternal and fetal 'circuits' were established, tritiated IgG (Ockleford & Clint, *Placenta* **1**, 1980) was introduced into the maternal circuit. Transport of this probe across the placenta was monitored by scintillation counting of samples taken from the venous return of the fetal circuit. After perfusion, tissue was fixed, resin-embedded and sections 0.5  $\mu\text{m}$  thick were prepared for autoradiography. The syncytiotrophoblast and the endothelial cells of the fetal capillaries were labelled. Silver grains were also associated with vesicles in the syncytium. The number of developed silver grains per unit area was significantly greater ( $P < 0.01$ ) in  $^3\text{H}$ -IgG perfused tissue than in control tissue not previously exposed to radiolabelled IgG.

Apparently much IgG becomes localised in vesicles in the syncytiotrophoblast. These vesicles are larger than micropinocytic vesicles. It is possible that some of the silver grains near the surface of the syncytiotrophoblast resulted from radioactive disintegrations in coated vesicles, although such light microscopic studies have insufficient resolution to determine if this is so.

The autoradiographic data indicating uptake and transepithelial transport is supported by the scintillation counting data which shows that maximal transport of the isotope is reached within 30 minutes of the addition of the  $^3\text{H}$ -IgG to the maternal circuit. We conclude that transport of at least part of the probe is accomplished in this system.

L.D. thanks the M.R.C. for support and C.D.O. is grateful to E.M.B.O. for supporting a visit to the University of Paris as a guest of Professor M. Panigel.

**D.19. The Harderian gland and its duct in the Mongolian gerbil (*Meriones unguiculatus*).** By A. P. PAYNE, H. S. JOHNSTON and J. MCGADEY. *Department of Anatomy, Glasgow University* (Fig. 11)

The gerbil Harderian gland has been widely studied in connection with the production of pheromones and thermoregulatory lipids, yet no description of its morphology has appeared. The gland is a tubulo-alveolar structure lined by a single layer of columnar/cuboidal epithelial cells exhibiting great uniformity (Fig. 11A). Nuclei are basal and spherical, with a corona of rough endoplasmic reticulum; binucleate cells are common. Cell apices contain numerous small lipid-filled vacuoles and the luminal surface bears microvilli. Small irregular mitochondria with dense matrices occupy the basal two thirds of the cell. The Golgi apparatus is not conspicuous. The dense cytoplasm contains a fine particulate matrix and is characterized by numerous clear 'slashes', often associated with a thin electron-dense membrane down one side. No sex differences were seen.

A network of myoepithelial cells surrounds the tubules. Interstitial cells include macrophages, plasma cells, mast cells and melanocytes: the latter are especially abundant and render the gland black/brown in colour. The tubule lumina contain solid accretions of porphyrin and lipid-filled vacuoles, together with considerable cytoplasmic debris and nuclei, particularly in the major ducts.

Within the gland the main duct is lined by a single layer of normal acinar cells. However, on leaving the gland there is an abrupt transition. The wall is thrown into folds with numerous clefts leading to narrow crypts. Three cell types are seen (i) normal acinar cells, (ii) cells with small dense apical granules and a variable number of large clear vacuoles (Fig. 11B) and (iii) cells packed with large dense granules and possessing an extensive Golgi area; lipid vacuoles are lacking (Fig. 11C). The first two types line the duct lumen, the second also lines the clefts, while the third type occurs only in the crypts. Some clefts contain dense geometric deposits with a regular layered crystalloid appearance. Very isolated pockets of cells similar to the ductal types occasionally occur deep within the gland. Mucous cells occur at the external opening of the secretory duct.

Lecture Theatre 3 09.00-11.00

**Marketing**

Lecture Theatre 3 14.00-17.30

**PIGS: NUTRITION AND REPRODUCTION IN THE SOW****(a) Sow productivity – the way ahead**

M. A. VARLEY, Rowett Research Institute, Bucksburn, Aberdeen

IN 1970, of the herds recording with the Meat and Livestock Commission, the percentage of pig producers weaning at three weeks of age or less was 2.3 per cent. This percentage rose to 47 per cent in 1981. Survey data also shows that producers who wean at three weeks of age or less, produce more piglets per sow per year than producers weaning at five weeks or over and the former group achieve greater profitability. Early weaning, therefore, is one important factor in the improvement of sow productivity in recent years but concurrent with this there is significant progress in the breeding, housing, nutrition and health status of sows.

A series of experiments demonstrated that the optimum lactation length is between three and four weeks. When weaning age is reduced below this optimum, a deleterious effect on the litter size at full term is seen.

However, early weaning disturbs the endocrine balance of the sow and this may be a cause of increased embryonic mortality. In the near future, it might be possible to precisely control some of these reproductive processes by the administration of exogenous hormones.

**(b) Nutritional influences on pig reproduction**

P. E. HUGHES, Department of Animal Physiology and Nutrition, University of Leeds

THE direct and indirect influences of nutrient intake on the reproductive performance of the pig is considered. The consequences of variation in the intake of both total feed and specific nutrients is discussed in relation to the various stages of the reproductive life of the female pig, ie, the pre-pubertal period, puberty to mating, pregnancy, lactation and the weaning to remating period. In addition to these direct effects of nutrition on reproduction, reference is made to indirect, longer-term effects of feed levels/specific nutrient intakes on the efficiency of reproduction. In particular, the effects of nutrient supply during lactation is discussed in relation to the subsequent fertility and fecundity of the sow. Possible mechanisms of action for such indirect nutritional effects, operating via liveweight/body condition changes, are proposed.

**(c) Effect of weaning age on sow productivity**

W. M. MILLER, Great Hatfield, Hull

**(d) Effect of age at first service on sow lifetime performance**

J. G. OLDHAM, 34 Ketwell Lane, Hedon, Hull

Lecture Theatre 4 09.00-11.00

**POULTRY: LEG PROBLEMS****(a) Pathological anatomy of avian skeletal abnormalities**

D. R. WISE, Department of Clinical Veterinary Medicine, Cambridge

THE skeletal anatomy of the normal fowl is illustrated and its development described and contrasted with that of the mammal. The pathological changes involved in the generalised bone dystrophies of rickets and chondrodystrophy are described. Thereafter, the localised abnormalities of dyschondroplasia, spondylolisthesis and twisted leg are discussed.

**(b) Nutritional aspects of leg weakness in poultry**

J. PORTSMOUTH, 15-19 Church Road, Stanmore, Middlesex

THE growth rate of chickens produced for meat has increased dramatically during the past two decades. Diets have also changed with less emphasis on imported cereals and marine proteins and more on home grown grain, cereal substitutes and vegetable proteins. The implication of these changes is discussed relative to mineral balance and biological availability.

Acid base balance and the effect which this aspect may have is reviewed. The involvement of specific vitamins and trace elements and the relationship between them in prevention of leg weakness is discussed with special emphasis on micronutrient availability and ration supplementation. Leg problems in both broiler breeder replacement stock and commercial layers are examined.

**(c) Leg weakness in poultry**

J. C. STUART, 21 Chapel Field Road, Norwich

'LEG weakness' is a term that covers a host of clinical conditions seen in all types of poultry. Possible causes include vitamin and other nutritional deficiencies, faulty management, genetical relationships, bacterial and viral infections. Each is briefly described and methods of control and treatment, where available, discussed.

Lecture Theatre 4 14.00-17.30

**IMMUNOLOGY: IMMUNITY IN THE FETUS AND NEONATE****(a) Cellular method of obtaining passive immunity**

C. D. OCKLEFORD, L. DEARDEN, Department of Anatomy, University of Leicester Medical School

ESSENTIALLY three organs, subtending similar transporting epithelia, are involved in passive immunity transfer. In species where passive immunity is conferred before birth these are the chorioallantoic and yolk sac placentae; after birth transfer occurs in the intestine. Similar cellular principles of antibody transport are utilised in the three organs.

Trans-chorioallantoic placental transport is selective (the only class of antibody transmitted is IgG), is mediated by an Fc  $\gamma$  receptor, occurs against a concentration gradient, becomes more efficient as pregnancy progresses and crosses trophoblastic tissue.

Syncytiotrophoblast contains many coated vesicles. These endocytic structures have polygonal ultrastructure. Coated vesicles are known to support the receptor mediated uptake of peptide containing molecules and particles. Fractions containing coated vesicles from human placental tissue pre-incubated with  $^3\text{H}$ -IgG also contain isotope. Evidence from yolk sac and neonatal epithelial transport studies indicates that these organelles cross the epithelium and release antibody after fusion with the basal surface membrane. Autoradiographic studies indicate that IgG accumulates in other organelles after fusion with coated vesicles. These may be transport intermediates or may represent a catabolic cul-de-sac.

A calculation of the concentration of antibody within coated vesicles and a consideration of the structure of coated vesicles suggest a model to account for observed physiological features of the transport.

**(b) Maternal influence on the neonatal immune response**

B. I. OSBURN, G. DUHAMEL, School of Veterinary Medicine, University of California, Davis

AN understanding of the functional immune system in ungulates is critical for providing adequate protection for the neonate. The immune system consists of local and systemic components. Both thymic (T) and bone marrow (B) derived lymphocytes are present in these systems and these contribute to cell mediated (T-cell) and humoral mediated (B-cell) immune responses.

Local immunity is concerned primarily with antigens found on mucosal surfaces. The thymic and bone cells come into contact with antigens on the surfaces and the responses, in the form of antibodies and cells, circulate to mucosal surfaces and the mammary gland. In contrast, systemic immunity is concerned with blood-borne infections. To assure adequate protection for the neonate, the local immune system of the dam needs to be exposed or hyperimmunised with enteric and respiratory agent antigens in order to provide the newborn with adequate protection.

The newborn obtains both thymic and bone cells as well as antibodies in colostrum. It is critical that these factors are present as the newborn is agammaglobulinaemic and immunologically depressed at the time of birth. Accessory factors such as monocytes and complement which assist the immune system are also deficient in the newborn. The role of antibodies in colostrum is critical for preventing enteritis and septicaemia. Although the function of T-cells is poorly understood at this time, they probably contribute to protective local immunity.

**ADVANCES IN IMMUNOLOGY****(c) Development of immunity in the respiratory tract**

W. P. H. DUFFUS, J. K. O'BRIEN, Department of Clinical Veterinary Medicine, University of Cambridge

## CHAPTER 3

# Structure of human trophoblast: correlation with function

L. DEARDEN and C. D. OCKLEFORD  
With a contribution from M. GUPTA

### *Contents*

1. Introduction . . . . .	70
2. Development of chorionic villi . . . . .	72
3. Anchoring villi . . . . .	73
4. Ultrastructure of the trophoblast . . . . .	74
4.1. Syncytiotrophoblast . . . . .	74
4.1.1. Microvilli . . . . .	74
4.1.1.1. Function of microvilli . . . . .	79
4.1.2. Vasculo-syncytial membranes (VSMs) . . . . .	80
4.1.3. Nuclei . . . . .	80
4.1.4. Syncytial knots . . . . .	81
4.1.5. Syncytial bridges . . . . .	81
4.1.6. Rough endoplasmic reticulum . . . . .	81
4.1.7. Mitochondria . . . . .	82
4.1.8. Golgi complex . . . . .	82
4.1.9. Ribosomes . . . . .	82
4.1.10. Polymeric cytoskeletal proteins . . . . .	83
4.1.10.1. Microtubules . . . . .	83
4.1.10.2. Microfilaments . . . . .	83
4.1.10.3. Intermediate filaments . . . . .	83
4.1.11. Myelin figures . . . . .	85
4.1.12. Glycogen . . . . .	85
4.1.13. Lipid droplets . . . . .	85
4.1.14. Secretion granules . . . . .	86
4.1.15. Iron-binding organelle . . . . .	86
4.1.16. Calcium deposits . . . . .	87
4.1.17. Iron . . . . .	87
4.1.18. Vacuoles . . . . .	87
4.1.18.1. Juxtannuclear vacuoles . . . . .	87
4.1.18.2. Lagoons . . . . .	88
4.1.18.3. Lysosomes . . . . .	88
4.1.18.4. Multivesicular bodies (MVBs) . . . . .	89
4.1.19. Vesicles . . . . .	90
4.1.19.1. Pinocytic vesicles . . . . .	90

4.1.19.2. Large macropinocytic and phagocytic vesicles . . . . .	90
4.1.19.3. Micropinocytic vesicles . . . . .	92
4.1.20. Fibrin on syncytium . . . . .	94
4.1.21. Intercellular junctions . . . . .	94
4.2. Cytotrophoblast . . . . .	95
4.2.1. Microvilli/filopodia . . . . .	95
4.2.2. Nuclei . . . . .	96
4.2.3. Nucleoli . . . . .	96
4.2.4. Nuclear envelope . . . . .	96
4.2.5. Endoplasmic reticulum (ER) . . . . .	96
4.2.6. Mitochondria . . . . .	96
4.2.7. Golgi . . . . .	96
4.2.8. Ribosomes . . . . .	96
4.2.9. Filaments . . . . .	96
4.2.10. Lipid . . . . .	97
4.2.11. Myelin figures . . . . .	97
4.2.12. Glycogen . . . . .	97
4.2.13. Glomerular body . . . . .	97
4.2.14. Granules and vesicles . . . . .	97
4.2.14.1. Lysosomes . . . . .	97
4.2.14.2. Secretion granules . . . . .	97
4.2.14.3. Pinocytic vesicles . . . . .	97
4.2.15. Junctions . . . . .	97
4.2.16. Fibrin and cytotrophoblast . . . . .	97
4.3. Non-villous trophoblast . . . . .	98
4.3.1. Cytotrophoblast cell columns . . . . .	98
4.3.2. Cytotrophoblastic shell . . . . .	99
4.3.3. Cell islands . . . . .	99
4.3.4. Giant cells . . . . .	100
4.4. Trophoblast layer adjacent to the amnion . . . . .	100
5. Acknowledgement . . . . .	105
References . . . . .	105

## 1. Introduction

The human placenta is a versatile organ. Its 10 m<sup>2</sup> (Aherne and Dunnill, 1966) of surface are convoluted to produce a discoid structure with a diameter of about 20 cm and with a weight of about 600 g. The trophoblastic tissue is organised on a branching basis to form a chorionic villous tree (Figs. 1 and 2). The sub-units of this structure are the chorionic villi. These are hollow and finger shaped. They are usually bathed in maternal blood derived from the uterine spiral arterioles.

The placenta carries out a diversity of functions during its relatively short life span, which is on average 280 days. It is involved in the transport of water and nutrients to the fetus, removal of waste products and exchange of gases. It also actively secretes both steroid- (Ryan, 1959; Zander, 1964) and peptide-containing hormones (Jones et al., 1943; Midgely and Pierce, 1962). All of these processes require a high degree of coordination and are performed simultaneously, so it is not surprising that placental tissue has a complex ultrastructure.

The placenta has been studied extensively using both light and electron microscopy (Wislocki and Bennett, 1943; Boyd and Hughes, 1954; Alvarez, 1964;

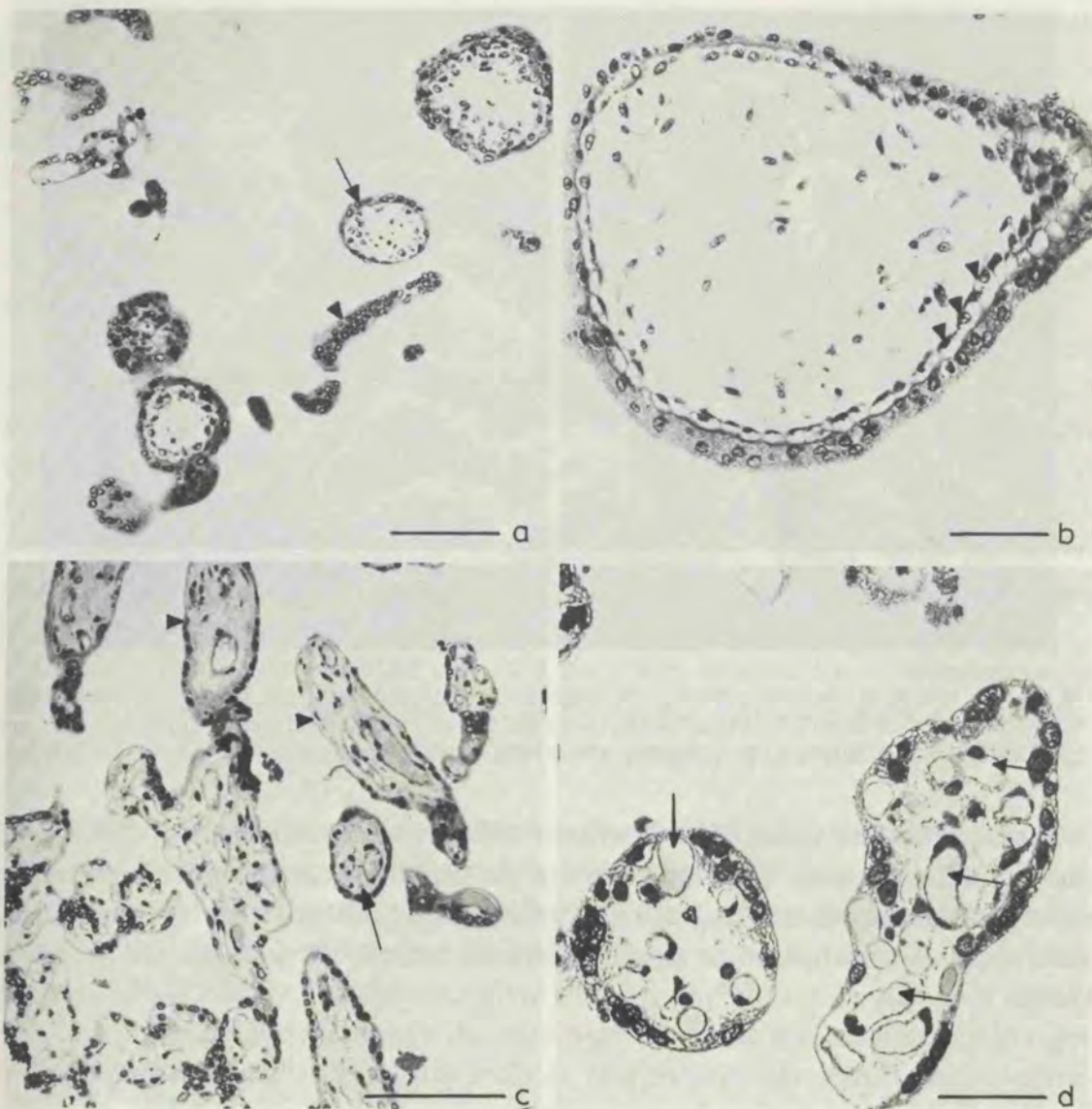


Fig. 1. (a) At low power 1st trimester chorionic villi are cut in transverse (arrow) and grazing longitudinal sections (arrowhead). Scale bar = 50  $\mu$ m. (b) At higher power the 1st trimester chorionic villus exhibits syncytiotrophoblast (\*) and cytotrophoblast (arrowheads) surrounding a mesenchymal core. Scale bar = 20  $\mu$ m. (c) At low power these term placental chorionic villi are also cut in transverse (arrow) and longitudinal sections (arrowhead). Scale bar = 50  $\mu$ m. (d) At higher power these term placental chorionic villi show virtually no cytotrophoblast, but a much more organised connective tissue core region which contains many fetal capillaries (arrows). Scale bar = 20  $\mu$ m.

Hamilton and Mossman, 1972; Fox, 1979) and there is much information available concerning placental ultrastructure and villous histology, from an early stage to term.

The placental trophoblast can be divided into cellular (cytotrophoblast) and syncytial (syncytiotrophoblast) components. The syncytiotrophoblast is a multinucleate tissue and is produced by fusion of initially separate cytotrophoblast cells. The cytotrophoblast generates all the other types of trophoblastic tissue (Boyd and Hamilton, 1970). These include the cells forming the cell columns, the cytotrophoblastic shell and the cell islands.

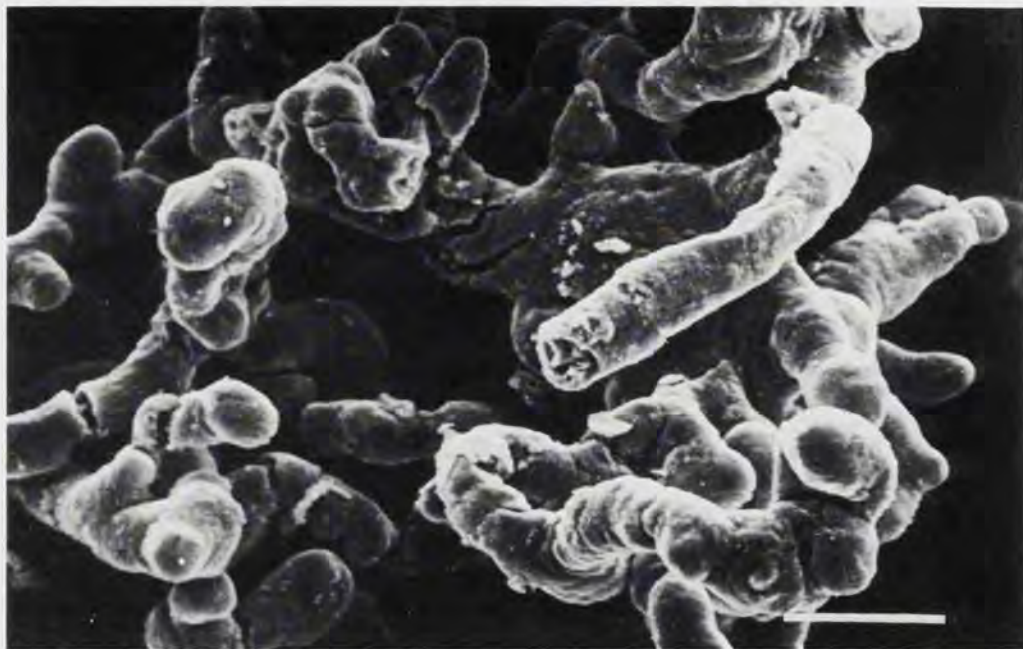


Fig. 2. This low power scanning electron micrograph of critical-point dried and gold-sputtered trophoblast exhibits the branching nature of the chorionic villous tree. Reproduced with permission from C.D. Ockleford, J. Wakely and R.A. Badley (1981) Proc. R. Soc. London, Ser. B. Scale bar = 100  $\mu$ m.

The trophoblastic tissue of the chorionic villi surrounds core zones of connective tissue continuous with Wharton's Jelly of the umbilical cord. This mesenchymal tissue is not trophoblastic and will not be considered in this article. Its properties, however, are described in an article published recently (Ockleford and Wakely, 1981).

## 2. *Development of the chorionic villi*

Between the 9th and 25th days of gestation there is a period of intense growth and differentiation, which results in the villi becoming established. Initially, vacuoles appear in the syncytium separated by the primitive villous projections or trabeculae; some of these vacuoles coalesce and produce the intervillous space. At first the trabeculae cover the whole surface of the conceptus forming the beginnings of the chorionic villous tree. As pregnancy progresses, the primitive villi orientated towards the uterine cavity regress to form the chorion laeve, while the villi on the decidua basalis side proliferate and develop into the chorion frondosum and ultimately the definitive placenta. The stimulus producing this regression is unknown but it has been suggested that it may be owing to a difference in nutritional supply after implantation (Boyd and Hamilton, 1970).

The villi are solid at first and are termed primary villi. They next develop a mesenchymal core containing fibroblasts, phagocytic Hofbauer cells (Enders and King, 1970) and collagen fibres and become secondary villi. The development of

foetal capillaries in the mesenchymal cores transform the villi into tertiary villi. Mature villi thus are composed of an outer layer of syncytiotrophoblast, a layer of cytotrophoblast (Langhans cells) resting on a basement membrane and an inner connective tissue core containing the foetal capillaries.

In the early stages of gestation (first trimester – see Fig. 1a,b) the villi are quite large in diameter, approximately 170  $\mu\text{m}$  (Fox, 1978b) and progressively decrease in diameter as term approaches (Fig. 1c,d) being on average approximately 40  $\mu\text{m}$  in diameter (Fox, 1978b).

Villous sprouts appear at about 10 wk, as protrusions on the sides and apices of the villi. They may develop mesenchymal cores and blood vessels and thus produce new villi. Some of the sprouts are reported to pinch off at their base and so enter the intervillous space (Boyd and Hamilton, 1970) and Douglas et al. (1959) report that these are often found in the maternal venous system. The significance of such transport is unknown but it has been suggested that it may affect circulating maternal antibody concentration and prevent graft rejection (Thomas et al., 1959).

Initially, the cytotrophoblast cells of a chorionic villus form a continuous layer beneath the syncytiotrophoblast but as pregnancy advances these become less prominent and in the term placenta there are very few cytotrophoblast cells present.

It is now generally accepted that the cytotrophoblast is the mitotic tissue of the placenta, giving rise to the syncytiotrophoblast, the cell columns, the cytotrophoblastic shell and the cell islands. Mitotic figures are only found in the cytotrophoblast and DNA synthesis has been shown only to occur here (Richart, 1961; Galton, 1962). The cytotrophoblast gives rise to the syncytium by fusion of mature cytotrophoblast cells resulting in the multinucleate tissue characteristic of the syncytiotrophoblast. Cells of an intermediate morphology between that of cytotrophoblast and syncytiotrophoblast have been found (Yoshida, 1964; Boyd and Hamilton, 1966). This suggests that the cytotrophoblast cells develop a morphology similar to that of syncytiotrophoblast prior to fusion. Evidence for fusion comes from micrographs in which intercellular membrane remnants have been found in the syncytium (Pierce and Midgely, 1963; Carter, 1964; Enders, 1965).

### 3. *Anchoring villi*

In addition to the chorionic villus there is another class of villus which fastens the foetal contribution of the placenta into the maternal endometrium. Examination of these villi, using scanning electron microscopy (Clint et al., 1979) has shown that these structures have a different type of surface ultrastructure from chorionic villi. Nomarski optical sections reveal that they are composed of solid trophoblast instead of having a mesenchymal core with blood vessels, as do the secondary and tertiary chorionic villi. It has been suggested by Clint et al. (1979) that these

structures are involved in supporting and suspending the chorionic villi and absorbing the mechanical strains to which they are subjected during pregnancy. They also suggest that these holdfast structures form pre-adapted weak spots 'designed' to break under stress. Rupture of these avascular structures would not have such potentially dangerous consequences as would rupture of a chorionic vilus leading to a possibly fatal mixing of foetal and maternal blood. This argument could also be extended to the syncytial bridges connecting the chorionic villi laterally. These too lack a vascular core and could be expected to yield bloodlessly if subjected to trauma.

#### *4. Ultrastructure of the trophoblast*

The two types of trophoblast will be dealt with in turn and will be described, each in terms of its characteristic complement of organelles.

##### *4.1. Syncytiotrophoblast*

Ultrastructural examination of the trophoblast (Figs. 5 and 6) shows there is considerable difference in morphology between the syncytiotrophoblast and the cytotrophoblast. The syncytiotrophoblast which is a true syncytium contains a higher concentration of organelles such as mitochondria, lysosomes, vesicles, vacuoles, microfilaments, microtubules and highly pyknotic nuclei. It also has a very electron-dense appearance owing to the abundance of endoplasmic reticulum and ribonucleoprotein. In contrast, the cytotrophoblast has little endoplasmic reticulum, a sparse population of organelles and has an electron-lucent appearance.

##### *4.1.1. Microvilli*

Electron microscopy has shown that the surface of the syncytium is covered with microvilli (Fig. 4). These are just visible at the light microscope level and were first described as a 'brush-border' by Katschenko (1885). Early in pregnancy these microvilli are long – approximately 1.5  $\mu\text{m}$  long at 10 wk (Tighe et al., 1967) and are positioned close together. As pregnancy progresses the microvilli become shorter, more branched and more separated. By term they are 0.8  $\mu\text{m}$  long (Tighe et al., 1967). Each microvillus appears to have a fibrillar core and the fibrils are sometimes seen to be continuous with fibrils in the syncytial cytoplasm of 7.5 nm in diameter.

The microvillous border shows considerable variation; some areas are reported to have no microvilli at all (Grosser, 1927; Wislocki and Bennett, 1943; Ludwig, 1974). Several scanning electron microscopy studies have been made to investigate this apparent variability in microvillous distribution (Dempsey and Luse, 1971; King and Menton, 1975; Clint et al., 1979).

King and Menton (1975) were unable to find any areas lacking microvilli al-

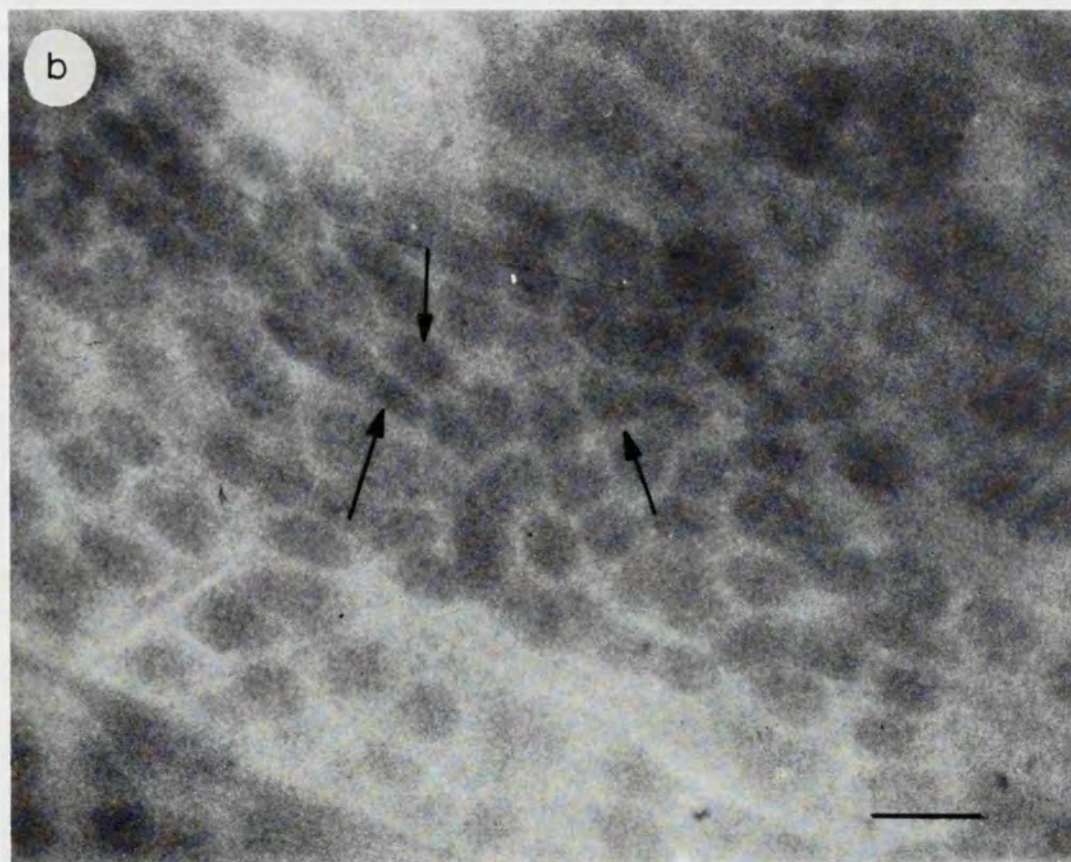
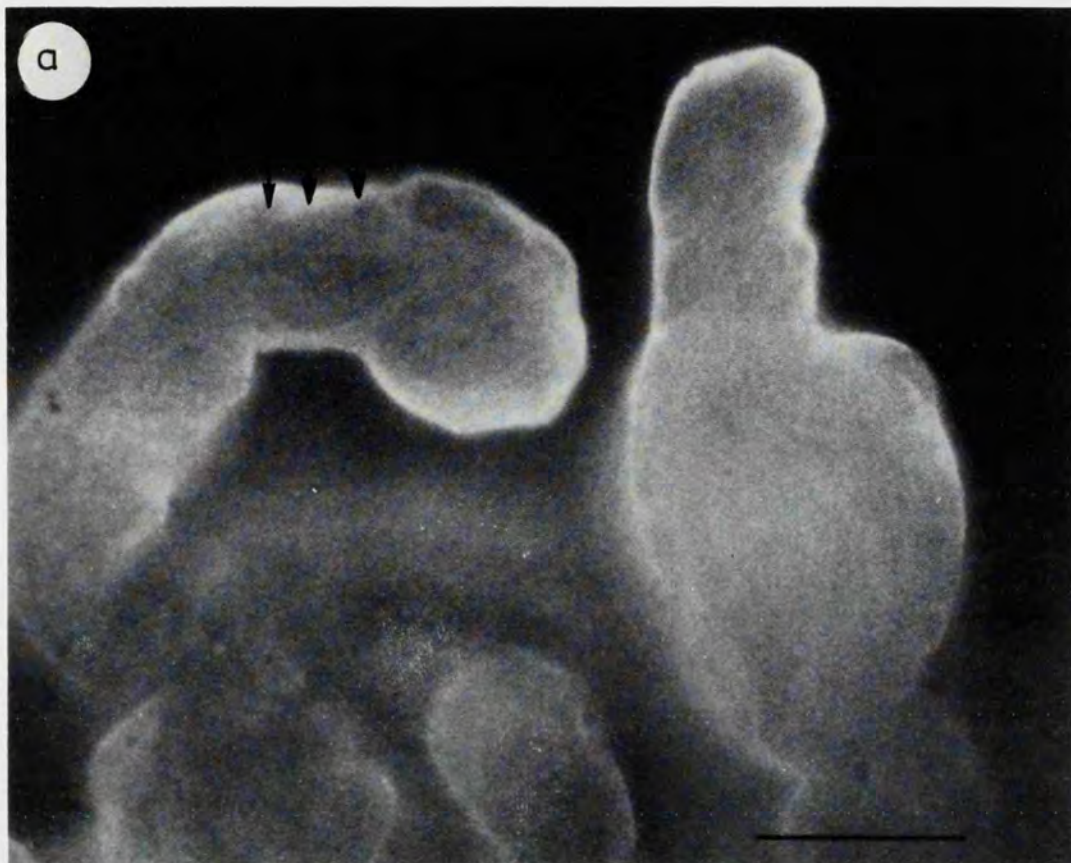


Fig. 3 (a) Indirect immunofluorescence microscopy of chorionic villi reveals a peripheral layer of tubulin (arrows) when focussed in the mid-plane of a villus. Reproduced with permission from C.D. Okleford, J. Wakely and R.A. Badley (1981) *Proc. R. Soc. London, Ser. B*. Scale bar = 10  $\mu$ m. (b) Arti-tubulin fluorescence of a chorion villus viewed 'en face' by focussing on the superficial surface of the trophoblast reveals a reticular pattern of staining (arrows). Scale bar = 2  $\mu$ m.

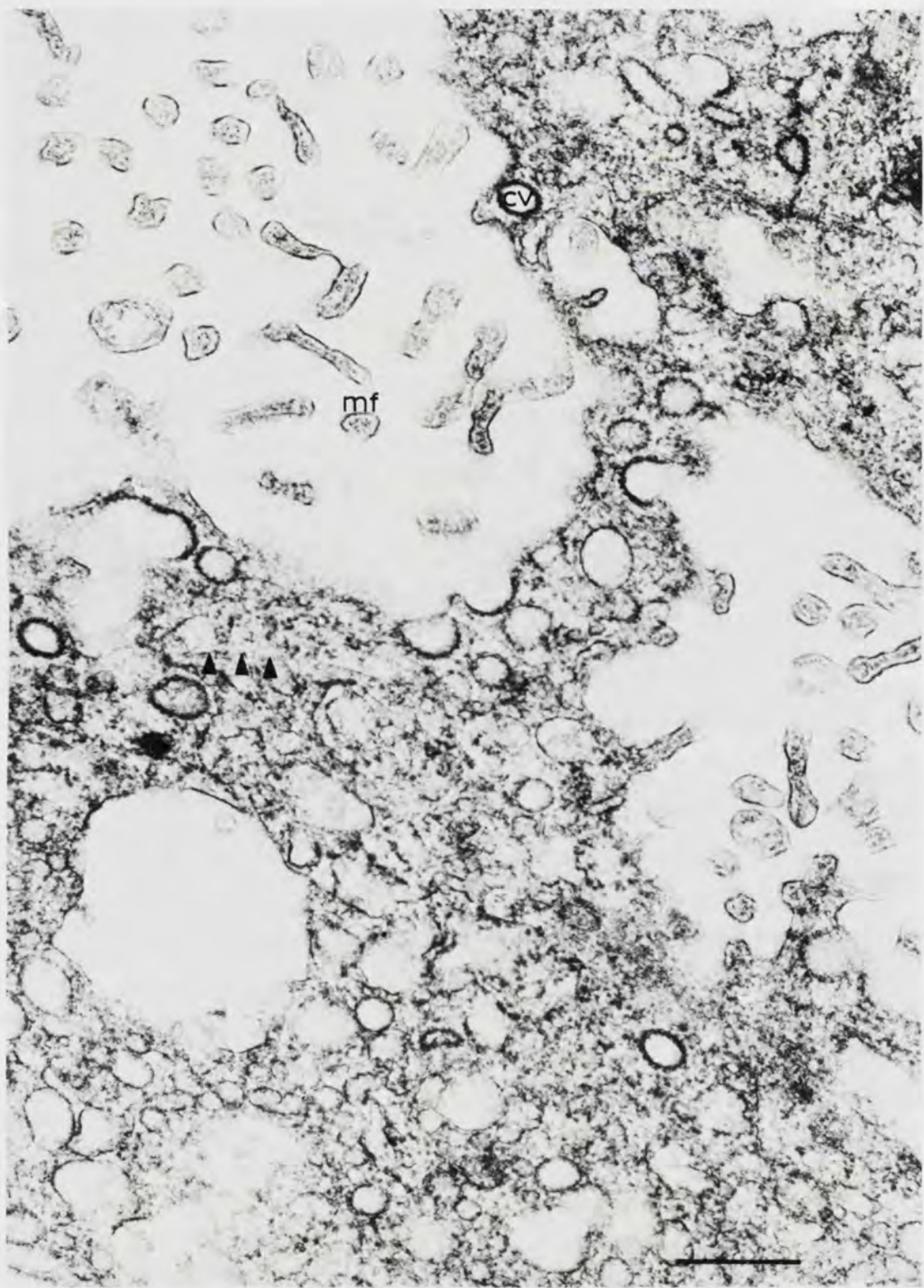


Fig. 4. Transmission electron micrograph of a section through the microvillous surface of the syncytiotrophoblast. The microvilli contain filaments (mf), 9 nm in diameter microtubules (arrowheads) are preserved using this method of fixation. Coated vesicles (cv) are commonly found components in this region. Reproduced with permission from C.D. Ockleford and A. Whyte (1977) *J. Cell. Sci.* Scale bar = 0.5  $\mu$ m.

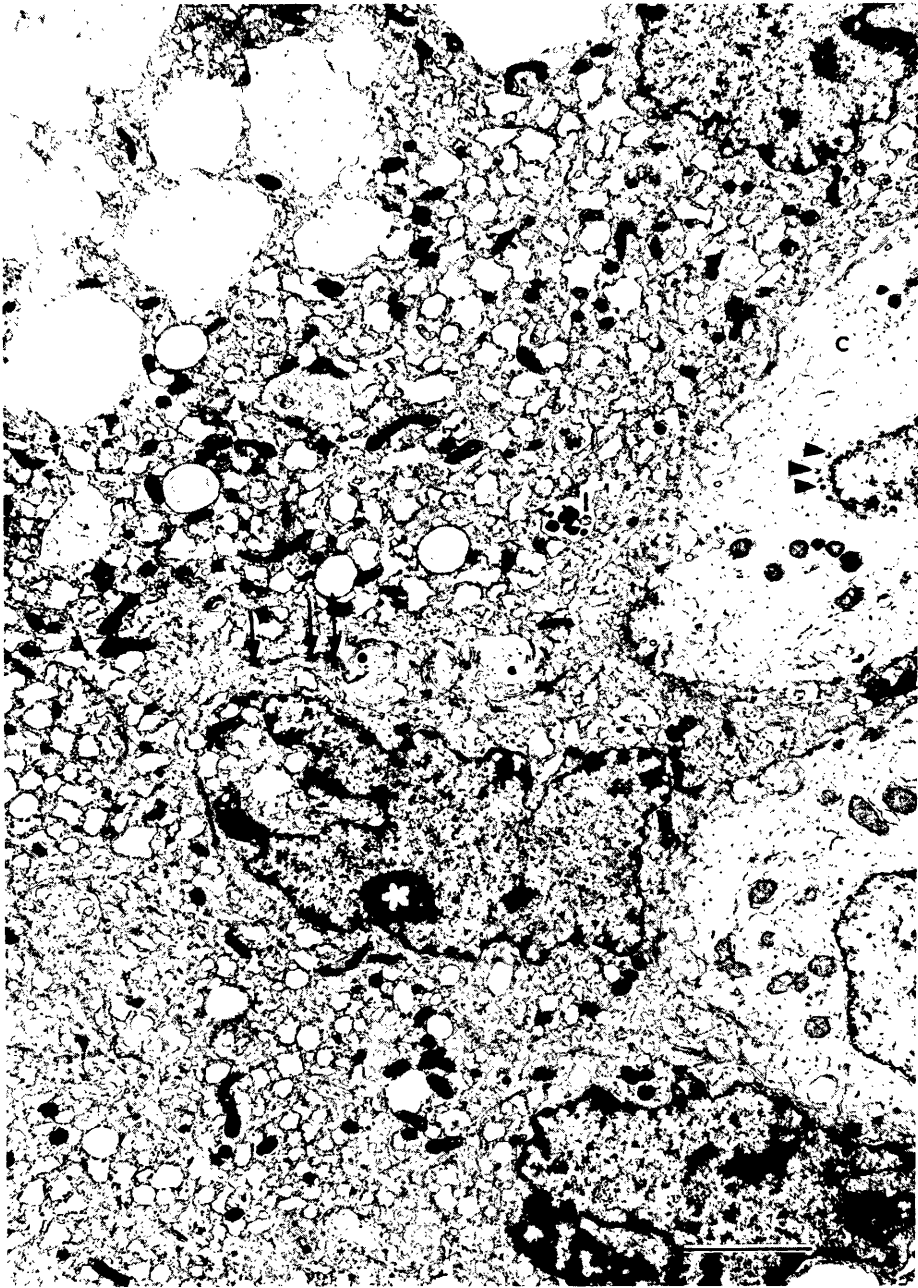
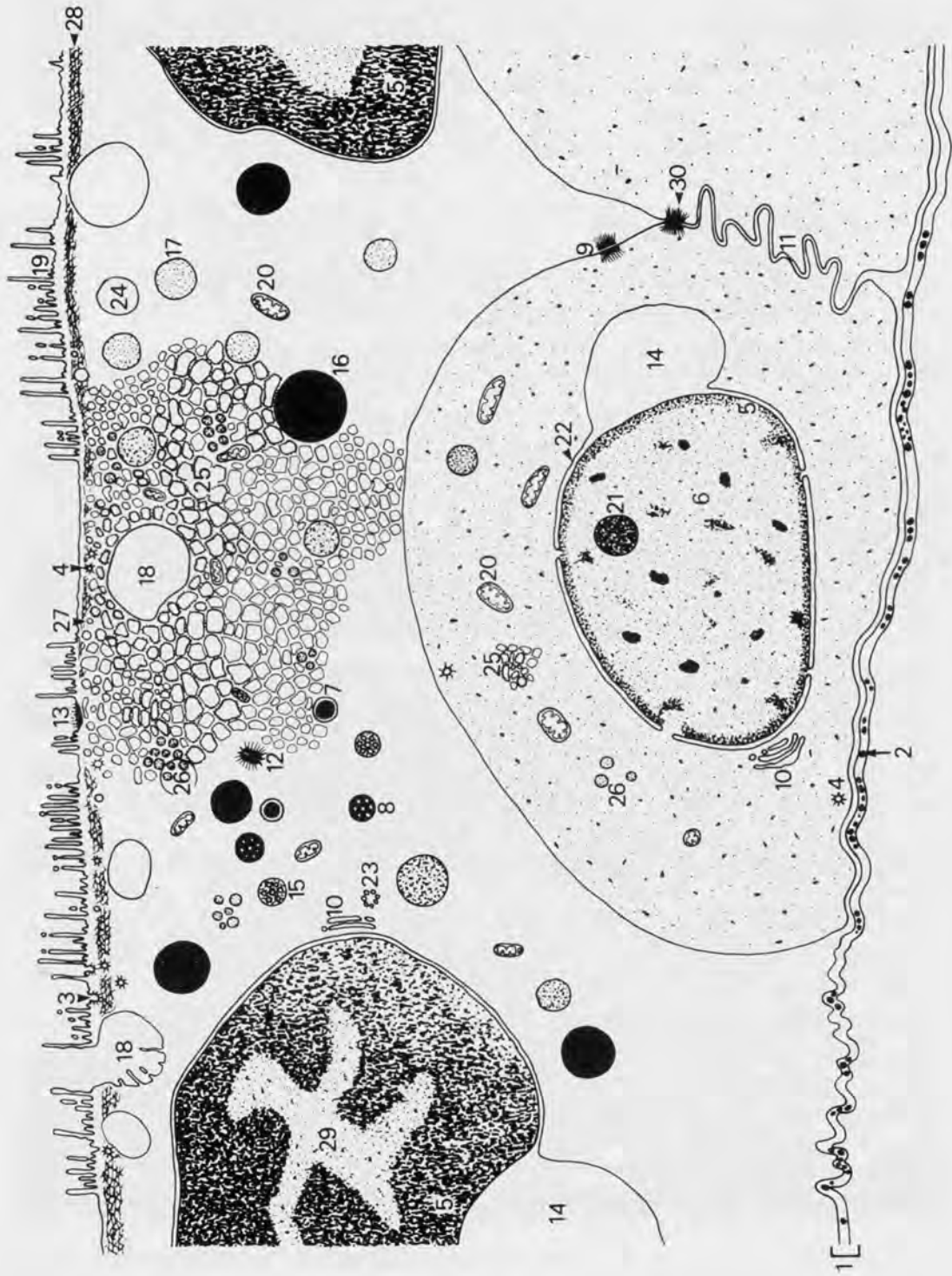


Fig. 5. Transmission electron micrograph of first trimester trophoblast. The cytotrophoblast cells (c) contain nuclei, the envelopes of which are densely studded with nuclear pores (arrowhead). One syncytial nucleus (\*) appears to have been incorporated recently into the syncytioplasm because traces of limiting membranes and associated desmosomes (arrow) remain. Also in the vicinity are secondary lysosome-like structures (l) which may have mediated the fusion process. Scale bar = 2  $\mu$ m.



though Clint et al. (1979) found a complete gradation of surface microvillar structures. Boyd and Hamilton (1967) and Panigel and Anh (1964) also noted the occurrence of such 'bald' areas as did Dempsey and Luse (1971). These smooth areas are randomly distributed and only occupy a small portion of the villus. The transition from microvillar covering to smooth area is gradual. The only areas to consistently lack microvilli are the vasculo-syncytial membranes (Fox and Agrofojo-Blanco, 1974).

*4.1.1.1. Function of microvilli* The function of these microvilli is uncertain, although several suggestions have been put forward.

(a) They may increase the surface area of the villi in contact with maternal blood and therefore possibly facilitate placental transfer.

(b) A similarity of the microvilli to the brush-border of the intestinal and renal epithelium (King and Menton, 1975) led to the suggestion that the microvilli may have a similar absorptive function. However, Boyd et al. (1968a) pointed out that there is only a superficial similarity between trophoblastic and these other epithelial microvilli. They are much less systematically arranged and show less morphological stability.

(c) An excretory function has been proposed (Salazar and Gonzalez-Angulo, 1967). Sometimes the ends of the villi are swollen and contain flocculent material and occasionally these can be seen pinching off into the intervillous space (Wislocki and Dempsey, 1955; Wakitani, 1961; Lister, 1963b). It is possible that these are artefacts resulting from poor control of  $Ca^{2+}$  levels in the fixative.

(d) Since there is a direct relationship between the density of microvilli and the degree of pinocytotic activity at that site (Fox, 1979), it has been suggested that the microvilli and their associated microfilaments are involved in vesicle closure and membrane flow (Allison and Davies, 1974).

(e) It has also been proposed that the microvilli increase the number and vari-

Fig. 6. A diagram which indicates the ultrastructural features of placental-disc trophoblast cells described in the text.

- |  |   |
|--|---|
| (1) Basal lamina                       | (17) Lysosome   |
| (2) Calcium containing granule         | (18) Macropinocytic vesicle   |
| (3) Coated pit                         | (19) Microvilli   |
| (4) Coated micropinocytic vesicle      | (20) Mitochondrion  |
| (5) Condensed chromatin                | (21) Nucleolus  |
| (6) Cytotrophoblast nucleus            | (22) Nuclear envelope   |
| (7) Dense body                         | (23) Pre-multivesicular body (Pre-MVB)  |
| (8) Dense multivesicular body (D-MVB)  | (24) Receptosome-like organelle   |
| (9) Desmosome                          | (25) Rough endoplasmic reticulum  |
| (10) Golgi apparatus                   | (26) Secretory granules   |
| (11) Interdigitating microvilli        | (27) Smooth micropinocytic vesicle  |
| (12) Intrasyncytial desmosome          | (28) Syncytioskeletal layer (microtubules, microfilaments and intermediate filaments) |
| (13) Iron-binding organelle            | (29) Syncytiotrophoblast nuclei   |
| (14) Juxtannuclear vacuole             | (30) Tonofilaments  |
| (15) Light multivesicular body (L-MVB) |   |
| (16) Lipid droplet                     |   |

ety of surface receptor sites (Dempsey and Luse, 1971), which will become internalised in coated vesicles (Ockleford and Whyte, 1977). In the case of receptors for transferrin there is now good evidence that these are present on microvilli and in coated vesicles (Booth and Wilson, 1981).

Whatever the function of the microvilli it seems that they have an important role, since if maternal nutrient supply is restricted there is a proliferation of the microvilli (Jones and Fox, 1979).

#### 4.1.2. *Vasculo-syncytial membranes (VSMs)*

These are areas on the chorionic villi which have a very thin syncytiotrophoblast, no cytotrophoblast layer, no nuclei and lack a microvillar border. Light microscopically, the thinned syncytium appears to be fused with the walls of the underlying foetal capillaries. However, ultrastructural examination shows that this is not a true fusion, just that the two areas are closely apposed (Strauss et al., 1965).

They have a random distribution and may appear in scanning electron micrographs as dome-shaped protrusions bulging into the intervillous space (Fox and Agrofojo-Blanco, 1974). It is not known how these structures are formed but their random distribution suggests that they are not derived by mechanical stretching, as was proposed by Pisarki and Topilko (1966).

The function of these regions is also unknown but it has been suggested that they are specialised areas developed to enhance gas exchange (Baker et al., 1944; Getzowa and Sadowsky, 1950; Hormann, 1958; Becker and Bleyl, 1961). However, this would only be important if epithelial resistance is a limiting influence on the rate of diffusion, and, according to Longo (1972), this is not the case. Comparative studies (see Steven, Ch. 4) of the placenta tend to support Longo's view because thicker 'placental barriers' in other species do not exhibit VSMs and evidently gas transport is sufficient. This debate, however, cannot be said to be closed because Fox (1967) reports that a deficiency of VSM in term placentae is associated with high incidence of foetal hypoxia.

Although the capillary and trophoblastic walls are thinner overall in the vasculo-syncytial membranes, immunofluorescence staining of polymeric cytoskeletal proteins in these areas (Figs. 3a,b and 4) show no obvious local reduction in the thickness of this component of the epithelium (Ockleford et al., 1981).

#### 4.1.3. *Nuclei*

The syncytial nuclei have coarse chromatin scattered throughout the nucleoplasm and aggregated around the nuclear envelope. Tangential sections through the nuclei show the presence of numerous nuclear pores 80 nm in diameter, a characteristic of synthetically active cells (Tighe et al., 1967).

In some of the mature villi the nuclear chromatin is highly pyknotic. Such nuclei are often found aggregated together into groups or syncytial knots.

#### 4.1.4. Syncytial knots

It has been suggested that this grouping together into knots is a sequestration phenomenon (Fox, 1965), collecting together aged nuclei as they are replaced by the proliferative activity of the cytotrophoblast. This idea is supported by the fact that only those nuclei in the knots show morphological changes associated with ageing (Fox, 1965; Boyd and Hamilton, 1970). Also villi with knots have a higher total number of nuclei than villi which have no knots.

#### 4.1.5. Syncytial bridges

Sometimes syncytial knots from adjacent villi fuse together forming an intervillous bridge. (In vitro fusion of knots has been demonstrated by Jones and Fox, 1977.) It has been suggested that these bridges form an internal strut system and act in the same way as has been proposed for the anchoring villi, absorbing stress and strain.

#### 4.1.6. Rough endoplasmic reticulum

The rough endoplasmic reticulum (RER) is a very prominent feature of the syncytium and contributes extensively to the vesiculated appearance of the cytoplasm. Maximal quantities of RER are observed after 10 wk of gestation (Tighe et al., 1967) and Boyd and Hamilton (1970) have observed that in the period immediately prior to parturition there is a reduction in the quantity of RER present. The RER is seen in the syncytium as cisternae, most of which are circular in cross-section and between 0.1 and 1  $\mu\text{m}$  in diameter (Ashley, 1965), but some have a 'peanut shape' cross-section to which Sawasaki et al. (1957) drew attention. It is these profiles which indicate that these cisternae are in communication with each other and form a canalicular system.

The RER cisternae also possess ribosomes on their external surface which distinguish them as part of the endoplasmic reticulum and separate from the other vesicles and vacuolar structures.

The RER cisternae are in communication with the juxtannuclear vacuoles and with the perinuclear space.

In some regions a transition can be seen from ribosome-covered RER into smooth cisternae. This is the smooth endoplasmic reticular system and more obviously forms a canal system (Boyd et al., 1968a).

#### 4.1.7. Mitochondria

These are numerous in the syncytium throughout gestation, as expected of an active tissue, and are round or elongated with characteristically lamellar cristae (Boyd and Hamilton, 1970). They are usually smaller than those found in the cytotrophoblast (Dempsey and Luse, 1971).

#### 4.1.8. Golgi complex

This is present in the syncytiotrophoblast (Boyd and Hamilton, 1970) and ac-

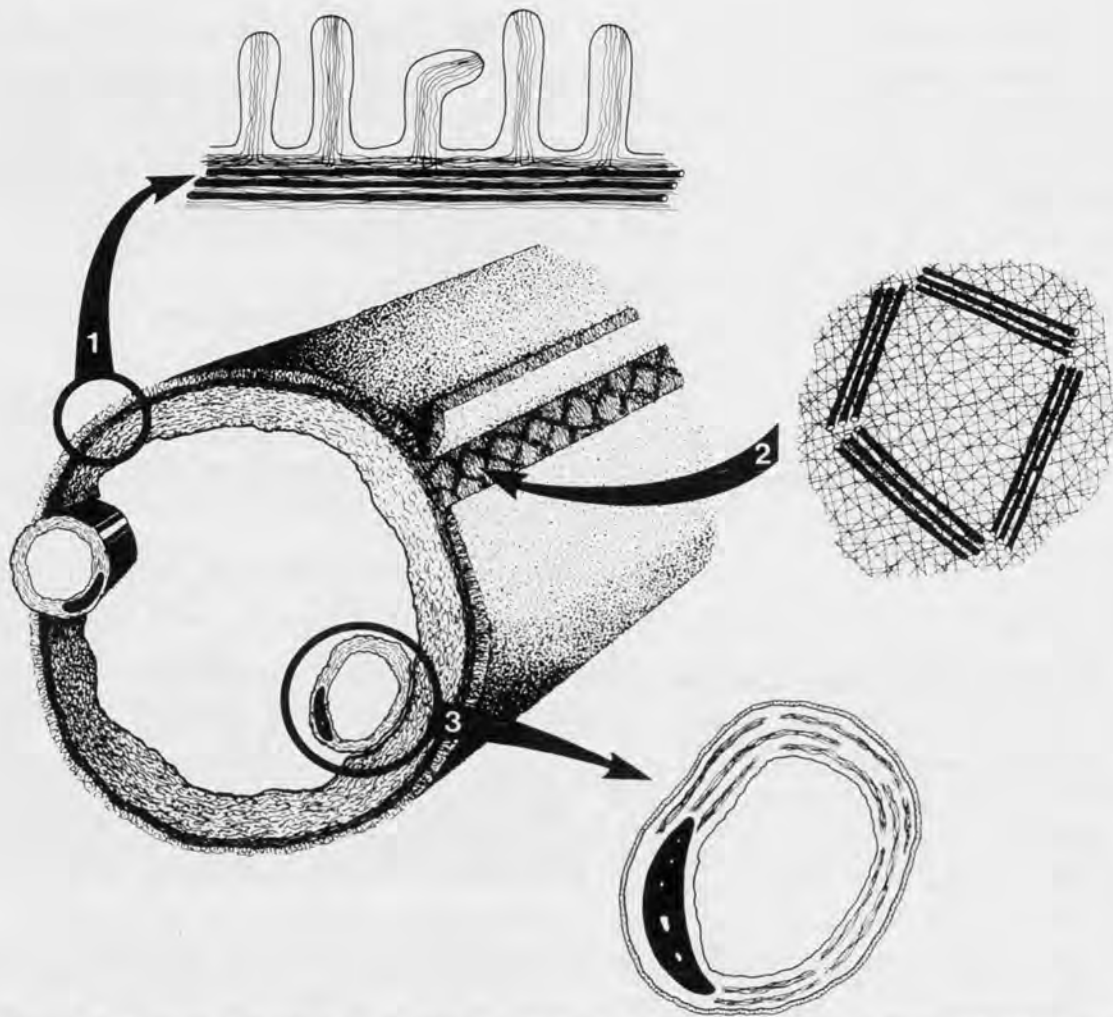


Fig. 7 A diagram indicating the positions where actin, tubulin, intermediate filament protein and fibronectin are found in the chorionic villus. The cortical layer containing the network of microtubules and the microfilament mesh has been given the name 'the syncytioskeletal layer'. (1) A section through the syncytioskeletal layer showing a mesh of actin microfilaments, some of which pass up into the microvilli, and relatively fewer microtubules. (2) A plan view of the syncytioskeletal layer which reveals that tubules are arranged in an open lattice network. (3) Enlargement of a transverse section through a foetal capillary. The wavy circumferential tresses in the cytoplasm of the endothelial cells represent intermediate filaments of vimentin. The outer layer of the capillary, the endothelial basal lamina is the site where fibronectin is localised. Reproduced with permission from C.D. Ockleford, J. Wakely and R.A. Badley (1981) Proc. R. Soc. London, Ser. B.

According to Ashley (1965) can be seen more easily in young placenta. In mature placenta it is often difficult to see owing to the intense vesiculation of the syncytial cytoplasm and because these organelles are smaller, rarer and less well organised than one would expect of a secretory tissue.

#### 4.1.9. Ribosomes

These are abundant, occurring both free in the syncytioplasm as polysomes and attached to the endoplasmic reticulum.

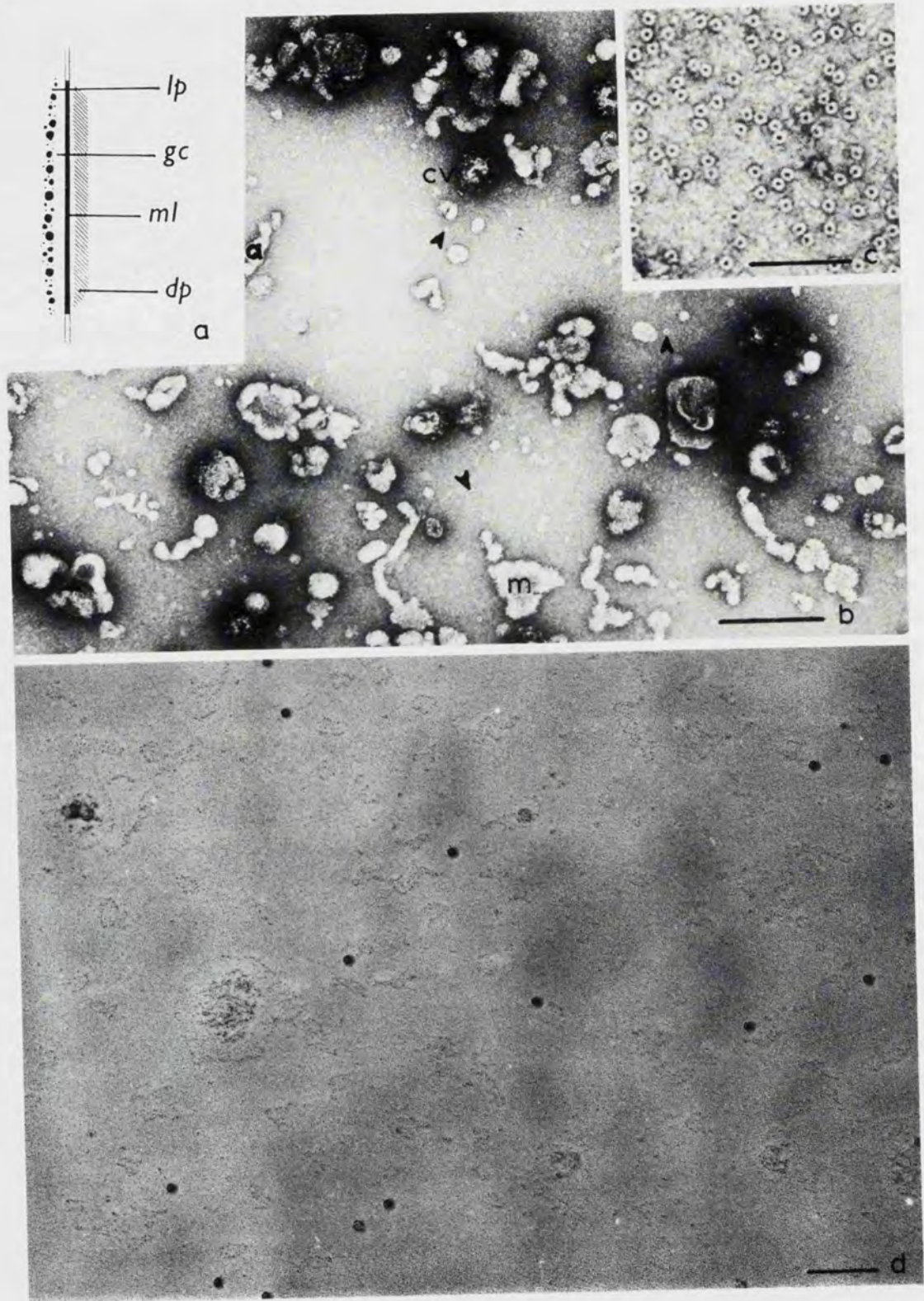
#### 4.1.10. *Polymeric cytoskeletal proteins (Fig. 7)*

Wislocki and Bennett (1943) have described a birefringent layer which exists just below the syncytial plasma membrane which is in contact with maternal blood. The implication of this result is that there are ordered linear arrays of molecules in this region. Our view is that at least part of this birefringence results from the presence of the 'syncytioskeletal layer' (Ockleford et al., 1981) which contains filamentous actin and microtubules.

**4.1.10.1. *Microtubules*** These organelles (Fig. 4) have a diameter of 24 nm and have been identified ultrastructurally (Ockleford and Whyte, 1977). Recently indirect immunofluorescent staining methods using antibody directed against the major protein of microtubules (tubulin) have indicated the presence of a layer in the syncytium sub-adjacent to the maternal cell surface where there is a high concentration of microtubules (Fig. 3a,b). En face examination of this layer reveals it has an open pattern in some places similar to chicken wire but in others arranged in longitudinal or circumferential bands around the villus (Ockleford et al., 1981).

**4.1.10.2. *Microfilaments*** These are 8 nm diameter filaments. In the placenta they have been identified just below the maternally opposed surface of the syncytiotrophoblast and directly beneath the plasma membrane. These filaments are probably involved in morphogenesis of microvilli (Ockleford et al., 1981) and possibly also in the process of endocytosis which leads to the formation of phagocytic and macropinocytic vesicles (Allison and Davies, 1974). As with tubulin the protein actin has been demonstrated by indirect immunofluorescence at this site. Unlike tubulin the actin-containing microfilamentous layer when viewed en face is complete (Ockleford and Wakely, 1981; Ockleford et al., 1981). It has recently been suggested that the anisometric shape of the villous tree probably owes its support to the actin and tubulin polymers, which coincide in position with a layer just beneath the syncytial cell surface which has been designated the syncytioskeletal layer (Ockleford and Wakely, 1981; Ockleford et al., 1981).

**4.1.10.3. *Intermediate filaments*** Unlike tubulin and actin which are widespread in different cell types, the proteins of intermediate filaments exhibit a degree of tissue specificity. For example, cytokeratins are found in cells of epithelia which have ectodermal ontogeny, whereas vimentin is characteristic of cells of mesenchymal origin. The filaments which these proteins form are morphologically very similar with a diameter of 10 nm. Indirect immunofluorescence microscopy has shown the presence of cytokeratins in the syncytioskeletal layer (Ockleford et al., unpubl. data). There is no staining of the term syncytium with a serum directed against desmin and vimentin under conditions where other cells in the same preparation are brightly fluorescent. These results support the view that trophoblast is an ectodermal derivative and interestingly parallel the results obtained by Jack-



son et al. (1980) showing the presence of cytokeratins in preimplantation mouse embryos only in the trophectoderm and not in the inner cell mass.

#### 4.1.11. Myelin figures

Residual bodies containing myelin figures are sometimes seen in the syncytial cytoplasm (Tighe et al., 1967).

Myelin figures consist of concentric electron dense membranes approximately 18 nm thick separated from each other by a space of approximately 6 nm (Salazar and Gonzalez-Angulo, 1967). They are most frequently found in late pregnancy and probably represent alterations in the molecular organisation of the phospholipids of the various cytoplasmic membrane systems (Salazar and Gonzalez-Angulo, 1967). The presence of myelin figures is usually interpreted as a sign of cellular damage, but in the placenta their occurrence is considered to be one of the ageing changes typical of this late gestational period (Salazar and Gonzalez-Angulo, 1967).

#### 4.1.12. Glycogen

Glycogen is found in the syncytium in small clusters and individual particles (Fox, 1978a). It is abundant in the cytoplasm and in the syncytial sprouts (Boyd, 1959). Examination of early chorionic villi shows glycogen-like material is present in the intervillous space and in the mesodermal villous core. Boyd (1957) proposes that this external glycogen is derived from erosion of endometrial glands and may be taken up by the syncytium and thus comes to be included in the vacuoles.

Since the syncytium is known to phagocytose such large particles as endometrial debris (Boyd, 1959) and blood cells (Clint et al., 1979) it is possible that particulate glycogen is taken up this way also. (See Chapter 7 by Contractor with regard to glycogen metabolism in the placenta.)

#### 4.1.13. Lipid droplets

These range between 0.4 and 1.0  $\mu\text{m}$  in diameter (Tighe et al., 1967). They are electron-dense, homogeneous and have no limiting membrane. They are most numerous in young placentae and are very sparse at term. It has been suggested that these lipid droplets are nutritive fat in transit from mother to foetus (Rhodin and Terzakis, 1962). If this was so it would be expected that fat would be found

---

Fig. 8. (a) Diagram of a differentiated region of iron binding to cell surface. Iron particles (Ip) are separated by an electron lucent layer (gc) from the membrane layer (ml). Beneath this and colinear with the iron particles is an electron dense plaque (dp). Reproduced with permission from C.D. Okleford and G. Menon (1977) *J. Cell Sci.* 25, 279–291.

(b) An isolated fraction of homogenised placenta negatively stained with uranyl acetate showing membrane fragments (m), coated vesicles (cv) and small annular profiles (arrowheads) which are probably ferritin molecules. Scale bar = 200  $\mu\text{m}$ . (c) Higher resolution images of the annular profiles described in (b). Scale bar = 0.1  $\mu\text{m}$ . (d) Low angle rotary shadowed images of ferritin molecules (arrows) which were isolated from placental homogenates by Dr. A. Booth. The shadowing was accomplished with platinum.

in other sites but little lipid is found in the cytotrophoblast or in the villous core.

These lipid droplets have also been suggested to contain oestrogen and progesterone (Wislocki and Bennett, 1943; Wislocki et al., 1948; Wislocki and Dempsey, 1955). When these hormones have a high level of output (at term) the amount of lipid present is very low (Amoroso, 1960). There is an obvious need to elucidate any correlation between the rate of steroid secretion and the number of lipid droplets present before making a definite statement that these droplets contain steroids. The possibility that the lipid represents stored precursors for membrane biosynthesis or the steroid hormone synthetic pathways, deserves serious consideration.

#### *4.1.14. Secretion granules*

These are round or oval in shape and have a moderate to great electron density. They vary in size from 50 nm to 2  $\mu$ m and were at first thought to be enclosed by a single smooth membrane (Yoshida, 1964). However, Tighe et al. (1967) report that the secretion granules they observed had a double limiting membrane.

Secretion granules are most common in the Golgi area and are present from 10 wk to term (Tighe et al., 1967). Their size appears to increase towards the syncytial surface. As they approach the surface Yoshida (1964) reports that they lose their dense appearance and their contents become flocculent. This seems to suggest that they are produced by the Golgi and liberate their contents into the maternal blood. Salazar and Gonzalez-Angulo (1967) also noted these flocculent granules and suggested they had an excretory function.

Yoshida (1964) suggests that these granules contain protein, possibly HCG or its precursor, but equally plausibly some of the granules may contain human chorionic somatomammotrophin (HCS), or any other proteinaceous placental product. Tighe et al. (1967) noted that the number of secretion granules increased towards term and suggested that this corresponded with the rising output of oestrogen and progesterone at this time.

Using peroxidase conjugated anti-HCG sera Dreskin et al. (1970) showed that HCG was only localised in the endoplasmic reticulum and there was no staining of the secretory granules. Again there is a need for clarification of the situation.

#### *4.1.15. Iron-binding organelle (Fig. 8a)*

An ultrastructural study of placental tissue incubated in the presence of ferric sodium citrate (Ockleford and Menon, 1977) showed accumulation of iron particles adsorbed to the cell surface in positions where an electron dense plaque was visible beneath the phospholipid bilayer (Fig. 8a). A narrow electron-lucent space between the iron particles and the phospholipid bilayer may indicate the presence of cell surface receptors such as transferrin. Transferrin is a component of the placenta (Booth and Wilson, 1981) and can be visualised immunocytochemically (King, 1976).

#### 4.1.16. Calcium deposits

Bargmann and Knoop (1959) and Terzakis (1963) described granular electron dense bodies associated with the basal lamina. They proposed that these were lipid deposits. However, they correspond with granular electron dense bodies described by Tighe et al. (1967) as calcium salts and their distribution correlates with that of calcium salts on the basal lamina using light microscope histochemistry.

Using the divalent cation pyroantimonate precipitation method, electron dense deposits indicating the presence of cations have been localised ultrastructurally to the basal lamina and its granules (Ockleford and Whyte, 1977).

Calcification has been regarded as an age-related change but there is no evidence that this particular process interferes with placental function. Fox (1978a) regards calcification as non-senescent since in some prolonged pregnancies calcium can be lost from the placenta.

#### 4.1.17. Iron

Dempsey and Wislocki (1944) examined the distribution of iron in the placenta and found the greatest concentration was in the syncytiotrophoblast. It was evenly distributed throughout the syncytial cytoplasm with a heavier deposit around the nuclear envelope. They suggest this perinuclear iron represents that which has been organically bound to the respiratory enzymes.

Some iron was also found in the Langhans cells, the cell columns and the cytotrophoblastic shell.

Wislocki and Dempsey (1946) report that these deposits diminish as pregnancy progresses. Iron is present complexed with protein in the form of haemosiderin and ferritin. Ferritin can be visualised as a tubular structure in negatively stained (Fig. 8b,c) and low-angle rotary shadowed (Fig. 8d) preparations of isolated fractions of placental homogenates.

#### 4.1.18. Vacuoles

The syncytiotrophoblast has a characteristically highly vesiculated appearance owing to an abundance of vesicles most of which are in the size range up to 150 nm in diameter (Boyd and Hamilton, 1970). However, there is considerable confusion in the literature concerning this wide variety of organelles and their functions. (At low magnification it is easy to confuse cisternae of the rough and smooth endoplasmic reticular systems with the fluid-filled components of the vacuolar system.)

Large vacuoles can be found such as the juxtannuclear vacuoles, lagoons, receptosomes, lysosomes, multivesicular bodies and macropinocytic vesicles. There is also a finer vacuolation consisting of micropinocytic vesicles.

*4.1.18.1. Juxtannuclear vacuoles.* These are large vacuoles approximately 0.8–10  $\mu\text{m}$  in diameter. They have a close relationship with the syncytial nuclei, frequently distorting the nuclei into crescentic shapes (Boyd et al., 1968b). They also communicate directly with the perinuclear space. Boyd et al. (1968a) suggest that

they are part of the endoplasmic reticulum since they have observed ribosomes lying along the thin walls of the vacuoles. In some micrographs they report that there are communications between the endoplasmic reticulum and the juxtannuclear vacuoles.

*4.1.18.2. Lagoons* These vacuolar structures occur throughout pregnancy in certain regions on the surface of the chorionic villi (Boyd et al., 1968a; Boyd and Hamilton, 1970). They are located immediately beneath the syncytial surface and like the juxtannuclear vacuoles are dilated and appear to be in communication with each other and have some similarities to the receptosome of cultured fibroblasts (Willingham and Pastan, 1980).

*4.1.18.3. Lysosomes* Lysosomes are numerous in the syncytiotrophoblast (Contractor, 1969; Corash and Gross, 1973, 1974). They are small round bodies 800–1400 nm in diameter (Tighe et al., 1967), have a single limiting membrane 6–7 nm thick (Rhodin and Terzakis, 1962) and usually have finely granular contents. These are separated from the single limiting membrane by a zone of low electron density 12 nm wide (Tighe et al., 1967). They stain densely and homogeneously for acid phosphatase (Contractor et al., 1977) and are variable in shape and distribution, although they are most numerous in the basal third of the syncytium aggregating near to the junction between the cytotrophoblast cells and the overlying syncytium (Contractor et al., 1977). They are present in greater numbers in the first trimester placenta (Jones and Fox, 1976) and as pregnancy proceeds their acid hydrolytic activity decreases (Corash and Gross, 1974).

Contractor et al. (1977) have proposed that their main role is the transformation of cytotrophoblast cells into syncytiotrophoblast. This idea is consistent with the fact that phospholipases occur in lysosomes from other cells (Smith and Winkler, 1968; Fowler and De Duve, 1969). Lysolecithin has been implicated in membrane fusion processes and can be produced by the action of phospholipase A1 on lecithin – a phospholipid constituent of membranes (Guttler and Clausen, 1969; Poole et al., 1970). If lysosomes are involved in membrane fusion and breakdown this would account for the presence of aggregations of primary lysosomes in the region of the cytotrophoblast-limiting membrane (Contractor et al., 1977) and the occurrence of free lysosomal enzymes in the space between the two plasma membranes (Contractor et al., 1977). Secondary lysosomes have been reported close to membrane fragments (Contractor et al., 1977) and other lysosomal structures have been seen to contain pieces of membrane (Rhodin and Terzakis, 1962). This strongly suggests that lysosomes are involved in membrane breakdown. Other functions have been proposed for these lysosomal structures including transfer and secretory mechanisms. However, the fact that their activity is reduced after the first trimester (Corash and Gross, 1974) suggests that their main role is during the time when they appear to be active in the remodelling of the placenta.

Evidence that they have a transfer function comes from the observation that in some of the lysosomes large granules can be seen and it is possible to trace transitions from these into multivesicular bodies (Tighe et al., 1967).

*4.1.18.4. Multivesicular bodies (MVBs)* MVBs consist of a number of membranous vesicles enclosed within another membrane (Sotelo and Porter, 1959). The average diameter of contained vesicles is approximately 50 nm (Tighe et al., 1967). MVBs have acid phosphatase activity (Contractor et al., 1977) although they do not seem to be autophagic. In addition, they also have an acid mucopolysaccharide coat on the inner surface of the limiting membrane and the outer surface of the individual vesicles. Tighe et al. (1967) believe that this implies that the small vesicles bud off from the limiting membrane.

Martin and Spicer (1973b) identified different types of MVB which they called pre-MVB, light MVB, dense MVB and dense bodies. These structures showed similar staining patterns with histochemical reagents which implied that they are related to each other. Martin and Spicer (1973b) propose that they are different states of the same organelle engaged in one basic function. All the different states of MVBs mentioned above are found quite frequently in the syncytiotrophoblast.

(i) *Pre-multivesicular body (Pre-MVB)*. These are most commonly found in the Golgi region. They consist of a circle of small vesicles surrounding a pale finely particulate centre area. The size of these vesicles is approximately 60 nm in diameter and Martin and Spicer (1973b) report a range of between 2 and 30 vesicles forming each cluster.

(ii) *Light multivesicular body (L-MVB)*. These are approximately 700 nm in diameter and consist of a number of vesicles again with a diameter of 60 nm enclosed in a membrane. The number of enclosed vesicles is variable again having a range of 2–30 (Martin and Spicer, 1973b). In addition to the vesicles another structure, the nucleoid is often present. This is approximately 200 nm in diameter and occupies about one-third of the L-MVB. It has no limiting membrane and consists of more dense particulate material than the matrix. The function of the nucleoid is unknown.

(iii) *Dense multivesicular body (D-MVB)*. Condensation of the L-MVB is thought to produce the dense MVBs (Martin and Spicer, 1973b). These are similar to the L-MVBs and often have nucleoids, but have a much more electron dense matrix. They also have a zone of exclusion of other organelles around them.

(iv) *Dense bodies*. These are smaller than the other dense MVBs, having a diameter of approximately 400 nm. They have a membrane enclosing a dark matrix. Usually there are no enclosed vesicles. Martin and Spicer propose that these dense bodies are the residues of MVBs. Rarely 'organoids' (Martin and Spicer, 1973b) are found within the dense bodies. These are regions which have a regular pattern of electron density.

(v) *Function of MVBs*. Martin and Spicer (1973b) propose that MVBs are involved in transport and suggest that they are able to selectively bind certain proteins for transplacental transport. In their view the unbound material is hydrolysed by lysosomes. MVBs are known to be involved in uptake of endocytosed protein in a variety of cell types (Kraehenbuhl and Campiche, 1969) and peroxidase and ferritin have been shown to appear in MVBs after a few minutes of

exposure in guinea-pig and bat placenta (Enders and Wimsatt, 1971; King and Enders, 1971) and a few hours later in the dense bodies.

The size of the enclosed vesicles in the MVBs is similar to the size of micropinocytotic vesicles. It may be that the MVBs take in the vesicles and break them open since the MVBs have been shown to have degradative enzyme activity (Martin and Spicer, 1973b). Since lysosomes have been observed to fuse with MVBs it may be that it is from these that the acid phosphatase activity of the MVBs is derived. The sequence of events may be fusion of coated vesicles with the MVBs, then fusion with lysosomes. Since Lin (1980) has provided evidence for the uptake of IgG by similar means there is direct evidence for this. It is, therefore, possible that the MVBs described by Martin and Spicer (1973b) may in fact correspond to the receptosomes described by Willingham and Pastan (1980) in fibroblasts, since they described the appearance of the receptosome as frequently containing intravesicular small, round, circular membraneous structures.

#### 4.1.19. Vesicles

These will be dealt with in turn.

*4.1.19.1. Pinocytotic vesicles* Pinocytosis occurs in the syncytium during the whole of the gestational period (Wislocki and Bennett, 1943; Boyd and Hughes, 1954; Wislocki and Dempsey, 1955; Wakitani, 1961; Rhodin and Terzakis, 1962; Lister, 1963b). Pinocytotic vesicles are most common in the surface membrane region and contribute to the general vacuolation of the syncytium. Pinocytotic vesicle formation occurs at the base of and between the microvilli (Ockleford, 1976) and there is a correlation between the density of the microvilli and the degree of pinocytotic activity at that site (Fox, 1979).

There are several types of pinocytotic vesicles in the syncytium (Simson and Spicer, 1973; Allison and Davies, 1974) which can be divided into two groups: macropinocytotic vesicles and micropinocytotic vesicles, depending on the size of vesicle.

*4.1.19.2. Large macropinocytotic and phagocytotic vesicles* These are greater than 300 nm in diameter (Boyd and Hamilton, 1970) and are easily resolvable using light microscopy. They are produced by invagination of the plasma membrane.

It seems probable that they are involved in uptake of fluid and large particulates. Fluorescent-labelled protein studies have shown that they mediate a non-selective form of molecular uptake (Wild, 1974) since there is little evidence from placental studies showing that there are any specific molecular receptors on their surface. In the case of the phagocytosis of maternal erythrocytes (Clint et al., 1979) it appears possible that if there are receptors they are localised at the tips of the microvilli on the invaginating surface. It has also been reported that these macropinocytotic vesicles may fuse with lysosomes and consequently their contents are expected to be degraded (Wild, 1974, 1975).

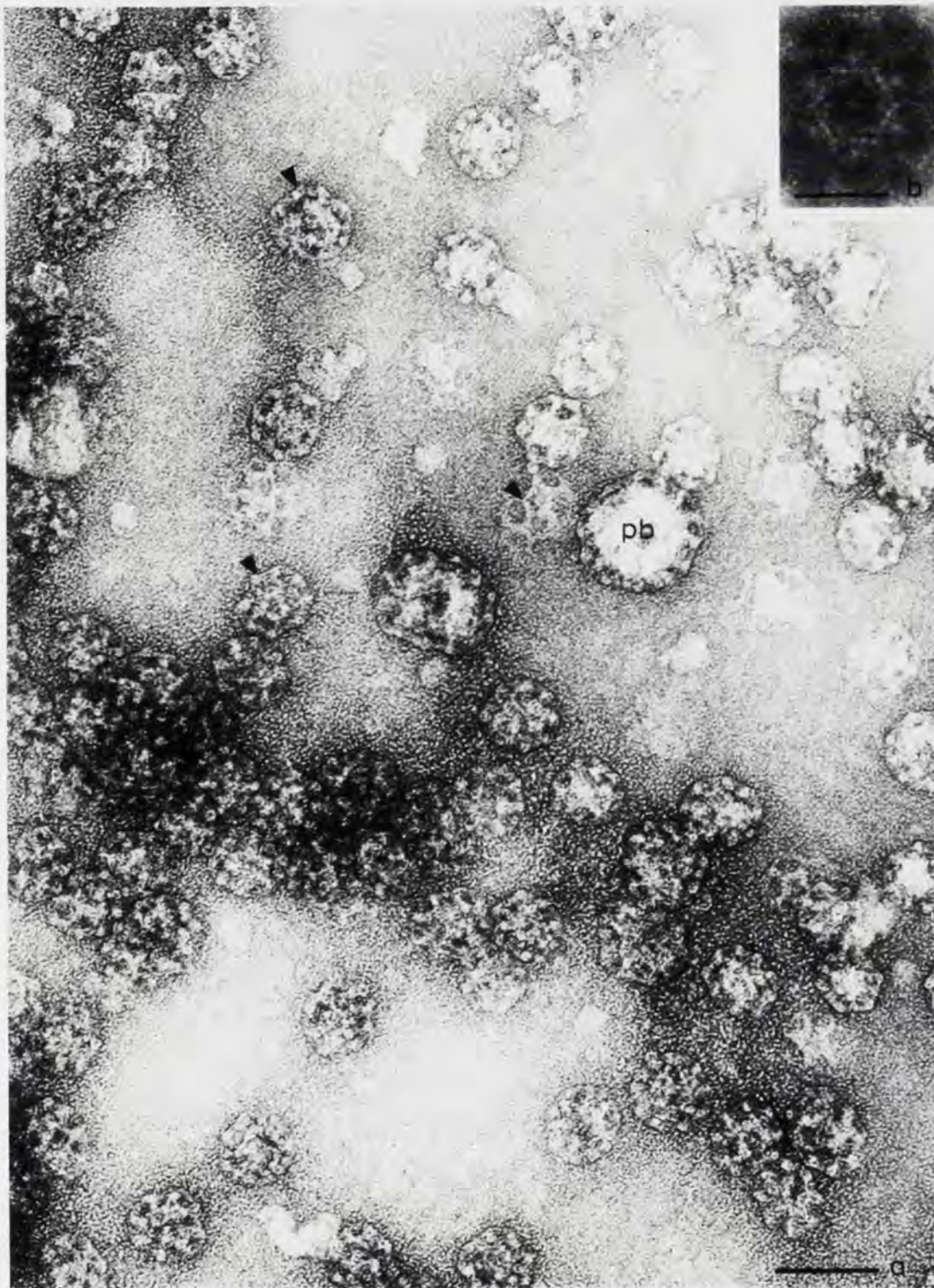


Fig. 9. (a) A preparation of human placental coated vesicles provided by Dr. A. Booth was negatively stained with uranyl acetate. Many clathrin lattices are visible (arrows) and some of these contain collapsed phospholipid bilayers (pb). Note the wide variation in the size of lattices, which is brought about by increasing the ratio of hexagonal to pentagonal units in the clathrin lattice. Scale bar = 75 nm. (b) A Markham rotation enhancement of one hexagonal facet of a clathrin lattice, showing a beaded substructure in the protein components of the walls of the hexagon (six-fold rotation). Reproduced with permission from C.D. Ockleford, K. De-Voy and H.M.K. Hall (1979) *Cell Biol. Int. Rep.* Scale bar = 50 nm.

4.1.19.3. *Micropinocytic vesicles* These can only be resolved using the electron microscope because of their small size (in general less than 200 nm). There are two main types: smooth micropinocytic vesicles and coated vesicles.

(i) *Smooth micropinocytic vesicles*. These are probably present in syncytiotrophoblast (Ockleford and Whyte, 1977). They range in size from approximately 70–100 nm in diameter (Wild, 1980) and are formed by membrane invagination. In macrophages they are not as sensitive to metabolic inhibitors as the macropinocytic vesicles (Nagura and Asai, 1976). There is no convincing evidence as yet that there are any associated receptors for specific proteins on their luminal surface in the placenta. Smooth micropinocytic vesicles in other tissues take in a variety of molecules including ferritin, myoglobin and colloidal iron (Bruns and Palade, 1968; Simionescu et al., 1973) in the concentration at which they are present in the extracellular space. There is some evidence in favour of these vesicles being capable of some degree of selection in uptake since in mouse omentum, smooth vesicles have been shown to transport ferritin particles but not colloidal gold (Fedorka and Hirsch, 1971). Smooth micropinosomes tend to fuse with lysosomes shortly after they have formed (Willingham and Pastan, 1980).

(ii) *Coated vesicles*. These have a similar size range to the smooth vesicles but are distinguishable from them by their characteristic outer coating structure (Fig. 9a). In section they have an electron-lucent inner lumen with a diameter of 50 nm (Kanaseki and Kadota, 1969). This is surrounded by a slightly more electron dense layer of material which is part of the glycocalyx. Enclosing these layers is a membrane which often appears as a single dense band, probably because of its small radius of curvature and has projections on its outer surface. Electron micrographs of replicas of the surface of these vesicles (Heuser, 1980) show that these projections appear as ridges, which are arranged in a polygonal network (Kanaseki and Kadota, 1969; Ockleford, 1976).

Markham rotation of isolated placental coated vesicles (Fig. 9b) (Ockleford et al., 1979) has shown that the polygons have 5- or 6-fold symmetry. This evidence supports the proposal that the polygonal network on the surface of coated vesicles is composed of regular pentagons and hexagons.

The major component of the coat of coated vesicles from human placenta has been found to be a protein with a molecular weight of 180,000 (Ockleford and Whyte, 1977). This protein (clathrin) (Pearse, 1975) is a constant component of coated vesicles from a variety of different tissues (Pearse, 1976; Blitz et al., 1977; Woodward and Roth, 1978).

Isoelectric focusing and SDS gel electrophoresis (Whyte, 1978) suggest that clathrin from human placental coated vesicles has an isoelectric point of 5.8.

Although the size of coated vesicles is variable, coated vesicles from human placenta have been found to have a unimodal size distribution (Ockleford et al., 1977).

Coated vesicles have been shown to be involved in selective protein uptake (Roth and Porter, 1964). In placenta the syncytiotrophoblast is known to selec-

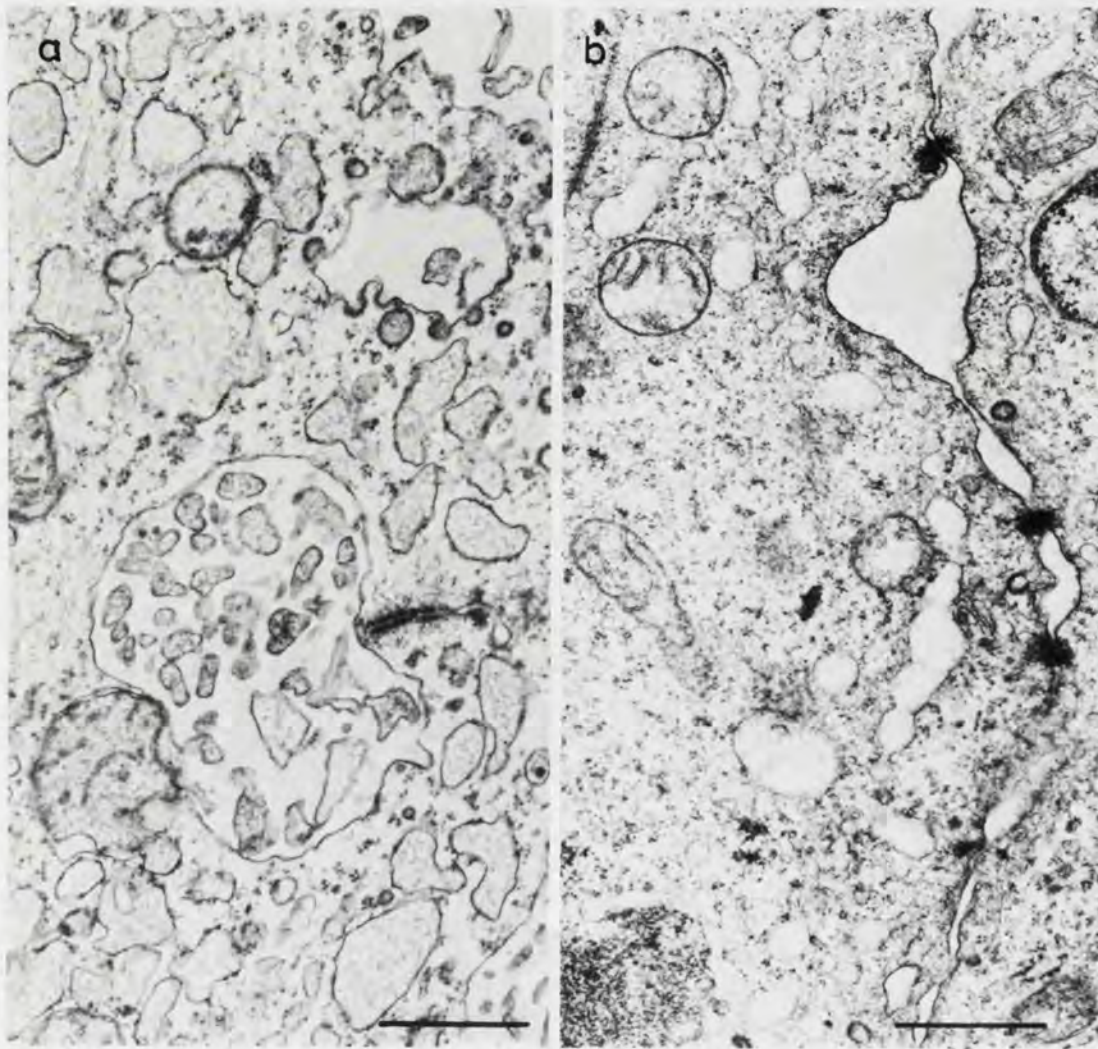


Fig. 10. (a) Transmission electron micrograph of a desmosome isolated in the syncytioplasm. Scale bar = 0.5  $\mu\text{m}$ . (b) Transmission electron micrograph of 3 desmosomes more conventionally positioned than those shown in Fig. 6. These hold together the cellular elements of the trophoblast. Scale bar = 0.5  $\mu\text{m}$ .

tively transport IgG (Bangham et al., 1958; Kohler and Farr, 1966) and maternal IgG can reach a higher concentration in the foetus than in the mother. Receptors for IgG have been demonstrated on the surface of human syncytiotrophoblast (Matre et al., 1975; Matre, 1977). IgG has also been shown to be present in micropinocytic vesicles of the syncytiotrophoblast (Lin, 1980). It is not possible to positively identify these as coated vesicles because the resolution is not adequate but it is likely that they are since they have a similar size and position.

Whyte (1980) has examined lectin binding in human trophoblast and found that the surface membrane of coated pits has certain saccharides present which are not present to the same extent on other parts of the surface.

Most of the coated vesicles are localised near the surface plasma membrane, very few being found deeper in the syncytium. Ockleford and Whyte (1977) have

estimated that over 89% of placental coated vesicles lie within 0.54  $\mu\text{m}$  of the apical plasma membrane. They suggest that after initial uptake of their specific protein the coated vesicles lose their clathrin coating or fuse with some other organelle before further transport occurs. It has also been reported that in cultured cells coated vesicles fuse with a specialised uncoated structure termed the 'receptosome' (Willingham and Pastan, 1980). These are large vacuolar structures and may correspond to the syncytial 'lagoons' described by Boyd et al. (1968a) and Boyd and Hamilton (1970) since they are found in a similar area.

Such an internalisation into a larger structure would explain the comparative lack of coated vesicles in the deeper parts of the syncytium.

#### 4.1.20. *Fibrin on syncytium*

Fibrin masses have been seen attached to the villous surface and sometimes erythrocytes can be seen trapped between these fibres (Dempsey and Luse, 1971). Sections through these fibrinous areas show that there are distinct gaps in the covering of trophoblast with a loose network of fibrin over the surface. This may represent a repair process in response to injury or damage to the trophoblast.

Foetal haemoglobin can now be identified and leakage of foetal blood into the maternal circulation has been detected in almost half of the cases investigated. The incidence of this leakage increases throughout pregnancy (Cohen et al., 1964). It is suggested that this leakage is a result of rupture of the delicate foetal blood vessels owing to increased pressure.

#### 4.1.21. *Intercellular junctions (Fig. 10a,b)*

Intercellular junctions have been described in both early and full-term placenta (Carter, 1964; Enders, 1965; Salazar and Gonzalez-Angulo, 1967; Tighe et al., 1967; Cavicchia, 1971; Metz et al., 1979; Metz and Weihe, 1980). Remarkably, desmosomes have been found joining pieces of membrane within the syncytium. These membrane remnants have been interpreted as being the remains of cytotrophoblast membrane which have fused to form syncytium (Salazar and Gonzalez-Angulo, 1967). The presence of such junctions also indicates that fusion of the cytotrophoblast cell membranes is one of the initial steps in syncytiotrophoblast formation.

Tight junctions are occasionally found in areas where two adjacent villi are very close together and their syncytial layers are in contact (Metz et al., 1979). Desmosomes have also been reported to occur in these areas (Metz et al., 1979). They note that the intervillous space is reduced to a small gap and membrane fusion can be seen at points along the villus, although there is no cytoplasmic continuity.

Desmosomes and tight junctions are also found between syncytial and cytotrophoblast cells (Cavicchia, 1971; Sideri et al., 1980). Thickening of the cell membrane is frequently seen in zones of contact between the syncytium and the basement membrane.

## 4.2. Cytotrophoblast

The cytotrophoblast (Figs. 5 and 6) is the germinative layer of the trophoblast and in the early placenta forms a continuous layer one cell thick beneath the syncytiotrophoblast. Cytotrophoblast is also found in the cytotrophoblastic shell, the cell columns and the cell islands. DNA synthesis is confined to the cytotrophoblastic nuclei (Richart, 1961; Galton, 1962) and it is now well established that the proliferative activity of the cytotrophoblast gives rise to the syncytiotrophoblast. It was once thought that the syncytial nuclei divided by amitosis and thus proliferation of the syncytium occurred (Van Cauwenberge, 1902; Florian, 1928; Bucher, 1959). However, the study by Galton (1962) revealed that in the cytotrophoblast there was a high incidence of nuclei with DNA values in excess of the diploid amount. This corresponds to DNA synthesis in interphase preparatory to division.

The syncytium was shown to have little or no intrinsic reproductive capacity when a unimodal distribution of diploid DNA values was found. This study eliminates the possibility of amitotic division by the syncytium since even amitotic division shows a period of DNA synthesis. Post-divisional synthesis is also eliminated since only a narrow distribution of DNA values was obtained and if DNA synthesis followed division one would expect a scatter of values from  $1n$  to  $2n$ .

The cells produced by division of the cytotrophoblast mature and appear to fuse together to become transformed into syncytium. This process of fusion may be mediated by lysosomes.

Further evidence that the syncytium is derived from the cytotrophoblast comes from the observation of cells intermediate in morphology between cytotrophoblast and syncytial cells (Yoshida, 1964; Boyd and Hamilton, 1966; Ockleford, unpubl. data). These intermediate cells have a more complex cytoplasm, contain more inclusions than the cytotrophoblast cells and have a well-developed endoplasmic reticulum. Other evidence in favour of cytotrophoblast cell fusion to form syncytium comes from electron micrographs which sometimes show a few remnants of intercellular membranes in the syncytial cytoplasm (Pierce and Midgely, 1963; Carter, 1964; Enders, 1965).

Some cytotrophoblast cells with nuclear morphologies which are intermediate between those of other cytotrophoblast and syncytiotrophoblast have been identified (Terzakis, 1963; Tighe et al., 1967).

### 4.2.1. Microvilli/filopodia

In addition to the microvilli which occur on the syncytial surface there are also microvillus-like filopodial projections from the cytotrophoblast cells. These 'microvilli' interdigitate with those from adjacent cytotrophoblast cells and with the basement membrane, although in the latter region the interdigitations are not so pronounced as they are where the syncytium is in contact with the basement membrane.

#### 4.2.2. *Nuclei*

The cytotrophoblastic nuclei have an average diameter of approximately 5  $\mu\text{m}$  (Boyd and Hamilton, 1970), and have a more uniform round or oval shape than the syncytial nuclei. The nucleoplasm is pale staining and the chromatin finely dispersed. There is some hetero-chromatin scattered in the nucleoplasm and in a thin line around the nuclear envelope (Martin and Spicer, 1973a).

#### 4.2.3. *Nucleoli*

There are usually 1–2 conspicuous nucleoli present. Stein et al. (1974) suggest that the presence of the nucleoli reflects the less differentiated and simpler state of the cytotrophoblast.

#### 4.2.4. *Nuclear envelope*

The nucleus is surrounded by a pair of limiting membranes interrupted by nuclear pores. These appear as gaps in the membrane when seen in section, bridged by a delicate septum. The perinuclear space is often connected to the endoplasmic reticulum.

#### 4.2.5. *Endoplasmic reticulum (ER)*

The ER is poorly developed and has few attached ribosomes.

#### 4.2.6. *Mitochondria*

There can be marked variations in the size of mitochondria in different chorionic villi. In some they are larger than syncytial mitochondria (Boyd and Hamilton, 1970), in others the reverse is the case (Rhodin and Terzakis, 1962; Lister, 1963a).

Mitochondria in the cytotrophoblast are not as numerous as in the syncytium (Wigglesworth, 1962; Lister, 1964; Hamilton and Mossmann, 1972). They are round or oval in shape and have well-defined cristae (Panigel and Anh, 1964) and a pale matrix (Dempsey and Luse, 1971).

#### 4.2.7. *Golgi*

This is usually found in a juxtannuclear position and is often more conspicuous than in the syncytium. In addition, the cisternae of the Golgi are quite dilated and therefore more prominent. Some of the vesicles in the Golgi area fuse with the Golgi cisternae (Rhodin and Terzakis, 1962).

#### 4.2.8. *Ribosomes*

There are a few ribosomes attached to the endoplasmic reticular system and an abundance of free ribosomes in the cytoplasm (Tighe et al., 1967).

#### 4.2.9. *Filaments*

Tighe et al. (1967) report the presence of fine fibrils 7.5 nm in diameter just below the plasma membrane and Boyd and Hamilton (1970) also claim there is a network of microfibrils present.

#### 4.2.10. Lipid

Lipid droplets are present in very small amounts (Boyd and Hamilton, 1970).

#### 4.2.11. Myelin figures

These have not been reported to be present in the cytotrophoblast.

#### 4.2.12. Glycogen

Glycogen is present in large amounts in young placenta (Yoshida, 1964). It diminishes and is absent or only present in small amounts in older placentae but can be found up to term in the cytotrophoblast cells of the chorion laeve.

Glycogen is also found in the basal plate cytotrophoblast cells and placental septa until the 7th to 8th month of gestation (Boyd and Hamilton, 1970).

#### 4.2.13. Glomerular body

An interesting structure has been found in the cytotrophoblast of the baboon's placenta (Wynn et al., 1971). It was named glomerular body by Hernandez-Verdun (1972) who noted its appearance in the syncytiotrophoblast of the rat and mouse, although no homologous or comparable structure has yet been reported in man. It is composed of entangled threads 40 nm thick, made up of fibrils (3–5 nm long) and particles. Biochemical analysis shows basic protein and associated RNA to be present (Hernandez-Verdun, 1972). He suggests that there is a relationship between the glomerular body and the absence of centrioles.

#### 4.2.14. Granules and vesicles

There are fewer inclusions in the cytotrophoblast than in the syncytium.

4.2.14.1. *Lysosomes* These are sparse or absent in the cytotrophoblast (Fox, 1978b).

4.2.14.2. *Secretion granules* Secretion granules are rare in cytotrophoblast cells.

4.2.14.3. *Pinocytic vesicles* Membrane associated vesicles are much less common than at the syncytial maternal surface.

#### 4.2.15. Junctions

A few tight junctions occur between the cytotrophoblast cells, but the majority of connections between them are desmosomal. Focal tight junctions also occur between syncytiotrophoblast and cytotrophoblast (Tighe et al., 1967; Cavicchia, 1971).

#### 4.2.16. Fibrin and cytotrophoblast

Fibrin deposits occur in the placental septa, cytotrophoblastic cell islands, syncytial buds and the cytotrophoblastic shell. (Similar to a sprout, a bud is a pro-

trusion from the surface of the trophoblast. However, a bud is an inward projection which occupies part of the villous core (Boyd and Hamilton, 1970.) Several layers of fibrin intervene between the trophoblast and the decidua. These are Langhans' layer (Langhans, 1877), which is located in the chorionic plate, Nitabuch's layer (Nitabuch, 1887), located in the basal plate, and Rohr's stria (Rohr, 1889), which is also in the basal plate but closer to the intervillous space. This layer is more irregular than the other two.

The amount of fibrin present increases during gestation (Boyd and Hamilton, 1970). Its source may be maternal blood, lymph or the interstitial fluids, since these both contain varying amounts of fibrinogen. It is thought that abscission at these fibrinous layers occurs at parturition.

#### *4.3. Non-villous trophoblast*

It was Wynn (1972, 1975) who drew attention to the ultrastructure of the non-villous trophoblast. This includes the cytotrophoblastic cell columns, the cytotrophoblastic shell and the cell islands. These cells have a much more complex ultrastructure than those of the villous cytotrophoblast and show some similarity to the intermediate type of cytotrophoblast cell sometimes seen in the syncytiotrophoblast, which has an ultrastructural complexity approaching that of the villous syncytium.

##### *4.3.1. Cytotrophoblastic cell columns*

These are developments from the tips of the tertiary villi. When the tertiary villi develop the mesenchymal core does not extend right to the very tips of the villi. These areas remain composed of cytotrophoblast with a thin covering of syncytium. During the early stages of development they extend and embed into the chorionic plate. They are often called 'anchoring' villi because of this attachment. Since they have no mesenchymal core they do not become vascularised and so foetal vessels do not penetrate the maternal decidua. The cell columns also produce lateral extensions which join with extensions from adjacent villi and form a continuous although somewhat irregular layer around the conceptus. This is the cytotrophoblastic shell.

It was once thought that these cytotrophoblastic cell columns disappeared at 3½ mth (Baker et al., 1944) but it has now been agreed that some do persist to term (Boyd and Hamilton, 1967).

The most striking feature of the cytotrophoblastic column cells is the large amounts of glycogen they contain. The cells also show marked basophilia in light micrographs owing to the large numbers of ribosomes which are present in the cytoplasm. The proximal cytotrophoblastic column cells are similar in ultrastructure to the Langhans cells but those cells which are more distal have a more prominent nucleus and an abundance of rough endoplasmic reticulum. This may indicate protein synthesis occurs here, possibly proteolytic enzymes to be used in

the invasion of the endometrium (Larsen and Knoth, 1971).

There are also numerous mitotic figures present in the column cells indicating that proliferation is occurring at a high rate, probably higher than that in the Langhans cells (Boyd and Hamilton, 1970).

In places the cytotrophoblastic cells in the columns have spaces between them; fibrinoid and particulate glycogen have been identified within these spaces (Boyd and Hamilton, 1970).

These cells also show microvillar projections which interdigitate with those from the adjacent cells in these spaces.

#### 4.3.2. *Cytotrophoblastic shell*

As stated previously the shell forms from the proliferative activity of the cytotrophoblastic cell columns and forms a layer around the conceptus.

Sometimes large spaces are found between the closely packed variously shaped cells of the cytotrophoblastic shell (Jung, 1908). Some contain maternal blood, others portions of vacuolated syncytium. Boyd and Hamilton (1970) suggest they are important in early embryonic nutrition.

The outer layer of the cytotrophoblastic shell becomes intermingled with the decidua and it is difficult to distinguish the junction between the two. However, in the basal plate there is a discontinuous layer of fibrinoid material which comprises Nitabuch's stria (Okudaira et al., 1971) and is considered to separate maternal and foetal cells (Nitabuch, 1887).

In this region syncytial streamers are present which extend into the endometrium. Some cells of the cytotrophoblast appear to be able to differentiate into syncytial giant cells (Anderson and McKay, 1966; Wynn, 1967).

#### 4.3.3. *Cell islands*

The cell islands are rounded isolated collections of cells partially covered by syncytium, occurring throughout the placenta to term. Their origin is much disputed, some authors being of the opinion that these cells are a special development of decidual cells, that is, they are of maternal origin (Klinger and Ludwig, 1957; Hormann, 1966); others believe they are foetally derived (Wislocki and Bennett, 1943; Boe, 1967; Boyd and Hamilton, 1967; Moe, 1969).

An argument in favour of the cell islands being maternal in origin comes from Klinger and Ludwig (1957) who showed that cell islands in placentae from two immature male embryos showed female sex chromatin. However, evidence from sex chromatin studies alone should be interpreted with care since not all diploid female cells show it and not all male diploid cells lack it. Taking account of shrinkage problems and the possibility of pyknotic nuclei being present, this evidence has not been found convincing (Ortmann, 1960; Boyd and Hamilton, 1970).

Evidence in favour of a foetal origin is strong since the appearance of the cell islands is very similar to that of the cell columns and both are very different from the maternal decidual cells (Moe, 1969). The cell islands do not show mitotic

activity, and Moe (1969) suggests that they are derived from the cytotrophoblastic cell columns.

Ortmann (1960) reported that the islands developed at the same time (approximately the 4th month) as the septa are developing, although they have been found much earlier than this (Boyd and Hamilton, 1970). Stieve (1952) considers that the islands fuse together to constitute the septa. Observations do show that they have similar cytological features to basal plate septa. An example would be the possession of intracellular cystic spaces (Boyd and Hamilton, 1970). It is possible that the cell islands seen in mature placenta may be cross-sections of the placental septa (Moe, 1969). The cell islands have an ultrastructure which suggests that they may have a secretory function, possessing a well-developed Golgi complex and abundant endoplasmic reticulum (Moe, 1969).

#### *4.3.4. Giant cells*

These remarkably large, non-microvillous and often multinucleated cells appear to be derived from trophoblastic tissue. They are present (many thousands) in the endometrium opposite the placental disc; they persist for several days after parturition and have no known function (Boyd and Hamilton, 1970).

#### *4.4. Trophoblast layer adjacent to the amnion*

As previously described, villi are initially present over the entire surface of the chorionic sac. As pregnancy advances, the chorionic villi towards the decidua basalis differentiate to form the definitive placenta (chorion frondosum). The villi towards the decidua capsularis regress forming the chorion laeve or reflected chorion. As the embryo increases in size, the villi upon this enlarging area of chorion slowly degenerate and atrophy. These atrophic remnants remain as frond-like processes upon the outer surface of the reflected chorion (Bourne, 1962).

By the middle of the 5th month of gestation the chorion laeve becomes much more extensive. It is no longer only in contact with the decidua parietalis, but has actually fused with it so that most of the uterine cavity is now obliterated. At this point, the chorion laeve consists of several layers of cytotrophoblast cells (Boyd and Hamilton, 1970). These authors suggest that the regression of the villi may be owing to a difference in nutritional supply after implantation. However, Bourne (1962) raises the following more precise possibilities.

- (1) The discoid placenta alone provides sufficient of the requirements of the conceptus.
- (2) Growth of the conceptus stretches the decidua constricting its blood supply. Thus the nutritional supply to the villi from the maternal side is restricted.
- (3) Growth of the conceptus renders the blood supply inadequate for maintenance of the villi.

Although the villi of the chorion laeve atrophy, the trophoblast cells between the villi remain alive, under normal circumstances, until term and may well retain



Fig. 11. A montage of a series of scanning electron micrographs across the breadth of the reflected amnion and chorion. The amnion is uppermost and the chorion is below. Erythrocytes (arrows) mark the trophoblastic layer which is permeated with blood vessels. Scale bar = 50  $\mu$ m.

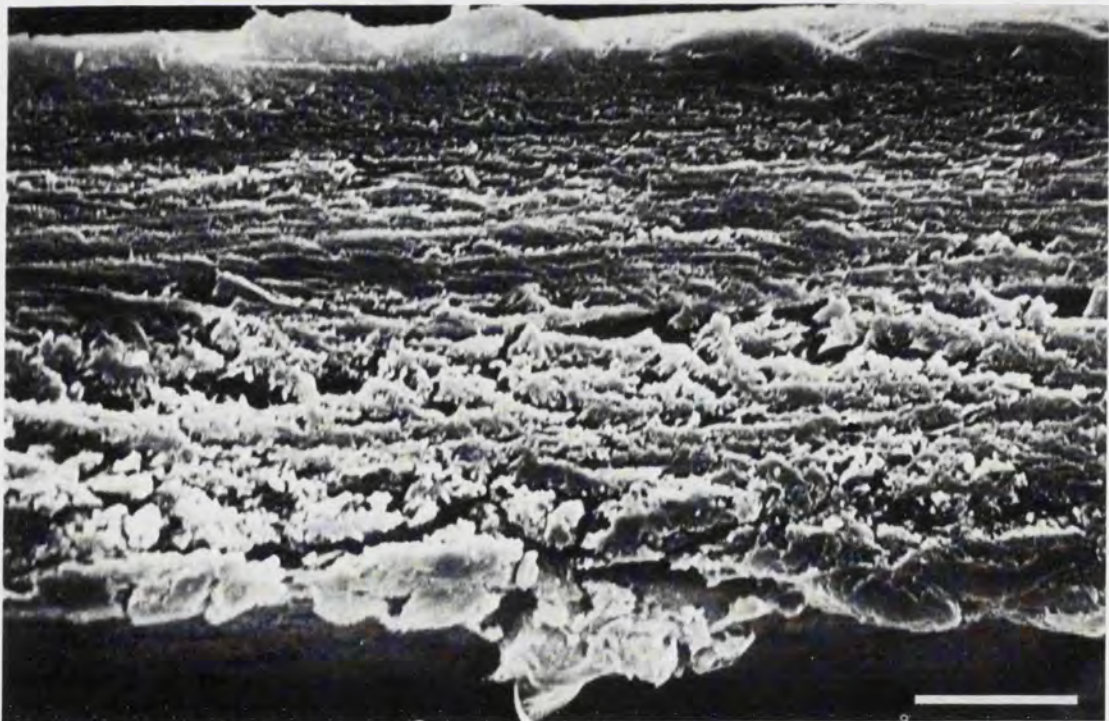


Fig. 12. A light micrograph of a 1  $\mu\text{m}$  section of resin-embedded reflected amnion and chorion shows the trophoblastic layer (t). The cuboidal amniotic epithelium (arrows) and some ectopic adherent foetal squamous cells from the opposite surface (arrowhead). Scale bar = 20  $\mu\text{m}$ .

Fig. 13. At low power this scanning electron micrograph shows the full thickness of the reflected amnion and chorion. The amniotic surface is uppermost. Scale bar = 40  $\mu\text{m}$ .

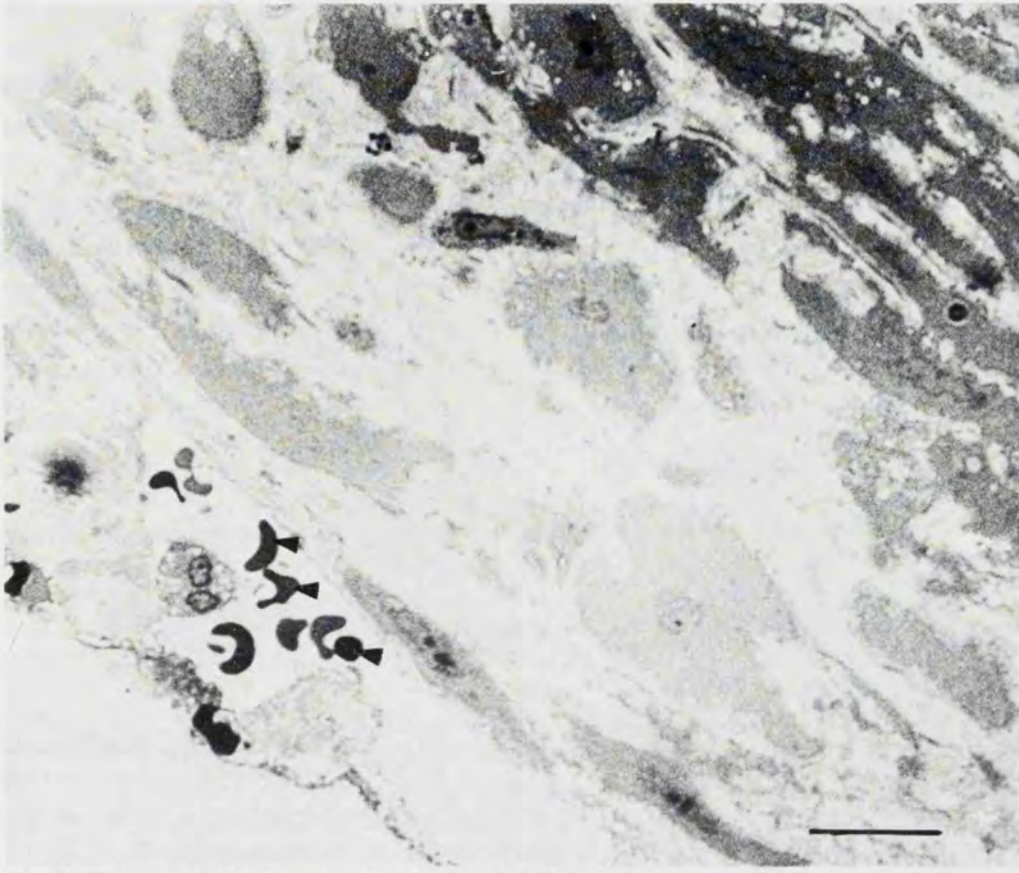


Fig. 14. Light micrograph of the trophoblastic portion of the reflected chorion shows the cellular as opposed to syncytial nature of the tissue. Red blood cells are present in an extensive sinus (arrowheads) in the tissue. Scale bar = 10  $\mu$ m.

Fig. 15. A scanning electron micrograph showing erythrocytes (arrows) interspersed between trophoblastic cells (t) of the chorion. Scale bar = 20  $\mu$ m.

their ability to transfer a small amount of material directly between the maternal organism and the foetus. (Structure of the chorion laeve and the trophoblast is shown in Figs. 11–15.)

The chorion laeve varies in depth from 0.2 to 0.02 mm and consists of four layers (Bourne, 1962, 1966). Starting on the inner aspect nearest to the amnion, these are as follows.

(1) The cellular layer: this layer is thin and consists of a fibroblast network usually present only in early pregnancy. The fibroblast network is similar to that present in the fibroblast layer of the amnion.

(2) The reticular layer: this forms the bulk of the chorion and consists of a loose reticular network in which fibroblasts and macrophages (Hofbauer cells) are embedded. Reticular fibres from this layer penetrate the trophoblast to bind the different chorionic structures together.

(3) The pseudobasement membrane: it consists of a narrow band of reticulin forming the basement membrane of the trophoblast and acts as its anchoring structure.

(4) The trophoblast: this consists of two to ten layers of trophoblast cells, closely applied to the maternal decidua and containing obliterated chorionic villi. These atrophic villi are expressed as oval or rounded bundles of fibrous tissue embedded between the trophoblast cells.

*Ultrastructure of chorion laeve.* Although the chorion laeve is present as a continuous and complete layer, the syncytium shows degenerative changes and is absent in most areas by term (Lister, 1968). Towards the end of pregnancy the outer surface of the chorion is covered with debris and degenerating cells. Below this debris, the cytotrophoblast cells are integrated by numerous, often complex, desmosomes. Intercellular spaces are formed between the desmosomes into which microvilli protrude. The cells show a number of pinocytic vesicles in close association with the cell surface. Prominent Golgi lamellae lie near to each nucleus. Cytotrophoblast cells contain little glycogen, few mitochondria and endoplasmic reticulum. Cytoplasmic filaments are also seen in abundance.

*Blood supply.* The reflected portion of the chorion contains blood vessels only during the stage of development in which the villi of the chorion laeve are vascularised and functioning. These vessels atrophy together with the villi which they have supplied, so that, at term, the reflected chorion contains few, if any, fetal blood vessels (Bourne, 1962; Boyd and Hamilton, 1970). Hoyes (1971) observed no indication of the persistence of a definitive circulation in the chorion laeve after the end of the 3rd month of gestation, although Lister (1968) has described capillary vessels containing blood cells in the mesenchyme of pathological material at term.

## 5. Acknowledgement

Dr. C.D. Ockleford and Miss L. Dearden thank the MRC for their support through project grant G979/939/SB. We should like to thank Mrs. S. Bulman and Mr. G.L.C. McTurk for expert technical assistance, Mrs. A. Chorley for the illustrations, Professor MacVicar and the obstetricians and gynaecologists of the Leicester Royal Infirmary for clinical co-ordination.

## References

- Aherne, W. and Dunnill, M.S. (1966) Morphometry of the human placenta. *Br. Med. Bull.* 22, 5-8.
- Allison, A.C. and Davies, P. (1974) Mechanisms of endocytosis and exocytosis. In: *Transport at the Cellular Level*. Editors: M.A. Sleight and D.H. Jennings, pp. 419-446.
- Alvarez, H. (1964) Morphology and physiopathology of the human placenta. 1. Studies of morphology and development of chorionic villi by phase contrast microscopy. *Obstet. Gynecol.* 23, 813-825.
- Amoroso, E.C. (1960) Comparative aspects of hormonal functions. In: *The Placenta and Fetal Membranes*. Editor: C.A. Villee, pp. 3-28. Williams and Wilkins, Cambridge.
- Anderson, W.R. and McKay, D.G. (1966) Electron microscope study of the trophoblast in normal and toxemic placentae. *Am. J. Obstet. Gynecol.* 95, 1134-1148.
- Ashley, D. (1965) Study of the human placenta with the electron microscope. Functional implications of a canal system in the trophoblast. *Arch. Pathol.* 80, 377-390.
- Baker, B.L., Hook, S.J. and Severinghaus, A.E. (1944) The cytological structure of the human chorionic villus and decidua parietalis. *Am. J. Anat.* 74, 291-326.
- Bangham, D.R., Hobbs, K.R. and Terry, R.J. (1958) Selective placental transfer of serum proteins in rhesus. *Lancet* ii, 351-354.
- Bargmann, W. and Knoop, A. (1959) Elektronenmikroskopische Untersuchungen an Placentarzotten des Menschen. *Z. Zellforsch. Mikrosk. Anat.* 50, 472-493.
- Becker, V. and Bleyl, V. (1961) Placentarzotte bei Schwangerschaftstoxicose und fetaler Erythroblastose im fluoreszenzmikroskopischen Bilde. *Virchows Arch. Pathol. Anat. Physiol.* 334, 516-527.
- Blitz, A.L., Fine, R.E. and Toselli, P.A. (1977) Evidence that coated vesicles isolated from brain are calcium sequestering organelles resembling sarcoplasmic reticulum. *J. Cell Biol.* 75, 135-147.
- Boe, F. (1967) Studies on the human placenta. 1. The cell islands in the young placenta. *Acta Obstet. Gynecol. Scand.* 46, 591-603.
- Booth, A.G. and Wilson, M.J. (1981) Human placental coated vesicles contain receptor-bound transferrin. *Biochem. J.* 196, 355-362.
- Bourne, G. (1962) *The Human Amnion and Chorion*, pp. 5-24. Lloyd-Luke Ltd., London.
- Bourne, G.L. (1966) The anatomy of the human amnion and chorion. *Proc. R. Soc. Med.* 59, 1127-1128.
- Boyd, J.D. (1957) The distribution of glycogen in early human placentae. *J. Anat.* 91, 595.
- Boyd, J.D. (1959) Implantation of Ova. In: *Memoirs of the Society for Endocrinology*, No. 6. Editor: P. Eckstein, pp. 26-34. Cambridge University Press, London.
- Boyd, J.D. and Hughes, F.W. (1954) Observations on human chorionic villi using the electron microscope. *J. Anat.* 88, 356-362.
- Boyd, J.D. and Hamilton, W.J. (1966) Electron microscopic observations on the cytotrophoblast contribution to the syncytium in the human placenta. *J. Anat.* 100, 535-548.
- Boyd, J.D. and Hamilton, W.J. (1967) Development and structure of human placenta from the end of the third month of gestation. *J. Obstet. Gynaecol. Br. Commonw.* 74, 161-226.
- Boyd, J.D. and Hamilton, W.J. (1970) *The Human Placenta*. W. Heffer and Sons, Cambridge.
- Boyd, J.D., Boyd, C.A.R. and Hamilton, W.J. (1968a) Observations on the vacuolar structure of the human syncytiotrophoblast. *Z. Zellforsch. Mikrosk. Anat.* 88, 57-79.
- Boyd, J.D., Hamilton, W.J. and Boyd, C.A.R. (1968b) The surface of the syncytium of the human chorionic villus. *J. Anat.* 102, 553-563.

- Bruns, R.R. and Palade, G.E. (1968) Studies on blood capillaries. Transport of ferritin molecules across the wall of muscle capillaries. *J. Cell Biol.* 37, 277-299.
- Bucher, O. (1959) Die amitose der tierischen und menschlichen Zelle. In: *Protoplasmatalogia. Handbuch der Protoplasma-forschung.* Editor: Heilbrunn. Kern und Zellteilung Amitose 1, 1-159.
- Carter, J.E. (1964) Morphological evidence of syncytial formation from the cytotrophoblast. *Obstet. Gynecol.* 23, 647-656.
- Cauwenberge, van, A. (1902) Recherches sur le role du syncytium dans la nutrition embryonnaire chez la femme. *Arch. Biol. Pans.* 23, 13-163.
- Cavicchia, J.C. (1971) Junctional complexes in the trophoblast of the human full term placenta. *J. Anat.* 108, 339-346.
- Clint, J.M., Wakely, J. and Ockleford, C.D. (1979) Differentiated regions of the human placental cell surface associated with the attachment of chorionic villi, phagocytosis of maternal erythrocytes and syncytiotrophoblast repair. *Proc. R. Soc. London., Ser. B.* 204, 345-353.
- Cohen, F., Zuelzer, W.W., Gustafson, D.C. and Evans, M.M. (1964) The mechanism of isoimmunization. 1. The transplacental passage of fetal erythrocytes in homospecific pregnancies. *Blood* 23, 621-646.
- Contractor, S.F. (1969) Lysosomes in human placenta. *Nature (London)* 223, 1275.
- Contractor, S.F., Banks, R.W., Jones, C.P.J. and Fox, H. (1977) A possible role for placental lysosomes in the formation of villous syncytium. *Cell Tissue Res.* 178, 411-419.
- Corash, L. and Gross, E. (1973) Sub-cellular constituents from human placenta. 1. Isolation and density distribution of lysosomes from term tissue. *Pediatr. Res.* 7, 789-811.
- Corash, L. and Gross, E. (1974) Subcellular constituents from human placenta. II. Isolation and density distribution of lysosomes from first trimester tissue. *Pediatr. Res.* 8, 774-782.
- Dempsey, E.W. and Wislocki, G.B. (1944) Observations on some histochemical reactions in the human placenta, with special reference to the significance of the lipoids, glycogen and iron. *Endocrinology* 35, 409-429.
- Dempsey, E.W. and Luse, S.A. (1971) Regional specialization in the syncytial trophoblast of early human placentae. *J. Anat.* 108, 545-561.
- Douglas, G.W., Thomas, L., Carr, M., Cullen, M.N. and Morris, R. (1959) Trophoblast in circulation blood during pregnancy. *Am. J. Obstet. Gynecol.* 78, 960-973.
- Dreskin, R.B., Spicer, S.S. and Greene, W.B. (1970) Ultrastructural localisation of chorionic gonadotrophin in term placenta. *Histochem. Cytochem.* 18, 862-874.
- Enders, A.C. (1965) A comparative study of the fine structure of the trophoblast in several haemochorial placentae. *Am. J. Anat.* 116, 29-67.
- Enders, A.C. and King, B.F. (1970) The cytology of Hofbauer cells. *Anat. Rec.* 167, 231-251.
- Enders, A.C. and Wimsatt, W.A. (1971) Transport and barrier function in the chorionallantoic placenta of the bat *Myotis lucifugus*. *Anat. Rec.* 170, 381-400.
- Fedorka, M.E. and Hirsch, J.G. (1971) Studies on the transport of macromolecules and small particles across mesothelial cells of the mouse omentum. 1. Morphological aspects. *Exp. Cell Res.* 69, 113-127.
- Florian, J. (1928) Über Syncytium im Trophoblast junger menschlicher der Embryonen. *Anat. Anz.* 66, erg Heft 211-221.
- Fowler, S. and Duve, de, D. (1969) Digestive activity of lysosomes. III. The digestion of lipids by extracts of rat liver lysosomes. *J. Biol. Chem.* 244, 471-481.
- Fox, H. (1965) The significance of villous syncytial knots in the human placenta. *Obstet. Gynaecol. Br. Commonw.* 72, 347-355.
- Fox, H. (1967) The incidence and significance of vasculosyncytial membranes in the human placenta. *J. Obstet. Gynaecol. Br. Commonw.* 74, 28-33.
- Fox, H. (1978a) The Pathology of the Human Placenta. Major Problems in Pathology. Vol. 7, pp. 1-37. Saunders, London.
- Fox, H. (1978b) Placental Structure. In: *Scientific Basis of Obstetrics and Gynaecology.* Editor: R.R. Macdonald, 2nd Edition, pp. 27-59. Churchill Livingstone, Edinburgh.
- Fox, H. (1979) The correlation between placental structure and transfer functions. In: *Placental Transfer.* Editors: G.V.P. Chamberlain and A.W. Wilkinson, pp. 15-30. Pitman Medical.
- Fox, H. and Agrofojo-Blanco, A. (1974) Scanning electron microscopy of the human placenta in normal and abnormal pregnancies. *Eur. J. Obstet. Gynecol. reprod. Biol.* 4, 45-50.
- Galton, M. (1962) DNA content of placental nuclei. *J. Cell Biol.* 13, 183-203.

- Getzowa, S. and Sadowski, A. (1950) On the structure of the human placenta with full-term and immature fetus, living or dead. *J. Obstet. Gynecol. Br. Emp.* 57, 388-396.
- Grosser, O. (1927) Frühentwicklung, Eihautbildung und Placentation des menschlichen und der Säugetiere, pp. 1-454. J.F. Bergmann, München.
- Guttler, F. and Clausen, J. (1969) Changes in lipid pattern of HeLa cells exposed to immunoglobulin G and complement. *Biochem. J.* 115, 959-968.
- Hamilton, W.J. and Mossman, H.W. (1972) Prenatal development of form and function. In: *Human Embryology*. Editors: W.J. Hamilton, J.D. Boyd and H.W. Mossman, pp. 83-159. Williams and Wilkins, Cambridge.
- Hernandez-Verdun, D. (1972) Etude cytochimique du corps glomérulaire dans le trophoblaste de souris. *J. Ultrastr. Res.* 40, 68-86.
- Heuser, J. (1980) Three dimensional visualisation of coated vesicle formation in fibroblasts. *J. Cell Biol.* 84, 564-583.
- Hormann, G. (1958) Versuch einer Systematik plazenterer Entwicklungsstörungen. *Geburtsh. Frauenheilkunde* 18, 345-349.
- Hormann, G. (1966) Über die sogenannten Septen, Inseln, Zysten, Furchen und die Randzone der menschlichen Plazenta. *Z. Geburtshilfe Gynaekol.* 165, 125-134.
- Hoyes, A.D. (1971) Ultrastructure of the mesenchymal layers of the human chorion laeve. *J. Anat.* 109, 17-30.
- Jackson, B., Grund, C., Burki, K., Schmid, E., Illmensee, K. and Franke, W.W. (1980) Formation of intermediate filaments and desmosomes in preimplantation mouse embryos. *Eur. J. Cell Biol.* 22, 377.
- Jones, G.E.S., Gey, G.O. and Gey, M.K. (1943) Hormone production by placental cells maintained in continuous culture. *Bull. Johns Hopkins Hosp.* 72, 26-38.
- Jones, C.P.J. and Fox, H. (1976) An ultrahistochemical study of the distribution of acid and alkaline phosphatase in placenta from normal and complicated pregnancies. *J. Pathol.* 118, 113-151.
- Jones, C.P.J. and Fox, H. (1977) Syncytial knots and intervillous bridges in the human placenta. *J. Anat.* 124, 275-286.
- Jones, C.P.J. and Fox, H. (1979) Ultrastructure of the placenta in prolonged pregnancy. *J. Pathol.* 126, 173-180.
- Jung, P. (1908) Beiträge für hestere Ei-einbettung beim menschlichen Weibe, pp. 1-112. Karger, Berlin.
- Kanaseki, T. and Kadota, K. (1969) The 'vesicle in a basket'. A morphological study of the coated vesicle isolated from nerve endings of guinea-pig brain with special reference to mechanisms of membrane movement. *J. Cell Biol.* 42, 202-220.
- Kastschenko, N. (1885) Das menschliche Chorionepithel und dessen Rolle bei der Histogenese der Plazenta. *Arch. Anat. Physiol. Leipzig. Jahr.* 451-480.
- King, B.F. (1976) Localization of transferrin on the surface of the human placenta by electron microscopic immunocytochemistry. *Anat. Rec.* 186, 151-160.
- King, B.F. and Enders, A.C. (1971) Protein absorption by the guinea-pig chorioallantoic placenta. *Am. J. Anat.* 130, 409-430.
- King, B.F. and Menton, D.N. (1975) Scanning electron microscopy of human placental villi from early and late gestation. *Am. J. Obstet. Gynecol.* 122, 824-828.
- Klinger, H.P. and Ludwig, K.S. (1957) Sind die Septen und die grosszelligen Inseln der Plazenta aus mütterlichem oder kindlichem Gewebe aufgebaut. *Z. Anat. Entwicklungsgesch.* 120, 95-100.
- Kohler, P. F. and Farr, P.S. (1966) Elevation of cord over maternal IgG immunoglobulin: evidence for an active placental IgG transport. *Nature (London)* 210, 1070-1071.
- Kraehenbuhl, J.P. and Campiche, M.A. (1969) Early stages of intestinal absorption of specific antibodies in the newborn. An ultrastructural, cytochemical, and immunological study in the pig, rat and rabbit. *J. Cell Biol.* 42, 345-365.
- Langhans, T. (1877) Untersuchungen über die menschliche Plazenta. *Arch. Anat. Physiol. Anat. Abl.* 5, 188-267.
- Larsen, J.F. and Knoth, M. (1971) Ultrastructure of the anchoring villi and trophoblastic shell in the second week of placentation. *Acta Obstet. Gynecol. Scand.* 50, 117-128.
- Lin, C.T. (1980) Immunoelectron microscopic localisation of immunoglobulin G in human placenta. *J. Histochem. Cytochem.* 28, 339-346.
- Lister, V.M. (1963a) Ultrastructure of the human placenta. I. The maternal surface. *J. Obstet. Gynecol. Br. Commonw.* 70, 373-386.

- List, V.M. (1963b) Ultrastructure of the human placenta. II. The fetal surface. *J. Obstet. Gynecol. Br. Commonw.* 70, 766-776.
- List, V.M. (1964) Ultrastructure of the early human placenta. *J. Obstet. Gynecol. Br. Commonw.* 7, 21-32.
- List, V.M. (1968) Ultrastructure of the human amnion, chorion and fetal skin. *J. Obstet. Gynecol. Br. Commonw.* 75, 327-341.
- Loro, L.D. (1972) Disorders of placental transfer. In: *Pathophysiology of Gestation*. Editors: N.S. Asai and C.R. Brinkman, Vol. 2, pp. 1-76. Academic Press, New York and London.
- Luöig, H. (1974) Surface structure of the human placenta. In: *The Placenta: Biological and Clinical Aspects*. Editors: K.S. Michissi and E.S.E. Hafez, pp. 40-64. Charles C. Thomas, Springfield, Illinois.
- Main B.J. and Spicer, S.S. (1973a) Ultrastructural features of cellular maturation and ageing in human trophoblast. *J. Ultrastruct. Res.* 43, 133-149.
- Main B.J. and Spicer, S.S. (1973b) Multivesicular bodies and related structures of the syncytiotrophoblast of human term placenta. *Anat. Rec.* 175, 15-36.
- Mae, R. (1977) Similarities of Fc receptors on trophoblast and placental endothelial cells. *Scand. J. Immunol.* 6, 953-958.
- Mae, R., Tonderr, O. and Endressen, C. (1975) Fc receptors in human placenta. *Scand. J. Immunol.* 4741-745.
- Me, I. and Weihe, E. (1980) Intercellular junctions in the full-term placenta. II. Cytotrophoblasts intravillous stroma cells and blood vessels. *Anat. Embryol. (Berlin)* 158, 167-178.
- Me, I., Weihe, E. and Heinrich, D. (1979) Intercellular junctions in the full term human placenta. Syncytiotrophoblastic layer. *Anat. Embryol. (Berlin)* 158, 41-50.
- Migley, A.R., Jr. and Pierce, G.B., Jr. (1962) Immunohistochemical localisation of human chorionic gonadotrophin. *J. Exp. Med.* 115, 289-294.
- Mo N. (1969) The cytotrophoblastic cell columns and the cell islands of the normal human placenta with particular reference to the nature of the intercellular material. *Acta Pathol. Microbiol. Scand.* 7, 401-408.
- Naart, H. and Asai, J. (1976) Pinocytosis by macrophages, kinetics and morphology. *J. Cell Biol.* 7, 19A.
- Nitbuch, R. (1887) *Beitrage zur Kenntniss der Menschlichen Placenta*, pp. 1-39. Stampfli, Bern.
- Ockeford, C.D. (1976) A 3-dimensional reconstruction of the polygonal pattern on placental coated vesicle membranes. *J. Cell Sci.* 21, 83-91.
- Ockeford, C.D. and Menon, G. (1977) Differentiated regions of human placental cell surface associated with exchange of materials between maternal and foetal blood: a new organelle and the binding criterion. *J. Cell Sci.* 25, 279-291.
- Ockeford, C.D. and Whyte, A. (1977) Differentiated regions of human placental cell surface associated with exchange of materials between maternal and foetal blood: coated vesicles. *J. Cell Sci.* 25, 23-312.
- Ockeford, C.D. and Wakely, J. (1981) The skeleton of the placenta. In: *Progress in Anatomy*. Editors: J. Harrison and R.L. Holmes, Vol. II, pp. 19-48. Cambridge University Press, London.
- Ockeford, C.D., Whyte, A. and Bowyer, D.E. (1977) Variation in volume of coated vesicles isolated from human placenta. *Cell. Biol. Int. Rep.* 1, 137-146.
- Ockeford, C.D., Devoy, K. and Hall, H. (1979) Image analysis of negatively stained human placental coated vesicles. *Cell Biol. Int. Rep.* 3, 717-724.
- Ockeford, C.D., Wakely, J. and Baddley, R.A. (1981) Morphogenesis of human placental chorionic villi: cytoskeletal, syncytioskeletal and extracellular matrix proteins. *Proc. R. Soc. London, Ser. B.* 22, 305-316.
- Okajima, Y., Hashimoto, T., Hamannaka, N. and Yashinara, S. (1971) Electron microscopic study on the trophoblast cell columns of human placenta. *J. Electron Microsc.* 20, 93-106.
- Ortmann, R. (1960) Morphologie der menschlichen Placenta. *Verh. Anat. Ges.* 106, 27-56.
- Pagd, M. and Ahn, J.N. (1964) Ultrastructure des cellules de Hofbauer dans le placenta humain. *R. Acad. Sci.* 258, 3556-3558.
- Pease B.M.F. (1975) Coated vesicles from pig brain: purification and biochemical characterisation. *Mol. Biol.* 977, 93-98.
- Pease B.M.F. (1976) Clathrin: a unique protein associated with intracellular transfer of membrane coated vesicles. *Proc. Natl. Acad. Sci. U.S.A.* 73, 1255-1259.

- Pierce, G.B., Jr. and Midgely, A.R., Jr. (1963) Origin and function of human syncytium giant cells. *Am. J. Pathol.* 43, 153-173.
- Pisarki, T. and Topilko, A. (1966) Comparative study of the vasculosyncytial membranes of the human placenta in light and electron microscopy. *Pol. Med. J.* 5, 630-638.
- Poole, A.R., Howell, J.I. and Lucy, J.A. (1970) Lysolecithin and cell fusion. *Nature (London)* 227, 810-813.
- Rhodin, J.A.G. and Terzakis, J. (1962) The ultrastructure of the human full term placenta. *J. Ultrastruct. Res.* 6, 88-106.
- Richart, R. (1961) Studies of placental morphogenesis. I. Radioautographic studies of human placenta utilizing tritiated thymidine. *Proc. Soc. Exp. Biol. Med.* 106, 829-831.
- Rohr, K. (1889) Die Beziehungen der Mutterlichen Gefäße zu den intervillösen Räumen der Placenta speciell zur Thrombose derselben ('Wiesser Infarkt'). *Virchows Arch. Pathol. Anat. Physiol.* 115, 505-534.
- Roth, T.F. and Porter, K.R. (1964) Yolk protein uptake in oocyte of the mosquito *Aedes aegypti*. *J. Cell Biol.* 20, 313-332.
- Ryan, K.J. (1959) Metabolism of C-16 oxygenated steroids by human placenta. The formation of estriol. *J. Biol. Chem.* 234, 2006-2008.
- Sálaraz, H. and Gonzalez-Angulo, A. (1967) The fine structure of human chorionic villi and placental transfer of iron in late pregnancy. *Am. J. Obstet. Gynecol.* 87, 851-865.
- Sawasaki, C., Mori, T., Inoue, T. and Shinmi, K. (1957) Observations on human placental membranes under the electron microscope. *Endocrinology Jpn* 4, 3-11.
- Sideri, M., Fumagalli, G., De Virgiliis, G. and Remotti, G. (1980) The morphological basis of placental endocrine activity. In: *The Human Placenta: Proteins and Hormones*. Editors: A. Kloppe A. Genazzani and P.G. Crosignani, pp. 339-348. Academic Press, London and New York.
- Simionescu, N., Simionescu, M. and Palade, G.E. (1973) Permeability of muscle capillaries to exogenous myoglobin. *J. Cell Biol.* 57, 424-452.
- Simson, J.V. and Spicer, S.S. (1973) Activities of specific cell constituents in phagocytosis (macropinocytosis). In: *International Review of Experimental Pathology*. Editors: G.W. Richter and MA Epstein, Vol. 12, pp. 79-118. Academic Press, New York and London.
- Smith, A.D. and Winkler, H. (1968) Lysosomal phospholipase A1 and A2 of bovine adrenal medulla. *Biochem. J.* 108, 867-874.
- Sotelo, J.R. and Porter, K.R. (1959) An electron microscope study of rat ovum. *J. Biophys. Biochem. Cytol.* 5, 327-342.
- Stein, L., Fernandes, J. and Lewandowski, H. (1974) The ultrastructure of the normal placenta. *J. Am. Osteopath. Assoc.* 73, 463-468.
- Stieve, H. (1952) Anatomie der Placenta und des intervillösen Raumes. In: *Biologie und Pathologie des Weibes*. Editors: Seitz and Amreich, pp. 109-146. Urban and Schwarzenberg, Berlin.
- Strauss, L., Goldenberg, N., Hirota, K. and Okydaira, Y. (1965) Structure of human placenta with observations on ultrastructure of the terminal chorionic villus. *Birth Defects, Orig. Art. Ser.* 1pp. 13-26.
- Terzakis, J. (1963) The ultrastructure of normal human first trimester placenta. *J. Ultrastruct. Res.* 9, 268-284.
- Thomas, L., Douglas, G.W. and Carr, M.C. (1959) The continual migration of syncytial trophoblast from the fetal placenta into the maternal circulation. *Trans. Assoc. Am. Physicians* 72, 140-48.
- Tighe, J.R., Garrod, P.R. and Curran, R.C. (1967) The trophoblast of human chorionic villi. *J. Pathol. Bacteriol.* 93, 559-567.
- Wakitani, T. (1961) Electron microscopic observations on the chorionic villi of the normal human placenta. 1. Electron microscopic observations of chorionic villi of normal human placenta. *Jpn Obstet. Gynecol. Soc.* 8, 208-224.
- Whyte, A. (1978) Proteins of coated micropinocytic vesicles isolated from human placenta. *Biochim. Soc. Trans.* 6, 299-301.
- Whyte, A. (1980) Lectin binding by microvillous membranes and coated pit regions of human syncytial trophoblast. *Histochem. J.* 12, 599-607.
- Wigglesworth, J.S. (1962) The gross and microscopic pathology of the premature delivered placenta. *J. Obstet. Gynecol. Br. Commonw.* 69, 355-365.
- Wild, A.E. (1974) In: *Transport at the Cellular Level*. Editors: M.A. Sleigh and D.M. Jennings. pp. 521-546. Cambridge University Press, Cambridge.

- Wild, A.E. (1975) Maternofetal transmission of immunoglobulin. In: Editor: W.A. Hemmings, pp. 155-167. Cambridge University Press, Cambridge.
- Wild, A.E. (1980) Coated vesicles: a morphologically distinct subclass of endocytic vesicles. In: Coated Vesicles. Editors: C.D. Ockleford and A. Whyte, pp. 1-25. Cambridge University Press, Cambridge.
- Willingham, M.C. and Pastan, I. (1980) Receptor mediated endocytosis in cultured fibroblasts: the receptosome. *Eur. J. Cell Biol.* 22, 203.
- Wislocki, G.B. and Bennett, H.S. (1943) The histology and cytology of the human and monkey placenta with special reference to the trophoblast. *Am. J. Anat.* 73, 335-450.
- Wislocki, G.B. and Dempsey, E.W. (1946) Histochemical age changes in normal and pathological placental villi. *Endocrinology* 38, 90-109.
- Wislocki, G.B. and Dempsey, E.W. (1955) Electron microscopy of the human placenta. *Anat. Rec.* 123, 133-149.
- Wislocki, G.B., Dempsey, E.W. and Fawcett, D.W. (1948) Some functional activities of the placental trophoblast. *Obstet. Gynecol. Surv.* 5, 604-614.
- Woodward, M.P. and Roth, T.F. (1978) Coated vesicles, characterisation, selective, dissociation and re-assembly. *Proc. Natl. Acad. Sci.* 75, 4394-4398.
- Wynn, R.M. (1967) Fetomaternal cellular relations in the human basal plate. An ultrastructural study of the placenta. *Am. J. Obstet. Gynecol.* 97, 832-850.
- Wynn, R.W. (1972) Cytotrophoblastic specializations: an ultrastructural study of the human placenta. *Am. J. Obstet. Gynecol.* 114, 339-353.
- Wynn, R.W. (1975) Fine structure of the placenta. In: *The Placenta and its Maternal Supply Line*. Editor: P. Gruenwald, pp. 56-79. Medical Technical Publishing Co., Lancaster.
- Wynn, A.M., Panigel, M. and McLennan, A.H. (1971) Fine structure of the placenta and fetal membrane of the baboon. *Am. J. Obstet. Gynecol.* 109, 638-648.
- Yoshida, Y. (1964) Ultrastructure and secretory function of the syncytial trophoblast of human placenta in early pregnancy. *Exp. Cell Res.* 34, 305-317.
- Zander, J. (1964) Progesterone in human blood and tissues. *Nature (London)* 174, 406-407.

## ABSTRACT

Transport of Immunoglobulin G across the human placenta. by  
Linda Dearden.

It is well known that Immunoglobulin G (IgG) is transported across the human placenta during gestation. However the route of this transport is not clear and the aim of this thesis is to elucidate the transport pathway.

A number of different methods and placental systems were employed to investigate the IgG transport pathway.

1. Human placentae were perfused with a human IgG probe using an isolated cotyledon method.
2. Dissected chorionic villi from both term and first trimester placentae were incubated in culture medium containing a human IgG probe.
3. Human placental cells were cultured and incubated with a human IgG probe.
4. Choriocarcinoma cells (BeWo) were cultured and incubated with a human IgG probe.

The IgG transport process was investigated at the light microscope level using tritiated IgG, and at the electron microscope level using colloidal gold particles coated with IgG. From these investigations new evidence was discovered concerning the transport of IgG across the human placenta.

In addition an extensive morphological study of the BeWo cells has provided much new information. There are clear indications in the structure of these cells, first of transformed state and secondly of their origin from trophoblast tissue.

Observations are presented of the in vitro differentiation of cultured cells towards the villous state of the parent tissue. Cytoplasmic characteristics and mutual positioning of these cells was noted which were similar to those of cytotrophoblast and syncytiotrophoblast in vivo. Bulbous projections were also noted in the culture cells both attached to the tissue and floating in the culture medium. These features may be related to the budding off and depbrtation of trophoblast in vivo.